PHOSPHORUS DYNAMICS IN A SHALLOW COASTAL LAKE SYSTEM, CANTERBURY, NEW ZEALAND

A thesis submitted in partial fulfilment of the requirements for the Degree of

Doctor of Philosophy in Water Resource Management

at the University of Canterbury

by

Alex Sean Waters

University of Canterbury

February 2016

Abstract

Te Roto o Wairewa/Lake Forsyth (Wairewa) is a small (6.3 km^2), polymictic, shallow (< 2 m), intermittently closed and open lake system on the south side of Banks Peninsula, New Zealand. The lake is hypertrophic and experiences regular algal blooms which are linked to high phosphorus (P) concentrations in the water column. This study investigates P dynamics in the lake and catchment, using field and laboratory investigations as well as geochemical modelling. The flux of P from the catchment to the lake was quantified, and the relative importance of internal P loading from the lake sediments determined. The important sedimentary P binding and release mechanisms were identified as well as the key environmental conditions controlling these mechanisms in the lake.

A P budget was developed for the lake using a mass-balance approach over a fifteen month period (December 2012- March 2014). More than 7000 kg $P.yr^{-1}$ was transported to the lake from the catchment. This flux occurred primarily as particulate associated P (80 % of total) during large flood events, particularly from the Okana River sub-catchment. The lack of a permanent opening to the sea resulted in the retention of 70 % of the external P load in the lake. This retained P was predominantly bound in the lake sediments. Mass balance calculations indicated that the flux of P from this sediment reservoir to the water column exceeded the external load during the summer months. Increases in total P (TP) concentrations during algal bloom events could only be explained by such internal loading.

P binding and mobility in the lake sediments were investigated by sequential chemical extraction, pore water chemistry and geochemical modelling. Surface sediments were highly enriched in P with total sedimentary P concentrations of around 1500 mg $P.kg^{-1}$. With depth, the concentrations of the more mobile P fractions (organic-P and P associated with Fe and Al (hydr)oxides) decreased, indicating the release and upward flux of orthophosphate (PO_4^{-3}) by organic decomposition and desorption from inorganic forms. In contrast the more refractory organic-P fraction and P associated with detrital apatite were immobile, and hence are progressively buried. The upward flux of released PO_4^{-3}, which is immobilised again in the shallower, more oxic sediments where PO_4^{-3} adsorbs to phases such as Fe and Al (hydr)oxides, explains the highly P enriched layer at the sediment surface. Geochemical modelling indicated that in the surface sediments this

cycle is affected by the rapid precipitation and dissolution dynamics of an amorphous Fe(III) (hydr)oxide such as ferrihydrite, and at depth by FeS_2 regulation of Fe availability. Secondary mineral phases such as $MnHPO_4$, strengite and vivianite may also exert some control over P binding in the sediments.

Trends in pore water chemistry indicated significant seasonal changes in redox conditions, with more reduced sediments at the surface during winter. This was due to decomposition of the increased amounts of organic matter present in the surface sediments during winter. A more oxidised upper sediment profile with less organic content existed during the early summer growing season (prior to algal bloom formation). This was consistent with the increased pool of Fe-bound P in the upper sediments observed in summer, which was then available for release when redox boundaries migrated upward again, as observed during periods of algal bloom formation.

The potential for release of P from the sediments, and the mechanisms which may promote this, were investigated by geochemical modelling and by laboratory experiments, which comprised a mixture of sediment core incubations and sediment slurry experiments. The potential for P release into an oxic, circum neutral-pH water column was negligible, likely due to the high ratio of reactive Fe to P in the sediments. Redox related P release from bed sediments began once the dissolved oxygen (DO) in the water column was completely depleted, and E_h was < 100 mV. Average release rates of 21 and 64 $mg.m^{-2}.d^{-1}$ were observed ($E_h \approx$ -200 and -300 mV respectively). pH related release was significant at pH > 9, and release rates from bed sediments of 3.3 and 11 $mg.m^{-2}.d^{-1}$ were observed (pH ≈ 9 and 10 respectively). These release rates have the potential to explain the increases in [TP] observed during algal blooms. pH-related release rates were significantly higher from resuspended sediment (78 and 100 $mg.m^{-2}d^{-1}$ in pH ≈ 9 and 10 respectively) than from the bed sediments. Geochemical modelling indicated that increased salinity would increase pH-related P desorption, as well as decreasing the P binding capacity of the sediments, due to the reductive dissolution of Fe hydroxides and Fe immobilisation as FeS_2. Salinity gradients across the sediment-water interface resulting from 'freshening' events in the lake, resulted in P release of up to 13 $mg.m^{-2}d^{-1}$.

Environmental conditions which may control P binding and release in the lake sediments were investigated by the use of DO and pH data loggers as well as spot sampling in the lake. Although the water column was generally well mixed and oxygenated, bottom water

anoxia did occur as ‘patchy’ spatially discrete and short lived (days, occasionally weeks) events. These occurred due to thermal stratification in macrophyte beds and the flux of organic material to the sediments from senescing macrophytes and algae. Salinity stratification may explain periods of variation in DO concentration associated with floods and lake openings. High salinity over longer time frames (4 months) was also correlated with high concentrations of chlorophyll-*a* in the lake. Macrophyte and algal photosynthesis produced water column pH > 9 and up to 10.5 for long periods of time, conditions compatible with significant sedimentary P release. Potential P release from observed DO and pH patterns was enough to explain observed increases in TP concentration associated with algal blooms.

In this research a combination of field and laboratory work, as well as geochemical modelling was used to determine key processes associated with P dynamics in Wairewa. The high external P load, coupled with high P retention, indicated that the management of water quality in the lake must address the flux of P from the catchment, especially that associated with flood events in the Okana sub-catchment. At the same time, the large reservoir of P in the lake sediments, and the importance of internal P loading processes, means that a response to external P load reductions is likely to be slow. Hence management of internal P loading should be considered. The key roles of redox potential and water column pH, the ‘patchy’ and short lived nature of low DO events, and the significant roles of macrophyte beds and salinity in the internal cyling of P in the lake, are all important findings for the management of Wairewa and shallow coastal lakes in general.

Table of Contents

List of Figures

Chapter 4

Chapter 5

List of Tables

Chapter 5

Chapter 6

Acknowledgements

First and foremost I would like to thanks my supervisors Prof Jenny Webster-Brown and Prof Ian Hawes for their support, advice and guidance throughout this project. In particular, thanks to Jenny for her leap of faith in believing in my ability, her trust in letting me get on with it, and her shear hard work in dealing with my questions, red herrings, and indecipherable manuscripts. Thanks to Ian for his advice on technical matters, for sharing his understanding of lake ecosystems, and his insights into scientific approach.

I would like to thank Ngai Tahu and the Wairewa Runanga, as well as the various landowners in the lake catchment, in particular Kinloch Farm and the farm manager Joe Power, for access on and around the lake.

Huge thanks to Suellen Knopick (Waterways Center for Freshwater Management), as well as Warwick Hill and Kelvin Nicholl (Lincoln University) for administrative, workshop and laboratory assistance. Also, Lynne Clucas and Roger Cresswell (Lincoln University), for their technical support and rapid sample analysis.

Thanks to all those people who supplied data and information. Staff at Environment Canterbury were invaluable, particularly Tim Davie for his support of this project and general enthusiasm regarding Wairewa. Also at ECan, Sian Barbour, Rachel Webster, Tony Grey, Jim Morrison and Alex Ring all helped with the supply of data, information and advice. Thanks also to Graham Harrington at Christchurch City Council, for sharing his work on lake level, area and volume relationships. At NIWA, Kathy Walters, Don Jellyman and Graham Horrell all provided data. Thanks especially to Graham for his friendship and support in Perugia.

Many thanks to David Hamilton, Mat Allan and Chris McBride (University of Waikato), for their support, advice and enthusiasm during my time in Hamilton. Although this didn't directly produce the results we were after, it provided many insights which were useful in other areas of this research.

Thanks also to my fellow students, particularly Hana Christensen, Jordan Miller, Neil Berryman and Phil Clunies-Ross, for their help in the field and laboratory, and Klaus Hammender for his assistance with WEPP.

This research was enabled financially by a University of Canterbury Doctoral Scholarship as well as support from Environment Canterbury and Meadow Mushrooms Ltd. The Royal Society of New Zealand- Canterbury Branch and the Waterways Centre for Freshwater Management both supported my travel to the 15th World Lake Conference in Italy. Many thanks for the support.

Thanks also to friends and family, in particular to Linda and Craig who put up with me staying at their house for long periods of time. Finally and most importantly, I would like to thank my wife Dallis for her continual support and encouragement, her belief in and understanding of the 'obsession', for putting up with my anti-social hours, and for her willingness to 'bring home the bacon' for many years.

Abbreviations

BD	Bicarbonate/dithionite (chemical extract)
CSA	Critical source area
DIC	Dissolved inorganic carbon
DO	Dissolved oxygen
DRP	Dissolved reactive phosphate
DW	Dry weight
EC	Electrical conductivity
ECan	Environment Canterbury Regional Council
EDTA	Ethylenediaminetetraacetic acid
EPC	Equilibrium phosphate concentration
HFO	Hydrous ferric oxide
IC	Ion exchange chromotography
ICOLL	Intermittently open or closed lake or lagoon
ICP-OES	Inductively coupled plasma- optical emission spectrometry
LOI	Loss on ignition
LOD	Limit of detection
LOQ	Limit of quantitation
masl	meters above sea level
NIWA	National Institute of Atmospheric and Water research
OLW	Overlying water column
ORP	Oxidation reduction potential
PBI	Post-bloom initiation
Q	Discharge (flow)
SD	Standard deviation
SEM-EDS	Scanning electron microscopy-energy dispersive X-ray analysis
SI	Saturation index
SS	Suspended solids
SOE	Sum of chemical extracts
TD	Total dissolved
TP	Total phosphorus
TLI	Trophic level index
TSP	Total sedimentary phosphorus
TSS	Total suspended solids
UOM	Uncertainty of measurement
UV	Ultra-violet light
Wairewa	Te Roto o Wairewa/Lake Forsyth
WEPP	Water erosion prediction project

Chapter 1: General Introduction

1.1 Motivation: The eutrophication of lake ecosystems.

The eutrophication of lake systems refers to the increasing primary productivity that occurs in response to nutrient inputs (Wetzel 2001). While these processes can be natural, problems arise from the much faster eutrophication which oftens results from greatly elevated nutrient inputs due to anthropogenic activities, including changes in catchment land use patterns, such as deforestation or agricultural activity (Schindler, 2006; Downs, et al 2008). The increased productivity is generally expressed as an increase in phytoplankton concentration and may result in seasonal or permanent algal 'blooms' which seriously degrade water quality, with detrimental impacts on biodiversity. Light attenuation and decreased dissolved oxygen levels in particular, have marked impacts on macrophyte, zooplankton, benthic and fish communities (Wetzel, 2001; Søndergaard, 2007; Schallenberg and Sorell, 2009). Such eutrophication is a well-documented phenomenon in lake ecosystems across the world (e.g. Jacoby et al, 1982; Kristensen et al, 1992; Kumar Das et al, 2009) and is a significant issue in a large number of New Zealand lakes (Verburg et al, 2010).

Primary productivity in lake systems is strongly limited by nutrient availability (Søndergaard, 2007). While numerous nutrients are critical for primary production, the dominant role of the macronutrients nitrogen (N) and phosphorus (P), in controlling phytoplankton biomass in lakes is well established (Wetzel, 2001; Abell et al, 2011). P is only bioavailable in the form of the soluble orthophosphate ion (PO_4^{-3}). The concentration of this ion in natural waters is reduced by its affinity for particulate sediment, as it is adsorbed onto clays and oxides minerals as well as organic/inorganic colloidal material. N generally occurs in lake waters in much higher concentrations than bioavailable P, and hence phytoplanktonic biomass may be limited by the lower availability of dissolved P. In addition N limitation may be a symptom of over fertilisation with P (Schindler, 1977) and may be circumvented by the fixation of atmospheric N by various bloom-forming cyanobacteria (Wetzel, 2001; Søndergaard, 2007). A 37 year experiment in the Experimental Lakes Area of Canada, in which Lake 227 was fertilised with annually constant amounts of P and decreasing amounts of N resulted in a shift of algal population

to N fixing species which were produced in proportion to P inputs (Schindler et al, 2008). However, many studies have also demonstrated nitrogen limitation in lake systems (eg: White et al, 1986) and such systems may also be co-limited, or experience a change in the limiting nutrient over time (Burger et al, 2007; Moss et al, 2013). In addition light may play an important role in limiting primary productivity (Burger et al, 2007).

Hence although different systems may be limited at times by various factors, P is of key importance in the cultural eutrophication of lake systems (Reynolds & Davies, 2001; Schindler, 2006; Abell et al, 2010; Kumar Das et al, 2009). Therefore understanding the sources and fate of P is considered to be critical to understanding the environmental state of lake ecosystems (Søndergaard, 2007) and hence to manage lake water quality.

1.2 Phosphorus dynamics in lake systems

1.2.1 External phosphorus loading to lakes

P delivery to a lake system from the lakes catchment, via various external pathways, is termed 'external loading'. Natural P inputs include particulate-associated and dissolved-P species sourced from run off and the resulting erosion in the lake catchment. While these processes may be greatly accelerated by human activities, point source nutrient-rich effluents such as sewage, industrial wastes and detergents have largely been controlled by regulation in developed nations (Carpenter et al, 1998; Schindler, 2006). However diffuse sources of nutrient pollution have been increasingly recognised as a major issue and are much more difficult to control. The strong affinity of particulate material for P means that non-dissolved forms predominate in the transport of P from catchment to lake (Pacini & Gachter, 1999). Erosion, which preferentially mobilises clay-sized particles and organic material, both of which can be strong P adsorbents, is exacerbated by land use activities such as deforestation and agriculture. In addition the intensification of agriculture, often requiring intense fertiliser application, increases the soil- bound store of P which in turn can increase the amount of P carried by eroded soils. These activities, without very careful control, can increase the external P loading of lake systems enormously (Carpenter et al, 1998; Schindler, 2006; PCE, 2013).

1.2.2 Phosphorous cycling within lakes

Once in the lake system, P may exist in a number of chemical forms (species). Dissolved orthophosphate (PO_4^{-3}) in the water column is directly bioavailable, while particulate-associated P will settle to the bottom of the lake as a result of sedimentation. This sediment can constitute a major reservoir of in-lake P (Wetzel 2001). In most lakes and particularly in shallow lakes there is a constant interaction between the near-surface sediment and the water column. While some sediment bound P will be immobilised permanently, various processes can occur which return some of the P from the sediment, to the lake water (Figure 1.1). This is referred to as 'internal P loading' and can be the major source of P contributing to eutrophication in the lake (Jacoby, 1982; Søndergaard et al, 2003; Gao et al, 2005; Christophoridis and Fytianos, 2006). Lake sediments can therefore be both a source and sink for P, and understanding the complex chemical and biological interactions between the sediment and water is critical for understanding eutrophication in a given lake system.

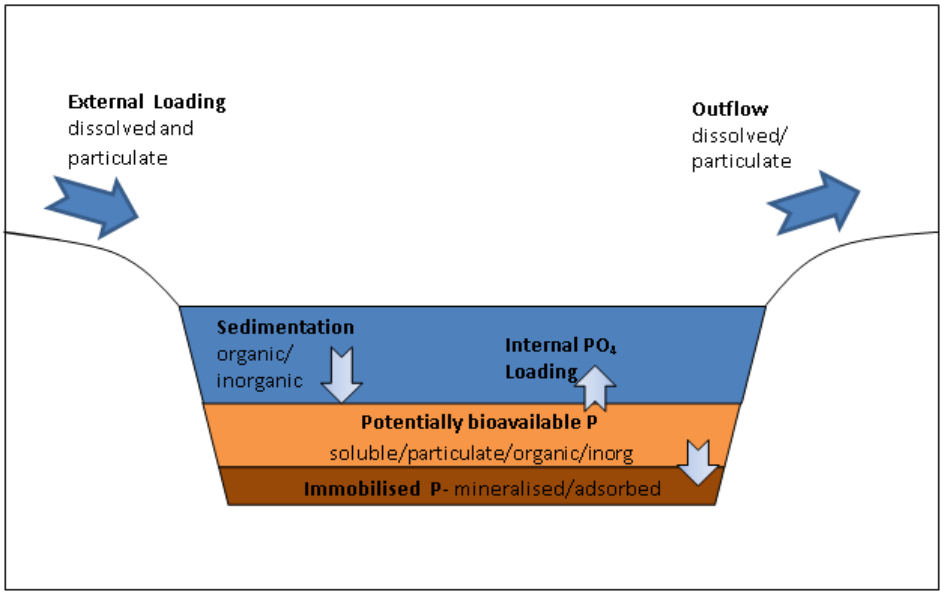

Figure 1.1 Simplified diagram of lake phosphorus dynamics (adapted from Søndergaard, 2007).

1.3 Shallow coastal lake systems in New Zealand

Shallow lake systems are common on the coasts of New Zealand. These systems are often naturally productive due to warmer temperatures and full depth photic zones, however, lying as they do, at the receiving end of often large catchments, they are susceptible to

eutrophication from increased sediment and nutrient inputs resulting from catchment disturbances and as a result they commonly have poor water quality. These systems have been the subject of some study (e.g. Hamilton and Mitchell, 1997; Drake et al, 2009) but have received relatively little research and management attention, relative to deeper inland lakes (Drake et al, 2011).

Significant numbers of these coastal lake systems are characterised by the lack of permanent outflows. High rates of long-shore drift create beach barrier systems which separate the lake from the adjacent ocean. Inflow volumes are insufficient to maintain permanent outflows to the sea and hence the lake system is isolated from the sea for long periods of time. Naturally, rising water levels and/or ocean wave action eventually break through the barrier resulting in lake outflows and lake-seawater interchange which results in varying levels of brackishness in the subsequently re-closed lake system. Artificial openings by excavation of the beach barrier are conducted in some systems to control lake levels and inundation of surrounding land or infrastructure. Such systems with natural or artificial openings, may be referred to as intermittently open and closed lakes and lagoons (ICOLLs) (Roy et al, 2001). The biogeochemistry of such ICOLLs has been the subject of much less research than estuarine or freshwater lake systems (Schallenberg et al, 2010), but is likely to be distinct from either.

1.4 Lake Forsyth/ Te Roto o Wairewa

Lake Forsyth/ Te Roto o Wairewa (referred to in this thesis as Wairewa) is a small (6.3 km^2), shallow lake on the southern side of Banks Peninsula (Figure 1.2). The lake catchment covers approximately 110 km^2, much of which is steep hill country used for pastoral agriculture. Inflows to the lake are predominantly from the Okana and Okuti Rivers which join near the lake to form the Takiritawai River (Figures 1.3 and 2.1). Lesser inflows occur from smaller stream tributaries and runoff which flow direct to the lake, as well as an unknown, but likely minor component contributed directly from groundwater. The lake is generally less than 2 m deep, and is separated from the sea by the eastern end of an active barrier-beach complex known as Kaitorete Spit. This narrow barrier (≤100 m) has evolved over 8000 years as an accumulation of material which has been transported north along the coast of the Canterbury Bight (Woodward and Schulmeister, 2005). The timing of the transition of the lake from marine estuary to

closed-in lake is uncertain but appears to be least 450 years BP (Woodward and Schulmeister, 2005). In the 19th century a lake outlet still existed and whalers, canoes and coastal traders accessed the lake from the ocean implying that the lake was open at least periodically (Jellyman and Cranwell, 2007). Currently the lake is a brackish ICOLL with a wide range of salinities (salinity=1-11 ‰ NaCl, mean 6 ‰ NaCl, Main et al 2003). Artificial opening of the lake to the sea first occurred in 1866 and now occurs approximately once a year in order to manage flooding of local roads and farmland (Soons, 1998; Reid et al, 2004; Woodward and Schulmeister, 2005).

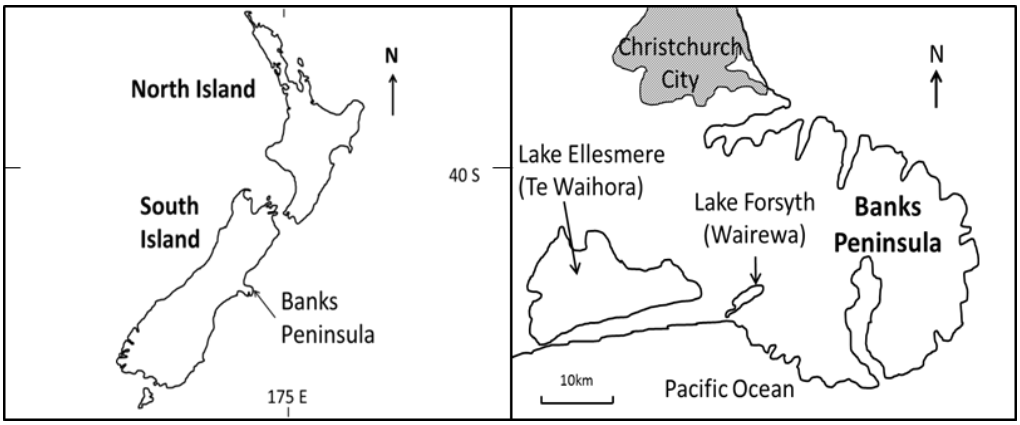

Figure 1.2 Location map for Lake Forsyth/Te Roto o Wairewa**.**

The main body of the lake is bounded at the north-eastern end by low lying marshy areas which are commonly inundated when the lake level is high. A narrow neck extends to the south-west through the gravels of the beach barrier complex toward the sea. The artificial openings of the lake are conducted at the western end of this neck. Originally openings were conducted directly through a 'cut' through the beach barrier to the sea, but since 2009 openings are conducted via a lake outlet canal which skirts bedrock cliffs to the beach opening site (Figure 3.1). The areal extent of the lake is variable depending on lake level with 6.3 km^2 being the average area during the budget period presented in Chapter 2. During that same period the average level of the lake surface was 1.91 masl with an average maximum depth of 1.86 m and an average depth across the lake of 1.56 m. The north-east end of the lake is generally shallower and shoals gently toward the north-east compared to the rest of the main body of the lake which is of consistent depth and shoals quickly at its edges. The neck has a slightly deeper channel which runs along its south-eastern bank. A New Zealand Oceanographic Institute bathymetric chart from 1978 indicated a small area of 4.1 m depth close to the opening sites at the south-west end

of the neck, however depth soundings by this author seemed to indicate that this deeper 'hole' no longer exists.

Wairewa is currently a turbid, hypertrophic lake, which experiences regular toxic blooms of cyanobacteria, predominantly *Nodularia spumigens* and less frequently *Anabaena spp*. Paleolimnological studies indicate that deforestation of the catchment predominantly after European arrival led to major increases in runoff and sediment to the lake, creating virtually freshwater conditions (Woodward and Schulmeister, 2005). Continuing nutrient input due largely to erosion of the P-rich, volcanic-derived soils of Banks Peninsula (Lynn, 2005), has led to declining water quality and toxic algal blooms. An increase in salinity, probably due to periodic openings, initiated a shift to more saline tolerant algal species such as *Nodularia spumigens*, the first recorded bloom of which occurred in 1907 (Main et al, 2003; Woodward and Schulmeister, 2005).

Figure 1.3 An aerial view of Lake Forsyth/Te Roto o Wairewa looking south toward the Pacific Ocean. The main tributary, the Takiritawai River can be seen entering from the bottom and the intermittent outflows occur from the end of the narrow tongue of water seen at the top (Photo; Kelvin Nicholls).

Nutrient levels are variable and often very high (see Section 1.4.1), and these high concentrations are commonly associated with algal blooms (Figure 1.4). However, the exact causative link between nutrient concentrations and bloom formation has not been established (Main et al, 2003). Nutrient speciation and dynamics in the catchment waterways and the lake, are largely un-researched, although seasonal and stream flow related variations in TP and dissolved PO_4^{-3} have been recorded (Main et al, 2003), and significant changes in in-lake dissolved PO_4^{-3} levels have been noted over very short time

frames (<1 hr) (Robertson, 2011). High P concentrations of up to 1600 mg kg^{-1} have been reported in the lake sediments (Main et al, 2003).

The poor water quality in Wairewa has had a major impact on lake biodiversity (Reid et al, 2004; Woodward and Schulmeister, 2005; Jellyman and Cranwell, 2007). The lake has long been a crucial food source for Ngai Tahu and is one of only two customary lakes in New Zealand. Te Wairewa Runanga have identified the rehabilitation of the lake as the priority issue in their area. A catchment wide approach to nutrient management with the aim of establishing a Mahinga Kai Cultural Park is proposed, but is unlikely to be successful if the current water quality issues cannot be addressed.

Figure 1.4 A bloom of *Nodularia spumigens* in Wairewa on 8 April 2013.

1.4.1 General water quality parameters

The regional authority, Environment Canterbury (ECan), monitors water quality in the lake. Key statistics for water quality parameters in the lake are presented in Table 1.1 for the period 1995 – 2014 (Statistical analysis conducted using Excel® 2010). Monthly averages are presented in Figures 1.5 and 1.6. Lake monitoring data was provided by S Barbour (ECan *pers comm).*

During the data period, dissolved oxygen (DO) concentrations and pH both display high average values and were relatively consistent with small standard deviations. Average pH is lower, and DO higher, during the winter months. The average and median EC were high, and highly variable, and showed a peak in late winter/early spring, likely due to lake openings in response to high winter rainfall events in the catchment. Total phosphorus

(TP), dissolved reactive phosphorus (DRP) and Chlorophyll a (chl-*a*) also showed high average, and highly variable, concentrations. The TP concentration was higher and had a higher range during the January-March period reflecting similar trends in chl-*a* concentrations. Water temperature showed a significant range and followed a predictable annual pattern of warmer temperatures during the summer months. The lake water temperature responded rapidly to air temperature, with changes occurring on a daily time scale (not shown).

Table 1.1 Key statistics for selected water quality parameters in Wairewa from long-term lake monitoring data collected by ECan over the period March 1995- October 2014.

	Temperature	**DO (mg.L)**	**pH**	**EC**
	^{o}C	$mg.L^{-1}$		$mS.cm^{-1}$
mean	13.40	10.28	8.21	9.22
SD	5.05	1.71	0.54	4.96
Median	13.40	10.30	8.10	8.70
Range	25.1 - 2.40	16.6 - 4.30	9.90 - 6.50	36.0 - 0.29
n	789	319	624	630
	Turbidity[1]	**TP[2]**	**DRP[3]**	**chl-*a*[4]**
	NTU	$mg.L^{-1}$	$mg.L^{-1}$	$ug.L^{-1}$
mean	28.9	0.238	0.019	96.9
SD	41,6	0.293	0.058	350
Median	14	0.140	0.004	33.8
Range	450 – 1.10	2.80 - 0.004	0.61 - 0.001	6790 - 0.100
n	634	547	542	800

1. A maximum value of 1500 NTU was considered to be an outlier and was removed from the data
2. Two values (14, 18 $mg.L^{-1}$) were considered outliers and removed from the data
3. Where concentrations were below detection a value of 0.5 x Detection Limit was used.
4. Three concentrations of >10000 $\mu g.L^{-1}$ were considered outliers and were removed from the data

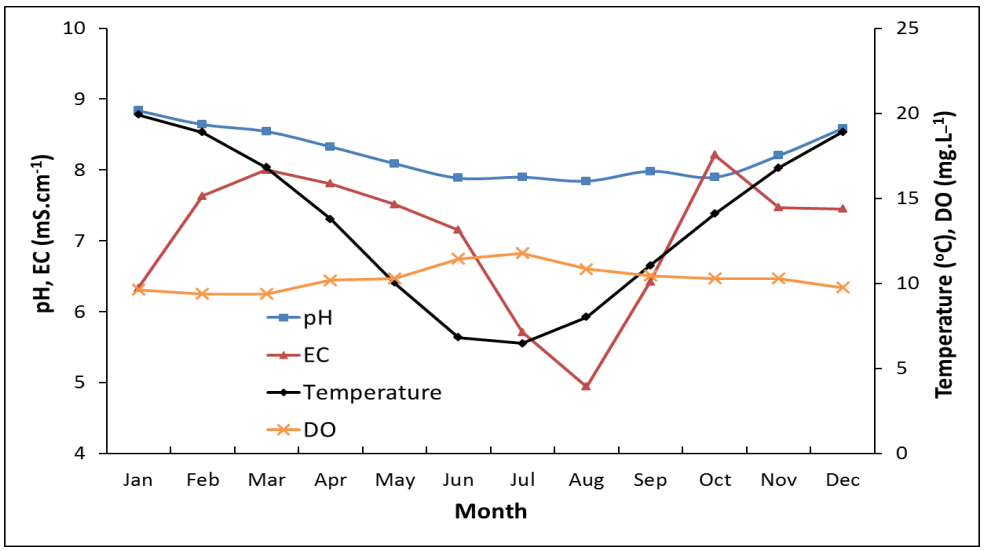

Figure 1.5 Monthly averages for key environmental variables in Wairewa over the period March 1995 – October 2014. Data is from long term monitoring data measured by ECan, at the main Environment Canterbury recorder site.

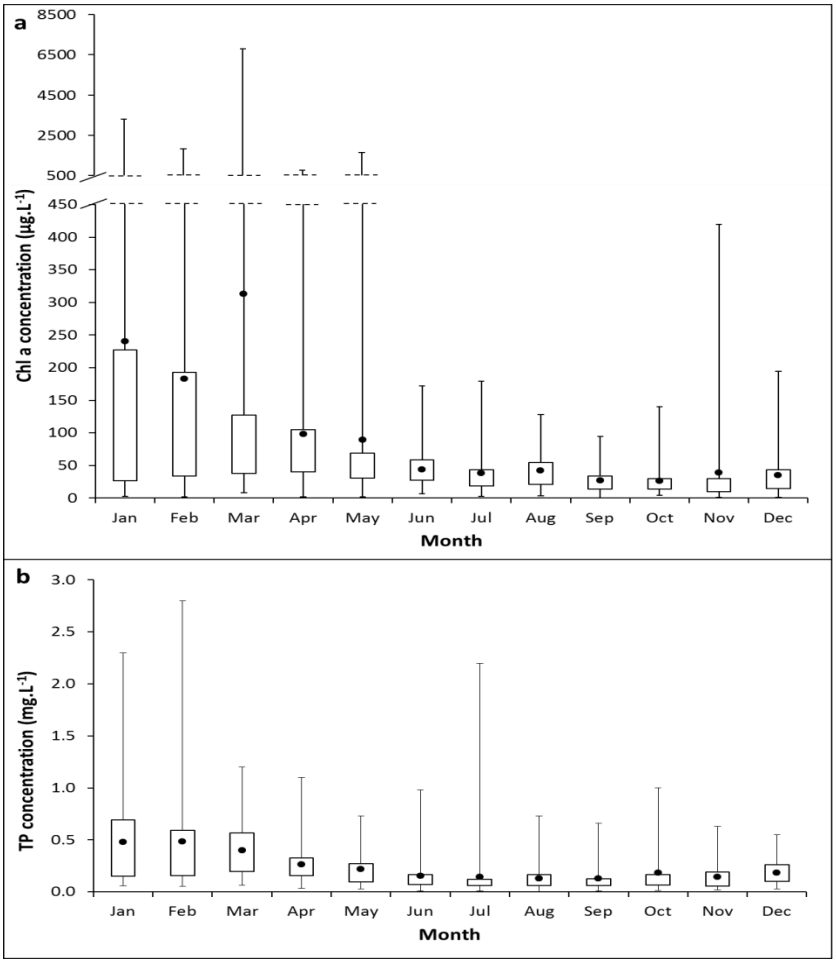

Figure 1.6 Box and whisker plots for monthly average concentrations of, (a) chl-*a*, and (b) Total Phosphorus concentrations, in Wairewa over the period. March 1995 – October 2014. Whiskers represent the maximum and minimum concentrations, boxes represent the 75th and 25th percentiles and the black circles are the mean concentrations. Data is from long term monitoring by ECan, at the main recorder site. Note the broken Y axis and maximum whiskers in plot (a). Very high mean values (> 75th percentile) may be affected by surface algal scum sampling.

1.5 Research rationale and questions

The dynamics of external and internal loading of phosphorus in lake ecosystems is complex and the relative contributions and drivers may be lake-specific. Limited research has been conducted on nutrient dynamics in ICOLL systems, particularly in New Zealand. As management responses to lake eutrophication are likely to be expensive, controversial and of a long term nature, there is an onus on lake managers to make decisions based on good quality, lake specific research, as well as the outcomes of community consultation. As such this research aims to identify the biogeochemical factors controlling P dynamics in Wairewa and in doing so illuminate key P cycling processes in New Zealand's shallow ICOLL systems. While the focus of this research has

been on geochemical processes, biological and geochemical processes are interlinked in lake systems and hence biological processes are discussed in this thesis where they affect, or are affected by, geochemical processes relating to P dynamics.

Specific research questions addressed in this study are as follow;

Q1. P loading.
What is the flux of P from the catchment and what are the key processes driving this flux? What is the relative importance of external and internal P loading?

Q2. P binding
How is P retained within the lake system?

Q3. P release
What biogeochemical mechanisms promote the release of P, from lake P reservoirs, to the water column?

Q4. Environmental conditions driving bloom formation
What are the environmental conditions that promote P binding and release in Wairewa, thus driving and sustaining algal blooms?

1.6 Thesis overview

This thesis has been set out in four broadly independent chapters (Chapters 2-5) which seek to answer the four research questions presented in Section 1.5. Each chapter is presented in the format of a scientific manuscript but reference may be made to other chapters in an effort to avoid repetition. A synthesis chapter integrates the overall findings and is followed by the final concluding chapter.

Chapter 2 presents a mass balance P budget for the catchment using hydrological and contaminant transport analyses to estimate the external loading of P from various areas of the catchment as well as the mass of P leaving the lake via outflows and seepage. P retained in the various P reservoirs within the lake system is estimated and a mass balance approach is used to provide a first order estimate of internal P loading. The research presented in this chapter has been published in the Journal of Hydro-environment Research; Waters, S., Webster-Brown, J.G. 2016. The use of a Mass Balance Phosphorus

Budget for Informing Nutrient Management in Shallow Coastal Lakes. *Journal of Hydro-environment Research 10. 32-49.*

Chapter 3 presents the findings from laboratory work and geochemical modelling investigations into how P is bound within the lake's reservoirs, with particular focus on the lake sediments. Temporal and spatial variations are quantified and explained.

Chapter 4 presents the findings from geochemical modelling and laboratory incubation experiments to identify the mechanisms which promote P release from the lake sediments.

Chapter 5 examines the range of environmental conditions that occur in the catchment and lake system, which may promote or inhibit internal loading of P. This utilises longer term monitoring data from ECan, as well as in-lake investigations conducted by the author.

Chapter 6 integrates the findings of the previous four chapters to present an annual biogeochemical cycle controlling P dynamics within the lake system. The findings are then used to comment on possible lake management approaches for the control of eutrophication in Wairewa.

Chapter 7 highlights the important findings of this research, presents a summary model of key mechanisms and processes affecting P dynamics in Wairewa, and concludes the thesis.

Chapters 3-5 are in preparation for publication in peer-reviewed journals.

Chapter 2: A Phosphorus Budget for Wairewa

2.1 Introduction

Eutrophication is considered in many jurisdictions to be the most pervasive water quality issue affecting surface waters (e.g. PCE, 2013; USEPA, 1996). The economic impact to society is significant (Le et al, 2010; Dodds et al, 2009) and major efforts are being made to prevent and manage eutrophication, and to rehabilitate already affected systems (e.g. EC, 2000). Management of nutrient loads to waterbodies has been a focus of regional authorities in New Zealand and abroad for many years however at a catchment scale these external loads commonly demonstrate high variability both spatially and temporally (Stamm et al, 2013). Hence attempts to quantify contaminant loading to lake systems either as areal loads or catchment exports, must reflect this variability (Cassidy and Jordan, 2011). P loads are likely to be delivered to a lake system from a variety of sources including highly episodic diffuse sources channelised into stream flows or flowing direct to the receiving waterbody, and more continuous point source and/or groundwater sources. Where significant point sources have been controlled, variable stream flows commonly dominate external P transport from the catchment to receiving lake systems (Pionke et al, 1996, Stamm et al, 2014).

Load estimates in lake inflows attempt to integrate instantaneous flow volumes and contaminant concentrations, but this seemingly simple concept can be problematic and prone to large errors (Cassidy and Jordan, 2011). Commonly stream concentrations are based on infrequent grab sampling associated with routine water quality sampling and the variability in concentrations between sampling events can lead to significant errors in estimated loads (Degens and Donohue, 2002; Johnes, 2007). A wide range of sampling schemes and data analysis techniques have been developed in an attempt to addresses these issues, including averaging methods, ratio-based estimators and regression techniques (Lechter et al, 1999; Cassidy and Jordan, 2011). Appropriate sampling and analysis approaches should reduce errors and provide valuable information on spatial and temporal variability in external P loading thus enabling targeted management interventions

While external loading provides the ultimate source of P, hydraulic retention times will control how much of the external load is retained in the lake system and hence how much may be available for internal loading processes. Quantification of the mass of P retained in various reservoirs in the lake should allow some validation of estimated external loading and retention rates while changes in the mass of reservoirs should provide some insight into the relative contributions of internal and external loading to lake water P concentrations.

Recently ECan has been developing a catchment management plan for the Wairewa catchment with an aim of rehabilitating the lake ecosystem. The complex process of P loading to shallow lakes means that management planning and interventions often need to be lake-specific and to be based on a good understanding of the P sources, sinks and transformation processes, in a specific lake system. This chapter aims to quantify, by the use of a mass balance budget approach, various loading pathways and repositories of P in Wairewa, as well as estimate areal loading and catchment export rates. Stream gauging, P concentration analyses, modelling approaches and water balance calculations have been used to estimate inflows and outflows of P to/from the lake. Sediment and biomass sampling and analyses have been used along with water sampling and monitoring data to estimate in-lake P reservoirs. The relative importance of external and internal loading in the fluctuations of in-lake P concentrations has also been established.

2.2 Methods

2.2.1 A Mass-balance P budget

To establish a mass-balance P budget for Wairewa, hydrological inflows and outflows to/from the lake over a discrete period of time, were measured, as were the P concentration in those flows.

The budget may be represented as;

$$\Delta P = (S_{in}+DR_{in}+GW_{in}+RD_{in})-(S_{out}+GW_{out}) \qquad \text{(eq 2.1)}$$

Where ΔP = change in P stored in the lake

S_{in} = P input to lake via stream flow

DR_{in} = P input to lake via direct runoff

GW_{in} = P input to lake via groundwater

RD_{in} =P input to lake via direct rainfall

S_{out} = P outflow from lake via lake opening, stream discharge

GW_{out} =P outflow from lake via seep through the beach barrier and to ground water.

The lake system was also considered as a biogeochemical cycle with in-lake reservoirs of P, and transfer processes between these reservoirs. Reservoirs of P were calculated for the estimated masses of lake water, sediment and macrophytes from the concentrations of P in the respective reservoirs. Fluxes between sediment and water column reservoirs were estimated from changes in the mass of water column reservoir P (see Section 2.3.4). These may include the direct release of P from organic material but this was not quantified as a separate flux. Statistical analyses were conducted manually in Microsoft Excel®.

2.2.2 Study site; the Wairewa catchment.

The Wairewa catchment is comprised of 110 km^2 of mainly steep hill country which falls from over 800 m in the northern catchment to sea level in the south (Figure 2.1). The catchment is predominantly in hill country sheep and beef agriculture, with scattered plantation forests and patches of native vegetation. Inflows to the lake are predominantly from the Okana and Okuti Rivers (which join to form the Takiritawai River shortly before entering the lake), but significant areas of hillslope drain to the lake via smaller ephemeral streams and runoff which flows directly to the lake. Stream gauging sites and areas of direct runoff are indicated in Figure 2.1. Lake outflows are via seepage through the beach barrier complex to the sea or via an intermittent, artificially opened channel through the same barrier (Figure 2.2). These openings now occur approximately once a year in order to manage flooding (Soons, 1998; Reid et al, 2004; Woodward and Schulmeister, 2005). ECan maintain a long term water quality monitoring programme on the lake. Water sampling for TP and DRP is conducted monthly or fortnightly during periods of algal bloom, while water level monitoring is continuous. The National Institute of Water and Atmospheric Research (NIWA) maintain a long established, continuous water level gauge on the Huka Huka stream in the upper Okana catchment as well as a weather station in the lower Okuti catchment (Figure 2.1).

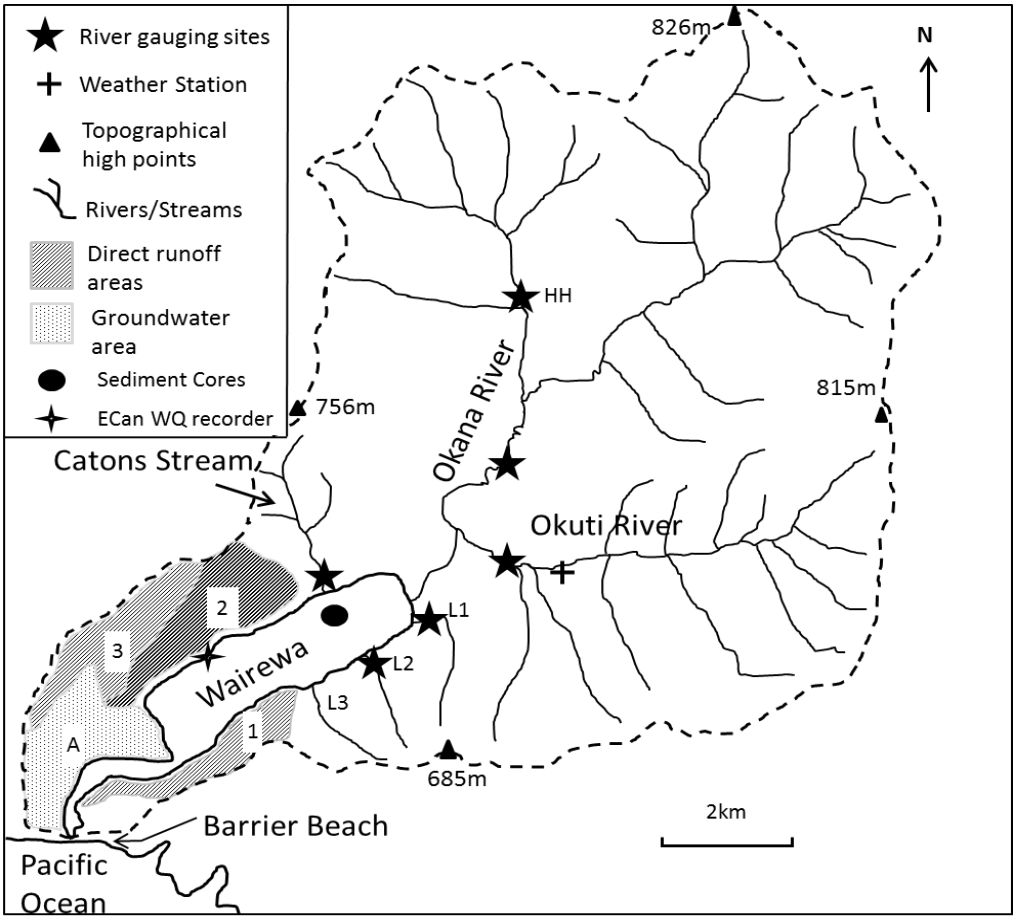

Figure 2.1. The Wairewa catchment, showing drainage patterns, the location of sites used for river gauging, and the direct-runoff catchment areas 1-3 referred to in the text. Groundwater storage area A, the Okuti weather station, ECan water quality recording site and sediment coring sites are also shown. HH= Huka Huka gauging station.

Figure 2.2 Outflow from Wairewa to the sea during an artificial opening on 19 April 2014.

2.2.3 Hydrology

2.2.3.1 Stream flows

Rating curves were established using water level and discharge data for the Okana and Okuti Rivers, and Catons, L1 and L2 streams (Figure 2.1). Level readings were obtained using capacitance water level loggers installed at these sites (Figure 2.3), which recorded levels at 10 min intervals for 15 months (3 Dec 2012 - 2 Mar 2014) for the Okana and Okuti Rivers and Catons Stream, and for 10.5 months (17 May 2013 – 2 Mar 2014) for L1 and L2 streams. Discharge (Q) data was obtained by manual stream gauging to calculate instantaneous stream Q. Gauging (Figure 2.4) was conducted in accordance with the USGS '6 tenths method' (Turnipseed & Sauer, 2010). Velocity measurements were taken with a Global Water FP111 flow probe. Q was obtained during low to high flow events over the summer and winter periods of 2012-2014. These rating curves allowed continuous Q to be obtained for low to high flows over the study period. Technical and safety issues prevented the gauging of very high flow Q. To extend the rating curves above maximum gauged Q for the Okana River (4.41 $m^3.s^{-1}$), a correlation was established between gauged Q and simultaneous Q from the Huka Huka gauging site (Figure 2.1). This correlation (R^2=0.86) was used to estimate very high flow Okana Q, from very high flow water level logger readings for the Okana River, and simultaneous Huka Huka discharges. These very high flow discharges were used to constrain the very high flow end of the rating curve.

The same process was used to determine very high flow estimates and a rating curve for the Okuti River (maximum gauged flow = 2.25 $m^3.s^{-1}$), except that the low-high flow correlation with the Okana River (R^2=0.78) was used instead of the correlation with Huka Huka. For the much smaller Catons, L1 and L2 streams, which are all ephemeral, the linear portion of the gauged ratings curve, (above 0.3 $m^3.sec^{-1}$ for Catons, and above 0.2 $m^3.sec^{-1}$ for L1 and L2) was extrapolated to very high flow levels. L3 stream (Figure 2.1) was not gauged but was assumed to have similar hydrological characteristics to L2 (see Section 2.2.5.1)

Figure 2.3 Downloading data from the capacitance level logger at L2

Figure 2.4 Stream gauging in a flooded Okuti River.

2.2.3.2 Direct Runoff

For the purposes of this study, direct runoff was considered to be that runoff which is not captured by the gauged tributaries, or L3. This has been calculated as two components, surface and subsurface runoff. Direct surface runoff has been modelled for areas 1-3 (Figure 2.1). These are areas of steep hill country which do not drain to significant tributaries and are characterised by sheet and rill erosion (Figure 2.5). Runoff from area 1

and 2 was included in the budget as direct runoff, while runoff from the hillslope of area 3 was assumed to drain to groundwater in the flat, porous gravel of area A and hence was included in the ground water portion of the budget. Surface runoff from these areas was modelled using the Water Erosion Prediction Project (WEPP) model from the US Department of Agriculture (ARS, 2012). The WEPP model is a process-based, distributed parameter, continuous simulation model (Laflan et al, 2004) which has been utilised extensively around the world for predicting water runoff and hillslope erosion processes (sheet and rill erosion) in small watersheds (e.g. Dehavri, 2014; Laflan et al, 2004; Rosewell, 2001). In a comparative study (Verma et al, 2010), WEPP proved more accurate in simulating annual runoff volumes, such as are required for this P budget research, than a similar model, the Hydrological Engineering Center's- Hydrological Modelling System. WEPP divides hillslopes into discrete 'overland flow elements' which have distinct soil, vegetation and land use characteristics. It then uses the fundamentals of weather processes, surface and subsurface hydrology, soil physics, plant growth, residue decomposition, overland flow hydraulics and erosion processes to simulate water runoff and the detachment, transport and deposition of sediment (Pieri et al, 2007). It was used here to predict the volumes of direct surface runoff water reaching Wairewa, based on a well published track record, good performance in a wide range of small watersheds (Laflan et al, 2004) and the fact that it has previously been utilised with success, to predict soil erosion in the Forsyth catchment (Hammender, 2013). Detailed information on general model parameters is available in Piere et al (2007). Catchment specific inputs were obtained from Hammender (2013) and hillslope specific inputs were from a variety of sources as detailed in Table 2.1.

Modelling was undertaken for the period 1 January-30 June 2013 (6 months) based on the available CLIGEN generated meteorological database and the model outputs were derived as 'event by event' runoff estimates (mm). These were then multiplied by the area of the slopes of interest to obtain a volume of direct surface runoff. The model was validated against the Catons Stream catchment area for which actual runoff was measured. The model predicted that direct runoff would result from rainfall events over eight days during May and June 2013. A Nash-Sutcliffe model efficiency coefficient (E) was calculated for the time series of daily runoff volumes during runoff events, to test model efficacy (Nash & Sutcliffe, 1970). E may range from $-\infty$ to 1 with 1 denoting a perfect fit of modelled and observed data and negative values indicating poor model

performance (Schaefli & Gupta, 2007). Where E > 0 the model prediction is better than the use of an overall mean. For the model validation in the Catons Stream catchment E = 0.1. While this was not as high as hoped for, it does provide a slightly improved estimate than the use of mean runoff. In addition model inaccuracies in the validation process were associated with the temporal distribution of the runoff rather than the estimation of the total runoff volumes required for the quantification of P loading from ungauged areas of the catchment. For the major flood event in June 2013, runoff intensity was overestimated by the model and the hydrograph indicated runoff over a longer time period, but total runoff volume (baseflow to baseflow) was correct to within 5%. On the basis of E > 0 and more importantly, a close agreement on total runoff volumes, the model has been utilised to predict total direct surface runoff volumes for the other slopes modelled in this study.

Table 2.1 Data input requirements for WEPP modelling of direct runoff

Data Input Files	Description/Inputs	Source
Hill Slope	Representative hill slope profiles; orientation, length steepness	20 m contours from 1:50000 topographical maps. http://www.freshmap.co.nz
Climate	Precipitation, temperature, solar radiation, wind using CLIGEN software.	File from Hammender (2013) based on data from National Climate Database, Okuti weather station 1 Jan 2013-30 June 2013 (6 months)
Soil	Particle size distribution, organic content, CEC[(a)], interill/rill erodibility, critical shear.	Steepland Soils from Hammender (2013) based on NZ[(b)] national soil database, spatial extension.
Land Management	Bare soil = fallow, Bedrock=pavement, Forest= 5yr perennial, Grass= permanent grass. Stocking rate =1cow/5ha, 1sheep/ha	Soil/rock % from oblique photos Forest from topographical maps Stocking rate from landowner.

(a) CEC= Cation Exchange Capacity
(b) NZ = New Zealand

Direct subsurface flow to the lake was calculated by use of a ratio of flood event surface runoff/total runoff derived for the Catons catchment. This was then applied, relative to

modelled surface runoff, to obtain direct subsurface runoff volumes for the slopes in areas 1-3 (Figure 2.1).

Figure 2.5 Silt runoff from 'direct runoff area 1' (see Figure 2.1) after a flood event in April 2014.

2.2.3.3 Groundwater

The lake catchment has limited groundwater storage capacity and no data is available on groundwater movements within these areas. Inputs to storage area "A" were estimated as direct runoff from area 3 (Figure 2.1), derived as described above. All of this runoff was assumed to enter the lake via groundwater, with no change in groundwater storage. A groundwater storage area also exists at the north-east end of the lake, however inputs to this area are considered to have been captured by flow data at the Okana and Okuti gauging sites which are upstream.

Seepage rates into the gravels of the accreted beach barrier at the southern end of the lake are poorly constrained with no direct measurement available. A lake water-balance approach was undertaken to estimate these rates using monitored lake levels, measured and modelled inflows, and direct rainfall to the lake. Outflows were calculated as described below (Section 2.2.3.5) and evaporation was calculated as a function of wind speed and air vapour pressure from the daily average evaporative heat flux (Fischer et al, 1979). A relationship between seepage and lake level was developed iteratively to reduce the difference between lake volumes predicted by the pre-seepage water balance and

actual lake volumes (Figure 2.6). The relationship (Daily Seep Rate (m^3) = 31022 x lake level (masl) - 1551.1) was assumed to be linear based on a well constrained rating curve (Horrell, 1992) across a similar beach barrier in the neighbouring Lake Ellesmere (Figure 1.2). A Nash-Sutcliffe model efficiency coefficient, E = 0.93 was calculated for the fit of water balance lake levels to observed lake levels. This indicates an excellent fit between observed and modelled data.

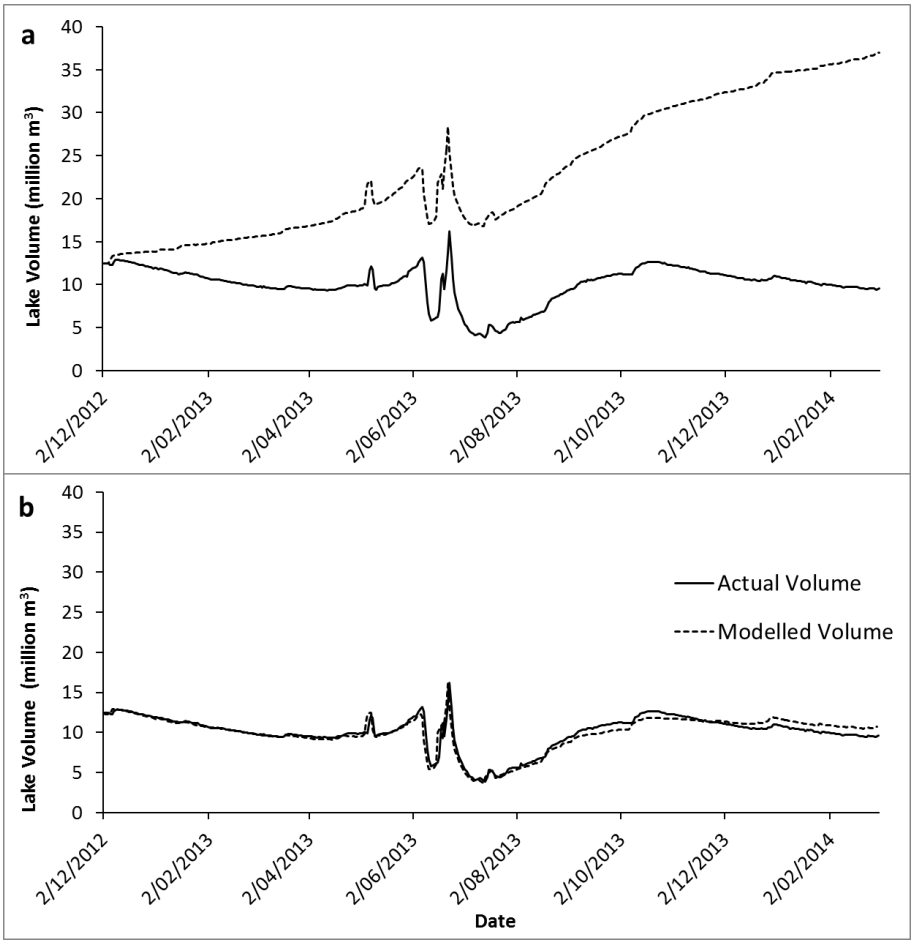

Figure 2.6 Lake volumes for Wairewa showing actual lake volumes and lake volumes calculated by water balance modelling using calculated inflows and outflows. a. Water balance before barrier seepage calculation. b. Water balance after barrier seepage calculations

2.2.3.4 Rainfall Direct

The volume of rain falling directly on the lake was calculated from lake area and rainfall data from the Okuti weather station (Figure 2.1).

2.2.3.5 Lake volume and outflows

Fifteen minute lake level data for Wairewa is recorded by Environment Canterbury. A relationship between lake level (masl) and lake volume (m^3) has been determined by Christchurch City Council (G Harrington, *pers comm*), as;

$$\text{Volume} = 684034x^2 + 4000000x - 211747 \text{ (where x=level in masl)} \quad \text{(eq 2.2)}$$

Changes in level and hence volume during artificial opening events, were used in this research to quantify the volume lost during the openings. Estimates of seepage across the beach barrier were subtracted from the volume lost, to obtain the volume lost due to the artificial opening.

2.2.4 Chemical analysis of P concentrations

2.2.4.1 Water

Water samples were collected in new 50 ml polypropylene centrifuge tubes, and transported on ice to the laboratory where they were frozen until analysis. Filtration of dissolved reactive P (DRP) samples was undertaken on-site through 0.45 µm MF-Millipore filters.

DRP was analysed by UV/visible spectrophotometric analysis using the Ascorbic Acid method (APHA 4500-P Method E). Total P (TP) was analysed by the same method after a persulphate digestion (APHA 4500-P Method B5) of unfiltered samples. The limit of detection was 0.002 $mg.L^{-1}$.

Stream sampling was planned and undertaken in order to sample seasonal, flow and hydrograph (rising and falling limbs) variability in P concentrations. Regular monitoring sampling was not undertaken.

2.2.4.2 Sediment and pore water

Lake sediment samples were collected in 25 cm cores using a Uwitec 90 mm X 60 cm sediment corer. Three cores (19 December 2011, 17 August 2012 and 5 Mar 2013) were collected from around the area indicated in Figure 2.1 for P analysis and P mass calculations. Cores were sectioned (1-5 cm = 1 cm increments, 5-15 cm = 2 cm increments, 15-25 cm = 5 cm increments), and samples transferred to new 50ml polypropylene centrifuge tubes for transport, on ice, to the laboratory. Pore water was

then immediately separated from the sediment by centrifuging at 4000 rpm for 40 mins, filtered through 0.45 µm Millipore membrane filters and frozen until analysis. As volumes were generally too small for analysis by spectrophotometry, the pore water samples were analysed for dissolved phosphorus by inductively-coupled plasma optical emission spectrometry (ICP-OES) at the Department of Soil and Physical Sciences, Lincoln University, New Zealand. The limit of quantitation for P on this instrument was 0.00455 mg/L^{-1}.

The sediment was also frozen until analysis. A sequential chemical extraction analysis was undertaken on the thawed samples, following the scheme used by Rydin (2000). More details of the sequential extraction procedure are given in Chapter 3, Section 3.2 While individual fractions have not been reported in this Chapter, the fraction of P bound to the readily reducible oxide/hydroxide phases (BD-P, as extracted using a $Na_2S_2O_4/NaHCO_3$ leachate) has relevance here and has been used to identify reactive or mobile P within the sediment cores.

2.2.4.3 Macrophytes

The TP concentration of the macrophyte biomass was obtained for duplicate samples by igniting at 550^oC and digesting in 1M HCl, using the method of Anderson (1976), followed by UV/visible spectrophotometric analysis for P, using the Ascorbic Acid method (APHA 4500-P Method E). Macrophyte sampling methods are discussed in Section 2.2.6.3

2.2.5 Mass calculations; P loads

2.2.5.1 Stream inflows

The mass of P (load) transported to the lake by stream flows was derived by multiplying the volume of water inflows by stream P concentrations. Stream P concentrations for all flows were derived from relationships established between sampled stream water P concentrations and simultaneous stream discharge. A wide variety of methods for establishing these load estimation relationships exist (Quilbe et al, 2006; Letcher et al, 1999) and the most appropriate method depends on many factors, including data resolution and field data collection programme (Letcher et al, 1999). Despite the relatively small number of samples used for this study, the sampling programme was designed to span seasons, flows, and differing parts of the hydrograph. As such, the

sampling programme was designed to enable the use of a ratings curve approach to load estimation. The ratings curve method is based on the extrapolation of contaminant concentrations over the time period of interest by developing a regression relationship between concentration and flow. Such extrapolations commonly use a power function relationship (e.g. Asselman, 2000; Quilbe et al, 2006; Diffuse Sources/NIWA, 2012) and a range of flow conditions must be sampled for this approach to be valid (Quilbe et al, 2006). The regression relationships used in this study are referred to here as 'load curves' (Figure 2.7) and take the form of power functions (Figure 2.7 and Table 2.2). Loads for flows above the maximum gauged flows, were derived by extrapolation of these power relationships. Nash –Sutcliffe model efficiency coefficients (E) were calculated to evaluate the fit of the load curves to measured concentration data (Table 2.2) and indicated very good model predictions. While a relatively small number of samples were used to derive the respective E coefficients, a further measure of the validity of the estimated loads was provided by comparison with mass of P residing in the lake sediment reservoir and known sedimentation rates for the lake (see Section 2.3.1.1). These comparisons also indicated that the estimations of load used here are appropriate. All the stream water samples used in load estimations were collected and analysed by the author.

The use of the ratings curve approach also allows data to be stratified to develop multiple relationships, for a single stream (Lechter et al, 1999). For the Okana and Okuti rivers, different load curves were evident between summer and winter, with summer TP concentrations being higher (for similar flows) than those in winter, particularly for the Okuti River (Figure 2.7). For the smaller tributary of Catons Stream there was either no difference between summer and winter TP concentrations, or there was not enough data to differentiate. Rather the stream data was stratified by flow with different power relationships above and below Q=0.16 m^3/s^{-1} (Table 2.2). These different load curves were used to calculate TP loads for the Okana and Okuti Rivers and Catons Stream.

Summer low flows ($Q < 0.55\ m^3.s^{-1}$) for the Okana and Okuti Rivers showed considerable scatter for TP, possibly reflecting prolonged periods of low flow with occasional short term and small, increases in flow i.e. low flow 'fresh' events, while in the L1 and L2 tributaries TP sampling data was insufficiently spread to allow a ratings curve approach. For all streams, DRP was poorly correlated with flow. For all of these, a mean TP or DRP concentration was used in an averaging estimator approach to load estimation (Tables 2.2

and 2.3) whereby continuous stream discharges were multiplied by the mean phosphorus concentrations (Degens & Donohue, 2002).

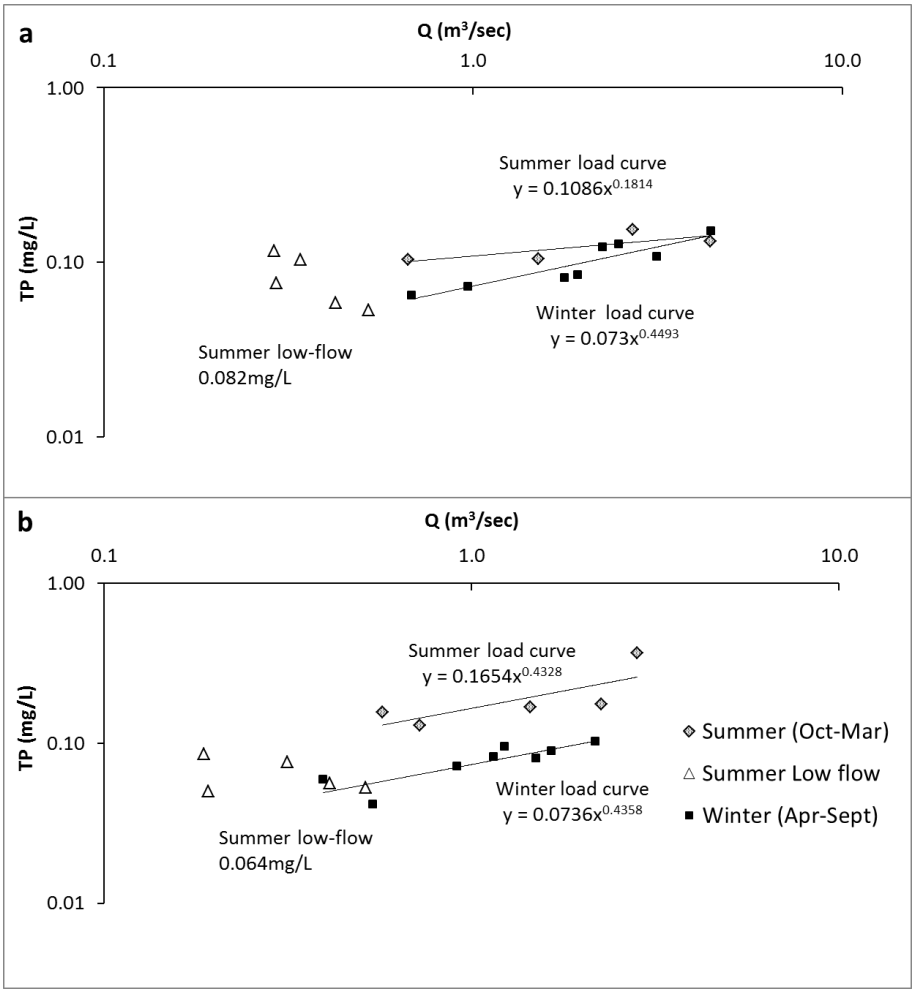

Figure 2.7 Discharge (Q) vs TP concentration plots for the Okana River (a) and the Okuti River (b), Wairewa's main tributaries, with summer and winter TP load curves indicated.

The level loggers for L1 and L2 streams were not in place for the entire period (15 months) and hence continuous flow data for L1 and L2 streams was limited to 10.5 months. In order to gain estimated TP and DRP loads for the entire period, multipliers were applied based on relative 15 month load/10.5 month load for adjacent catchments (Table 2.4). The load delivered to the lake by Stream L3 (Figure 2.1) was assumed to be L2 x 1.067 based on relative catchment sizes and very similar aspect, vegetation cover and topography.

Table 2.2 Total phosphorus load estimation; method, relationships and model fit. TP= total phosphorus concentration (mg.L^{-1}), Q=stream flow (m^3.s^{-1}), r^2= regression coefficient, E= Nash-Sutcliffe Model efficiency coefficient, SD= standard deviation

Rating Curve Approach				
Stream	Stratification	Regression Equation	r^2	E
Okana	Summer Q>0.55	TP=0.1086 x $Q^{0.1814}$	0.59	0.53
	Winter	TP=0.073 x $Q^{0.4493}$	0.83	0.82
Okuti	Summer Q>0.55	TP=0.1654 x $Q^{0.4328}$	0.57	0.53
	Winter	TP=0.0736 x $Q^{0.4358}$	0.73	0.78
Catons Stream	Q>0.16	TP=0.1571 x $Q^{0.2107}$	0.91	0.97
	Q<0.16	TP=0.0986 x $Q^{0.0746}$	0.44	0.84

Averaging Estimator Approach			
Stream	Stratification	Mean TP	SD
Okana	Summer Q<0.55	0.082	0.028
Okuti	Summer Q<0.55	0.064	0.016
L1	All season, all flow	0.091	0.024
L2	All season, all flow	0.099	0.012

Table 2.3 DRP Load Estimation; Mean flow-specific and seasonal DRP concentrations utilised in P load calculations as well as standard deviations (SD).

Stream	**DRP (mg.L^{-1}) Summer Average**				**DRP (mg.L^{-1}) Winter Average**	
	Q<0.55 m^3.s^{-1}		**Q>0.55 m^3.s^{-1}**			
	Mean	SD	Mean	SD	Mean	SD
Okana River	0.029	0.016	0.038	0.006	0.025	0.004
Okuti River	0.030	0.012	0.046	0.016	0.023	0.008
	All Season Mean				**SD**	
Catons Stream	0.022				0.012	
L1	0.031				0.003	
L2	0.049				0.011	

2.2.5.2 Direct runoff inflows

A range of TP and DRP loads were calculated for direct surface runoff. An upper estimate was based on the average concentrations (TP=0.463 mg.L^{-1}, DRP=0.109 mg.L^{-1}) from five samples of direct runoff collected immediately after three separate rainfall events, as well as ten samples analysed from rainfall simulation experiments (Miller, 2013). These

concentrations were likely to represent high intensity runoff at, or near, runoff peaks. A lower estimate was derived from the average TP and DRP concentrations (0.138 $mg.L^{-1}$ and 0.037 $mg.L^{-1}$ respectively) calculated for Catons Stream during a high rain fall event (June 2013). The mass of P transported to the lake by direct surface runoff was derived from the volume of water inflows and the concentrations discussed here. As the estimate of direct runoff water volume was based on WEPP modelling (with a 6 month climate database, Jan- June 2013), a multiplier was applied to estimate the TP load over the total 15 month period based on relative 6 and 15 months loads exported by Catons Stream (Table 2.4). Loads for direct subsurface flow were based on measured P concentrations in adjacent catchments i.e. loads from area 1 (Figure 2.1) were calculated from mean DRP concentrations for L2, while area 2 subsurface loads were calculated from the mean DRP for Catons Stream (Table 2.3). The mass of P transported to the lake by direct subsurface runoff was derived from the volume of subsurface water inflows and the concentrations discussed here.

2.2.5.3 Groundwater inflows

Groundwater P concentrations were not available from catchment aquifers, however a single sample was obtained from water seeping from subsoil after a rainfall event in August 2012. The DRP concentration (0.007 $mg.L^{-1}$) obtained for this sample was used to calculate a lower estimate of the P load entering the lake from groundwater area 'A' (Figure 2.1). The average DRP concentration for Catons Culvert (Table 2.3) was used to calculate an upper estimate for groundwater load. The mass of P transported to the lake by groundwater was derived from the volume of water inflows and the concentrations discussed here. As with the direct runoff, a multiplier was used to gain an estimate of the DRP load over the total period (Table 2.4).

Table 2.4 Multipliers used to convert loads from a partial period to the full study period (15 months). CS= Catons Stream, OR = Okuti River, mo= month.

Load Source	Multiplier Equation	Multiplier
Direct Runoff	= CS load (15mo)/CS load (6mo)	TP =1.15
		DRP =1.24
Groundwater	= CS load (15mo)/CS load (6mo)	DRP =1.24
L1 & L2 streams	= OR load (15mo)/OR load (10.5mo)	TP =1.23
		DRP =1.24

2.2.5.4 Rainfall direct

The deposition of P to the lake from rainfall was calculated as the product of rainfall volume reaching the lake directly and the concentration of P in the rainfall. Rainfall P concentrations were not measured as part of this study and data is very sparse for the east coast of the South Island of New Zealand. Larned and Schallenberg (2006) report the results of five rainfall samples taken from three different localities around nearby Lake Ellesmere. An average total dissolved P concentration of 0.009 $mg.L^{-1}$ was reported and is used here to calculate rainfall deposition.

2.2.5.5 Lake opening outflows

Lake water P concentrations, used to calculate the P removed from the lake by outflow, were derived from water monitoring data from the regional council (S. Barbour, ECan, *pers comm).*

Three artificial lake openings occurred during the research period. The first opening was over the period 10-11 May, 2013. TP (0.034 $mg.L^{-1}$) and DRP (0.017 $mg.L^{-1}$) concentrations were used from ECan's lake monitoring (14 May 2013) to calculate P outflow. The second opening was for the period, 8-12 June 2013. TP (0.048 $mg.L^{-1}$) and DRP (0.005 $mg.L^{-1}$) concentrations were used from ECan's lake monitoring (10 June 2013) to calculate P outflow. The third opening was over the period 18 June -21 July 2013. TP (0.076 $mg.L^{-1}$) and DRP (0.031 $mg.L^{-1}$) concentrations were used from Ecan's lake monitoring (8 July 2013) to calculate P outflow. The mass of P lost from the lake due to lake openings was derived by multiplying the volume of water outflows by the concentrations discussed here.

2.2.5.6 Beach barrier seepage outflows

A range of P removed from the lake by seepage through the beach barrier was calculated by using the mean and median DRP concentrations for the lake over the study period (Table 2.5). The mean gave an upper load estimate, while the median gave a lower load estimate. Beach barrier seepage was calculated only for dissolved P, as most particulate-bound P will be filtered out by passage through the lake sediment and the substrate of the beach barrier. The mass of P lost from the lake due to beach barrier seepage was derived by multiplying the volume of seepage outflows by the concentrations discussed here.

Table 2.5 Key statistics in for Wairewa Water Quality over the research period, from monitoring sampling by Environment Canterbury and analyses by the authors. Concentrations are in $mg.L^{-1}$.

	TP	DRP
Max	0.191	0.039
Mean	0.085	0.010
SD[(a)]	0.033	0.010
Median	0.082	0.005
Min	0.034	0.001
n	41	41

(a) SD= standard deviation

2.2.6 Mass calculations; P reservoirs

2.2.6.1 Lake water column

The mass of P contained in the lake water column was derived from lake volume and TP concentrations observed in the lake. Maximum and minimum concentrations (Table 2.5) during the 15 month research period were used to provide the range of figures in Table 2.8. Concentrations were derived from samples collected and analysed by the authors and from water monitoring data from Environment Canterbury (S. Barbour, *pers comm).* Changes between sampling dates in the calculated mass of P, net of inflow and outflow P loads, were used to indicate fluxes between sediment and the water column.

2.2.6.2 Sediment

Total P concentrations in the sediment derived by summation of all fraction concentrations targeted by the sequential extractions, were used along with sediment density figures obtained from sediment cores, and lake area, to calculate the total P reservoir in the lake sediments to a depth of 25 cm. Sediment pore water was treated as a separate reservoir based on analysed concentrations and sediment densities (Table 2.8). Lake area was calculated from lake levels by the relationship determined by the Christchurch City Council (G. Harrington, *pers comm)* as;

$$\text{Area } (m^2) = (16.504L^3 - 128.19L^2 + 434.88L + 159.88) \times 10000 \qquad \text{(eq 2.3)}$$

(where L = level in masl)

2.2.6.3 Lake macrophytes

A macrophyte biomass survey was conducted in March 2013. Four sites in the northern half of the lake where macrophyte beds were regularly present, were surveyed by diving with a ring-net sampler of known area. Triplicate weed samples collected in the sampler at each site were weighed. Two sub-samples were transported to the laboratory for drying and TP analysis. Biomass results from the diving survey were combined with visual observations of macrophyte density to provide an estimate of biomass in the lake. Areas of differing density were delineated using the track function in a Garmin cx60 handheld GPS, and the area inside the tracks calculated in Freshmap® mapping software (www.freshmap.co.nz). The southern end of the lake was not surveyed, but much lower and highly variable macrophyte densities have been observed there over the period of this research. A lower estimate of biomass was obtained by assuming no macrophyte growth at the southern end of the lake, while an upper estimate was obtained by assuming equal macrophyte growth at the southern and northern ends of the lake. The total P contained in the macrophyte reservoir was derived from the calculated biomass and P concentrations in that biomass. The calculated range of biomass is likely to be a maximum as macrophyte density during the sampling period was high relative to other periods.

2.2.7 Uncertainties in P load and reservoir calculations

A ± 25% uncertainty in P load calculations was assumed for all P loads in this study, based on analytical and measurement errors inherent in P concentrations and flows as determined for the Okana River. The TP concentration error of ± 15% was based on a 95% confidence interval for replicate analyses of P standards and stream water samples. The error associated with water flow was calculated by applying an 'uncertainty of measurement' analysis (0.5 x the smallest feasible measurement unit) to flows up to the highest gauged flow (4.5 $m^3.sec^{-1}$). A 95% prediction interval was then calculated and applied to flows extrapolated above 4.5 $m^3.s^{-1}$. This use of a prediction interval allows for the key assumption that the regression relationship established at low to high flows can be extrapolated to very high flows.

A ± 20% uncertainty is assumed for all P reservoirs in this study, based on a 95% confidence interval for replicate sediment extractions, testing both experimental uncertainty and variability between sediment samples taken in close proximity. This

uncertainty allows for the assumption that the analysed sediment P concentrations are representative across the lake bed.

2.3 Results

2.3.1 P load transported to the lake

2.3.1.1 Streams (S_{in})

Table 2.6 presents the results of P loads transported to the lake as calculated from the load estimation methods. Just under 9000 kg of P were transported into the lake over the 15 month study period. Table 2.6 also presents the P loads delivered by significant flood events during this period.

Table 2.6 also presents the P loads delivered as TP, particulate P (the difference between TP and DRP) and DRP. Overall 81% of the P load transported to the lake by streams is associated with particulate material.

Table 2.6 TP and DRP loads delivered to Wairewa by stream flows, direct runoff, ground water and rainfall over the 15 month research period. The flood events in columns 4 and 5 are the 1 and 5 events respectively, which transported the greatest amount of P during the period.

Source	TP load (kg)	% of total catchment TP load	% of source TP load in one flood	% of source TP load in five floods	DRP load (kg)	% of source TP load as Particulate P	% of source TP load as DRP
Okana River	6202	68	71	80	1010	84	16
Okuti River	2295	25	46	64	632	74	26
Catons Stream	277	3	54	86	39	86	14
L1 Stream	58	0.63	42	48	20	66	34
L2 Stream	30	0.33	63	69	15	50	50
L3 Stream	32	0.32	63	69	16	50	50
Total Stream	8894	97	63	75	1732	81	19
Direct Runoff	148	1.6	42	-	60	59	41
Ground water	11	<0.1	-	-	11	0	100
Rainfall Direct	88	0.96	-	-	-	-	-
Total Catchment	9141	100	61	73	1803	80	20

The Okana River delivered the greatest P load to the lake, with over 70% of this delivered in a single flood event (June 2013). The Okana and Okuti Rivers together transported 93% of the catchment TP load, with 60% transported by these two rivers in the June 2013 flood event alone. 15 min loads and cumulative loads for Okana and Okuti Rivers (Figure 2.8), confirm the importance of flood events on the delivery of P to the lake. Even these P load values are likely to underestimate the importance of such events, because in the June 2013 flood event, water levels overtopped the level loggers and hence estimated flows reflect the highest reading of the level logger rather than the actual water level. The Okana River level logger was overtopped for approximately 24 hrs and the Okuti River level logger was overtopped for approximately 5 hrs.

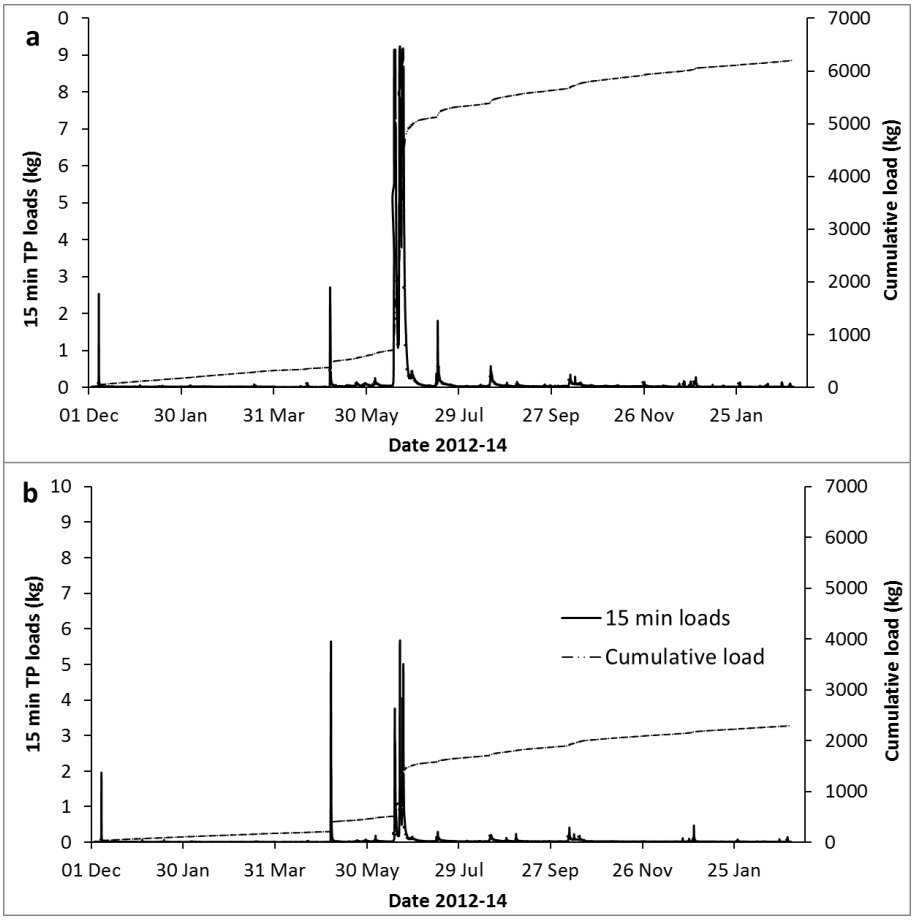

Figure 2.8 15 minute and cumulative TP loads for the Okana River (a) and the Okuti River (b), the two main tributaries of Wairewa.

The external P loads calculated by the mass balance approach utilised in this study appear reasonable based on flow regimes, sedimentation rates and the mass of P in the lake sediments. Table 2.7 presents flow statistics for the Huka Huka long term flow gauge site

for the ten years, 2004-2013, which indicated that the 2013 flow regime was very close to the annual average for the decade. The mean, median and 75th and 25th percentile flows in 2013 were close to the ten year averages. The twelve months of 2013, comprises the main time component of the 15 month research period, and included almost all the major loading events of the period (Figure 2.8), hence the flow regimes over the research period appear to be representative of catchment averages.

Table 2.7 Flow statistics (l.s^{-1}) from the long term flow gauge on the Huka Huka stream tributary of the Okana River.

	2004	2005	2006	2007	2008	2009	2010	2011	2012	2013	Mean	SD
Max	4890	1632	5127	1080	3776	2193	3409	5296	12120	5051	4457	3100
75th	178	155	151	151	243	199	307	171	166	202	192	49
Mean	184	143	270	131	251	187	253	169	253	209	205	50
Median	78	98	127	87	85	90	100	117	107	98	99	15
25th	44	55	63	57	49	47	38	72	70	52	55	11
Min	18	34	24	44	29	24	25	48	53	41	34	12

The Nash-Sutcliffe model efficiency coefficients (Table 2.2) indicated that the regression relationships utilised to calculate load estimations for the main tributaries are a good fit to the observed data. However, although the sampling was undertaken to target a wide range of flows, these relationships are based on a relatively small number of observations, and validation of the loads delivered to the lake was also sought by comparison with the sediment P reservoir and sedimentation rates. Two estimates of sedimentation rates for Wairewa were available. Woodward & Shulmeister (2005) derived an average rate of 2.7 mm.yr^{-1} since 1895 based on pollen dating of sediment cores, while Painter (2014) derived a rate of 2 mm.yr^{-1} based on sediment yields from the Huka Huka catchment. Using these two sedimentation rates and the annual mass of P retained in the lake as ascertained by this research, the top 10 cm of lake-wide sediment should contain a P mass of 1.88 and 2.54 t, respectively. The average top 10 cm sediment P reservoir as analysed in the lake (Table 2.8) contained 2.1 t which gave a sedimentation rate of 2.4 mm.yr^{-1} The close agreement of the annual P load retained in the lake with the P mass contained in the sediment reservoir, and hence the agreement of the calculated sedimentation rate with previous sedimentation estimates confirmed that the P loads calculated in this study are reasonable

The importance of flood events in P transport is evident from Table 2.6. The hydrograph for the research period is presented in Figure 2.9 along with the key statistics for the main flood events. The dominance of the June 2013 flood event is evident is both plots, and the amount of P transported in single large events (Table 2.6) is an important research finding in terms of management responses. The average recurrence interval of the flood on which this finding is based is therefore of importance. The average recurrence interval of the June 2013 event has been calculated at 1.6 years by ECan (T Davie, ECan, *pers comm*). It is apparent then that the June 2013 event was not exceptional and that the importance of large flood events for P loading in the catchment, reported in this study, is valid.

2.3.1.2 Direct runoff (DR_{in})

Direct runoff transported an estimated TP load of 148-403 kg to the lake over the 15 months. The upper estimate for these loads was derived from runoff samples collected during or immediately after high intensity rainfall events. The WEPP model used to predict runoff, appeared to over-predict runoff intensity, but more accurately predicted total runoff volumes over the longer time frames taken to return to pre-flood levels. Hence the lower estimate for the load was considered more realistic as it was derived from an average concentration for Catons Stream discharge over a longer time frame flood event (June 2013). This lower estimate was therefore used in Table 2.8 which illustrates the insignificance of the direct runoff loads relative to stream loads. The lower direct runoff P load estimate was also used in the P budget (Section 2.3.3).

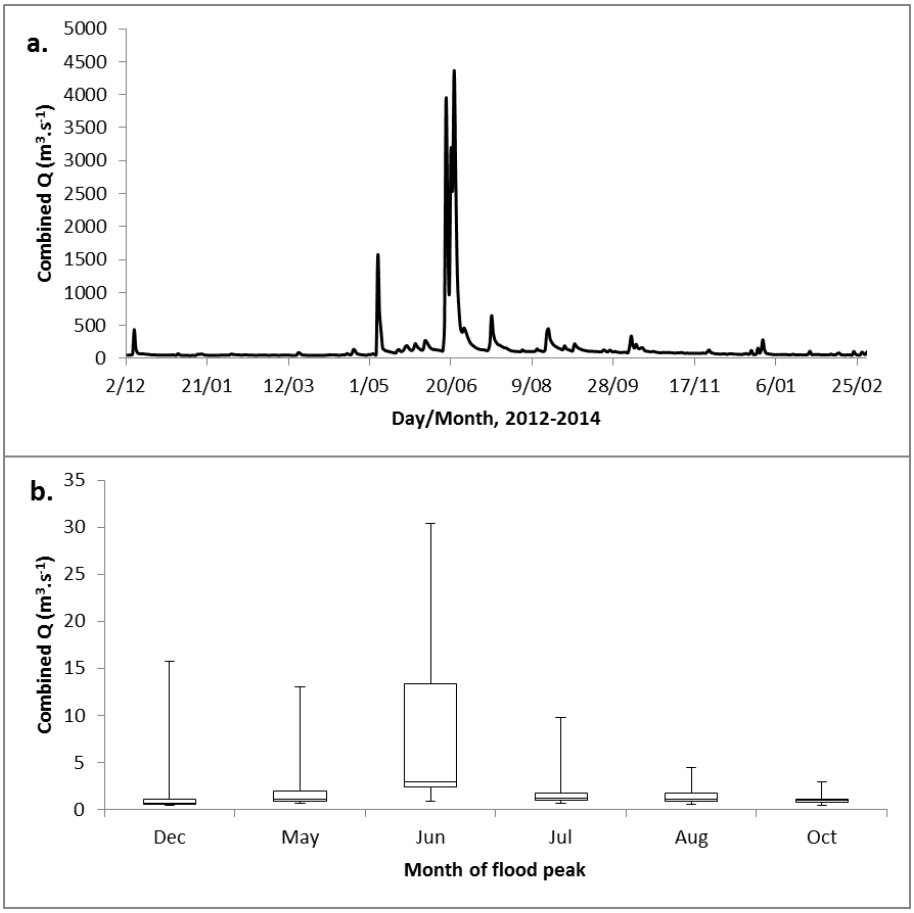

Figure 2.9 (a). The combined Okana and Okuti River hydrograph for the research period. (b). Box and whisker plots for the six largest flood events (by peak flow) in the research period, showing combined Okana and Okuti flow maximum, minimum, 75th and 25th percentile and median flows. The December 2012 event, while having a large peak flow, was very short lived and in terms of P load was smaller than the October 2013 event. Hence the December event is not included in the five flood events of Table 2.6.

2.3.1.3 Groundwater (GW_{in})

The calculated load to the lake from the groundwater storage area "A" (Figure 2.1) was 7-15 kg and a mid-range value was used in the P budget (Section 2.3.3). Table 2.8 illustrates the low inflow of P to Wairewa from groundwater relative to inflows from streams.

2.3.1.4 Rainfall direct (RD_{in})

Direct rainfall is estimated to have delivered 88 kg of P to the lake over the 15 month period. This was based on a 'total dissolved P' sample analysis (Larned & Schallenberg, 2006) so does not include particulate material. In addition dry deposition of wind blown particulates cannot be estimated from available data.

2.3.2 P load transported from the lake (S_{out} and GW_{out})

A total P load of 2580 kg was calculated to have been transported out of the lake during the artificial opening events that occurred over the 15 months. Of this, 957 kg (35%) was transported as DRP. The initial 2 day opening event (10-11 May) transported a TP load of 106 kg (DRP= 38 kg), the second opening (8-12 June) transported a TP load of 346 kg (DRP=36 kg) and the final opening (18 June- 14 July) transported a TP load of 2128 kg (DRP=868 kg).

Seepage through the beach barrier transported 142-261 kg of P out of the lake during the 15 months, all of which was assumed to be DRP. A mid-range figure is used in Table 2.8 and Figure 2.12.

Hence, of the total outflow P load of 2782 kg, 93% was via the artificial lake opening events.

2.3.3 P budget and reservoirs

Inflow and outflow P loads over the 15 months, showed that approximately 6355 kg of P were retained in the lake over this period (Table 2.8).

The highest and lowest concentrations of TP recorded in the lake during the period of this research were 0.191 $mg.L^{-1}$ (10 April 2013) and 0.034 $mg.L^{-1}$ (sampled and analysed by ECan, 14 May 2013) respectively. These analyses illustrated the temporal variability which occured in the lake and were used, in conjunction with lake level at the time of analysis, to calculate the range of TP in the lake water-column reservoir (Table 2.8). The sediment and pore water P ranges in Table 2.8, were based on the maximum and minimum P concentrations, measured in three sediment cores, taken at different times.

The lake sediment constitutes a very large reservoir of P, relative to the water column or macrophytes. The sediment depth intervals shown in Table 2.8 were selected based on relative P enrichment and mobility, as observed in the cores (refer to Chapter 3). Analysis of core profiles showed that the top 5 cm of the sediment is enriched in P relative to the deeper sediments, on a mass per dry weight basis. Comparison between summer and winter cores also showed that P in the upper 10 cm appeared to be more mobile than in deeper sediments (refer to Chapter 3, Figures 3.27 and 3.28). At a depth of >10-15 cm the sediment P appeared to be relatively immobile. Further work conducted to more fully

understand the dynamics of P in the sediment reservoir is presented in Chapters 3, 4 and 5.

Table 2.8 The P budget for the 15 month study period and the P reservoirs in the lake. The % shown for the sediment reservoirs, is the % of the total 0-25 cm sediment P reservoir. Sediment pore water is from depths of 0-25 cm. The range given for P reservoirs is for high and low estimates.

P Budget		P Reservoirs	
Budget Component	**Total P (kg)**	**Reservoir**	**Total P (kg)**
S_{in} Stream flow	8894	Lake water column	140-2470
DR_{in} Direct Runoff	148	Macrophytes	100-150
GW_{in} Groundwater flow	7	Sediment; Pore water	245-1660
RD_{in} Rainfall Direct	88	Sediment; 0-5cm	92600-118300 (18-20%)
S_{out} Lake opening	2580	Sediment; 0-10cm	182500-244200 (36-41%)
GW_{out} Beach Barrier Seep	200	Sediment; 0-25cm	502000-600400 (100%)
ΔP retained in lake	6357		

2.3.4 P variations in the lake

Increases in the mass of P in the water column reservoir between lake sampling dates, minus the mass of P delivered as external loads, were used to estimate fluxes from the sediment to the water column. The total flux over the period of study was 2214 kg P, approximately 25% as compared to the total external load. When only the summer, low stream-flow, months were considered, the internal sediment to water column flux was 1632 kg compared to 1289 kg transported to the lake from the catchment. This summer internal flux calculated by mass balance, occurred over a sum of 79 days, providing a flux rate of 3.26 $mg.m^{-2}.day^{-1}$. This rate and the total load is a minimum due to the low frequency of sampling (between weekly and monthly).

Figure 2.11a provides insight into the internal flux over a shorter time period and illustrates a period of time (5 March- 10 April 2013) during which the water column TP concentration varied significantly and was associated with algal bloom formation.

Chlorophyll-*a* concentration increased over this time by 17x (0.008-0.141 mg.L^{-1}). The TP concentration increased over the period by 0.077 mg.L^{-1}, an increase of 100%. This was a period of low stream flows in the catchment, when the maximum possible increase in lake TP concentration from external loading alone was 0.011 mg.L^{-1}, an increase of only 15%. Hence the TP concentration increase exceeded that which could be explained by external loading, confirming that internal loading from lake sediment was a major source of P to the water column during periods of algal bloom formation. Figure 2.11b illustrates the maximum relative contribution of internal and external P loads to changes in the water column TP reservoir, again showing that external loads played a minor role in the TP increase during a period of algal bloom formation.

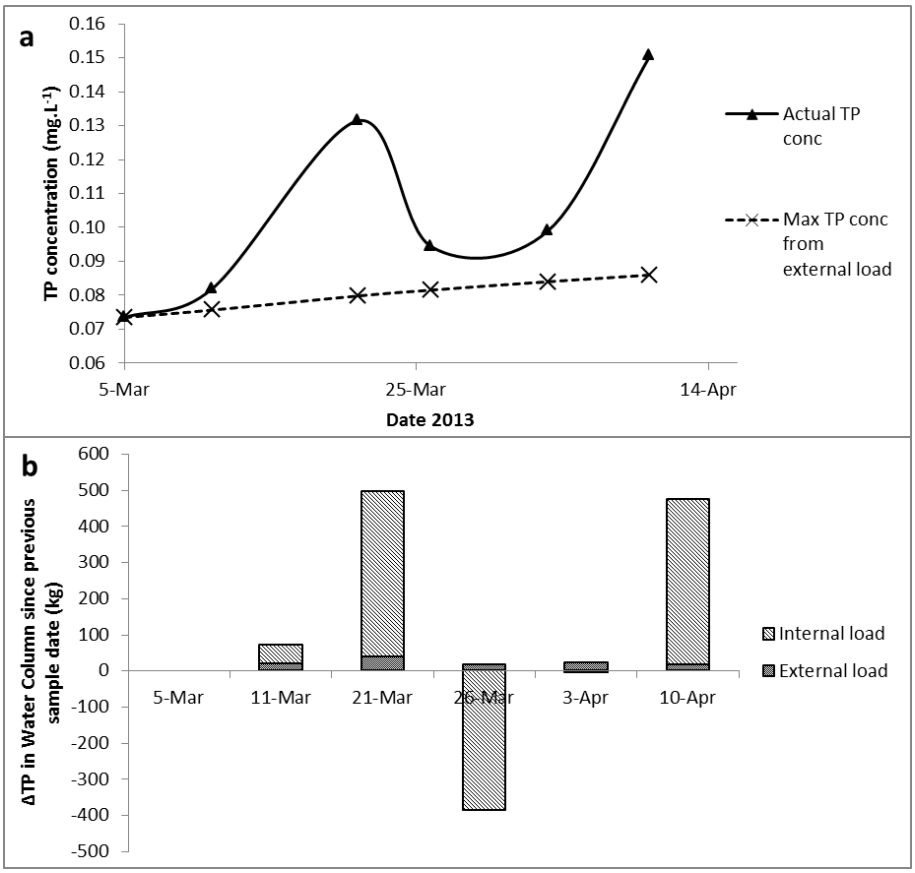

Figure 2.11 Changes in water column TP in Wairewa. a- Actual TP concentrations observed in the lake water column are compared with the maximum concentrations that would result from external loads. b- Changes in the water column TP reservoir since the previous sampling date, showing both external and internal load contributions

The flux from the sediment to the water column over the period 3-10 April was at least 10.6 mg.m^{-2}.day^{-1}. Again this rate was a minimum, due to the infrequent sampling. The mass balance approach also does not take into account potential water column variability.

During a large flood event between 10 June and 8 July 2013, >5450 kg of P was transported to the lake from the Okana and Okuti catchments, and 2150 kg was transported out of the lake during artificial openings. More than 3300 kg was therefore retained in the lake. Lake water analysis on those dates showed a net change of -31 kg within the lake water column. Hence a minimum flux from the water column to the sediment of 18 $mg.m^{-2}.day^{-1}$ was required between these dates.

2.4 Discussion

2.4.1 The P budget: External P loads

The annual P budget for Wairewa (Figure 2.12) illustrates the dominance of stream flows (97%) on external P loading in the lake. The two largest lake tributaries, the Okana and Okuti rivers provided the vast majority of the external load with the Okana River alone transporting 68% of the lake's total annual, external P load. The ephemeral streams (Catons, L1, L2 and L3 streams) were much less significant, transporting less than 5% of the total annual load. Direct runoff inputs from the steep slopes on the south-east and north-west sides of the lake comprised < 2% of P loads to the lake. As expected calculated groundwater contributions to P loads were very small (0.1%). No direct measurement of groundwater movements or P concentrations were available, however the limited size of the potential groundwater storage areas, the modelled recharge volumes of area "A", the affinity of particulate material for P, and the very small effect that the beach barrier seepage had on the budget (3% of stream inflow), indicated that the contribution of ground water to the budget was likely to be very small.

With no natural outlet, limited seepage outflows across the beach barrier and infrequent artificial openings, the calculated hydraulic retention in the lake was relatively high (0.15yr, based on average annual lake volume/total inflows). This retention rate is in the upper end of the range in 18 shallow coastal lakes, elsewhere in the South Island of New Zealand, studied by Kelly et al (2013), which have a median hydraulic retention time, calculated by the same method, of 0.08 yrs. Consequently the flushing rate in Wairewa is low and the retention of P in the lake system is very high (70% of inflows). This P retention coefficient (R_p) of 0.7 is at the higher end of published data. Kelly et al (2013) reported modelled R_p values of between -0.7 and 0.85 with median and means of 0.46 and 0.26 respectively for 19 shallow coastal lakes in Southland, New Zealand. Similarly Kiov

et al (2013) report median and mean R_p values of 0.5 and 0.46 respectively for 54 lakes and reservoirs worldwide.

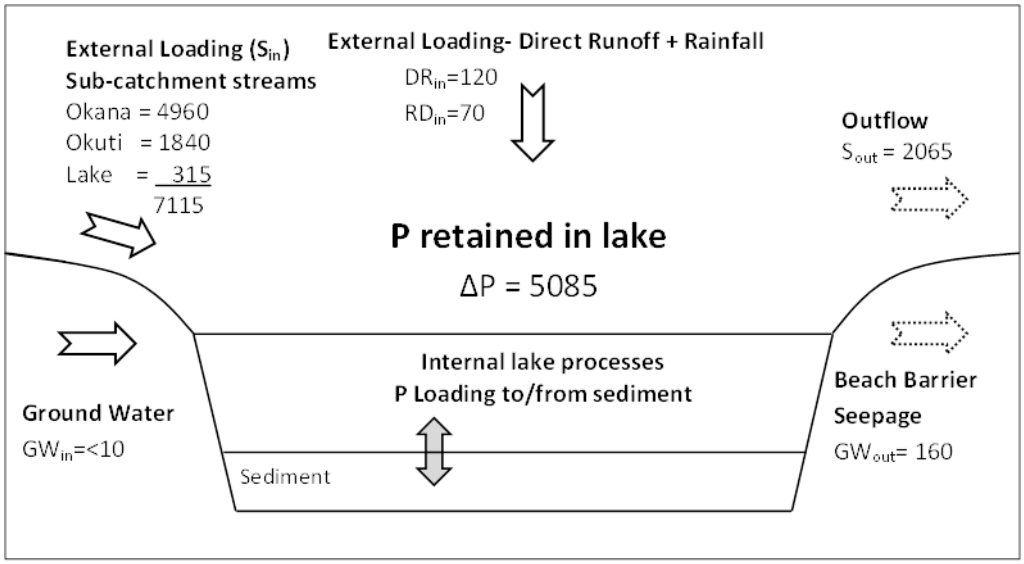

Figure 2.12 An annual P budget for Wairewa. Loads are in kg. The 'Lake' sub-catchment includes Catons, L1, L2 and L3 streams.

The areal P load to Wairewa was 3.16 $mg.m^{-2}.d^{-1}$, based on total annual catchment load. In a review of 57 intermittently open and closed lakes and coastal lagoons (ICOLLs), in New South Wales, Australia, Scanes (2012) concluded that an areal P load of >1.6 $mg.m^{-2}.d^{-1}$ was characteristic of lakes with less than 'moderate environmental quality'. Subsequently an upper areal P load limit of 1.5 $mg.m^{-2}.d^{-1}$ has been suggested for Waituna Lagoon in Southland, New Zealand, as well as for New Zealand ICOLLs in general (Wriggle, 2012). Waituna Lagoon, which is currently declining in environmental condition has an areal P load of around 2 $mg.m^{-2}.d^{-1}$. It is apparent then that the areal P load to the Wairewa ICOLL is well above levels considered appropriate for the maintenance of environmental conditions. A P load reduction of 3840 $kg.yr^{-1}$ (53%), is required to reach the suggested ICOLL guideline. The effect of catchment characteristics on areal P loads was evident in a comparison with the neighbouring Lake Ellesmere which has an areal P load of 0.24 $mg.m^{-2}.d^{-1}$ (derived from Larned & Schallenberg, 2006 and Horell, 1992). While Wairewa is smaller relative to its catchment size, a much higher proportion of the catchment is in hill country, facilitating higher rainfall and greater soil erosion. In addition its soils are volcanically derived and high in P relative to the greywacke derived soils of the flatter Ellesmere catchment (Lynn, 2005).

2.4.1.1 The importance of flood events

The investigation of P sources in Wairewa indicated a very clear trend in the temporal distribution of P transport in the catchment. The majority of P was transported to the lake as particulate associated P during flood events (Table 2.6). Over 60% of the P load during the 15 month study period was delivered to the lake via a single flood event and >70% of the P load was transported during the five largest flood events over that period. The effect of these flood events on the TP load to the lake can be clearly seen in Figure 2.8, where the cumulative TP load transported by the Okana River increased enormously (x7) over the June 2013 flood event. The TP load in the Okuti River was not as flow sensitive as the Okana River (Table 2.6) but the majority of the load was still transported during the big flood events. These trends are similar to results seen in other studies conducted in hill-country catchments (e.g. Pionke et al, 1996). In a review of small Wisconsin catchments 50-76% of annual TP loads were associated with storm flows, with a small number of storms dominating the load (Danz et al, 2010). The strong affinity of particulate material for P and the greater erosive power of overland flow associated with low frequency, high intensity rainfall events (McDowell et al, 2004) explains the flood sensitivity of P transport in the catchment.

2.4.1.2 Critical Source Areas

The Wairewa catchment can be broken down into three distinct sub-catchments (Figure 2.1), the Okana and Okuti River sub-catchments and the 'lake' sub-catchment, which includes Catons, L1, L2 and L3 streams as well as runoff areas 1-3. Figure 2.12 presents the annual P loads from each of these sub-catchments and Table 2.9 presents the annual yields. These sub-catchment yields allowed the identification of critical sources areas (CSAs) for P loading to the lake.

The importance of the identification of CSA's as a tool for addressing the management of P related eutrophication, is well established in the literature (Meals et al, 2008; McDowell et al, 2004; Daniel et al, 1998). CSA's combine source factors, which indicate a high potential for P loss, with transport factors which transform potential loss into actual loss (Gburek et al, 2000). The Okana sub-catchment was clearly the most significant contributor to external P load to Wairewa, both in total annual load and yield. The reasons for the high yield were not investigated further but are likely to include both source

factors such as soil types and artificial P sources (fertiliser and residential impacts), and transport factors such as runoff intensity and erosion of hill slopes and stream banks. Transport factors in the form of reduced erosion due to more extensive forest cover likely explain the lower yield in the Okuti sub-catchment. The very minor role of the direct runoff and ephemeral streams of the 'lake' catchment in the annual load, and the significantly lower yield, were perhaps more surprising. At first glance the slopes adjacent to the lake, with obvious rill and sheet erosion features, seemed likely to be significant sources of soil-associated P load to the lake, however Table 2.9 clearly indicates these slopes to be of much less concern than the Okana sub-catchment. This is likely due to the rarity of erosion events resulting from the altitude and aspect of these slopes relative to prevailing weather systems, but may also reflect factors such as land use (extensive pasture cover and significant areas of native vegetation), a lack of prolonged stream-bank erosion and/or soil types.

Table 2.9 Relative TP yields from the total catchment and sub-catchments of Wairewa. The 'Lake' catchment includes Catons, L1, L2, L3 streams, direct runoff and groundwater inputs.

Catchment	Area (km^2)	Catchment yield ($kg.km^{-2}.year^{-1}$)
Total	102	71
Okana	54	91
Okuti	27	68
Lake	21	21

The catchment yields presented in Table 2.9 are high compared to those for several shallow lakes in Southland, New Zealand, where yields between 16-52.5 $kg.km^{-2}.year^{-1}$ were reported (Schallenberg & Kelly, 2012). However a review of exports from New Zealand pasture country reports yields of 30-170 $kg.km^{-2}.year^{-1}$ (Quinn & Stroud, 2002), while Young et al (1996) report yields of 50-150 $kg.km^{-2}.year^{-1}$, and 10-70 $kg.km^{-2}.year^{-1}$ for North American mixed agricultural land and south-east Australian improved pastures respectively. Hence it seems that the yields from the catchments surrounding Wairewa are high, but not unusual for agricultural watersheds.

2.4.2 P Reservoirs and internal P loading

The importance of flushing rates on P loading has been previously identified (Reitzel et al, 2005; McDowell et al, 2004; Dillon, 1975) and Wairewa's large external TP loads and the limited outflows have resulted in very high P retention in the lake. Combined with the predominance of particulate associated P in these external loads, and subsequent sedimentation in the lake, the high R_p has resulted in a large legacy reservoir of sediment associated P (Figure 2.13). Temporally variable amounts of the retained P were present in the water column and standing macrophytes, however these reservoirs were very small relative to the sediment. The enriched surface sediments and the potentially mobile nature of the P in the upper 10 cm of sediment (see Chapter 3) provide a large source for P for internal loading.

Internal P loading is common in lakes with significant sediment P reservoirs such as that seen in Wairewa (Jarvie et al, 2013; Søndergaard et al, 1999; Carpenter et al, 1998). While external loading is the ultimate source of the P in Wairewa, internal loading must be responsible for many of the short term fluctuations in water column P concentration. Summer fluxes of P from the sediment to the water column exceeded external loads. With the mass balance data, it is impossible to separate the role of sediment resuspension from the release of DRP which would be available for immediate uptake by algae. However the changes in water column TP concentration in Wairewa over the period 5 March-10 April 2013, were much greater than could be explained by external loading, and accompanied algal bloom formation. The flux from the sediment to the water column was likely to have initially been as dissolved P, and the change in water column TP was due to uptake by phytoplankton, rather than increased suspended sediment. Hence internal loading due to biogeochemical processes producing fluxes of DRP from the sedimentary P pool, were likely to be responsible for those water column TP concentration changes that are associated with cyanobacteria blooms. These processes are further explored in Chapters 3 - 6.

The calculated minimum internal P flux rate in Wairewa of 10.6 $mg.m^{-2}.day^{-1}$ for the period 3-10 April 2013, is low compared with reported rates in other lakes. Sondergard et al (1990) reported short term sediment to water column P fluxes as high as 200 $mg.m^{-2}.day^{-1}$ with a summer average of 40 $mg.m^{-2}.day^{-1}$. Reitzel et al (2005) and Burger et al (2007) have reported rates of 22-32 and 2.2-85.6 $mg.m^{-2}.day^{-1}$ respectively in

shallow lakes. The low rate reported here for Wairewa during April 2013 is likely to be an artefact of infrequent sampling and ECan monitoring data during January-February 2004 showed a flux rate of 61 $mg.m^2.d^{-1}$ based on changes in DRP in the water column. Further work refining internal loading rates in this lake is presented in Chapters 4-6.

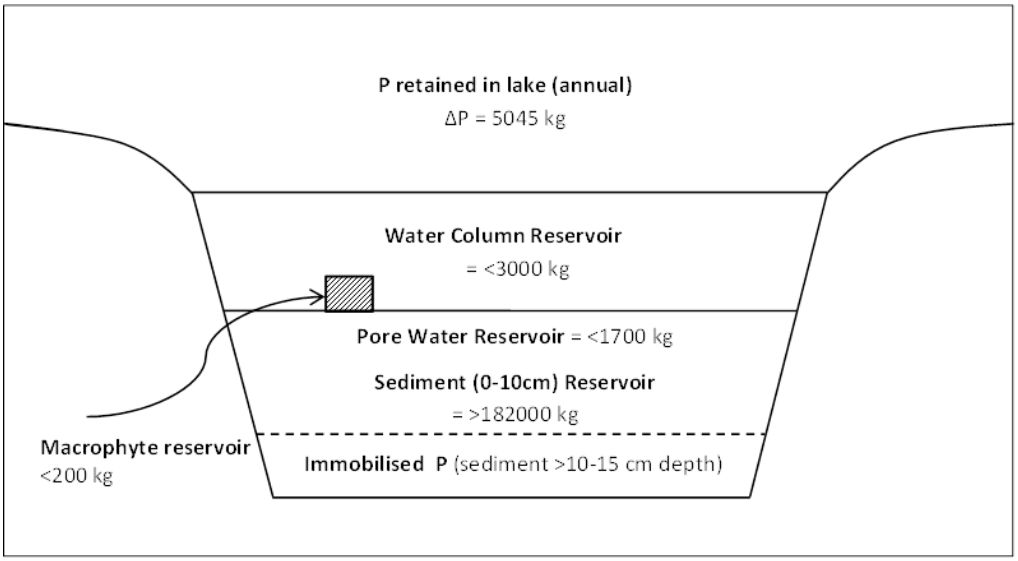

Figure 2.13 Reservoirs of P in Wairewa

2.4.2.1 Recommendations for P budgets and monitoring programmes

Development of a meaningful P budget involves the analysis of complex and dynamic hydrological and biogeochemical systems. The development of the budget presented in this study has highlighted some important parameters. Stream-flow gauging must be conducted over a long enough time frame to capture representative flow variations, and must include large flood events. The time frame required for this is likely to be catchment specific, based on the 'flashiness' of catchment streams, the return periods of large flood events and seasonal variation in P concentrations. The accuracy of any P budget will also be affected by sampling frequency, with continuous monitoring offering the most accurate results (Cassidy and Jordan, 2011). Such monitoring conducted over longer time frames and at high frequency would significantly increase the confidence in load estimations. Methodologies and instrumentation used for flow/level gauging must be sensitive enough to measure the lowest stream flows, but also capable of very high flow analysis. Significant uncertainties in the budget presented here were largely a result of our inability to gauge very high-flow flood events. Use of technology such as acoustic doppler current profilers may enable better estimates of very high flows and hence significantly reduce these uncertainties. Site selection for hydrological gauging is

important for the ability to capture these very high flow flood events and also determines the extent to which sub-catchments can be delineated. Analysis of external load P concentrations should span base flows and variable intensity flood events with flood sampling conducted on rising and falling limbs as well as the flood peaks. The intensity of sampling will depend on flood characteristics and is likely to be catchment and stream specific. Base and flood flows should be sampled over different seasons.

Accurate determination of internal loading rates by mass balance is dependent on sampling frequency in the lake water. In this study, weekly sampling over a period of significant increase in primary productivity was enough to determine the relative importance of external and internal loading however it was not enough to directly determine maximum flux rates. This is likely to require much higher frequency sampling and/or specific laboratory or lake based experiments as presented in Chapters 4 and 5.

2.5 Conclusion

The mass balance P budget presented for Wairewa identified key sources and sinks for P in this lake system. More than 9000 kg P was delivered to the lake over the research period, 68% of which came from a single critical source area, the Okana sub-catchment. P associated with suspended particulate material accounted for 80% of the external P load transported into the lake, and 61% of the load delivered over the study period was transported during a single flood event. A reduction of 53% in the external P load is necessary to achieve a recommended areal loading guideline for ICOLL's. As the lake has no permanent outflow, the high external load and low flushing rates have created a large legacy reservoir of P in the lake sediments, with 70% of external P loads retained in the lake. It is the release of this P from the lake sediments, rather than fluctuations in external loading, that control P concentrations in the lake water column during the blooms of nitrogen-fixing cyanobacteria. These key attributes of P dynamics in the lake catchment, will allow informed management decisions and direct actions to reduce P loading to the lake and subsequent lake eutrophication. The results indicate the importance for lake management purposes of targeting both external and internal P loading processes in the catchment.

2.6 Key Research Findings

- External P load >7000 $kg.yr^{-1}$
- External P load was dominated (80%) by particulate material transported during large flood events.
- The Okana sub-catchment was the dominant critical source area.
- Sub-catchment P yields ranged from 21-91 $kg.km^{-2}.y^{-1}$
- The areal P loading rate = 3.16 $mg.m^{-2}.d^{-1}$
- The average hydraulic retention time = 0.15 year.
- The P retention coefficient (R_p) = 0.7
- The sedimentation rate = 2.4 $mm.y^{-1}$
- Sediment is the dominant in-lake P reservoir.
- Internal loading > external loading during summer months.
- Internal loading provides P for uptake during algal bloom events
- A P flux, from sediment to water column, of at least 10.6 $mg.m^{-2}.d^{-1}$was observed during a seven day period of increasing [TP] in the water column.

Chapter 3: Phosphorus Binding in the Wairewa sediments

3.1 Introduction

Phosphorus (P) is essential to biological metabolic processes but is commonly the least bioavailable macronutrient in aquatic systems. P is present in igneous and sedimentary rocks and predominantly occurs as the minor but ubiquitous calcium phosphate mineral, apatite ($Ca_4(PO_4)_3(OH,Cl,F)$). Weathering of these rocks is the ultimate source of P, released as phosphates, to the global P cycle (Bengtsson and Sjoberg, 2009), where P is cycled between biotic and abiotic forms. The transfer of P between biotic and abiotic realms is bacterially mediated (Weiner, 2008) and biotic P forms often predominate in freshwater systems (Wetzel, 2001). These are present as organic molecules such as deoxyribose and ribose nucleic acids, phospholipids, nucleotide phosphates and phosphonates, as well as non-organic molecules produced by biological processes such as polyphosphate and pyrophosphates (Turner et al, 2005).

Biological uptake of P is in the form of orthophosphate (PO_4^{-3}). This may be produced initially by weathering of P minerals as discussed above, or from the mineralisation of organic forms. Either way the bioavailability of phosphate is severely restricted by its reactivity. Phosphate readily forms soluble complexes with cations (eg NaH_2PO_4), or may be precipitated as a mineral phase with Ca, Fe, Mg, Al or Mn (e.g. vivianite, $Fe_3(PO_4)_2.8H_2O$) (Moore and Reddy, 1994). In addition phosphates have a strong adsorption affinity for the surfaces of the (hydr)oxides of metals such as Fe (Wang et al, 2013), Mn (Appelo and Postma, 1999) and Al (Li et al, 2013). Metal (hydr)oxides, particularly Fe (hydr)oxides such as hydrous ferric oxide (HFO), are dominant sorbents in nature due to their wide dispersal, rapid precipitation and the ability to coat other materials (Dzombak and Morel, 1990). A general consensus about P sorption mechanisms at the surface of the metal (hydr)oxides holds that ligand exchange reactions form inner sphere complexes between phosphate and hydroxyl groups (Li et al, 2013). Such sorption is thought to occur in a two-step process with an initial rapid (minutes to hours) adsorption/desorption on particle surfaces, followed by a slower (days-months) diffusion from the surface into the interior of the particle (Froelich, 1988). Adsorption

also occurs at the surfaces of clay minerals (Froelich 1988) and organic material (Bengtsson, 2009). The availability of phosphate for biological uptake in a lake system is strongly controlled by such sorption processes (Weiner, 2008). Weakly adsorbed fractions are likely to be more mobile than strongly adsorbed or precipitated mineral forms. P weakly adsorbed to surfaces by electro-static processes may be released easily by ion exchange, while more strongly adsorbed P on metal (hydr)oxide surfaces may require competition by other ligands, or dissolution of the adsorbing surface in order to be released.

The sedimentation of organic and particulate-associated P has resulted in a large reservoir of P in the sediment of Wairewa (Chapter 2). The dominance of this sedimentary P pool and the importance of in-lake fluxes between sediment and the water column, means that understanding the partitioning of P in this sediment is key to understanding the dynamics of P in the lake system. Much research effort has been invested to analyse specific sedimentary P fractions (Bostrom et al, 1982; Condron & Newman, 2011). Simple, single reagent extraction procedures such as EDTA extractions, are commonly used by soil and sediment scientists, in particular to gain an understanding of metal adsorption in soils. (e.g. Fangueiro et al, 2002). EDTA is a chelating agent that is commonly used due to its ability to slowly dissolve metal (hydr)oxides (Chang & Matijevic, 1983; Ngwick & Sigg, 1997) and hence release adsorbed species. More complex sequential chemical extraction techniques have been favoured for P fractionation, whereby sediment is exposed to a succession of chemical reagents which are intended to target specific binding forms of P (Pettersen et al, 1988). Sequential extraction schemes used to target P cannot unambiguously extract P bound to specific phases (Kopacek et al, 2005; Søndergaard, 2007). Rather, the P extracted in each step is operationally defined relative to the extraction reagent. The non-specificity and potential redistribution of P during extraction steps are limitations, but despite these shortcomings the extraction schemes yield reproducible results that allow a description of the dominant binding mechanisms and compounds in a given sediment (Søndergaard, 2007) and provide insights into potential mobility and bioavailability. Typical sequential extraction schemes target loosely bound, soluble or ion-exchangable P, P fractions adsorbed to metal oxyhydroxides, organic P, Ca-mineral bound P, and residual phases.

This chapter describes research to determine the geochemistry of P in the lake sediments in Wairewa and to determine the mobility, and temporal variability of various P fractions.

P fractions were investigated through the use of chemical sequential extraction. In an attempt to circumvent the lack of specificity inherent in the extraction scheme, geochemical modelling was used to investigate P binding species which are likely to be present in the sediment under prevailing chemical conditions. An understanding of the key binding mechanisms will inform research into factors controlling the release of P from the sediments into the lake water column (Chapter 4 and 5) which potentially drives and/or sustains algal bloom events in the lake.

3.2 Methods

3.2.1 Sediment and water sampling

Lake sediment and pore water samples were collected and processed as detailed in Section 2.2.4. Sampling sites are presented in Figure 3.1. Surface sediments reported here are from the top 1cm of the core. When coring, the sediment was extruded until level with the top of the corer and then the corer was tipped slightly to drain free flowing water. Very limited organic 'floc' at the sediment/water interface made distinction of the sediment surface easy. Sediment cores (Table 3.1) were generally collected and processed under air (i.e. oxic atmospheric conditions) although three cores were collected under nitrogen in order to assess the difference between sampling and processing under oxic and anoxic conditions (F10 C9) and, in the case of F12 C4 to provide pore water chemistry for geochemical modelling. In this research, core samples are denoted by the sample site and a 'C' number e.g. F11 C1 (Table 3.1), while surface sediments are denoted by the sample site and an "S" number e.g. F11 S5. Elements and compounds are referred to by their chemical annotation and square brackets […] are used to denote concentration. The water column above a sediment core is referred as the over-lying water (OLW).

Seasonal differences were noted between cores (as discussed in Section 3.3). Cores were sampled for sediment and pore water analysis in order to investigate these differences, as well as the differences between sites F11 (abundant macrophytes), F12 (few macrophytes) and F10 (southern end of the lake). Core F11 C2 (sediment and pore water) was used as the winter core. Cores F11 C3 (sediment and pore water) and F12 C5 (pore water only) were used as summer cores sampled prior to algal bloom formation. These are referred to as summer pre-bloom cores in this research. F11 C1 and F12 C7

(sediment and pore water) were used as summer cores sampled during algal bloom events. These are referred to as summer post-bloom initiation (PBI) cores. Core F12 C6 and C8 and F10 C10 (Table 3.1) are not referred to in this chapter but are used for the research presented in Chapter 5. The factors influencing differences between sites are discussed in Chapter 5 rather than this chapter.

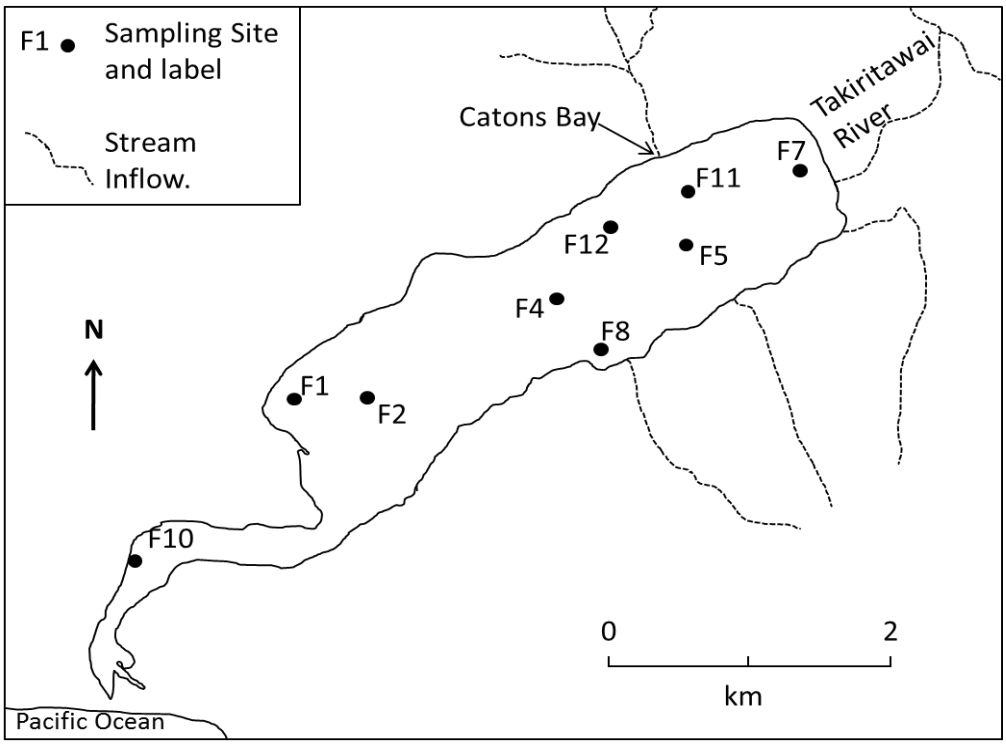

Figure 3.1 Wairewa showing sediment sampling sites. Cores were collected from sites F11, F12 and F10. The other sites were used for surface sediment sampling only. Samples from sites F1, F5 and F8 are not referred to in this chapter but are included in Chapter 5.

Table 3.1 Details of sediment cores used in this research. SE = sequential extraction. PWC = Pore water chemistry. 'Atmosphere' refers to conditions under which sample processing was conducted (either air or N_2 in a glove bag)

Sample Site	Core Number	Sampling Date	Season	Algal bloom	Analysis Type		Atmosphere
					SE	PWC	
F11	C1	Dec 2011	Summer	Yes	✓	✓	O_2
	C2	17 Aug 2012	Winter	No	✓	✓	O_2
	C3	5 Mar 2013	Summer	No	✓	✓	O_2
	C4	23 Dec 2013	Summer	Yes		✓	N_2
F12	C5	5 Mar 2013	Summer	No		✓	O_2
	C6	23 Dec 2013	Summer	Yes		✓	N_2
	C7	7 Oct 2014	Summer	Yes	✓		O_2
	C8	20 Oct 2014	Summer	Yes		✓	O_2
F10	C9	10 Oct 2014	Summer	Yes	✓	✓	$N_2 + O_2$
	C10	20 Oct 2014	Summer	Yes		✓	O_2

3.2.2 Analytical methods for water samples

3.2.2.1 Lake and pore water analysis

Lake water and sediment pore water was analysed for P as detailed in Chapter 2, Section 2.2.4. Major ion analyses were by DIONEX ion exchange chromatography (IC) at the Department of Soil and Physical Sciences, Lincoln University, New Zealand. Anion limits of detection (LOD) are presented in Table 3.2. Dissolved trace element analyses were conducted on samples filtered through 0.45 µm Millipore membrane filters and acidified with concentrated ultrapure HNO_3 to pH < 2. Analysis was by inductively-coupled plasma optical emission spectrometry (ICP-OES) at the Department of Soil and Physical Sciences, Lincoln University, New Zealand. These analyses are referred to in this research as 'total dissolved' (TD) concentration. The limits of quantitation (= 10 x (standard deviation of concentration blank measured 7 times)) are presented in Table 3.2. Dissolved inorganic carbon (DIC) was analysed for by infrared gas analyser (IRGA) using the method described in Hawes et al (2011).

Table 3.2 Limits of detection (LOD) for DRP and major anions analysed by analysed by spectrophotometry and ion chromatography respectively, and limits of quantitation (LOQ) for trace elements analysed by ICP-OES.

Spectrophotometry- Limit of Detection			
Species	LOD ($mg.L^{-1}$)		
DRP	0.002		
Major Anions- Limit of Detection			
Anion	LOD ($mg.L^{-1}$)	Anion	LOD ($mg.L^{-1}$)
Chloride	0.005	Bromide	0.02
Nitrate-N	0.02		
Trace Elements- Limit of Quantitation			
Element	LOQ ($mg.L^{-1}$)	Element	LOQ ($mg.L^{-1}$)
Aluminium	0.00213	Manganese	0.00008
Calcium	0.00031	Sodium	0.00107
Iron	0.00065	Phosphorus	0.00455
Potassium	0.00729	Sulphur	0.00744
Magnesium	0.00037	Zinc	0.00015

3.2.3 Analytical methods for sediment

3.2.3.1 Sediment weights and loss on ignition

Wet weight to dry weight (DW) ratios were determined by drying a sediment sample at 105^{o} C for 24 hours. The sample was weighed prior to and after the drying process. These samples were then ignited at 550^{o} C for 4 hours. The weight loss during ignition (LOI) gives a percentage of organic material by the following;

$$LOI_{550}=((DW_{105}-DW_{550})/DW_{105}) \times 100 \quad \text{(eq 3.1)}$$

Further ignition at 950^{o} C for 2 hours gives a loss on ignition percentage by the following;

$$LOI_{950}=((DW_{550}-DW_{950})/DW_{105}) \times 100 \quad \text{(eq 3.2)}$$

The weight of carbonate in the original sample is the weight loss due to ignition at 950^{o} C x 1.36 (Heiri et al, 2001).

3.2.3.2 Sediment grain size

Sediment grain size is an important factor in determining mechanisms and rates of solute transfer between sediments and the water column (Das, 2008). Sediment grain size was analysed to determine spatial variability along the lake by sampling surface sediments at five sites along the lake. Variability with sediment depth was determined by analysis of sediments from two cores, from sites F12 and F12 respectively. Analysis was by Horiba LA-950V2 laser scattering particle size distribution analyser at the Environmental Laboratory of Civil and Natural Resources Engineering, University of Canterbury using a refractive index of 1.556.

3.2.3.3 Scanning electron microscopy

Scanning electron microscopy using energy dispersive X-ray analysis (SEM-EDS) was used to determine semi-quantitative chemical composition of sediment particles using spot spectra. This data was then used to estimate mineralogy by stoichiometry. Analysis was conducted at the University of Canterbury using a JEOL JSM-6100 scanning microscope with an Oxford Aztec EDS system with a 50mm^2 X-max silicon drift detector. An accelerating voltage of 20kV was used. Sediment samples were suspended in deionised water and then filtered onto 0.45 µm Millipore membrane filters. These were dried at 105^{o}C for 24 hrs prior to carbon coating for analysis.

3.2.3.4 Sediment; Sequential chemical extractions

A comparison was made between the use of a Tessier et al, (1979) sequential extraction scheme and a Psenner et al (1988) style scheme adapted slightly from that described in Rydin (2000). For the comparison, four surface sediment samples from different sites were extracted using the two different schemes and the total sediment P (TSP) obtained from the sum of the extracts (SOE) were compared with TSP obtained by HNO_3 extraction (as described below). The Rydin style extraction SOE averaged 99.9% of the TSP by HNO_3 (Standard deviation = 5.7%). In contrast the Tessier style extraction SOE averaged 73.5% of the TSP by HNO_3 (Standard deviation = 7.5%). The Rydin sequential extraction scheme was chosen for use in this research on the basis of these better performances in P recovery and is presented in Figure 3.2. Also, the early steps of the scheme (a-c below) mimic processes which may result from in-lake environmental conditions and hence may give some indication of the mass of P susceptible to mobilisation by these processes. A shortcoming of P sequential extraction schemes is the potential for re-adsorption of P between steps of the extraction scheme (Kopacek et al, 2005). This is considered a particular problem in carbonate rich sediments (Ruban et al, 1999). The low carbonate content of the Wairewa sediment (see Section 3.3.1.3) and the close agreement of the SOE with TSP determined by HNO_3 digestion indicates that while some re-adsorption may occur it is limited in its effect. The Rydin scheme was adapted slightly in that the Residual-P was ascertained by a HNO_3 acid digestion following the HCl step, and the total extracted P was calculated by the sum of the extracts P (see Section 3.2.3.7, below).

The P forms targeted by the extraction steps are as follows;

a. NH_4Cl-P;

   NH_4Cl is a neutral salt which is considered to extract very loosely bound and soluble P by ion-exchange.

b. BD-P;

   The bicarbonate/dithionite ($NaHCO_3/Na_2S_2O_4$) step is a reducing reaction. The bicarbonate is used to control pH. This reagent targets P forms which are sensitive to redox conditions such as P absorbed to reactive (hydr)oxides of Fe and Mn.

c. NaOH-rP and NaOH-nrP;

The NaOH-reactive P (rP) step extracts remaining P forms which are sensitive to pH change such as P strongly adsorbed to Al hydroxides and to less reactive Fe and Mn (hydr)oxides as well as organic particulates and clays. Also targeted in this step and detected after a persulphate digestion to determine NaOH-non-reactive P (nrP), is easily degradable organic-P (including bacteria incorporated P), which is the difference between NaOH-nrP and NaOH-rP.

d. HCl-P;

The HCl step targets remaining P forms which are mobile at low pH. This is likely to include Ca associated P such as apatite and P adsorbed or co-precipitated with carbonates, as well as more refractory oxides that are not affected by previous steps.

e. Res-P;

Residual P is extracted with a strong acid digestion (HNO_3) and is considered to include refractory organic and inert inorganic forms.

f. Total P;

Total sediment P is considered to be the sum of the extracted P forms (SOE). This is further discussed below.

A weight of recently thawed wet sediment equivalent to approximately 0.5 g dry weight sediment, was weighed into 50 ml polypropylene centrifuge tubes. For each step of the extraction procedure 25 ml of the appropriate reagent was added. The tube was then placed on an end over end shaker for the appropriate time before being centrifuged at 4000 rpm for 15 minutes. The supernatant was then removed for analysis and the next reagent added. Supernatants were stored at 4^{o} C for analysis within 48 hrs.

The NH_4Cl, NaOH, digested NaOH, HCl and HNO_3 supernatants were analysed for reactive P by UV/visible spectrophotometric analysis using the Ascorbic Acid method (APHA 4500-P Method E). Calibration curves for these analyses were constructed using standards made up in the media of each sequential extraction reagent. Supernatant dilution using deionised water, was tested during the method development and was then

used throughout the research for diluting both samples and standards. These dilutions and the cuvette lengths for UV/visible spectrophotometric analysis are presented in Table 3.3. The limit of detection for these analyses was 0.002 $mg.L^{-1}$. The digestion of the NaOH supernatant was by persulphate (APHA 4500-P Method B5). The bicarbonate/dithionite (BD) supernatant was unable to be analysed by spectrophotometric methods due to interference by CO_2 bubbling and therefore was analysed by ICP-OES at the Department of Soil and Physical Sciences, Lincoln University, New Zealand. The limit of quantitation for P on this instrument was 0.00455 $mg.L^{-1}$. As most Al (hydr)oxides phases are soluble at pH = 10, ICP-OES analysis was also used to quantify Al concentrations in a number of NaOH extracts from surface sediments.

All sediment concentrations reported in this research are per dry weight of sediment unless otherwise stated.

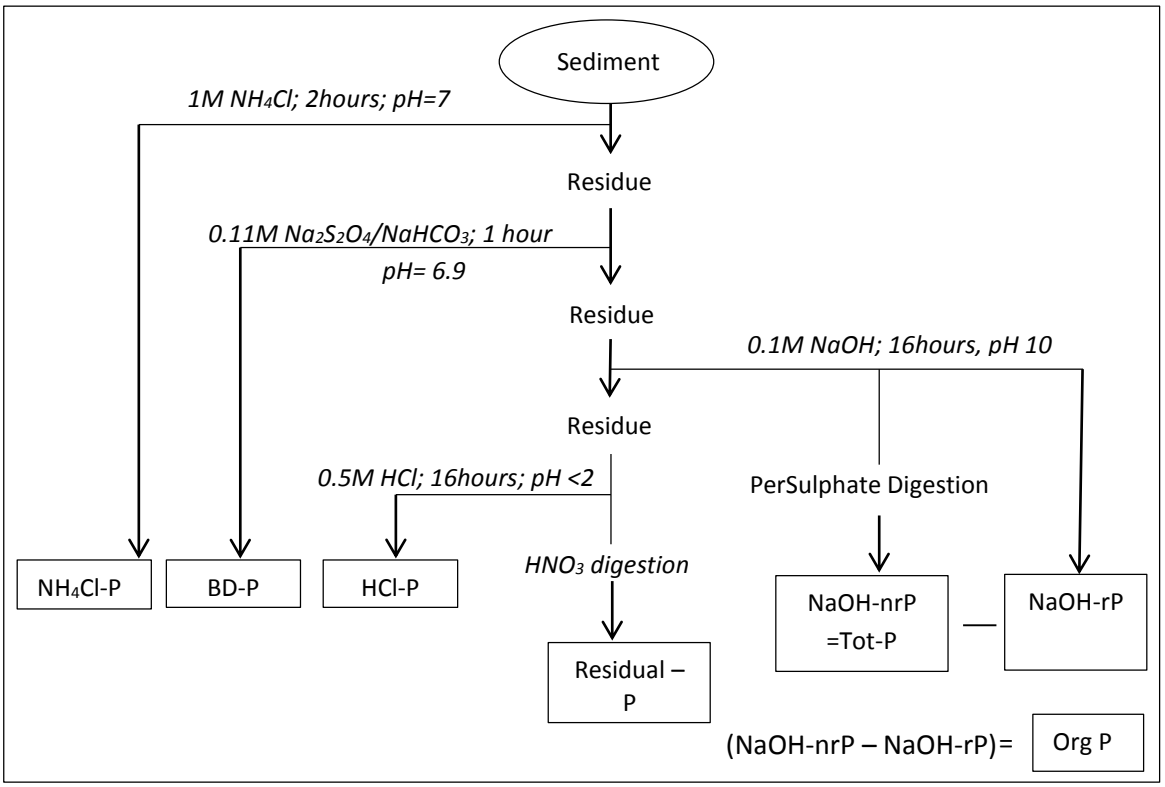

Figure 3.2 Sequential extraction scheme used on Wairewa sediments. Adapted from Rydin (2000).

Table 3.3 Dilutions with deionised water and cuvette length used for UV/visible spectrophotometric analysis of extraction scheme reagents.

Extraction Reagent	Dilution with DI water	Cuvette lengths
NH_4Cl	1:10	5 cm
NaOH	1:20	2 cm
Digested NaOH	1:10 prior to digestion	2 cm
HCl	1:20	2 cm
HNO_3	1:20	2 cm

3.2.3.5 The effects of sampling and processing sediment under nitrogen or oxygen atmospheres

Pore water chemistry

For the purposes of evaluating the effects of processing sediment and pore water under oxidising conditions, a single core (F10 C9) was collected and processed under a nitrogen atmosphere using a glove bag inflated with O_2-free nitrogen. The core was halved and sediment and pore water from one half was transferred into nitrogen purged centrifuge tubes for analysis. The pore water was processed and analysed as detailed in Section 3.2.2 while the sediment was analysed by chemical sequential extraction as detailed in Section 3.2.3. However in the case of the sequential extraction the first two steps were conducted in nitrogen purged centrifuge tubes. The other half of the core (sediment and pore water) was exposed to oxygen for a period of time representative of normal processing time frames and were then transferred into unpurged centrifuge tubes for analysis. Data from the two analysis methods are presented in Appendix 2.

Figure 3.3 presents the depth profiles for redox sensitive elements in the pore water. The profile for total dissolved Fe was affected significantly with a much reduced [TD-Fe] in the upper 8 cm of the O_2-processed sediment. A peak was still evident in this TD-Fe profile but was deeper, occurring at 8 cm as opposed to the 4-5 cm peak in the N_2-processed sediment. The [TD-P] was also diminished above 8 cm in the O_2-processed sediment but much less so than for TD-Fe and the same basic profile was evident for both O_2- and N_2-processed profiles. It appeared then that the pore water profiles of [TD-Fe] are affected by oxidation during sample collection and processing, and that the [TD-Fe] must be interpreted with this in mind. Despite this, pore water profiles observed in most O_2-

processed cores (e.g. Figure 3.17) did have very significant [TD Fe] peaks with similar trends as those processed under N_2.

Profiles for [TD-Mn] and [TD-S] were similar in the two processing atmospheres. When combined with the limited impact on the [TD-P] profiles, and the observed [TD-Fe] peaks, this meant that while the actual [TD-P] and in particular [TD-Fe] in O_2-processed cores may be expected to be diminished, the trends may still be used in conjunction with [TD-Mn] and [TD-S] to identify important redox thresholds.

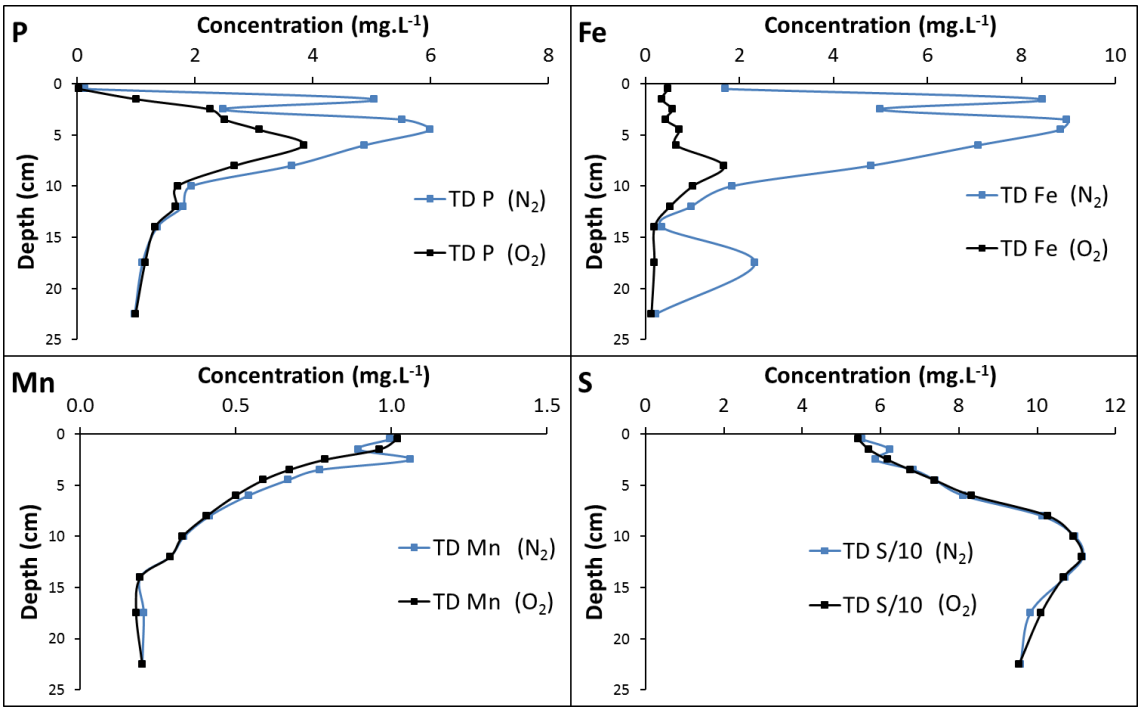

Figure 3.3 Depth profiles for redox sensitive elements in sediment pore waters from the same core, extracted under N_2 and O_2 atmospheres. All analyses are as total dissolved concentrations.

Sequential extraction of sediment

Figure 3.4 presents selected depth profiles for P fractions from sequential extractions for sediments from the same core processed under O_2 and N_2 atmospheres. The [TSP] profiles for the two processing atmospheres were very similar except for the upper 2 cm. These upper sediments showed concentrations in the O_2 processed core were higher by 150 $mg.kg^{-1}$ and 65 $mg.kg^{-1}$ at depths of 0 - 1 and 1 - 2 cm respectively. These differences were comprised of higher [BD-P] and [Org-P] in the O_2 processed samples. The differences in the TSP were 9 and 4% of the total respectively, well within the uncertainty of measurement. In addition, a complete redox related incorporation of all the pore water

TD P into the TSP would result in a maximum increase of only 5.6 $mg.kg^{-1}$. It was apparent then that the significantly higher [TSP], [BD-P] and [Org-P] in the O_2 processed sediment were due to sample variation rather than redox related transformation during sampling and processing. The differences apparent in the NH_4Cl-P fraction were more significant and consistent. The N_2 processed sediments had a much greater [NH_4Cl-P] in the surface sediments (1.6 $mg.kg^{-1}$ compared with 0.4 $mg.kg^{-1}$ at 0 - 1 cm) and at depths below 15 cm. Redox related changes in the Fe binding capacity of the sediment may explain the changes seen in [NH_4Cl-P]. Processing of sediment under an O_2 atmosphere increased the precipitation of Fe(III) phases (as evidenced by the decrease in soluble Fe^{+2} in the pore water) which may rapidly adsorb P leading to the very slight increase observed in [BD-P], and the significant decreases seen in [NH_4Cl-P]. The [NH_4Cl-P] were of low enough magnitude to be significantly impacted by the observed changes in pore water concentrations.

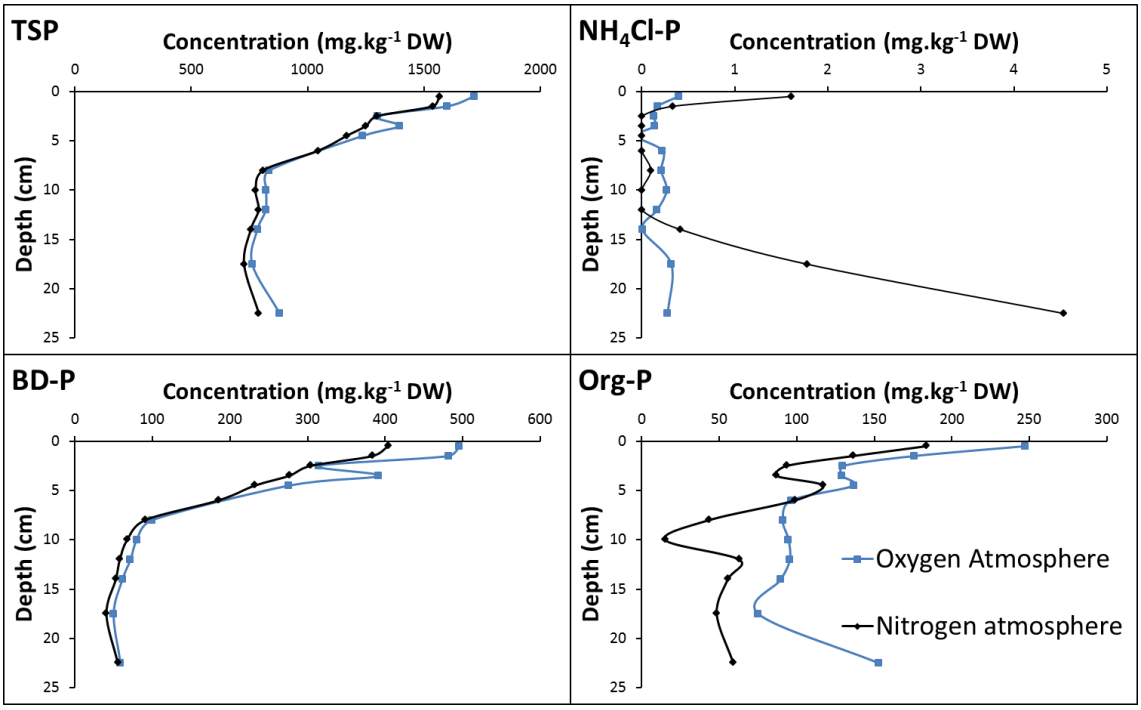

Figure 3.4 Depth profiles for selected P fractions from sequential extractions conducted on sediments from the same core sampled and processed under N_2 and O_2 atmospheres.

3.2.3.6 EDTA Chemical Extraction

An EDTA extraction was conducted on a single surface sediment sample from site F12 (sampled 1 February 2013) in order to investigate the relationship of P release rates to those of Fe and Mn. A sediment sample of 0.51 g was mixed in 5 mls of deionised water

before extraction in 250 ml of 10 mM EDTA at a temperature of 30^{o} C and a pH of 6.97 for 48 hrs. The pH was maintained by manual additions of 5M NaOH and 2M HCl as required. 10 ml samples were taken at various time intervals and these were centrifuged at 4000 rpm for 15 mins prior to filtering through 0.45 µm MF Millipore filters. Sediment left on the filter was washed back in to the reaction vessel with 10 ml of the EDTA solution. Samples were analysed for trace element concentration by ICP-OES.

3.2.3.7 Total Sediment P (TSP)

Three methods of determination for TSP in lake sediments were used and compared. The first is discussed above in Section 3.2.3.4 and comprises the sum of the extracted P forms (SOE) in the sequential extraction scheme. The second method was a nitric acid digestion based on the US EPA (1994) method 3051. Due to equipment availability, our digestion utilised a hotplate for heating rather than a microwave. Many common methods of 'total' element digestion and analysis actually determine 'total recoverable concentrations' as they do not recover the recalcitrant fraction often bound in silicate minerals (Duzgoran-Aydin et al, 2011). However in a study on Florida soils by Chen & Ma (1998), total recoverable concentrations obtained for P by US EPA method 3051 were approximately equal to actual total concentrations. In this research approximately 1 g of sample was gently boiled in a covered teflon beaker in 10 ml concentrated HNO_3 for 2 hours. A further 10 ml of 10% HNO_3 was added and heating continued for another 1 hour at which stage the cover was removed from the beaker and heating continued for a final hour. This was made up to a known volume and analysed by UV/visible spectrophotometric analysis using the Ascorbic Acid method (APHA 4500-P Method E). Comparisons of TSP in 12 sediment core samples determined by HNO_3 digestion and by the SOE approach indicated an average difference of 10%, with greater recovery of P by the SOE approach.

A third method used followed Anderson (1976), and involved the ignition of a dry sediment sample at 550^{O} C for 4 hours before boiling in 25 mls of 1M HCl for 15 minutes. This was made up to a known volume and analysed by UV/visible spectrophotometric analysis using the Ascorbic Acid method (APHA 4500-P Method E). Digestion and analysis of three samples from different core depths by ignition + HCl achieved a 96% recovery compared to the SOE approaches. A further comparison between the HNO_3 and ignition + HCl methods on two samples at step e (Residual-P) of the sequential extraction scheme above, indicated a 93% recovery of P by the ignition +

HCl method, relative to the HNO_3 method. The results of these comparisons indicated that the SOE approach results in higher recoveries of P than the acid digestions. Due to this, the SOE approach to estimating TSP is used, except where a TSP concentration is required for a sample for which a sequential extraction has not been conducted. In these cases an HNO_3 digestion as described above is utilised.

3.2.4 Data quality control and uncertainties

For all water analysis methods, standard and blanks were run prior to any analysis. For P analyses in the sequential chemical extractions, separate calibration curves were constructed for each extraction reagent. Sample spikes were used during the calibration process to check good P recovery. Each run of extraction samples was proceeded by analysis of a standard solution.

Uncertainties associated with the spectrophotometric analysis of dissolved reactive PO_4^{-3}-P (DRP) were determined by 95% confidence intervals associated with replicate analyses of standards and natural water samples and hence include accuracy and precision in the uncertainty estimates. The uncertainty of measurement (UOM) for DRP was 10% where [DRP] < 0.009mg/L^{-1} and 5% for [DRP] > 0.009 mg.L^{-1}. The UOM for TP was 15% for all concentrations. The limit of detection for spectrophotometric analysis of DRP was determined from the analysis of twenty blanks. The mean concentration + three times the standard deviation was 0.002 mg.L^{-1}, which was considered to represent the limit of detection.

A 20% UOM is assumed for sediment concentrations based on a 95% confidence interval for replicate sediment extractions testing both experimental uncertainty and variability between samples taken in close proximity.

Table 3.2 presents limits of quantitation and detection for trace elements and major anions respectively, as determined for the respective analytical methods by the Department of Soil and Physical Sciences, Lincoln University.

3.2.5 Geochemical Modelling

Geochemical modelling was undertaken to investigate changes in aqueous speciation in sediment pore water and the stability of mineral phases that may bind P in the lake sediments and water column. The U.S. Geological Survey PhreeqcI (version 3.1.2)

graphical user interface (Charlton et al, 1997) to the geochemical PHREEQC computer model (Parkhurst and Appelo, 1999), was used. This version was released on March 3, 2014 and was downloaded from http://wwwbrr.cr.usgs.gov/projects/GWC_coupled/phreeqci/. PHREEQC is used here to conduct solution modelling, whereby a chemical analysis of water is used to calculate the distribution of aqueous species and mineral saturation indices, by ion association modelling. PHREEQC iteratively adjusts the concentration of an element to obtain equilibrium with a specified phase, or to obtain charge balance. The distribution of redox elements among their valence states can be set by a specified pe value, or any redox couple for which data are available. The program utilises various databases of thermodynamic data and options include PHREEQC.dat, MINTEQ.dat and WATEQF.dat. This study utilises MINTEQ.v4.dat, as this has the most comprehensive thermodynamic data relevant to P species and mineral phases.

PHREEQC is a well utilised and tested geochemical modelling program used extensively in many geochemical settings such as acid mine drainage (e.g. Waters and Webster-Brown 2013), contaminant leaching (e.g. Tiruta-Barna, 2008), biogeochemical reactions in soils (e.g. Wissmeier and Barry, 2010) and contaminant transport in groundwater (e.g. Postma et al 2007). The model has been used successfully in various lake settings (e.g. Oelbner and Guth, 2003; Andersen et al 2011) and for P dynamics in lakes (e.g. Berg et al, 2004; Das et al, 2009). The main limitation of the model for use in speciation and mineral stability is the assumption of all reactions proceeding to equilibrium. Hence the model predicts thermodynamic possibilities rather than accurately predicting phases that are present in the modelled system. Kinetic hindrances may favour formation of one mineral form over another, more thermodynamically stable, form. Also the model uses ion association reactions to calculate activity coefficients, an approach which is less accurate at high ionic strengths such as in sea water.

Two modelling approaches were taken in this research as described below, both based on solution chemistry only. Surface complexation modelling was conducted at a later stage of this research (refer to Chapter 4): Pore water chemistry for both modelling approaches was from a summer core (F11 C4) which had been processed under a nitrogen atmosphere. The pH conditions were not analysed in this core and so pore water pH was taken from a core sampled at site F12, under similar OLW conditions (pH = 8.80) as for F11 C4 (pH = 8.88). Redox condition were set as described below.

i. In the first approach (variable chemistry approach) the pore water chemistry from varying depths was used. Input chemistry is presented in Table 3.4. Redox conditions were estimated for each depth from the pore water chemistry profile, and from the redox pair (O^{-2}/O^{0}, Fe^{+2}/Fe^{+3} and HS^{-}/SO_4^{-2}) calculations presented in Table 3.5. Temperature was from the OLW temperature. This approach was taken in order to provide data on the stability of key mineral phases which may affect P binding, at the various sediment depths, under the redox profile of core F11 C4.

Table 3.4 Pore water chemistry for core F11 C4 used as input for PHREEQC solution modelling. pH is taken from a core from site F12, redox is estimated, and temperatures are taken from the surface sediment pore water in core F11 C4. The chemical form in which the variables were input into the model is included. Pore water analyses from surface sediment F11 S5 0-1 cm are also shown. This was used in the redox pair calculations in Table 3.5, as well as in Chapter 4**.**

Model inputs		**Concentration ($mg.L^{-1}$) for elements at specified depths**							**F11 S5**
Variable	**Input as;**	**0-1 (cm)**	**1-2 (cm)**	**2-3 (cm)**	**5-7 (cm)**	**9-11 (cm)**	**13-15 (cm)**	**20-25 (cm)**	**0-1 (cm)**
Al	Al	0.079	0.156	0.127	0.094	0.265	0.246	0.041	0.027
Ca	Ca	39.1	46.8	48.9	47.7	42.0	47.1	16.1	5.90
Fe	Fe	14.8	41.9	35.3	7.36	1.26	0.482	0.196	0.0427
K	K	51.0	56.8	57.9	68.7	75.8	91.1	24.6	6.80
Mg	Mg	102	116	124	125	114	133	46.4	15.5
Mn	Mn	2.69	3.03	2.41	1.09	0.915	0.970	0.297	0.142
Na	Na	706	759	773	851	887	1011	302	107
P	P	0.215	4.32	2.87	0.722	1.09	1.54	0.709	0.028
S	S	29.1	12.23	5.11	0.864	1.63	1.48	0.168	16.3
Zn	Zn	0.025	0.082	0.012	0.005	.004	0.106	0.026	-
Cl	Cl	1191	1277	1314	1453	1480	1567	1610	190
Br	Br	4.87	5.27	5.48	6.12	6.17	6.49	7.16	0.911
NO_3-N	NO_3	0.069	0.048	0.035	0.034	0.023	0.022	0.052	0.043
HCO_3	C	393	620	679	726	585	656	656	58.6
pH	pH	6.97	7.16	6.78	6.56	6.89	7.32	7.63	7.27
Redox	pe	4.5	0.7	0	-4	-4	-4	-4	13
Temp	^{o}C	20	20	20	20	20	20	20	19.6

ii In the second approach (fixed chemistry approach) modelling was conducted with pore water chemistry taken from the surface sediment of core F11 C4 0-1

cm depth (Table 3.4). Redox conditions were then altered (see Section 3.3.2.2) without changing pore water chemistry. This approach was taken to provide data on the effect of changing redox conditions on a given sediment, and to isolate the redox effect from the effect of different initial water chemistry. This was intended to illuminate both the effect of redox changes on the surface sediments, as well as to provide insights into the effect of differing redox profiles on pore water species and mineral stability at differing sediment depths.

Table 3.5 Examples of redox conditions calculated as pe using PHREEQC. Dissolved oxygen concentrations were used in the O^{-2}/O^{0} calculations. Solution chemistry from the pore water of sample F11 S5 0-1 cm was used in the Fe^{+2}/Fe^{+3} and $HS^{-}/SO4^{-2}$ calculations.

Redox Pair = O^{-2}/O^{0}	
Dissolved oxygen mg.L^{-1}	**pe**
12	13.64
4	13.52
2	13.44
1	13.37
$0.1x10^{-27}$	6.99
Redox Pair = Fe^{+2}/Fe^{+3}	
Fe^{+2}/Fe^{+3} ratio	**pe**
Fe^{+3} = 99.999% of Tot Fe	10.02
Fe^{+2} = 99.999% of Tot Fe	0.0205
Redox Pair = HS^{-}/SO_4^{-2}	
$HS^{-}/SO4^{-2}$ ratio	**pe**
SO_4^{-2} = 99.999% of Tot S	-3.37
HS^{-} = 99.999% of Tot S	-4.62

3.3 Results

3.3.1 Sediment characterisation

3.3.1.1 Grain size analysis

Table 3.6 presents key grain size data for five sites distributed along the lake, while Figure 3.5 plots the mean and standard deviation data against the distance from the northern end of the lake. The main tributary enters the lake from the north and this is the dominant source of sediment to the lake (see Chapter 2). The most common grain size was around 9.4 µm with the mean size ranging from 12.58 to 9.28 µm. This was

consistent with observations of grain size under SEM. More than 99 % of grains in all samples were between 5 and 50 µm which puts the lake sediment in the "silt" category according to the Wentworth (1929) classification scheme. Grain size decreased slightly in a southerly direction along the lake with the greatest change occurring between F7 and F12 at the northern end of the lake. The standard deviation decreased from north to south indicating a slightly better sorted sediment at the southern end. Neither of these trends was statistically significant.

Sediment grain size distribution with depth at two sites is presented in Table 3.7 and Figure 3.6. The sediment fined slightly with depth and appeared less well sorted near the surface. However, overall the sediment grain size was consistently distributed across the lake and through the sediment pile.

Table 3.6 Key statistics of grain size distribution along the length of Wairewa. The dominant inflow (Takiritawai River) is at the N end of the lake. (n = not reported by analyser)

Site	Distance from N end of lake (km)	Range (µm)	Median (µm)	Mean (µm)	SD (µm)
F7	0.38	6.72 - 77.0	10.36	12.58	7.99
F12	1.50	6.72 - 51.5	9.95	10.58	3.85
F4	2.18	5.87 - 59.0	9.31	10.08	4.32
F2	3.75	5.86 - 19.9	9.60	10.36	4.11
F10	5.66	5.86 - 19.9	9.07	9.28	1.94

Table 3.7 Key statistics for grain size (µm) vs depth at two core sites. (n= not reported by analyser)

Depth	Range		Median		Mean		SD	
(cm)	F12	F10	F12	F10	F12	F10	F12	F10
0-1	6.72-51.5	6.72-51.5	9.97	9.72	10.52	10.16	3.60	3.16
1-2	6.72-51.5	5.87-19.9	9.95	9.06	10.58	9.28	3.85	1.94
2-3	6.72-51.5	6.72-44.9	9.87	9.31	10.44	9.66	3.63	2.71
4-5	6.72-44.9	5.87-19.9	9.76	9.14	10.15	9.34	2.95	1.92
7-9	5.80-44.9	5.87-19.9	8.69	8.59	9.16	8.86	2.95	1.96
11-13	5.87-44.9	5.87-19.9	9.01	8.63	9.56	8.89	3.46	1.95
15-20	5.87-51.5	5.87-17.4	9.22	8.36	9.76	8.61	3.71	1.86

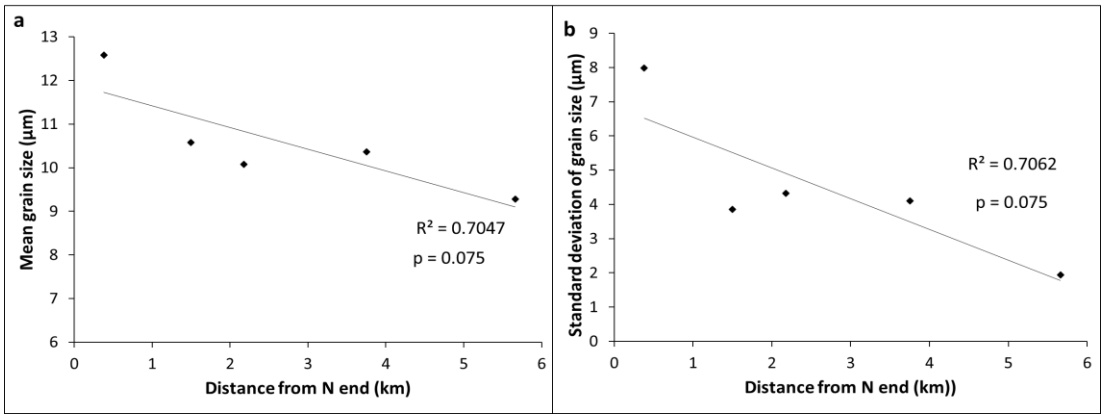

Figure 3.5 (a) Mean and, (b) standard deviation for grain size data plotted against distance from the north end of the lake

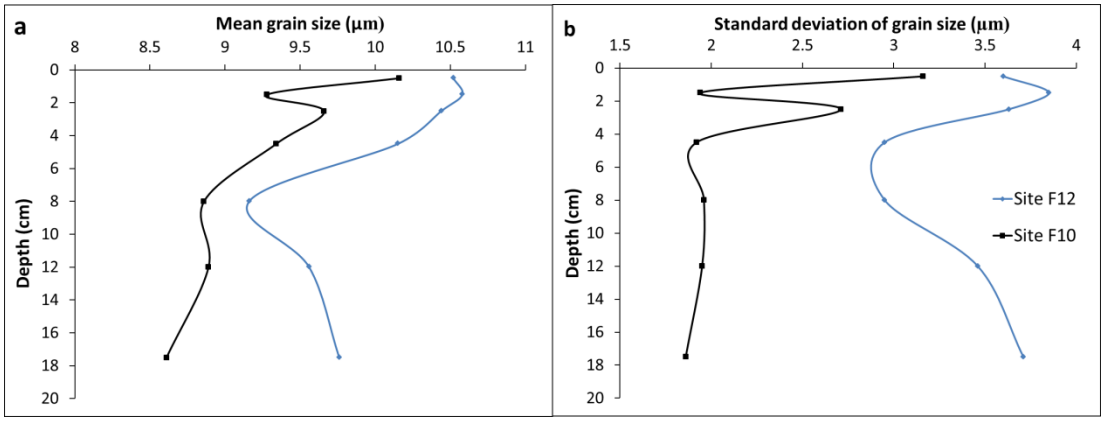

Figure 3.6 (a) Mean and (b) standard deviation plotted against depth for two sites; F12 and F10.

3.3.1.2 Sediment Density

The mass per area and density of sediment and pore water calculated in core F11 C3 are presented in Table 3.8. These densities have been used to calculate sediment P reservoirs in Section 2.2.6 and areal release rates for pH related slurry experiments in Chapter 4. Sediment density increased uniformly with depth at an average rate of increase of 17.5 $kg.m^{-3}.cm^{-1}$.

Table 3.8 Mass/area and density for sediment and pore water for core sections sampled in Core F11 C3. DW = dry weight.

Core section (cm depth)	Mass/area (kg.m^{-2})		Density (kg.m^{-3})	
	DW Sediment	Pore water	DW sediment	Pore water
0-1	2.81	12.27	280.87	1226.83
1-2	2.29	6.97	228.55	697.26
2-3	3.60	7.58	359.80	757.69
3-4	3.44	6.98	344.00	697.98
4-5	3.92	7.75	391.87	775.31
5-7	8.73	16.18	435.95	808.16
7-9	7.58	15.05	378.86	751.88
9-11	9.65	16.50	482.11	824.48
11-13	9.19	13.18	459.34	658.34
13-15	10.57	14.15	527.97	707.08
15-20	29.48	27.58	589.30	551.33
20-25	33.75	25.99	674.52	519.47

3.3.1.3 Organic matter and carbonate contents

Organic matter and carbonate contents determined by loss on ignition for varying depths in three summer cores and one winter core are presented in Table 3.9.

Table 3.9 Organic material and carbonate contents for selected sediment depths from three summer cores (F11 C1, F11 C3, F12 C7) and one winter core (F11 C2), as determined by LOI.

Depth (cm)	F11 C1		F11 C3		F12 C7		Summer Average		F11 C2	
	Org	Carb	Org	Carb	Org	Carb	Org	Carb	Org	Carb
	Weight %									
0-1	11	2	13	2	9	2	11	2	16	2
1-2	7	1	12	2	10	2	10	2	13	2
2-3	7	-	8	2	10	2	8	2	8	2
5-7	6	2	9	2	9	2	8	2	8	2
11-13	5	2	8	3	6	2	6	2	6	2
20-25	5	2	4	2	6	2	5	2	5	2

The lake sediments were relatively low in organic matter (≈ 10 – 15 %) and very low in carbonates (2 %). Organic and carbonate contents were consistent between summer cores, and averaged 11 and 2 % of dry sediment weight respectively at the surface. The organic matter was higher in the winter core than the summer cores. This difference decreased with depth over the upper 2 cm, below which there was no seasonal difference. Organic contents decreased with depth while carbonate contents stayed constant.

Correlations between LOI analyses and sequential extraction P fractions can provide insight into the specific phases that bind P in the various fractions of the sequential extraction scheme. Figure 3.7 presents a plot of organic material determined by LOI versus [Org-P] and [Res-P] fractions for three summer and one winter core (all depths). The strong correlations observed between [Org-P] and LOI (R^2 = 0.72 – 0.91) confirmed that LOI is largely comprised of organic matter. The correlation (R^2 = 0.79 – 0.95) between [Res-P] and LOI confirmed that a high proportion of the Res-P fraction is also likely composed of refractory organic material.

When sediment carbonate content was plotted against HCl-P there was no correlation (R^2 = 0.03). The HCl-P sequential extraction fraction targets Ca associated P and the lack of correlation with carbonates indicated that the Ca-P is not associated with a Ca-carbonate phase.

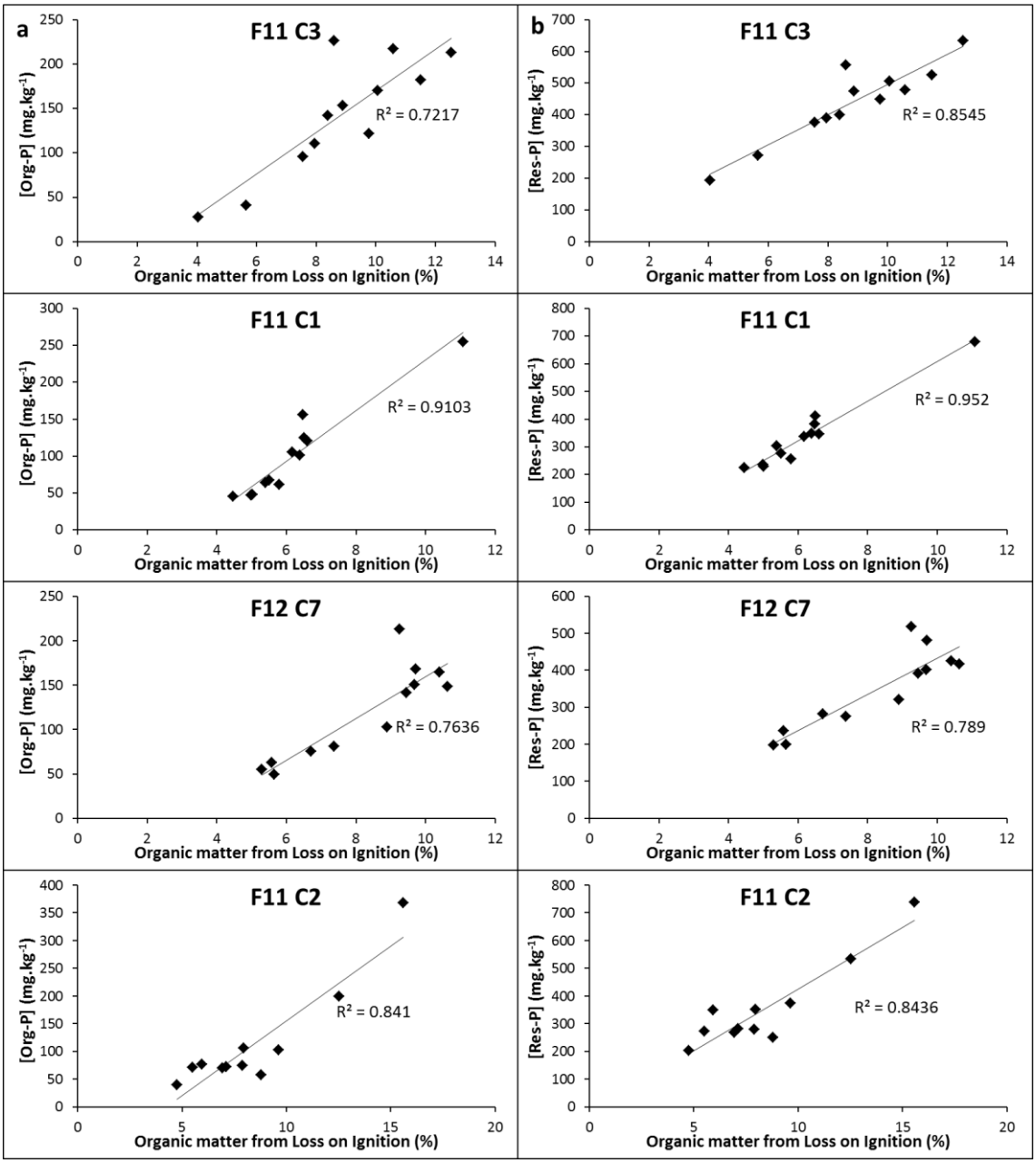

Figure 3.7 Organic matter determined by LOI versus (a) [Org-P] and (b) [Res-P], from sequential extractions on sediments from all depths. $p < 0.001$ for all plots.

3.3.1.4 Reactive Fe and Mn sediment concentrations and Fe:P, Mn:P ratios

Table 3.10 presents the range of reactive [Fe] and [Mn], as targeted by the BD step of the sequential extraction procedure, as well as the Fe:P, Mn:P and Fe:Mn molar ratios in the BD extracts from the sequential extraction of four cores (F11 C1, C2, C3, F12 C7). The reactive Fe concentrations were high but decreased rapidly with depth as did the reactive Mn concentrations, however the Fe concentrations were an order of magnitude higher

than Mn. High Fe:P ratios (> 2) have been used to suggest an adsorption relationship (Gunnars et al, 2002; Nyenje et al 2014), and this was observed in the Wairewa sediments down to about 10 cm depth. The low Mn:P ratio suggested little adsorption of P onto Mn (hydr)oxides. The high Fe:Mn ratio suggested the significant dominance of Fe (hyd)roxides in the redox sensitive fraction of the sediment.

Figure 3.8 presents reactive [BD-Fe] and [BD-Mn] plotted against [BD-P] as determined by the BD extraction step in the sequential extractions, for the same four cores. There was a strong (R^2 = 0.97) correlation between [Fe] and [P] in all cores suggesting a strong relationship between reactive Fe and P. The [Mn] and [P] correlations were not as strongly positive as the Fe correlations and showed more variability between cores. It was apparent then that easily reducible Fe mineral phases were strongly associated with P in the sediment while Mn phases were not so significant.

Table 3.10 The range in Fe and Mn concentrations and molar ratios of Fe, Mn and P in the BD extract of the sequential extractions from four cores (F11 C1, C2, C3 and F12 C7).(n=4).

Depth (cm)	Fe (mol.kg^{-1})		Mn (mol.kg^{-1})		Fe:P		Mn:P		Fe:Mn	
	low	high	low	high	low	high	low	high	low	high
0-1	0.0993	0.1923	0.0019	0.0158	8.92	19.4	0.17	0.85	12.2	51.1
1-2	0.0630	0.0981	0.0012	0.0027	10.2	13.2	0.17	0.55	22.9	76.7
2-3	0.0170	0.0970	0.0007	0.0030	7.87	13.4	0.10	1.40	5.64	102
3-4	0.0080	0.0715	0.0002	0.0009	5.81	12.8	0.08	0.18	33.1	130
4-5	0.0070	0.0620	0.0002	0.0022	3.77	12.4	0.06	0.44	16.2	178
5-7	0.0083	0.0379	0.0002	0.0004	4.52	12.9	0.05	0.24	23.3	173
7-9	0.0069	0.0132	0.0001	0.0004	4.22	6.10	0.06	0.24	21.4	96.4
9-11	0.0040	0.0103	0.0002	0.0004	2.59	5.40	0.09	0.28	10.1	63.3
11-13	0.0006	0.0087	0.0002	0.0004	1.49	4.95	0.11	0.47	3.17	45.1
13-15	0.0023	0.0067	0.0002	0.0005	2.35	3.76	0.12	0.46	7.31	31.4
15-20	0.0005	0.0030	0.0002	0.0004	0.99	1.99	0.20	0.41	2.38	10.0
20-25	0.0008	0.0016	0.0002	0.0002	0.80	1.67	0.23	0.41	2.91	7.28

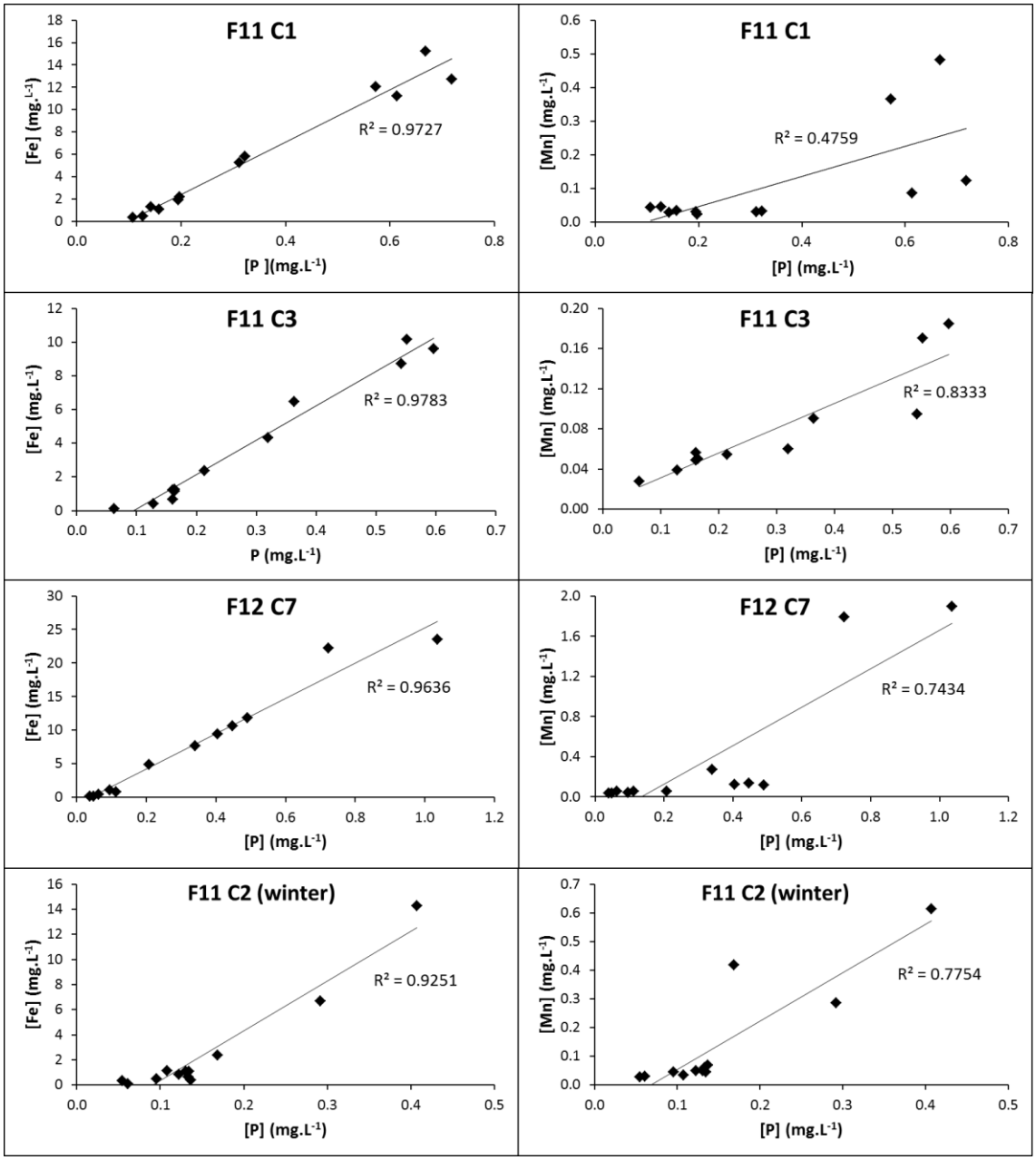

Figure 3.8 Fe and Mn versus P concentrations in the BD extracts from all depths for sediment cores. $p < 0.001$ for all plots except F11 C1 Mn vs P for which $p < 0.05$.

3.3.1.5 pH-sensitive Al in the surface sediment, and the Al:P ratio

Figure 3.9 plots sedimentary Al and P concentrations, for nine surface sediment samples, as analysed in the NaOH extracts from sequential extraction procedures. The Al concentrations ranged from approximately 1100 to 1900 $mg.kg^{-1}$ and were well correlated with the [NaOH-rP]. The Al:P molar ratios ranged from 8.5 to 15 which indicated a probable adsorption relationship. These results confirmed that the NaOH-rP step of the

sequential extraction scheme targeted P associated with Al (hydr)oxides, although P adsorbed to recalcitrant Fe (hydr)oxides and clays were also likely to be targeted.

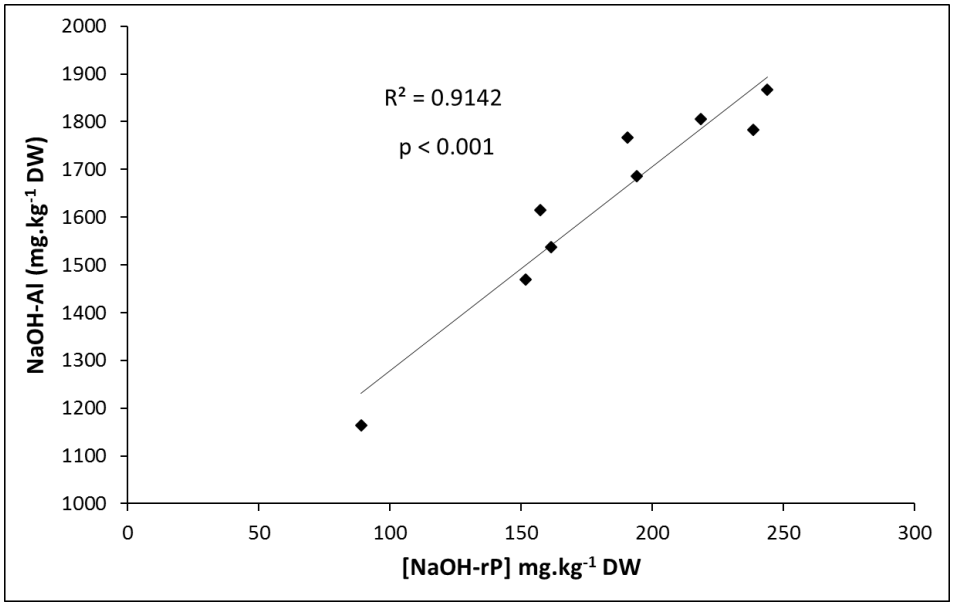

Figure 3.9 Sedimentary P and Al concentrations in the NaOH extracts from nine surface sediments.

3.3.1.6 Sediment mineral phases

Geochemical modelling of mineral stability

Table 3.11 presents saturation indices for selected mineral phases from PHREEQC modelling using the pore water chemistry from core F11 C4 and using the variable chemistry approach (see Section 3.2.5). The modelling predicted precipitation of over-saturated mineral phases (SI > 0) and dissolution of under-saturated phases (SI < 0).

The F11 C4 pore water was saturated with respect to the Fe(III) (hydr)oxide minerals ferrihydrite and hematite, down to around 3 cm depth and with respect to the Fe(III) phosphate mineral strengite, down to 2 cm. The pore water was variously under and over-saturated with respect to the Fe(II) phosphate mineral vivianite throughout the core, while pyrite was consistently over-saturated below 5-7 cm. The manganese oxides were all under-saturated throughout the core (example of Birnessite in Table 3.11), while the mineral $MnHPO_4$ was over-saturated. The manganese carbonate mineral, rhodochrosite was near-saturated down to depths of 3 cm and again at deeper levels and might be expected to form with a slight change in conditions. The aluminium hydroxide gibbsite was over-saturated throughout the core as was the Ca-PO_4 mineral hydroxylapatite.

Table 3.11 Saturation indices (SI) for key mineral phases at various sediment depths, as predicted by PHREEQC modelling using the variable chemistry approach. SI > 0 predicts mineral precipitation, SI < 0 predicts mineral dissolution. Redox was estimated from the pore water chemistry of the summer post-bloom initiation core (see Section 3.3.2.1), F11 C4. pH values were used from a core taken under similar lake conditions as F11 C4

Depth (cm)	redox (pe)	pH	Ferrihydrite Amorphous Fe(III) hydroxide	Hematite Fe_2O_3	Strengite $FePO_4.2H_2O$	Vivianite $Fe_3(PO_4)_2.8H_2O$	Pyrite FeS_2
0-1	4.5	6.97	4.32	16.49	1.79	-0.36	-100
1-2	0.7	7.16	2.01	11.88	0.39	5.35	-50.3
2-3	0	6.78	0.1	8.06	-1.07	3.76	-35.3
5-7	-4	6.56	-5.25	-2.64	-6.65	-0.08	7.95
9-11	-4	6.89	-5.03	-2.2	-6.73	-1.01	8.82
13-15	-4	7.32	-4.18	-0.5	-6.49	0.98	8.45
20-25	-4	7.63	-3.53	0.8	-6.57	-1.42	2.19

Depth (cm)	Birnessite MnO_2	$MnHPO_4$	Rhodochrosite $MnCO_3$	Gibbsite $Al(OH)_3$	Calcite $CaCO_3$	Hydroxylapatite $Ca_5(PO_4)_3OH$
0-1	-11.63	2.28	-0.64	1.91	-1.36	0.39
1-2	-18.45	3.59	-0.21	2.07	-0.88	5.30
2-3	-21.47	3.18	-0.72	2.2	-1.27	2.96
5-7	-30.71	2.15	-1.33	2.11	-1.54	-0.02
9-11	-29.46	2.43	-1.08	2.47	-1.27	2.11
13-15	-27.74	2.68	-0.55	2.13	-0.71	4.76
20-25	-26.91	2.17	-0.6	1.09	-0.76	3.63

Scanning electron microscopy

SEM analysis of the sediment supports the grain size analyses (Section 3.3.1.1), with grain size ≈ 10 μm appearing very common. Table 3.12 presents trends in At % for Fe, S and P from SEM-EDS map sum spectra, from sediments of different depths in a summer core (F11 C4). Fe was highest in the surface sediment and then was reasonably consistent with depth. P decreased with depth while S increased. This increase in S minerals with depth is apparent in Figure 3.10. Element spectra from spot analyses of individual grains of these S minerals indicated that they are FeS_2 These grains were generally framboidal in habit (Figures 3.11 and 3.12). Although more common in the deeper sediments, the framboidal pyrite was also present in the surface sediments. Element mapping and spot spectrum analysis also identified Fe (hydr)oxide (Figures 3.13 and 3.14) and apatite

(Figures 3.14 and 3.15) minerals and indicated the co-existence of Fe(hydr)oxides and FeS_2 (Figure 3.14) in near surface sediments (3 – 4 cm).

Figure 3.16 presents an EDS element spectrum for a precipitate filtered from the pore water of sediment from core F11 C4, 2-3 cm depth, which had been allowed to oxidise after sampling. The precipitate was an Fe (hydr)oxide which confirms the potential for precipitation of Fe (hydr)oxides from pore waters when they are oxidised. The analysis also confirms the association of P with these hydroxides. Mn was not identified in the analysis indicating that Mn (hydr)oxides did not precipitate.

Table 3.12 Atomic % for selected elements as analysed by SEM-EDS map spectra, in sediments from differing depths in core F11 C4. nd = not detected.

Sediment depth (cm)	Fe	S	P	Mn
	(At %)			
0-1	2.7	0.4	0.3	0.0
3-4	2.1	0.5	0.2	nd
5-7	1.7	0.7	nd	nd
13-15	2.0	1.1	0.1	nd

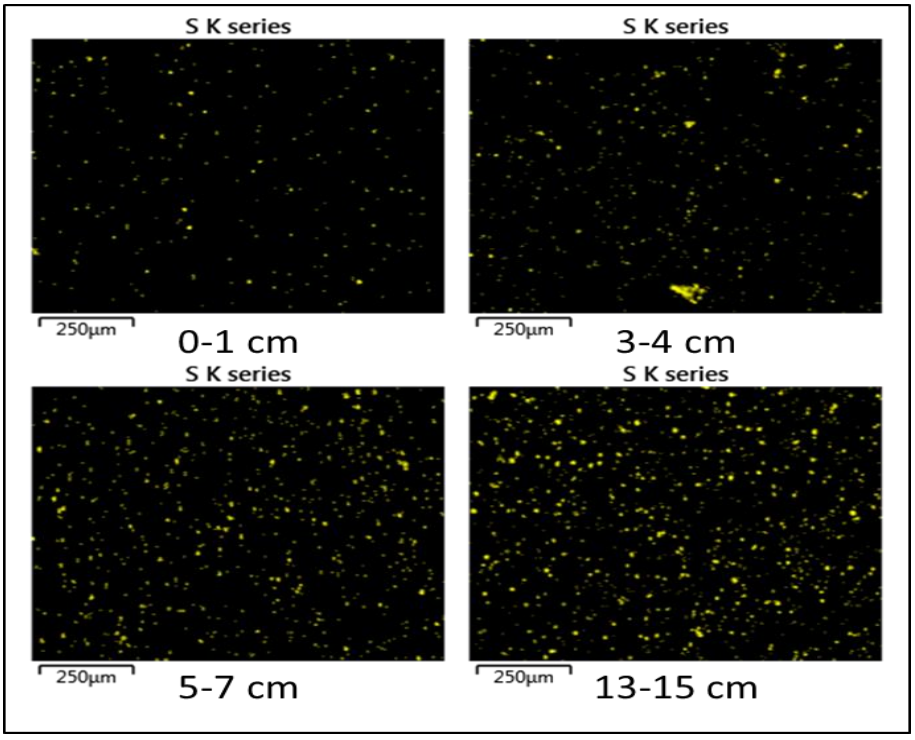

Figure 3.10 SEM-EDS element maps (100x magnification) for S for sediments from differing depths in core F11 C4. Yellow indicates S bearing mineral phases.

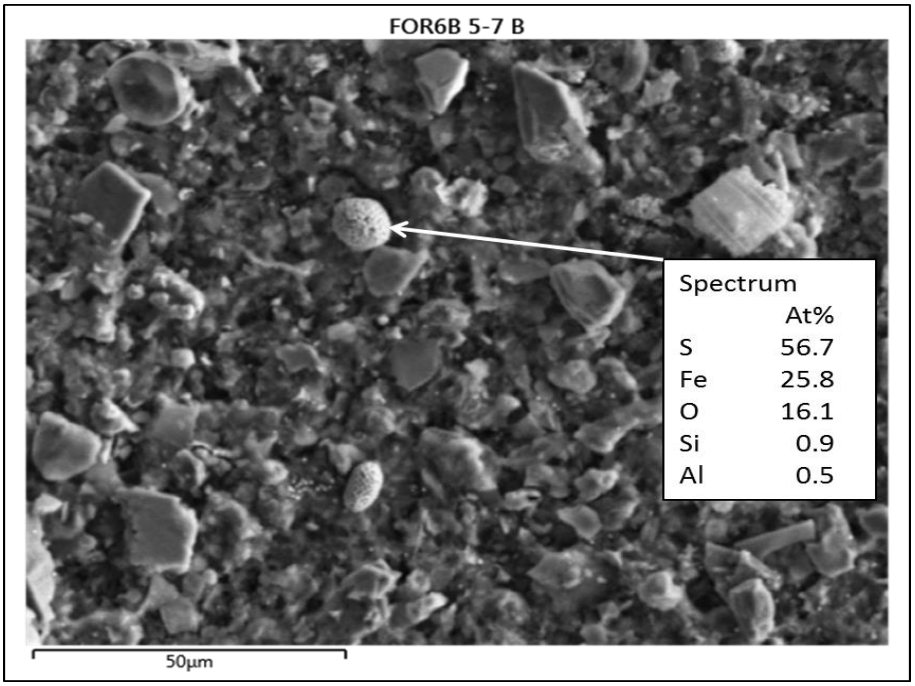

Figure 3.11 SEM image (800x magnification) of core F11 C4 sediment from 5-7 cm depth with an EDS spot spectrum (At %) from a framboidal FeS_2 grain indicated by the arrow. A similar grain can be seen approximately 50 µm below the identified grain.

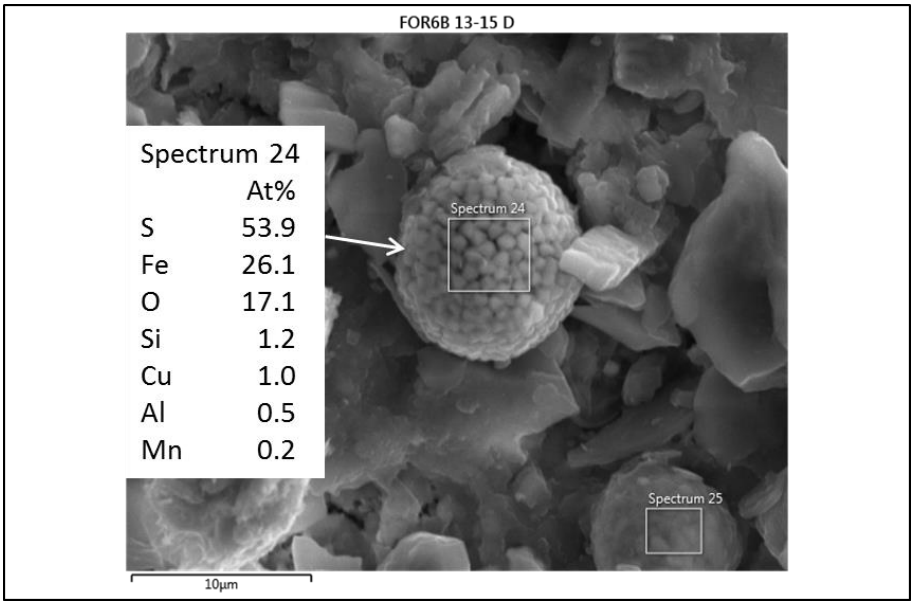

Figure 3.12 SEM image (2000x magnification) of core F11 C4 sediment from 13-15 cm depth with an EDS spot spectrum (At%) from a framboidal FeS_2 grain indicated by the arrow.

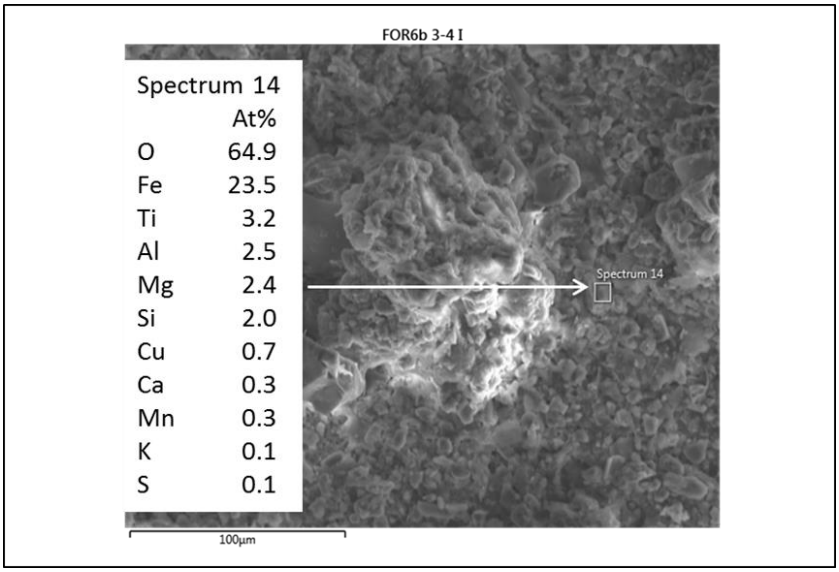

Figure 3.13 SEM image (400x magnification) of core F11 C4 sediment from 3-4 cm depth with an EDS spot spectrum (At%) from a Fe (hydr)oxide mineral indicated by the arrow.

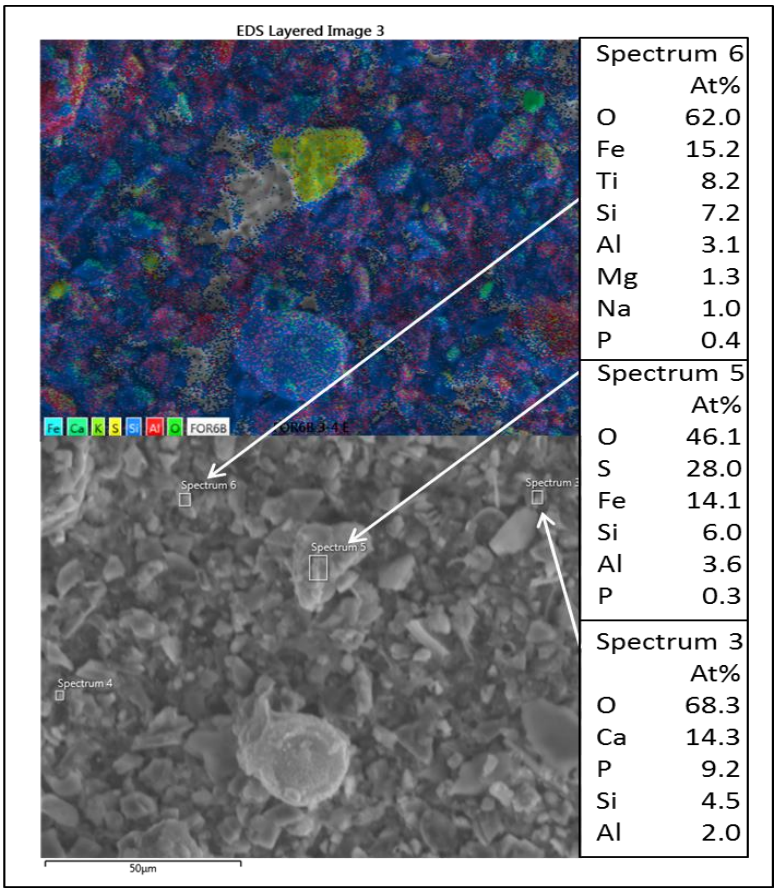

Figure 3.14 A layered element map (top) and image (bottom) of sediment from core F11 C4 3-4 cm, with EDS spot spectra analysis positions marked. Spectra indicate co-existing Fe (hydr)oxide, FeS_2 and apatite. (800x magnification).

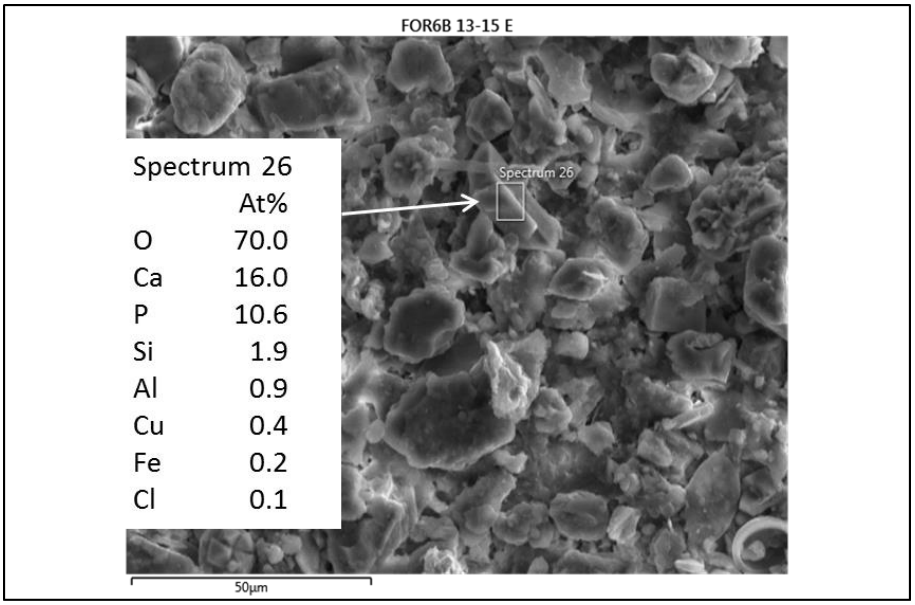

Figure 3.15 SEM image (800x magnification) of core F11 C4 sediment from 13-15cm depth with an EDS spot spectrum (At %) from a euhedral apatite grain ($Ca_4(PO_4)_3(OH,Cl,F)$ indicated by the arrow.

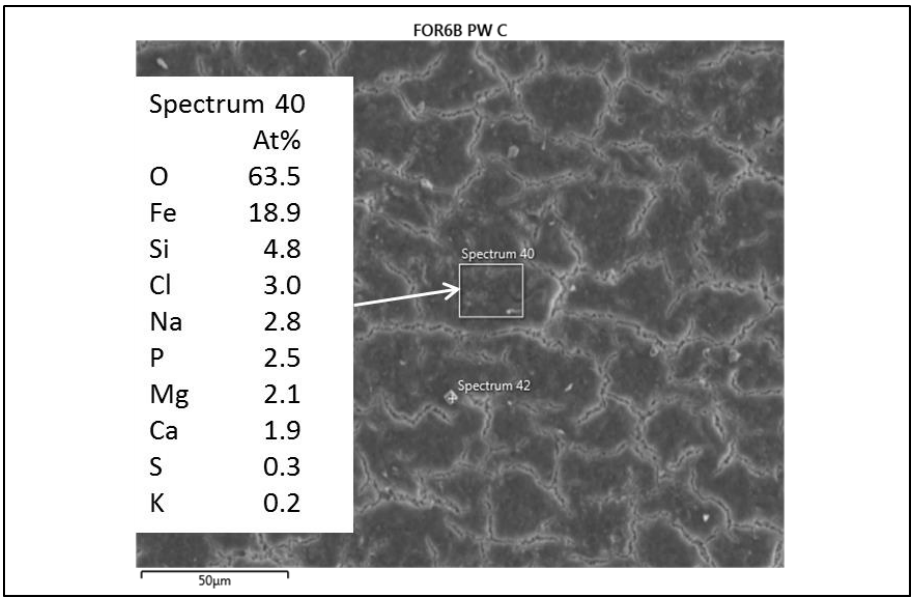

Figure 3.16 SEM image (800x magnification) and an EDS spectrum (At%) of a Fe(hydr)oxide precipitate filtered from F11 C4 2-3 cm pore water which was allowed to oxidise prior to filtration.

3.3.2 Sediment pore water chemistry and redox conditions

Pore water chemistry for a core processed under a N_2 atmosphere (F11 C4) is presented in Table 3.4. This is one of few cores processed under N_2 and as such represents chemical

concentrations unaffected by oxidation during processing (see also, Section 3.2.3.5). Pore water chemistry for other cores is presented in Appendix 2.

The dissolved concentrations of Na, Cl, K and Mg were moderately high, reflecting the brackish nature of the lake. The increase with depth of these elements may be related to changing salinities in the lake over time (See Chapters 4 and 5). [TD-S] was high in the upper sediments and decreased with depth, as did [TD-Fe] and [TD-Mn]. pH was measured in a separate core (see Section 3.2.5) and was generally circum-neutral with a slight increase with depth to 7.63 at 20-25 cm depth.

3.3.2.1 Depth profiles

Figure 3.17 presents the total dissolved concentrations for P, Fe, Mn and S in the pore water of four summer cores, from two different sampling sites. Two of these were sampled prior to algal bloom formation (pre-bloom) and two were sampled during bloom events (post-bloom initiation, PBI).

The two pre-bloom cores from different sites showed similar trends in pore water chemistry with sediment depth. TD-Fe concentrations were stable or slightly increasing for the first few cm below the water-sediment interface, after which a steep increase occurred to a peak at about 10-12 cm, below which concentrations decreased. Marked changes in the slope of the [TD-Fe] with depth curves occurred at 2 - 3 and 3 - 4 cm, and were likely caused by a redox threshold below which Fe reducing conditions prevail. TD-Fe concentrations peaked at 0.039 and 0.065 $mg.L^{-1}$, and the increasing [TD-Fe] reflected the reduction of insoluble Fe(III) phases to soluble Fe(II) species. TD-Mn concentrations showed a similar threshold with slight increases down to 1 - 2 and 2 - 3 cm reflecting reduction of Mn(III) and Mn(IV) to more soluble Mn(II). Below this, concentrations decreased. The TD-S concentrations were relatively stable or showed slight decreases down to 10 cm, below which more rapid decreases occurred, likely caused by a S(VI) to S(-II) (SO_4 to S) reduction reaction. The corresponding decrease in [TD-Fe] and [TD-S] below 10 cm likely indicates precipitation of Fe and S as FeS and/or FeS_2. The P concentration increased slightly below the Fe(III)/Fe(II) threshold but then more significantly below the S(VI)/S(-II) threshold.

The two post-bloom initiation (PBI) cores (Figure 3.17) showed distinct differences in pore water chemistry from the pre-bloom cores described above. The Fe(III)/Fe(II)

threshold at 2 - 4 cm seen in the pre-bloom cores was not evident in the PBI cores. In addition the peak in [TD-Fe] was two orders of magnitude higher in the PBI cores relative to the pre-bloom cores (8.26 $mg.L^{-1}$ in F12 C8 and 0.065$mg.L^{-1}$ in F12 C5) and was also shallower, at 5 cm in the PBI cores as opposed to 10 cm in the pre-bloom cores. One of the PBI cores (F11 C1, Fig 3.16) had a significant [TD-P] peak which coincided with the [TD-Fe] peak at 5 cm depth. This [TD-P] peak was also observed in other core profiles taken during blooms (e.g. Figure 5.12). [TD-Mn] peaks were higher and more pronounced in the PBI cores and occurred at 2-3 cm depth coinciding with the upper edge of the [TD-Fe] peak. The significant decrease in [S] which marked the S(VI)/S(-II) redox threshold, was also at shallower depths in the PBI cores than in the pre-bloom cores. It was apparent then that the redox profile was compressed upwards in the summer PBI cores relative to the pre-bloom cores, with more reducing conditions closer to the sediment surface.

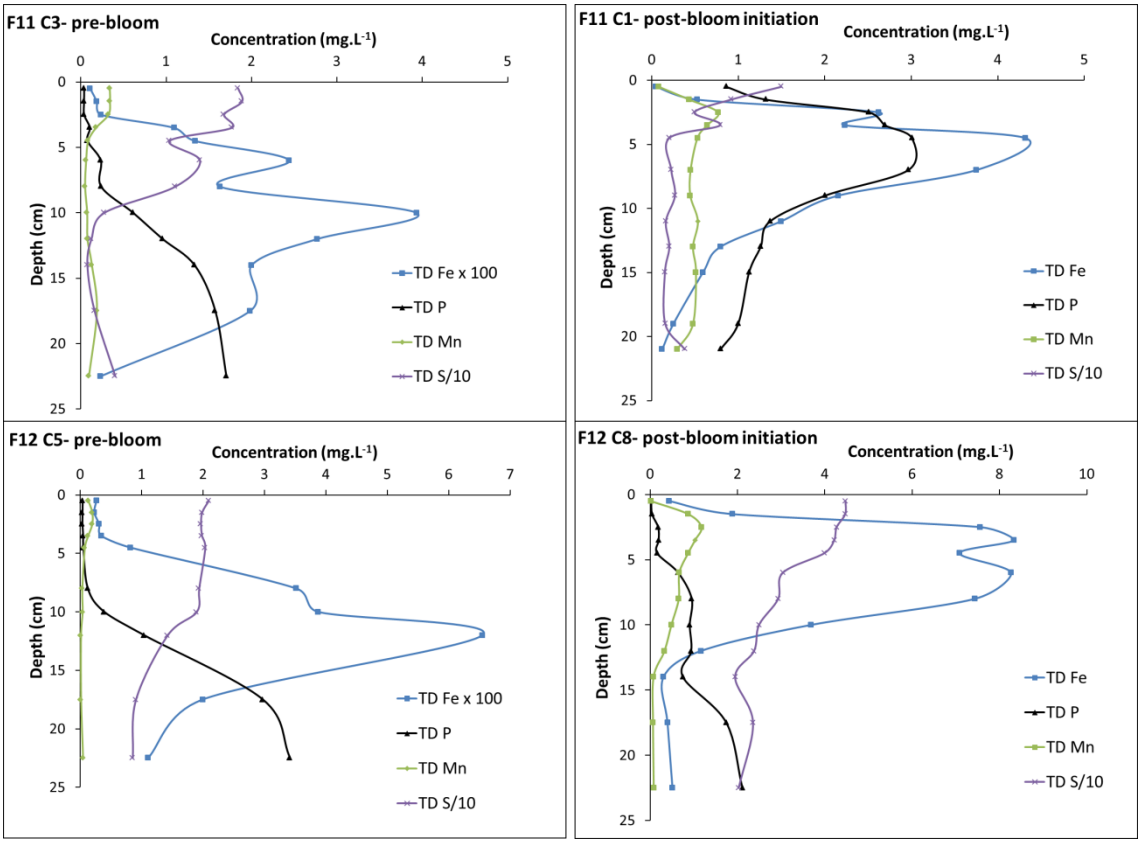

Figure 3.17 Pore water chemistry profiles with depth for four summer sediment cores from two locations. Two of these, F11 C3 and F12 C5 (pre-bloom) were sampled prior to algal bloom formation in the lake. Note that [Fe] is shown at 100 x actual concentrations for these two cores. The other two, F11 C1 and F12 C8 (post-bloom initiation, PBI) were sampled after the beginning of an algal bloom event. TD = total dissolved**.**

Figure 3.18 presents the pore water chemistry for a core sampled during winter (F11 C2). The [TD-Fe] for a summer pre-bloom core (F11 C3) is included for comparison. The pore water chemistry profiles can be compared to those for summer cores in Figure 3.17. The [TD-Fe] in the surface sediments of the winter core was an order of magnitude higher than the pre-bloom summer cores while the [TD-Fe] in the surface sediment pore waters of the PBI cores was an order of magnitude higher again. Whereas the [TD-Fe] in all the summer core pore waters increased substantially with depth to achieve peak concentrations, in the winter core the [TD-Fe] increased only slightly in the first few cm and then decreased with depth. The [TD-Mn] was also elevated between 3-10 cm in the winter sediment compared to the summer pre-bloom profiles. These trends indicated that the upper sediment (<10 cm) experienced a lower redox potential during winter, than during early summer (pre-bloom summer cores), resulting in greater concentrations of reduced, soluble Fe and Mn in the pore water. Pore water [TD-P] in the winter core was slightly higher near the surface than the pre-bloom summer cores, but was significantly lower at depths >10 cm.

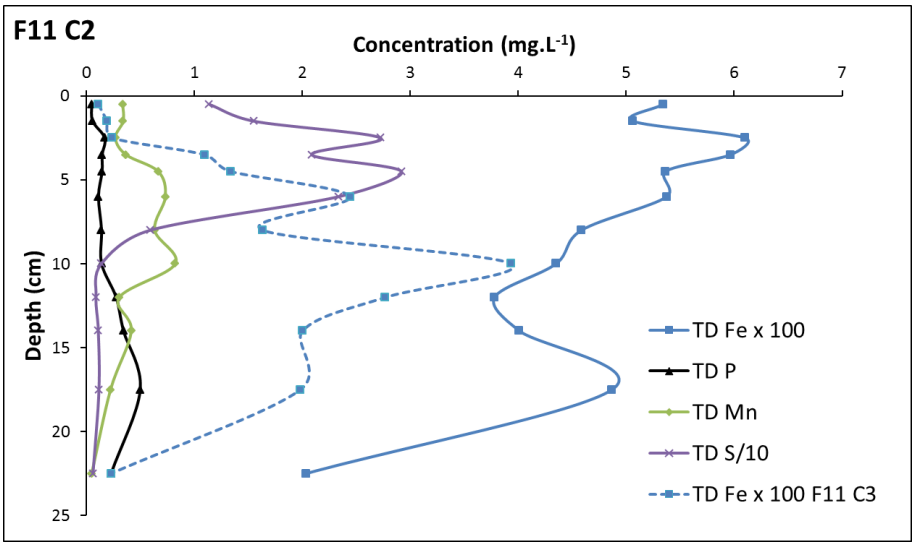

Figure 3.18 Depth profiles for pore water chemistry, for a sediment core sampled during winter. TD = Total dissolved. The [TD Fe] profile from summer core F11 C3 (Figure 3.16) is included for comparison.

3.3.2.2 Geochemical modelling of pore water speciation

Figure 3.19 presents the concentrations of redox affected aqueous species which are key to sediment P binding, in the pore water of core F11 C4, from PHREEQC modelling using the variable chemistry approach (see Section 3.2.5).. The concentration of Total Fe(III) (hydr)oxide species decreased to near 0, by 2 cm depth, while [Fe^{+2}] increased to a

maximum at the same depth. Mn was present almost entirely as reduced Mn(II) at all depths. Low concentrations of Mn(III), and no Mn(IV) or Mn(VI) were predicted. Total [Fe-PO_4 complexes] increased to a 2 cm depth maximum, due to the higher [Fe] in the pore water at this depth. The total [S] profile showed slightly higher concentrations than the SO_4^{-2} profile and the gap between these at depths shallower than 5 cm represents various SO_4 complexes especially $MgSO_4^0$, $NaSO_4^-$ and $CaSO_4^0$. At depths below 5 cm S was largely present as sulphide.

Generally in this core, oxidised forms of Fe and S predominated in the surface sediments, with Fe decreased below 1cm depth. Mn was reduced at all depths, and by 6 cm depth S also is largely in reduced forms.

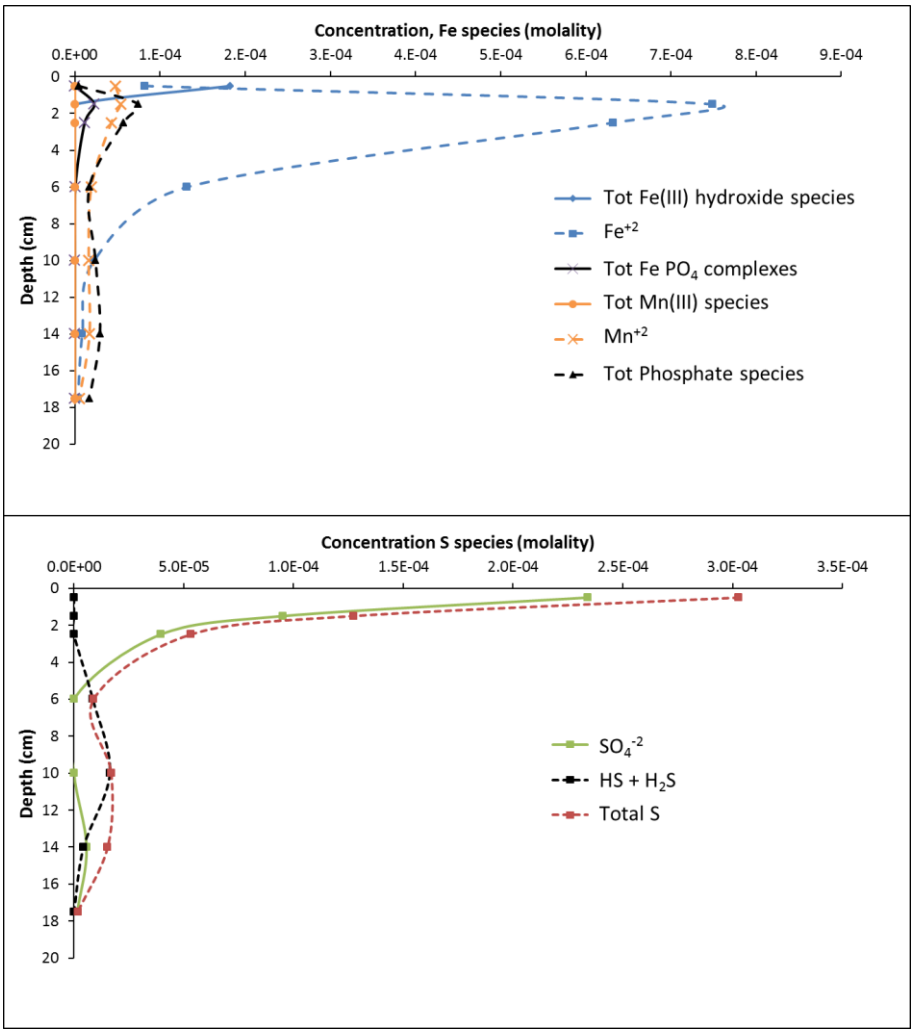

Figure 3.19 Key redox sensitive Fe, Mn and S aqueous species with depth, modelled by PHREEQC using the variable chemistry approach and pore water chemistry from core F11 C4. Total phosphate species are also shown.

The effects of changing redox conditions

Figure 3.20 presents the concentrations of redox sensitive aqueous species from PHREEQC modelling, using the fixed chemistry approach (see Section 3.2.5) and changing the redox conditions. [Fe(III) (hydr)oxide species] decreased steeply as pe dropped below 6 and were replaced by increasing [Fe^{+2}]. Reduced forms of Mn ((Mn(II) + Mn(III)) were the predominant Mn species in all redox conditions with increases in the Mn(III) as redox conditions became more oxidisng. At high redox (pe=13) oxidised Mn concentrations (Mn(VI) + Mn(VII)) were orders of magnitude lower than Fe(III) (hydr)oxide concentrations and the [oxidised Mn] decreased very rapidly as pe droped below 13. The [SO_4^{-2}] remained stable until pe drops below -2 at which stage it decreased steeply while the combined concentrations of sulphide species HS^- and H_2S increased along with [Fe sulphide complexes].

This modelling suggested that oxidised Mn species were minor components of the pore water chemistry and would be the first species to be reduced, followed by Fe(III) (hydr)oxides at pe < 6. At -2 < pe < 5 soluble Fe^{+2} becomes dominant, while at pe < -2 Fe sulphide species begin to form as SO_4^{-2} is reduced to HS^- and H_2S species.

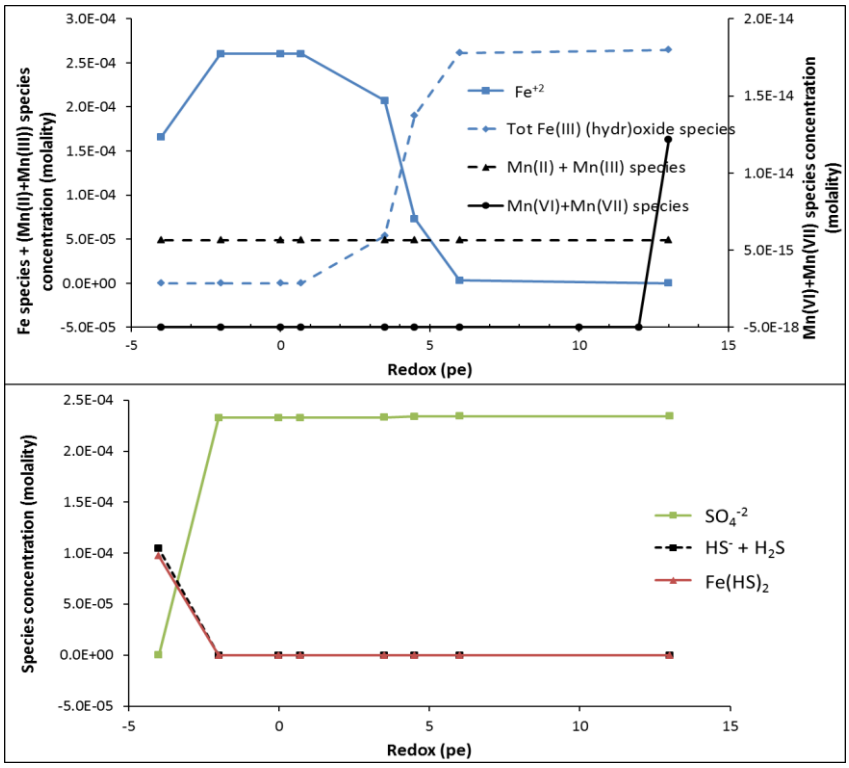

Figure 3.20 Concentration changes in redox sensitive species of Fe Mn and S modelled using the pore water chemistry of F11 C4 sediment from 0-1 cm depth, and using the fixed chemistry approach.

Figure 3.21 presents the effect of changing redox conditions in pore water from core F11 C4 on saturation indices (SI) for selected mineral phases. SI's of < 0 indicate a phase is unlikely to precipitate and that already precipitated minerals will dissolve. Oxidised Mn(IV) mineral phases such as birnessite (MnO_2) became unstable at pe < 10, while Fe(III) (hydr)oxide mineral phases continued to be stable at much lower redox conditions, down to pe ≤ 0. Al (hydro)xides were thermodynamically stable with SI > 0 under all modelled redox conditions. Fe(III) PO_4 phases such as strengite ($FePO_4.2H_2O$) remained stable down to pe = 2 and below this Fe(II) PO_4 phases such as vivianite ($Fe(PO_4)_2.8H_2O$) remain stable. Iron sulphide phases such as pyrite (FeS_2) were stable at pe < -2.5.

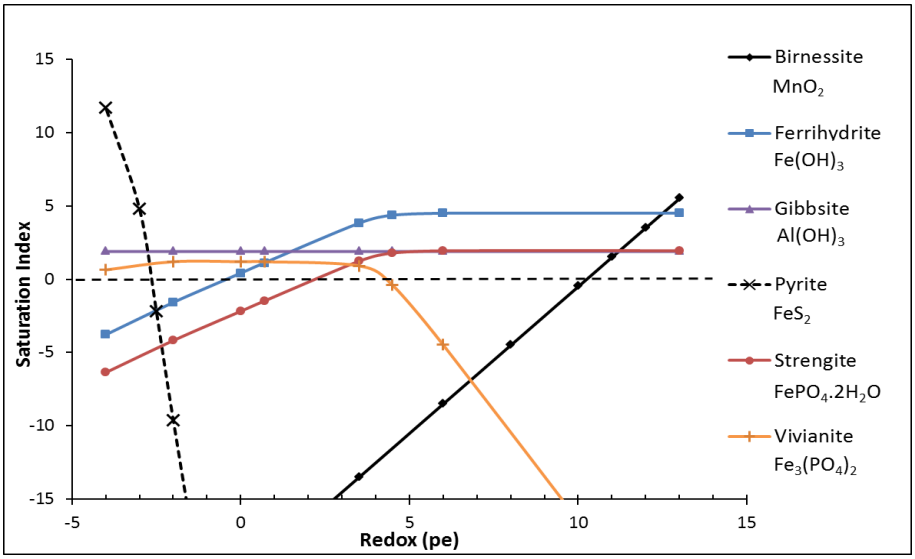

Figure 3.21 Redox related changes in saturation indices for representative mineral phases, modelled using the pore water chemistry from core F11 C4 and the fixed chemistry approach.

PHREEQC modelling was also used to test the hypothesis that redox conditions are the dominant mechanism causing the temporal variations seen in the pore water profiles discussed in Section 3.3.2.1. In order to isolate the effect of redox from the effect of dynamically changing pore water chemistry, a fixed chemistry approach was taken (see Section 3.2.5) using pore water chemistry from the sediment of core F11 C4 0-1 cm. Due to this approach the modelled species concentrations were unlikely to reflect actual concentrations, but the concentration trends could still be used to provide insight into the effects of changing redox conditions in the sediment pile, and to help interpret the temporal changes seen in Wairewa sediment pore water chemistry.

Three redox profiles used in the modelling are presented in Table 3.13. These were estimated from the pore water chemistry of three cores, which were interpreted as representing different redox regimes in the lake sediment. The results of this modelling are presented in Figures 3.22 (aqueous species) and 3.23 (saturation indices). Figure 3.23 also shows the redox profiles in graphical form. The actual pore water chemistry profiles of the cores on which the modelled redox profiles were based (F11 C3 (summer pre-bloom), F12 C8 (summer post-bloom initiation) and F11 C2 (winter)), are presented in Figures 3.17 and 3.18 respectively.

Table 3.13 Redox conditions used for modelling of depth profiles of chemical species and mineral stability using the fixed chemistry approach. Redox profiles were estimated from the pore water chemistry in three cores representing different redox conditions.

Depth (cm)	Redox (pe) profile estimated from pore water chemistry of;		
	F11 C2 (Winter)	F11 C3 (Summer Pre-bloom)	F12 C8 (Summer PBI)
0-1	3.5	13	4.5
1-2	3.5	6	3.5
2-3	0.7	6	0.7
5-7	0	3.5	0
9-11	-4	0	-4
13-15	-4	-4	-4
20-25	-4	-4	-4

The modelled [Fe^{+2}] profiles in Figure 3.22 accurately reflected the shape of the [Fe] curves in the respective cores from which the redox profiles were estimated, confirming that the temporal changes seen in the pore water chemistry profiles in Wairewa sediment cores, can be explained by redox conditions.

The peak of the [Fe^{+2}] curves became shallower as more reducing conditions were simulated in the shallower sediments, culminating in a significant increase in the [Fe^{+2}] at the sediment/water interface (Fig 3.22 c). At the same time [Fe(III) hydroxide species] declined significantly in the upper sediments with decreasing pe. The depth at which [SO_4^{-2}] declined steeply and [$Fe(HS)_2^0$] increased, became shallower as conditions become more reducing.

The SI for ferrihydrite decreased with depth (Figure 3.23), with the steepest decrease occurring in the more reduced pore water profile. In the pre-bloom profile, ferrihydite

remained stable down to around 10 cm, while in the winter and PBI cores it remained stable only down to 5 cm. The SI for MnO_2 in the surface sediment quickly decreased to SI << 0 as redox decreased and MnO_2 was only stable in the upper 1 cm of the pre-bloom core. Pyrite became stable at a shallower depth in the more reduced redox profiles. The SI's for strengite decreased in the upper sediments, a trend which was accompanied by an increase in the SI's for vivianite.

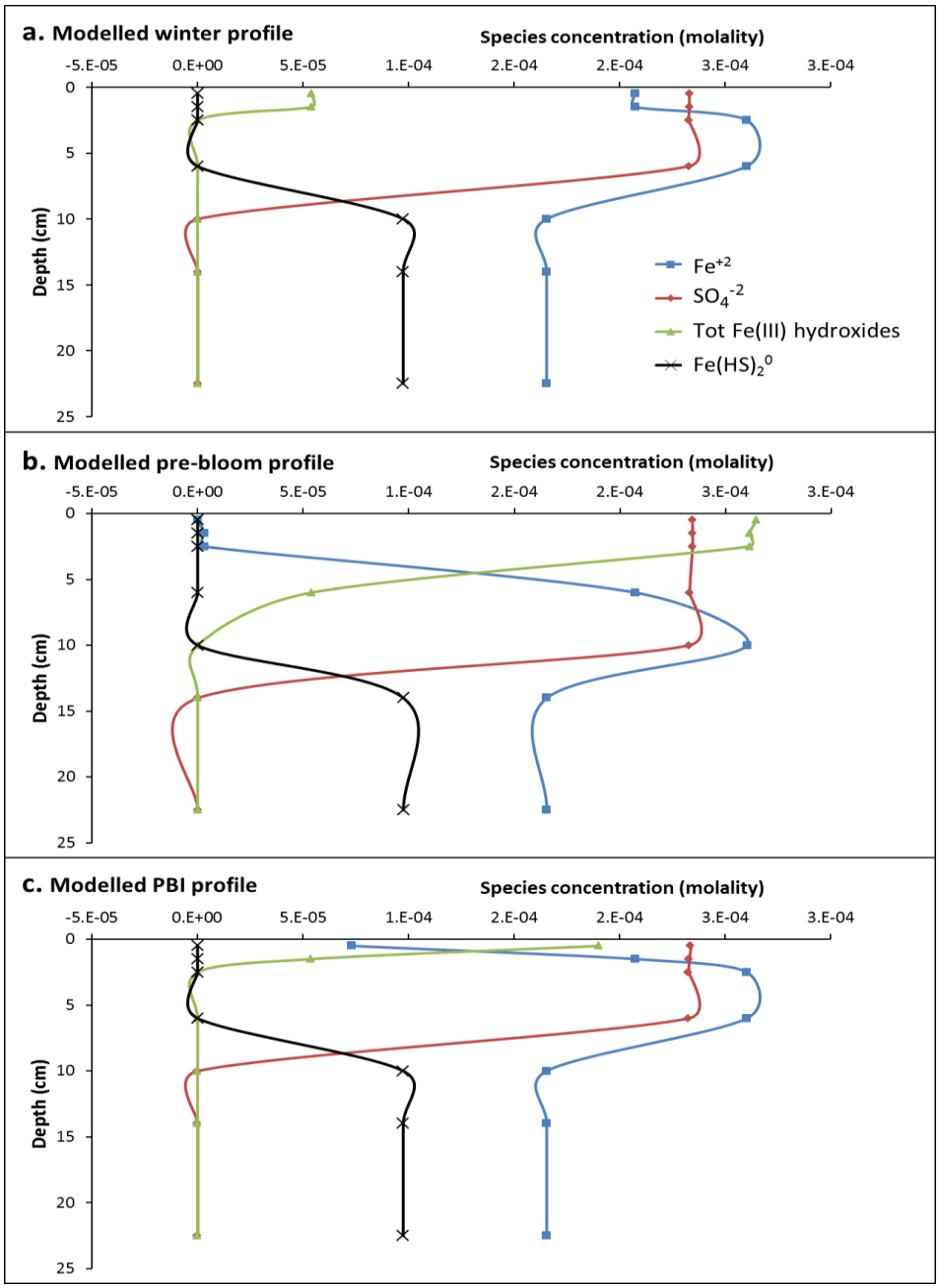

Figure 3.22 Modelled seasonal changes in Fe and S species in pore water with sediment depth, from solution modelling using the pore water chemistry of F11 C4 0-1 cm and the fixed chemistry approach. Depth profiles are based on varied redox conditions (Table 3.13) estimated from pore water chemistry relationships in cores; (a) F11 C2 (winter), (b) F11 C3 (summer pre-bloom), (c) F12 C8 (summer PBI)

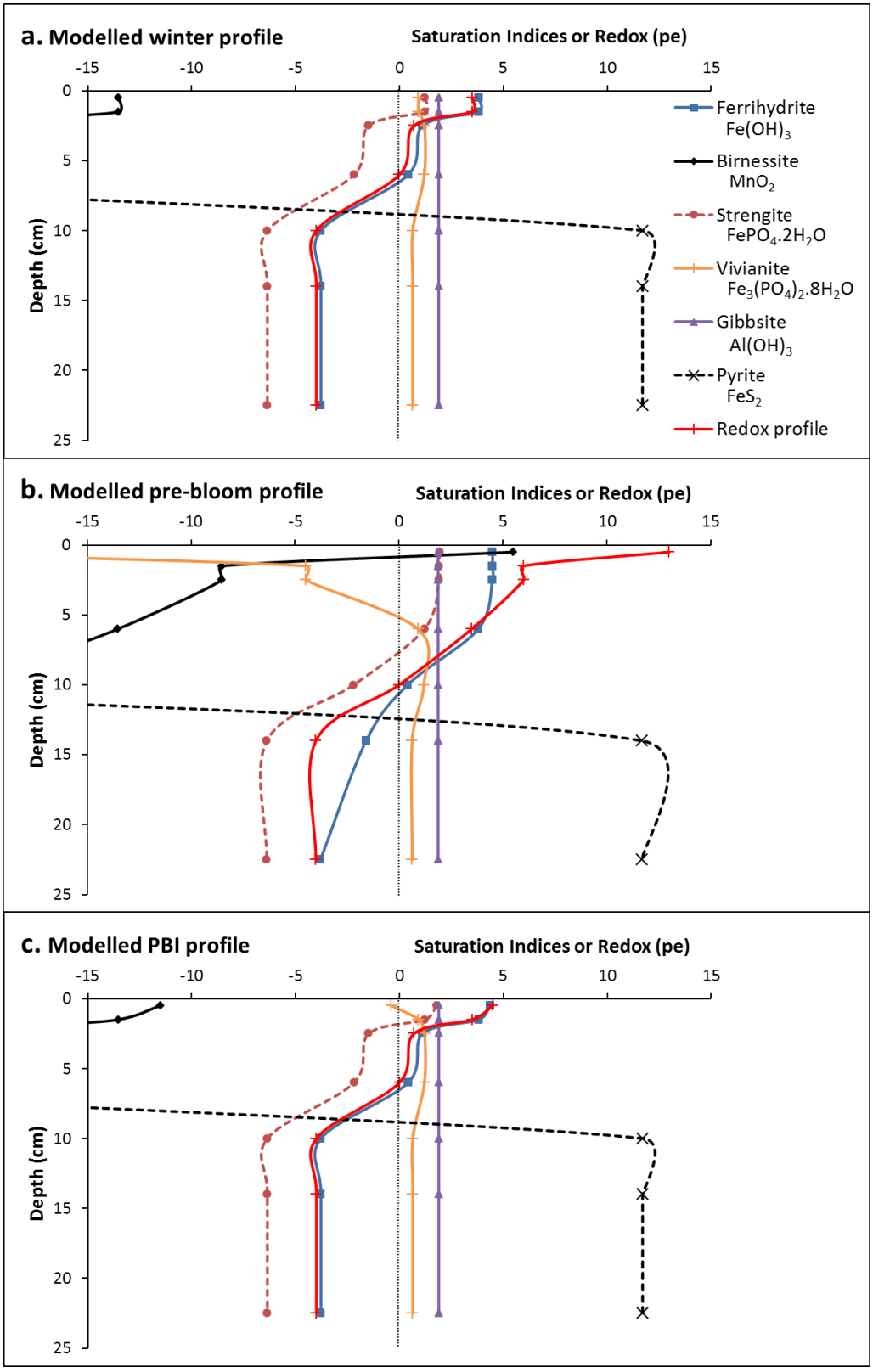

Figure 3.23 Modelled seasonal saturation indice profiles with sediment depth using the pore water chemistry of core F11 C4 0-1cm and the fixed chemistry approach. Depth profiles are based on varied redox conditions (Table 3.13) which have been estimated from pore water chemistry relationships in cores (a) F11 C2, (b) F11 C3, (c) F12 C8

The effect of changing [Fe] on Fe-phase stability

The effect of changing [Fe] in the pore water on the stability of Fe phases for given redox conditions, was also modelled. This modelling is somewhat problematic as, in the natural system, the analysed pore water chemistry is representative of the redox conditions of that particular sediment and hence, changing redox conditions would naturally result in changing chemical concentrations. However, modelling a static concentration while changing redox conditions, does give some insight into likely effects on mineral phase stability. Figure 3.24 presents the saturation indices under various redox conditions and [Fe].

Increasing [Fe] increased the stability of ferrihydrite shifting SI = 0 from pe = 1 to pe = -1. Similarly for strengite and vivianite, the SI increased with increases in [Fe]. However pyrite stability was little affected.

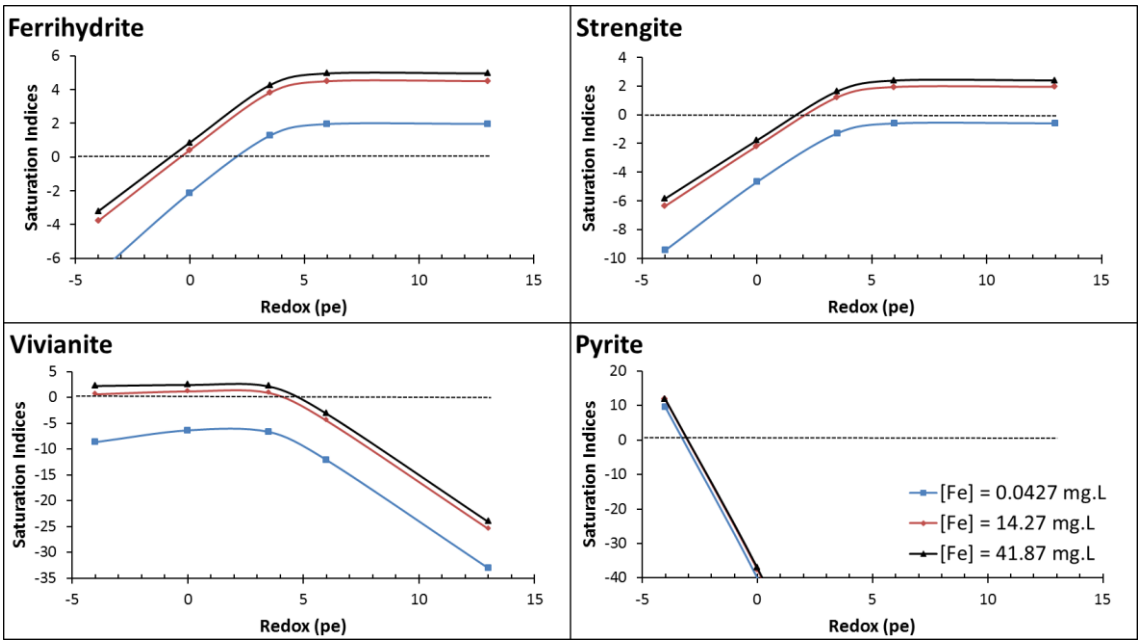

Figure 3.24 The effect of Fe concentration on saturation indices under varying redox conditions modelled in PHREEQC. [TD-Fe] from F11 S5, F11 C4 0-1 cm, and F11 C4 1-2 cm were used for the low, medium and high values respectively.

The effect of increased [S] in reduced sediments

PHREEQC modelling was used to assess the effects of changing [S] on key species and saturation indices in reduced sediments (pe = -4). Table 3.14 presents the changes in total Fe-$HS_{(aq)}$ ($Fe(HS_2)^0$ + $Fe(HS)_3^-$) and total Fe-$PO_{4(aq)}$ ($FeHPO_4^0$ + $FeH_2PO_4^+$ + $FeHPO_4^+$ + $FeH_2PO_4^{+2}$) complexes, as well as pyrite, Fe(hydr)oxides and Fe-PO_4 mineral saturation

indices. Increasing the [S] significantly increased the proportion of Fe present as total Fe-$HS_{(aq)}$ complexes and simultaneously decreased the proportion present as total Fe-$PO_{4(aq)}$ complexes. The proportion of [P] present as Fe-$PO_{4(aq)}$ complexes also decreased. At the same time vivianite became undersaturated with increasing [S], while strengite, pyrite and ferrihydrite were undersaturated at all S concentrations. The more crystalline Fe (hydr)oxide, goethite was close to saturation at the lowest [S] and became increasingly undersaturated with increasing [S], while hematite was saturated at lower [S] and undersaturated at the two highest S concentrations.

Table 3.14 The effect of changing [S] in a reduced sediment (pe=-4), on total Fe-$HS_{(aq)}$ and total Fe-$PO_{4(aq)}$ species as well as the saturation indices for key mineral species as predicted by solution modelling in PHREEQC.

[S]	**Tot Fe-HS species**	**Tot Fe-PO_4 species**	**Tot Fe-PO_4 species**	**Strengite**	**Vivianite**	**Pyrite**
$mg.L^{-1}$	(% of total [Fe])		(% of total [P])	Saturation Indices		
16.5	19	0.15	5.69	-6.26	0.95	11.41
29.1	37	0.12	4.50	-6.36	0.64	11.7
100	94	0.01	0.01	-7.36	-2.38	12.09
725	100	0.00	0.00	-9.69	-9.35	11.99

[S]	**Ferrihydrite**	**Goethite**	**Hematite**
$mg.L^{-1}$	Saturation Indices		
16.5	-3.67	-0.93	0.51
29.1	-3.78	-1.04	0.30
100	-4.80	-2.06	-1.74
725	-7.12	-4.38	-6.39

The effect of increasing pH on Al (hydr)oxide stability in oxic surface sediments

Al (hydr)oxide phases have been shown to adsorb P, and to dissolve at the pH of the NaOH extraction step of the sequential extraction scheme (pH = 10). Geochemical modelling was used to assess the effect of increasing pH in the lake water column (pH = 6.5 – 10) on the stability of Al (hydr)oxides in the oxic surface sediments. Table 3.15 presents the results of this modelling. Diaspore is the only phase for which the SI remains above 0 at pH = 10. In contrast the amorphous $Al(OH)_3$ phase is under-saturated down to pH = 6.5. The remaining phases become under-saturated at varying stages between $6.50 < pH < 10$.

Table 3.15 The effect of pH on the saturation indices for Al(hydr)oxide phases predicted by PHREEQC modelling of oxic sediments. 'am' indicates an amorphous phase.

pH	$Al(OH)_3$ am	Al_2O_3	Boehmite (AlOOH)	Gibbsite ($Al(OH)_3$)	Diaspore (AlOOH)
	Saturation indices				
6.50	-0.52	0.80	1.68	2.04	3.43
7.00	-0.67	0.51	1.54	1.89	3.29
8.00	-1.55	-1.25	0.66	1.01	2.40
9.00	-2.51	-3.11	-0.29	0.04	1.46
10.00	-3.54	-5.23	-1.33	-0.98	0.41

3.3.3 Sedimentary P binding and flux

3.3.3.1 P fractionation

Table 3.16 presents sequential extraction results for the surface sediments of three summer cores and one winter core. Further sequential extraction data from surface sediment analyses is presented in Appendix 1. The total sedimentary P (TSP) concentrations in the summer surface sediments were relatively consistent between the cores, ranging from 1465-1549 $mg.kg^{-1}$ with an average of 1517 $mg.kg^{-1}$. In the summer cores the redox sensitive BD-P fraction (reactive Fe and Mn (hydr)oxides) represented 25% of the total, while the pH sensitive NaOH-rP fraction (absorbed to less reactive Fe (hydr)oxides and Al (hydr)oxides) represented just under 20% of the total. A repeat sequential extraction on summer core F12 C7, which missed the reducing BD step and instead used the high pH NaOH-rP step directly after the NH_4Cl step, indicated that around 25% of the redox sensitive BD-P fraction was also sensitive to high pH desorption. If this is applied to the average figures in Table 3.17, then around 30% of the total P is susceptible to high pH related desorption. Summer core organic-P comprised around 15% of the TSP pool and the remaining 43% consisted of the less mobile HCl-P (apatite + refractory oxides) and the Res-P (refractory organics). The winter surface sediment data shown in Table 3.16 are discussed below in Section 3.3.3.2.

Table 3.16 P fractions in the surface sediments (0-1 cm depth) of three summer core (F11 C1, F11 C3, F12 C7) and one winter core (F11 C2). The 'NaOH-rP only' fraction from Core F12 C7, is the P in an NaOH extract, without the preceding BD extraction.

Fraction	F11C1	F11C3	F12C7	Summer Average		F11 C2	
	mg.kg^{-1}	mg.kg^{-1}	mg.kg^{-1}	mg.kg^{-1}	% total	mg.kg^{-1}	% total
Total P	1539	1465	1549	1517	100	1518	100
NH_4Cl-P	9	2	1	4	>1	0.5	>>1
BD-P	332	345	474	384	25	200	13
NaOH-rP	284	240	248	257	17	324	21
Org-P	254	212	168	212	14	367	24
HCl-P	236	245	345	275	18	255	17
Res-P	423	421	314	386	25	370	24
NaOH-rP only			373				

Sequential extraction data for full core depths are presented for two summer cores. Table 3.17 presents P fractions with depth for the summer pre-bloom core F11 C3 while Figure 3.25 presents phosphorus fraction profiles with depth, for summer PBI core F11 C1. These were typical of the profiles seen in all summer cores analysed by sequential extraction (Table 3.1). The data for other analysed cores is presented in Appendix 1. In F11 C1 and C3, [TSP] showed a general trend of significant P enrichment in the surface sediments and decreasing concentration with depth. The greatest concentration decrease occurred in the top few cm of the core. This decrease in [TSP] with depth was mirrored by decreases in [BD-P], [NaOH-rP] and [Org-P]. The [NH_4Cl-P] depth profile showed a similar steep decrease just below the surface sediment. The concentration then remained more consistent down to a depth of 12 cm, below which concentration increased. [HCl-P] was relatively stable with increasing depth, while [Res-P] showed a steep decrease in the upper two cm of the core followed by a more stable concentration profile with increasing depth.

Figure 3.26 presents P fractions as a percentage of [TSP] at different depths in core F11 C1. It is apparent that the changes in concentration of the various P fractions with depth seen in Figure 3.25 resulted in significant changes in the proportions of the various fractions. [BD-P], [NaOH-rP] and [Org-P] all decreased as a percentage of the decreasing [TSP], while the proportion of [Res-P] and, in particular, the [HCl-P] fraction increased.

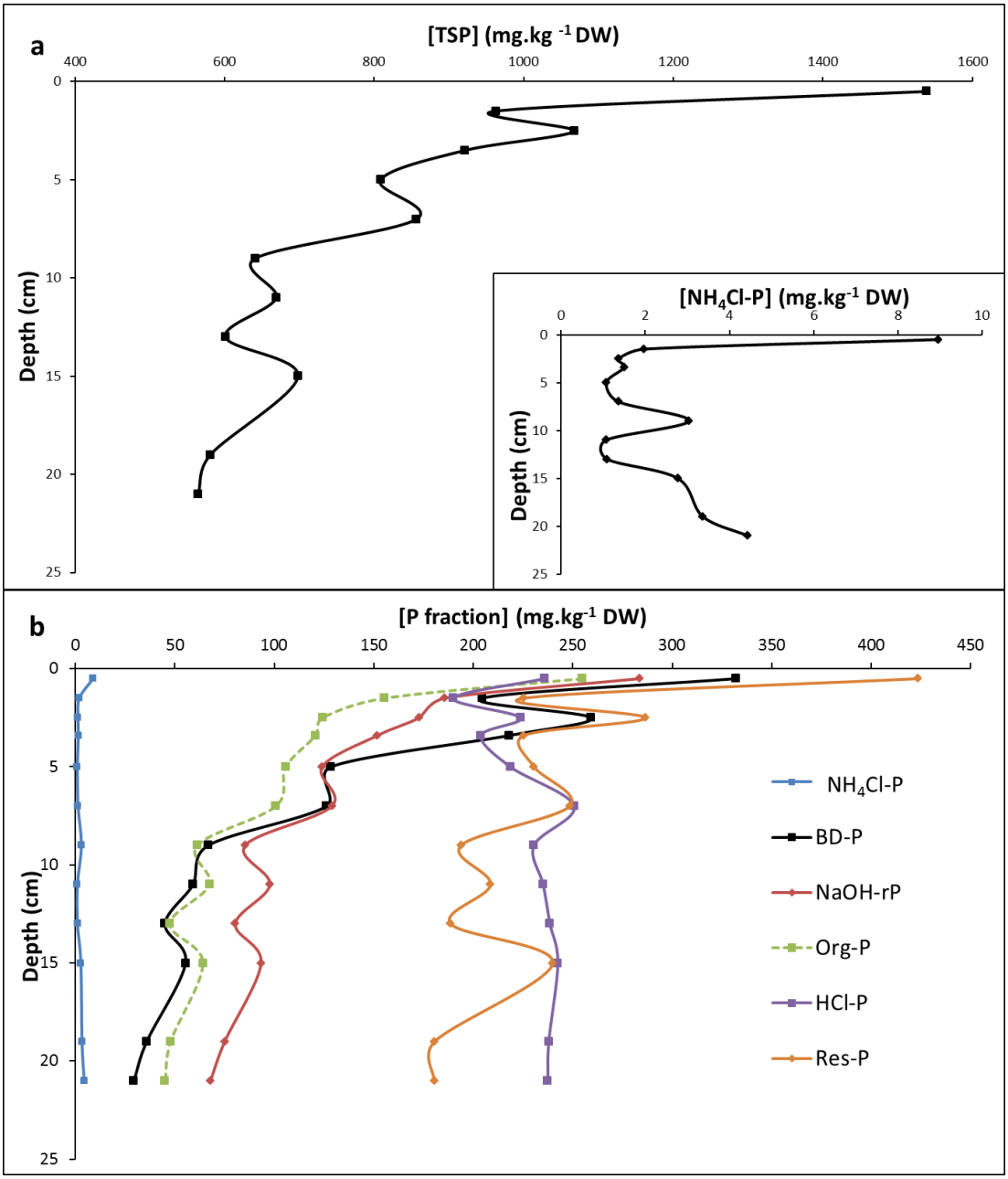

Figure 3.25 Sediment (dry weight = DW) concentrations of (a) total sediment phosphorus (TSP), and (b) phosphorus fractionation, with depth below the sediment/water interface, for core F11 C1. The inset in plot (a) provides better resolution of the NH_4Cl-P fraction.

Table 3.17 P fractions (mg.kg^{-1} DW) with depth (cm) from a sequential extraction of core F11 C3, as well as the total dissolved P (TDP) in the sediment pore water.

Depth	NH_4Cl-P	BD-P	NaOH-rP	Org-P	HCl-P	Res-P	TSP	TDP
cm	mg.kg^{-1}.DW							
0-1	1.45	345	240	213	245	421	1465	0.040
1-2	0.00	298	239	182	238	344	1301	0.038
2-3	0.00	236	154	142	252	257	1041	0.040
3-4	0.00	175	165	153	268	322	1083	0.106
4-5	0.00	150	148	170	242	336	1046	0.079
5-7	0.00	76.9	123	226	230	330	986	0.235
7-9	0.00	69.5	128	217	238	262	915	0.240
9-11	0.00	70.4	129	122	245	328	895	0.615
11-13	0.09	68.9	119	95	224	281	789	0.960
13-15	0.81	71.5	147	110	248	280	858	1.33
15-20	1.73	50.4	105	41.1	247	230	676	1.58
20-25	4.56	23.0	45.4	27.4	197	166	463	1.71

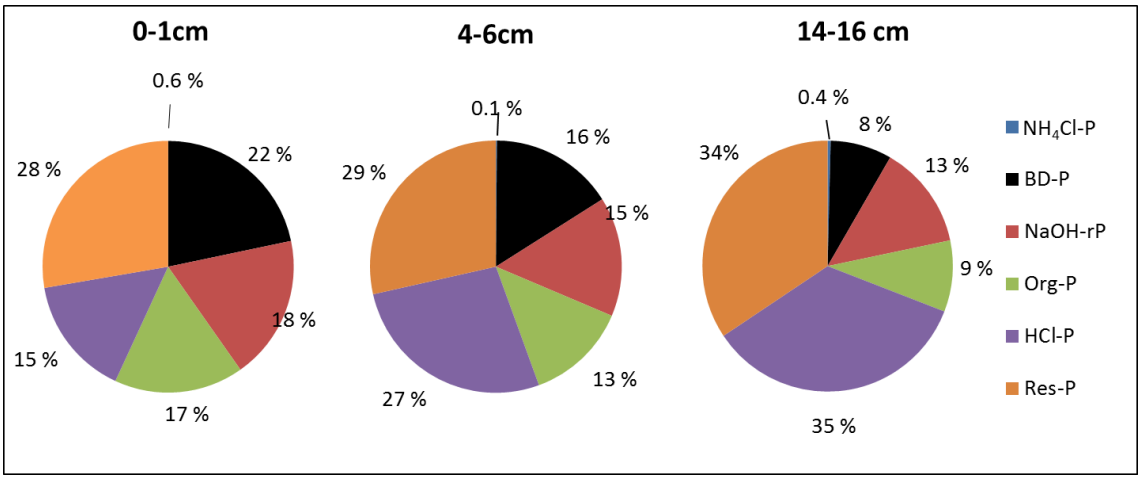

Figure 3.26 Phosphorus fractions as a percentage of TSP at different depths in core F11 C1 as determined by sequential extraction.

3.3.3.2 Seasonal variability

The sedimentary P pool showed significant and consistent changes over time, particularly between seasons. The change in the surface sediment Org-P fraction between summer (average = 14%) and winter (24%) shown in Table 3.16 reflects this. This winter increase in surface sediment Org-P was offset by a decrease in BD-P (summer = 25%, winter =13%). These trends were consistent with those observed in other surface sediment sampling, the data for which is presented in Appendix 1.

Figure 3.27 and 3.28 present depth profiles of the TSP and P fractions from sequential extractions, respectively, for a representative summer core (F11 C1) and a winter core (F11 C2). The [TSP] was the same at the surface, but the winter core showed a slightly lower [TSP] at mid-depth (3-7 cm). This seasonal change in [TSP] was within the uncertainty of measurement and may reflect sample variability. At depths >10cm, the cores showed similar TSP concentrations. When the individual P fractions were compared between seasons however, it was apparent that the concentrations of the more mobile fractions, [NH_4Cl-P] and [BD-P] were substantially higher during the summer months, down to at least 10 cm. The same seasonal variation was seen in the [BD-Fe] but not in [BD-Mn] (Figure 3.29), hence the variability was associated with reactive Fe and not reactive Mn phases. The [NaOH-rP] fraction was higher in the summer core from 3-7 cm depth. The [Org-P] was highly enriched in the surface sediments during winter but was reasonably consistent between the cores below the surface. The [HCl-P] was relatively consistent between seasons as was the [Res-P].

The differences observed in the pore waters of summer pre-bloom and summer PBI cores (Figure 3.17) were not observed in the sequential extraction results. Figure 3.30 presents depth profiles for the most mobile P fraction (BD-P), for summer pre-bloom and PBI cores. It is apparent that the depth profiles were quite similar.

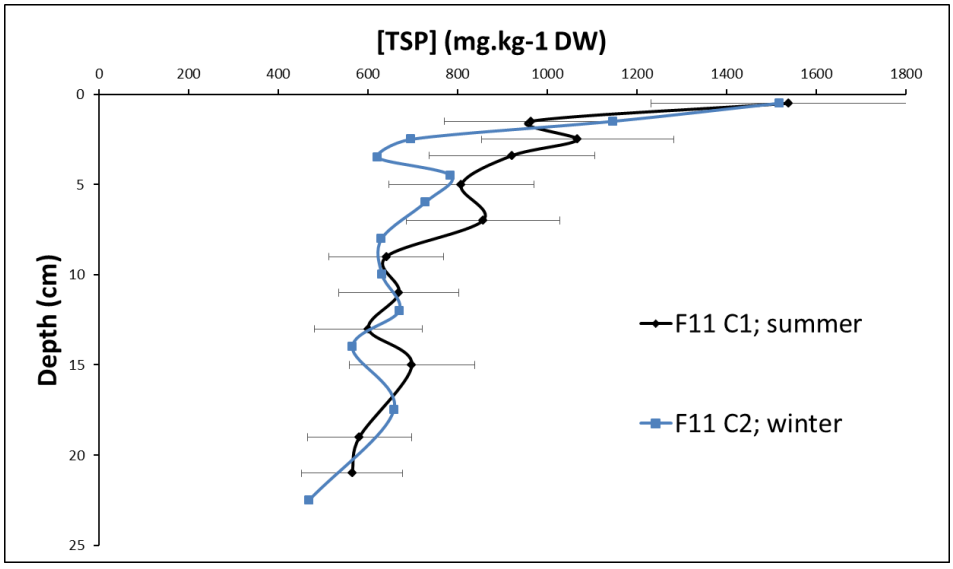

Figure 3.27 Depth profiles for total sedimentary phosphorus in summer and winter cores as determined from sequential extractions. 20% error bars (see Section 2.2.7) are shown for summer curve only.

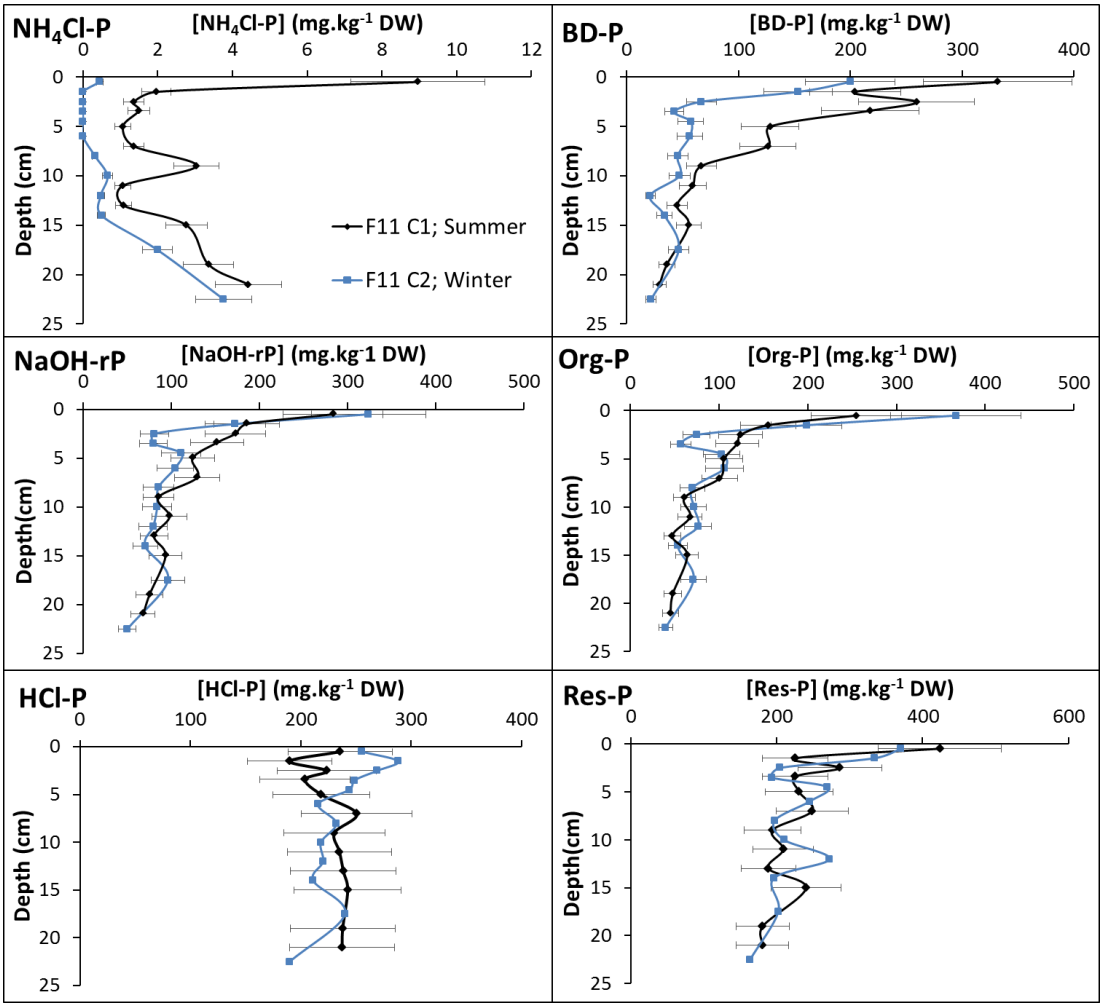

Figure 3.28 Depth profiles for sedimentary phosphorus fractions determined by sequential extraction for summer and winter cores. Error bars are 20 %. For the HCl-P and Res-P error bars are only shown for the summer curve to avoid confusion.

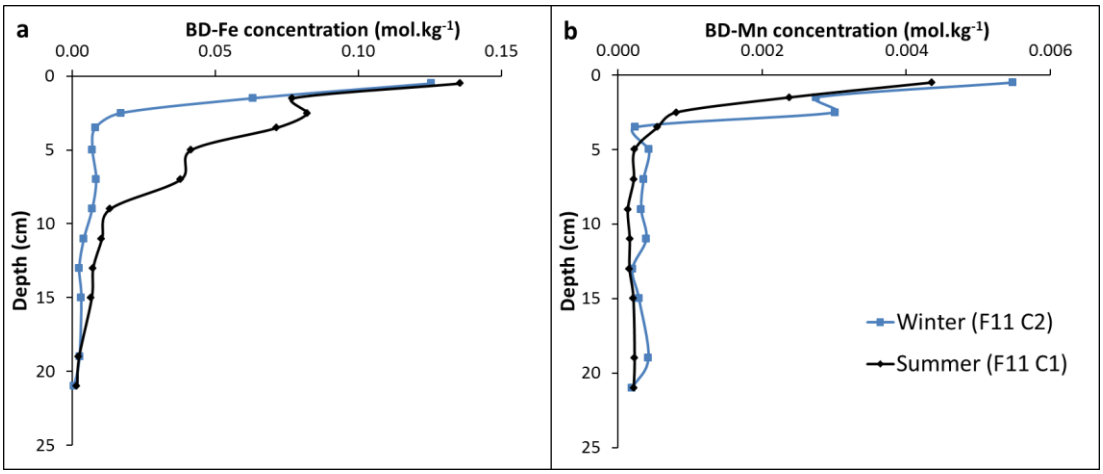

Figure 3.29 Reactive (a) Fe, and (b) Mn, concentrations with depth in the BD extracts of a winter and summer core.

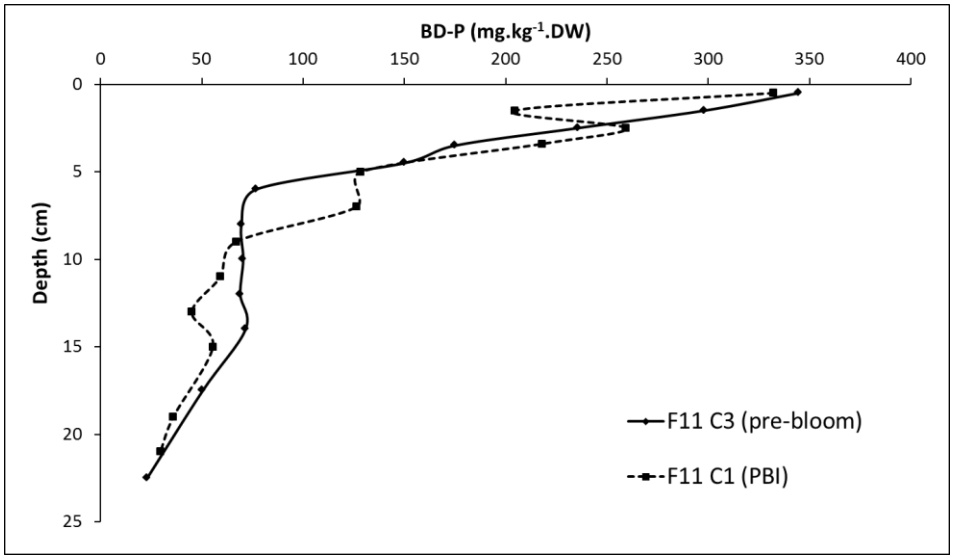

Figure 3.30 Depth profiles for BD-P in a pre-bloom and PBI summer core.

3.3.3.3 EDTA Extraction

Molar ratios were calculated over time for Fe, Mn and P from the EDTA extraction and are presented in Table 3.18. The Fe:P ratio started at approximately 2 and increased to > 2.5 by 120 mins and then continued to increase. Fe:P ratios of around 2 have been used to suggest Fe bound P in the sediment is produced by precipitation of Fe phosphates, whereas Fe:P > 2.5 suggest an adsorption relationship (Nyenje et al, 2014). The Mn:P ratio was low at the beginning and increased to around 0.9 by 480 minutes. This is suggestive of a mineral precipitation relationship rather than adsorption. The high Fe:Mn ratio suggests significant dominance of Fe over Mn in the sediment.

Table 3.18 Molar ratios for Fe, Mn and P over time, from an EDTA extraction on surface sediment from site F12.

Time (mins)	Molar ratios		
	Fe:P	Mn:P	Fe:Mn
60	2.05	0.319	6.44
90	2.37	0.358	6.64
120	2.52	0.392	6.43
180	2.92	0.499	5.87
300	3.83	0.759	5.06
360	3.84	0.802	4.79
420	4.01	0.850	4.73
480	4.14	0.879	4.72
1440	4.54	0.745	6.10
2880	5.33	0.644	8.29

3.4 Discussion

3.4.1 Sediment character and P concentration

The Wairewa sediments consisted of well sorted silts with abundant reactive Fe, and low carbonate concentrations. These silts showed a slight fining towards the southern end of the lake as the distance from the Takaritawai River, the main tributary, increased. Organic matter was highest in the surface sediments and was seasonally variable, with higher organic content during the winter than the summer. A steep decrease in organic matter with sediment depth was evident year round.

The [TSP] in surface sediment samples was reasonably consistent, both spatially and temporally, at around 1500 $mg.kg^{-1}$. Data on TSP concentrations in shallow lakes in New Zealand is scarce, but Lake Horowhenua, a shallow, eutrophic system on the west coast of the North Island has reported P concentrations of 700 $mg.kg^{-1}$ (2011), down from 1300 $mg.kg^{-1}$ in 1988 (Gibbs, 2011). Søndergaard (2007) reported a median value for 32 shallow Danish lakes of 2000 $mg.kg^{-1}$, while Gao et al (2005) reported values of between 1130 and 3450 $mg.kg^{-1}$ in the eutrophic Dianchi lake in south-western China. Hence the TSP concentrations in Wairewa are high but consistent with other eutrophic lake systems.

The sediments in Wairewa showed very significant decreases in [TSP] with sediment depth. The decrease was most pronounced just below the surface with a 29% decrease at 2 cm depth in core F11 C3, a rate of decrease of 260 $mg.kg^{-1}.cm^{-1}$. The rate of decrease remained relatively steep from 2 cm down to 9 cm (53 $mg.kg^{-1}.cm^{-1}$) below which the decrease continued but at a lesser rate (6 $mg.kg^{-1}.cm^{-1}$). This P distribution pattern is common in lake sediments (Søndergaard, 2007) and has been used to indicate an increasing external P load (eg: Gao et al, 2005). However in Wairewa there is no history of recent increases in external load, and the enriched upper sediments are more likely the result of internal P mobility. The decrease with depth of [BD-P], [NaOH-rP] and [Org-P] relative to the consistent concentrations of the more refractory Res-P and HCl-P fractions also suggest a P mobility provenance for the depth gradients. Such upward fluxes of P within the sediment, rather than changes in external loading rates, have been inferred in other lake systems, to explain similar depth gradients (e.g. Moore and Reddy, 1994; Rydin, 2000; Søndergaard, 2007). The causes of this flux of P from deeper to shallower sediments in Wairewa, are discussed further in Section 3.4.3.

3.4.2 Pore water chemistry

3.4.2.1 Seasonal changes in redox conditions

The depth profiles of redox sensitive species in sediment pore waters provided an insight into the dominant processes controlling P binding in the Wairewa sediments, and demonstrated significant seasonal variation. Pore water chemistry profiles differed significantly between winter, summer pre-bloom, and summer PBI cores. These changes indicated distinct seasonal redox conditions with important implications for P binding.

A winter core pore water profile showed a high surface [TD-Fe] relative to the summer pre-bloom pore water. The [TD-Fe] then decreased below the near-surface sediment, indicating Fe(III) to Fe(II) reduction was occurring in the surface sediments. The steep decrease in [TD-Fe] below 3 cm, coupled with the decrease in [TD-S] indicated S(VI)→S(-II) reduction, and precipitation of FeS phases was occurring high in the sediment profile. A similar profile to this was produced experimentally in fully anoxic lake sediments by Lijklema & Hieltjes (1982). An approximation of this winter profile was also replicated in this research, by geochemical modelling of anoxic conditions. This confirmed that the observed pore–water chemistry in the winter core, could be explained by a fully anoxic sediment profile (Figure 3.31). These conditions likely result from decomposition of the increased organic matter in the surface sediment of the winter core, which results from sedimentation of biota at the end of summer/autumn period. Chen et al (2014) demonstrated that the addition of cyanobacterial biomass to the sediment surface increased both Fe(III) and S(VI) reduction in the sediments of the shallow Lake Taihu in China.

In contrast the [Fe] in the pore waters of the pre-bloom summer cores were lower in the surface sediments and increased to a marked peak at mid-core depths (Figure 3.31). These lower TD-Fe concentrations were due to higher redox potentials relative to the winter core, especially in the sediments above the TD-Fe peak. These conditions cause the oxidation of Fe(II) to Fe(III), and the precipitation of Fe (hydr)oxides, thus decreasing the [TD-Fe]. Below the Fe peak, [TD-Fe] decreased steeply, coinciding with a steep decrease in [TD-S], likely due to the reduction of S(VI) to S(-II), and the precipitation of Fe sulphides. These pore water profiles were replicated using geochemical modelling of oxic surface sediments, confirming the role of redox in the pore water trends. The inferred

higher redox conditions in the upper core were consistent with the increase in [NH_4Cl-P] and [BD-Fe] in the sequential extraction profiles of the summer cores, and is likely associated with increasing oxygen production in the lake water column during spring increases in primary productivity and/or lower oxygen demand due to the diminished pool of organic matter in the surface sediments. Increased bioturbation in spring may also oxygenate the upper sediments.

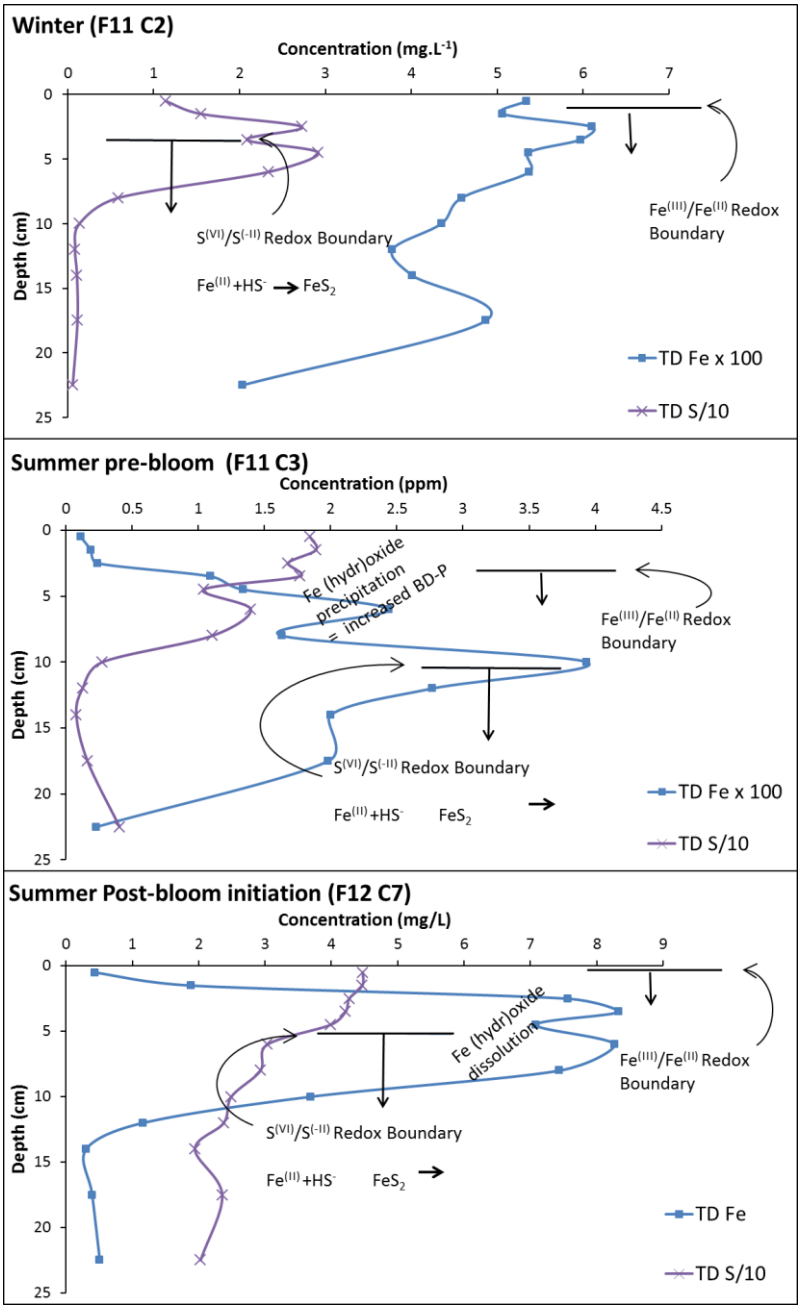

Figure 3.31 Pore water profiles for various sediment cores showing the temporal changes in the depth of redox boundaries between winter, pre-bloom and post-bloom initiation cores. Note the different scales for TD Fe.

Pore water profiles from cores sampled during algal blooms, (summer PBI) were distinct from summer pre-bloom cores due to the upwardly compressed redox profiles they displayed. The pore water [TD-Fe] was much higher (> 2 orders of magnitude) than pre-bloom cores, and the peak was closer to the sediment surface. [TD-Mn] was also higher and displayed a peak in the near surface sediments, while the [TD-S] began to decrease with depth from higher in the sediment than in the pre-bloom cores. These trends were consistent with the Fe(III) to Fe(II), and S(VI) to S(-II) reduction thresholds being closer to the sediment surface than in the pre-bloom cores. These summer PBI pore water profiles were replicated using geochemical modelling of an upwardly compressed redox profile, confirming the role of redox in the pore water trends. The significantly increased [TD-Fe] in these PBI profiles, relative to pre-bloom and winter profiles, was due to the upward compression of the redox profile taking place in a sediment (pre-bloom initiation) which had an increased mass of redox sensitive Fe (hydr)oxides, shown by the increased mass of BD-Fe in the upper 10 cm of the summer sediments. Such seasonal compression of redox zones in the upper sediments has been noted in other studies (e.g. Koretsky et al, 2006) and in the Wairewa sediments was consistently associated with periods of high primary productivity. The lower redox potential in the near-surface summer PBI sediments was likely due to increased oxygen demand resulting from warmer temperatures and rapid increases in primary productivity, and/or a redox 'event' such as stratification and deoxygenation occurring in the lake water column.

The change observed in Wairewa surface sediment redox conditions from anoxic in winter to oxic in early summer, differs from that reported in shallow Danish lakes. Søndergaard et al (1999) reported more oxidising conditions during winter and more reducing conditions in the summer, as a result of changes in oxygen demand during periods of low- and high-temperature related, biological activity. The different conditions in Wairewa may be explained by the relatively low organic matter in the sediments during summer, which increased to an autumn/winter maximum following sedimentation of cyanobacteria. The lower redox potential in the surface sediments of the later-summer PBI cores in Wairewa is more consistent with the Danish lake data.

Hence, Wairewa sediments appeared to go through a seasonal change in redox conditions. The increased organic matter in the surface sediments during winter results in more reducing conditions in the sediment. In early summer the decrease in organic material in the surface sediments and the increasing primary productivity in the water column

produce more oxic conditions in the upper sediments, with resulting precipitation of Fe(hydr)oxides in the upper 10 cm. Later in the season a deoxygenation 'event' in the water column, and/or greatly increased oxygen demand associated with algal blooms, results in anoxic conditions throughout the sediment profile which dissolves the recently precipitated Fe (hydr)oxides causing the high TD-Fe concentrations seen in the pore water of the upper sediments.

3.4.3 P binding phases

3.4.3.1 The role of Fe minerals

Pore water chemistry, the sequential extractions and geochemical modelling all provide insights into which mineral phases are likely to be binding P in the Wairewa sediments. In the more oxic near-surface sediments nearly a quarter of the extractable P was bound up in the BD-P. The BD extraction targets reactive Fe and Mn (hydr)oxides, however the strong correlation between reactive [BD-Fe] and [BD-P], the high Fe:P molar ratios in the BD extracts, the high [Fe] relative to [Mn] in both the BD and EDTA extractions and the lack of re-precipitated Mn in the re-oxidised pore water, all indicated that most of the P in the redox sensitive BD extract was Fe bound.

Pore water chemistry indicated that in the upper sediment, redox conditions favour the formation of Fe(III) (hydr)oxide mineral phases, and geochemical modelling indicated the stability of Fe(III) (hydr)oxides down to 2-3 cm, even in the post-bloom initiation cores which have compressed redox profiles. Ferrihydrite, hematite (Fe_2O_3) and goethite (FeO(OH)) were all variably super-saturated in these upper sediments. The more crystalline Fe (hydr)oxides (hematite and goethite) may persist in reducing conditions for some time, which may explain some of the BD-P in the deeper sediments. However the seasonal variation in the [BD-P] correlated with variation in [BD-Fe] rather than [BD-Mn], suggesting that BD-P is predominantly associated with Fe(III) (hydr)oxide phases which are very reactive and may precipitate and dissolve over relatively short time periods, and in response to small changes in redox conditions. Such observations are strongly indicative of the formation of amorphous ferrous hydroxides such as ferrihydrite, which is common in such surface sediments and may precipitate from rapid hydrolysis of Fe^{+3} or oxidation of Fe^{+2} (Schwertmann et al, 1987).

The surface area, crystallinity and morphology of Fe (hydr)oxides are the best indicators of their abilities to adsorb P (Barber, 2002). Less crystalline, higher surface area (hydr)oxides, have higher adsorption capacities. As such ferrihydrite, which has a high surface area (100-600 $m^2.g^{-1}$, Dzombak and Morel, 1990; Barber, 2002), exhibits greater adsorption capacities than more crystalline Fe (hydr)oxides such as goethite, hematite and lepidocrocite (Enyard, 1993; Strauss et al, 1997). Reactive Fe:P mole ratios of > 2 suggested an adsorption relationship between these two elements at sediment depths of < 10 cm.

Sediment grain size is also an important component of sediment adsorption capacity and hence the transfer of solutes between sediment and the lake water column, and the thickest Fe and Mn (hydr)oxide coatings have been found to occur on silt sized sediment grains such as those found Wairewa (Das, 2008). The predominance and distribution of fine silts observed in the lake sediment is likely to contribute to the adsorption capacity of freshly precipitated ferrihydrite as the precipitation is likely to occur as a coating on these fine grained particles (Horowitz & Elrick, 1987; Stone & English, 1993). Hence it appears that an amorphous Fe(III) (hydr)oxide is a major phase controlling P binding and mobility in the upper, more oxic sediments.

Fe may also bind P in the oxic sediments as strengite ($FePO_4.2H_2O$). The saturation indices for this mineral were positive in the oxic sediments of core F11 C4, above a sediment depth of 2 cm. Below this depth Fe phosphate minerals may be present as the Fe(II) phosphate mineral, vivianite ($Fe_3(PO_4)_2.8H_2O$) which has been reported from other reduced lake sediments (e.g. Fagel, 2005). Geochemical modelling predicted vivianite formation in the F11 C4 pore waters and a reactive Fe:P ratio < 2.5 at depths greater than 10 cm in this core may indicate the presence of vivianite. However the high [TD-S] relative to [TD-Fe] in the Wairewa sediment pore waters is likely to limit the importance of this secondary mineral. In the deeper anoxic sediments vivianite may be the directly dissolved by H_2S, and Fe^{+2} immobilised by FeS_2 precipitation as described by Fagel et al, (2005) and Katsev et al (2006). Geochemical modelling indicated both increased concentrations of $Fe\text{-}HS_{(aq)}$ complexes and decreased concentrations of $Fe\text{-}PO_{4(aq)}$ complexes, as a result of increased [TD-S] in the pore water, and vivianite became undersaturated as FeS_2 precipitation decreased the [TD-Fe], and dissolved, releasing PO_4^{-3} to the pore water. This may in part explain the increasing [TD-P] seen in the deeper

pore waters of cores F11 C3 as well as F12 C5 and C8, and is consistent with the findings reported in Gachter and Mueller (2003).

The [S] is an important control on P binding to Fe minerals in the sediment and is thought to be the key factor in long term retention of P in sediments (Katsev et al, 2006). Fe-bound P may be mobilised when Fe (hydr)oxides are reductively dissolved by H_2S (Katsev et al, 2006; Weston et al, 2006), while P mobilisation at depth is increased by the Fe-phosphate mineral dissolution, as discussed above. In addition the upwards flux of P released by such mechanisms may not be matched by an upward flux of Fe due to Fe immobilisation by FeS_2 precipitation. Therefore when the upward flux of P reaches more oxidising conditions in the shallower sediments, sufficient Fe may not be available to immobilise all of the mobile P (Smolders et al, 2006; Jordan et al, 2008; Hartzell et al, 2012). Significant FeS_2 precipitation was evident in the Wairewa sediments, with pyrite saturation occurring below 6 cm depth in core F11 C4, and pore water chemistry reflecting control of [TD-Fe] by FeS below the [TD-Fe] maxima. SEM results illustrated that FeS_2 precipitation occurred throughout the sediment cores, right up to near surface, and H_2S odour has been detected in the surface sediment (Section 5.3.3.3), indicating the redox thresholds are, at times, moved upward even further such that $SO_4^{-2} \rightarrow HS^-$ reduction occurs at or above the sediment surface.

3.4.3.2 Other mineral phases

Manganese

Mn oxides have also been reported to be strong adsorbents of P in oxic waters and sediments (e.g. Post, 1999). Despite a negative surface charge, the presence of transition metals and alkaline earth cations bound to the mineral surface can allow hydrous manganese oxides to strongly adsorb anions such as PO_4^{-3} (Kawashima et al, 1986). Birnessite (MnO_2) type minerals form in a wide range of environmental conditions, including eutrophic lakes (Frieed et al, 1997) and are fine grained and poorly crystalline, providing for excellent adsorption potential (Post, 1999) and high reactivity to redox conditions.

Modelled saturation indices in core F11 C4 pore water indicated that birnessite was unlikely to be present, at least in the winter and summer post-bloom initiation profiles. Pore water chemistry profiles showed [TD-Mn] increasing slightly just below the surface

sediments and an increased concentration in the post-bloom initiation profiles relative to winter and summer pre-bloom profiles. This is consistent with the reduction of oxidised forms of Mn (Jones et al, 2011). However the low Mn:P molar ratios (< 1) and the lack of seasonal variation in [BD-Mn] indicated that Mn (hydr)oxides were only a minor component of the BD-P fraction, and are insignificant when compared to the Fe (hydr)oxide component. This was supported by the EDTA extraction which suggested that the Fe:P relationship is one of adsorption (Fe:P > 2, Nyenje et al, 2014), while the Mn:P ratio approaches 1 and hence is more likely to indicate a non-adsorption, mineral relationship.

Pore water profiles indicated a decreasing [TD-Mn] in the sediments deeper than 3 cm, a trend often explained in other studies by precipitation of a Mn(II)-bearing mineral phase in anoxic conditions (e.g. Jones et al, 2011). Geochemical modelling indicates $MnHPO_4$ is supersaturated at all levels in the Wairewa sediment and this phase has been noted in various other studies of lake sediments (Ho et al, 2013; Jalali & Moharami, 2013). EDTA is known to form Mn-EDTA complexes (Trfunovic et al, 2000) and so might be expected to dissolve $MnHPO_4$ during an EDTA extraction. This may explain the Mn:P ratio in the EDTA extract discussed above. Geochemical modelling also indicated that another Mn(II) bearing mineral phase, rhodochrosite ($MnCO_3$) approached saturation in the sediment pore waters, but LOI analyses indicated that carbonates are likely to be very a minor component of the Wairewa sediments.

Aluminium

Al hydr(oxides) are known to strongly adsorb P (Reitzel et al, 2005; De Vicente et al, 2008) and are considered to comprise the majority of the NaOH-rP sequential extraction fraction in many lake sediments (e.g. Lukkari et al, 2007; De Vicente et al, 2008). In the Wairewa sediments the NaOH-rP fraction comprised a significant portion of the TSP and the strong correlation of Al and P concentrations in the NaOH extract indicates that the Al (hydr)oxides are an important binding phase.

Geochemical modelling indicated that amorphous Al (hydr)oxide, which may be expected to have a higher sorption capacity than more crystalline phases (Gerard, 2015), were undersaturated in the Wairewa sediment pore waters and hence would not be expected to precipitate in these sediments. More crystalline forms such as Gibbsite ($Al(OH)_3$) were saturated throughout the sediment core pore waters, and hence are not

expected to be reactive to observed change in sediment redox conditions but may react to increased pH as discussed in Section 3.4.4.1.

Calcium

Calcite is also known to bind P in lake sediments (Søndergaard et al, 2003), however several studies have shown that calcite adsorption of PO_4^{-3} is of minor importance where amorphous Fe (hydr)oxides are abundant (Golterman, 1988, Jensen et al 1992). The low carbonate content of the Wairewa sediments and the lack of a correlation between carbonate content and the HCl-P fraction, as well as the geochemical modelling, which indicated that calcite is under-saturated, suggest that calcite binding is not important in Wairewa.

The other important Ca-PO_4 phase is apatite ($Ca_4(PO_4)_3(OH,Cl,F)$ which was observed in the SEM analysis of the sediments. Apatite is thermodynamically stable in the lake sediments as saturation indices indicated saturation with respect to hydroxylapatite at all depths. However, the kinetics of apatite formation indicate that these grains are likely to be detrital rather than authigenic (Oxmann & Schwendenmann, 2015). This is consistent with the euhedral morphology of the grains observed under SEM, and the fact that the [HCl-P fraction] which is considered to consist of Ca-P, was consistent throughout the sediment profile, indicating its lack of reactivity.

3.4.3.3 The effect of redox changes on P binding phases

Pore water chemistry indicates that redox conditions in the sediment profiles are likely to be the major control on changing mineral stability in the sediments. As the water column and/or sediments become more reducing due to organic decomposition and/or deoxygenation of the water column, the first redox reaction will be the dissolution of Mn (hydr)oxides. This will be followed by the reduction of Fe (hydr)oxides, which can remain stable down to very low oxygen concentrations, especially the more crystalline phases such as hematite and goethite which may persist in anoxic sediments for prolonged periods of time. Strengite may be replaced by vivianite in the anoxic sediments although with a further decrease in redox potential, and the presence of significant dissolved sulphide, vivianite dissolution may result in P release into sediment pore waters. The occurrence of this mechanism of P release in Wairewa sediments is supported

by observed increased [P] in deeper pore waters and decreasing P on sediments with depth in SEM EDS spectra.

The potential effects of upwardly compressed redox profiles on mineral stability is seen in Figure 3.23, where Mn (hydr)oxides (e.g. Birnessite) become under-saturated in the surface sediment, Fe (hydr)oxide and strengite stability is decreased closer to the surface sediments, and FeS_2 becomes stable at shallower depths. Al (hydr)oxides (e.g. Gibbsite) which may adsorb PO_4^{-3}, are unaffected by redox changes at all depths of the sediment as is $MnHPO_4$.

3.4.4 P fractionation and flux in the sediments

The conditions observed in the pore water chemistries of the Wairewa sediments and the effects of these on mineral phase stabilities, can be used to help interpret the results of the sequential extractions. This has enabled conclusions to be drawn regarding P binding and mobility within the sediments. Concentration decreases with depth and/or seasonal changes, as discussed below, indicate that the NH_4Cl-P, BD-P, NaOH-rP and Org-P fractions comprise a 'mobile' P pool within these sediments, while the HCl-P and Res-P fractions comprise a more refractory immobile pool.

3.4.4.1 Mobile P fractions

Loosely bound P

The NH_4Cl-P fraction represents the most mobile fraction of very loosely bound P (Rydin, 2000; Søndergaard, 2007) and has been reported as comprising up to 25% of TSP in shallow Lake Søbygard in Denmark (Søndergaard, 2007). In Wairewa this fraction was generally a very small component (< 0.5 %) of the [TSP] and is considered relatively insignificant as a source of P although it will reflect pore water P concentrations. The [NH_4Cl-P], after a drastic decrease just below the surface sediment, showed a gradual increase in the deeper sediments, reflecting the increased [P] in the deeper pore waters, and indicating a more labile pool of P in the deeper sediment.

Redox sensitive P

As discussed in Section 3.4.3.1, the BD-P fraction in the Wairewa sediments was strongly associated with Fe (hydr)oxides and in the surface sediments of the summer cores this fraction comprised a high (25 %) proportion of the [TSP]. This is at the higher end of

reported values. While Rydin (2000) reported a similar proportion (26 %) in a shallow eutrophic Swedish lake, Gao et al (2005) reported much lower values (up to 5 %) in the eutrophic Dianchi lake, while Kisand and Noges (2003) reported [BD-P] at < 10 % of [TSP] in two Estonian eutrophic lakes. The high proportion of P associated with Fe (hydr)oxides in Wairewa indicated that significant mobility may be expected in response to the changing redox conditions observed in the pore water chemistry, and indeed significant decreases in [BD-P] were observed in the reduced surface sediments, during winter. The steep decreases in the [BD-P] observed with depth, which indicated an upward flux of P from low to high redox potential, also displayed significant seasonal variation reflecting the changing redox conditions discussed in Section 3.4.2.1.

pH sensitive P

The NaOH-rP fraction represents pH sensitive P and is often interpreted to be comprised largely of P adsorbed to Al (hydr)oxides (Rydin 2000, De Vicente et al, 2008) but, also includes P adsorbed to more resistant Fe (hydr)oxides. Variable proportions of this fraction have been reported from other lakes with Rydin (2000) reporting 3% NaOH-rP in Sweden's Lake Erkin and Gao et al (2005) reporting 20-30% NaOH-rP in the shallow Dianchi Lake in southwestern China. In Wairewa this P fraction comprised a significant proportion (17 %) of TSP in the surface sediments during summer. Slightly higher concentrations (21%) were observed in the winter sediment, likely due to the lower water column pH.

Rydin's (2000) definition of the mobile P pool in the sediments Sweden's Lake Erkin, excluded NaOH-rP based on a lack of surface enrichment of this fraction. Al hydroxides, are unaffected by changing redox conditions at depth. As such one may expect this fraction to be relatively immobile in the sediment, however the Wairewa sediments show a definite upward enrichment of the NaOH-rP fraction.

High pH in lake sediment pore waters may result in the release of P from Al (hydr)oxides due to pH related desorption and dissolution of Al(hydr)oxides (Kopacek et al, 2005). The maximum pH observed in Wairewa sediment pore water was pH = 7.98 at a depth of 15-20cm (see Section 5.3.4.2). A pH = 8 is high enough to cause desorption from Al (hydr)oxides (Gerard, 2015) and an increase in pore water [TD-Al] with depth was observed in some cores (e.g. F11 C1, see Appendix 2) which may indicate some dissolution of Al(hydr)oxides. Hence the upward flux of the NaOH-rP fraction observed

in the Wairewa sediments may be due to release from Al(hydr)oxides, however this P fraction is also likely to include PO_4^{-3} absorbed to clays (Gerard, 2015) and to more recalcitrant Fe (hydr)oxides (e.g. hematite, goethite) which are mobilised in the sediment by long term exposure to low redox conditions

Organic P

The Org-P fraction includes P associated with non-refractory organic matter such as algal material settled from the water column, as well as bacterial incorporated P. Values of 20 - 30% of TSP in Dianchi lake (Gao et al, 2005), and 29 % in Lake Erkin, Sweden (Rydin, 2000) have been reported. In comparison the [Org-P] in the Wairewa summer surface sediments was relatively low at 14% of [TSP]. This low [Org-P] was consistent with the relatively low organic matter (11%), as determined by LOI. In the winter surface sediment, an increased [Org-P] was observed (24%), reflecting the sedimentation of algal material at the end of the summer growth period. The increased [Org-P] in the winter core was almost entirely offset by the decrease in [BD-P], reflecting an apparent seasonal cycling of P between mineral and organic forms in response to redox changes and organic decomposition. In this cycle, P released by the dissolution of Fe (hydr)oxides, due to the changes in the sediment redox profile observed in the summer PBI cores, is taken up by algae in the water column. The sedimentation of algae and other organic particulate material in late summer and autumn then increases the winter [Org-P] in the surface sediments, while the subsequent decomposition of the organic material in winter and spring releases PO_4^{-3}, which is then available to be re-adsorbed onto Fe (hydr)oxides. In the continuing cycle, increased oxygen demand during rapid summer increases in primary productivity, causes a decline in redox potential in the surface sediment, reducing Fe(III) phases once again, and re-releasing P for algal uptake. These processes have also been reported in other lake systems (e.g. Smolders et al, 2006; Hupfer & Lewandowski, 2008; Geurts et al, 2010).

The [Org-P] decreased steeply with sediment depth. The 80 % decrease in [Org-P] at 20 cm depth relative to the surface in core F11 C4, indicated that only a small proportion of the organically bound P accumulated at the surface is permanently buried. The majority is instead mineralised and released. Different organic-P compounds degrade at different rates and hence may progressively release P during burial and diagenesis (Reitzel et al, 2007).

3.4.4.2 Immobile P fractions

The HCl-P fraction is considered to be largely comprised of P associated with Ca phases such as apatite (Rydin, 2000; Søndergaard, 2007; De Vicente et al, 2008), which in Wairewa is thought to be largely detrital. HCl-P values of 20% (Søndergaard, 2007) and 15% (Rydin, 2000) of TSP, reported in shallow Danish lakes, are similar to the values observed in the Wairewa (18%). This fraction appeared to be largely immobile with no seasonal or depth variation observed.

The Res-P fraction is considered to comprise of refractory organic material (Rydin, 2000; Søndergaard, 2007) and inert inorganic P (Rydin, 2000). In the Wairewa sediments there was a strong correlation between the organic matter determined by loss of ignition, and both Org-P and Res-P, suggesting a significant proportion of the Res-P is indeed refractory organic material. This fraction comprised 25% of the Wairewa [TSP], which is comparable with Sweden's Lake Erkin (16-26% of TSP) (Rydin, 2000). This fraction is relatively immobile with no seasonal variation observed. The slight decrease observed with depth is likely to be due to slow decomposition with increasing burial.

3.4.4.3 Summary of P fluxes

The temporal changes evident in the P-fraction depth profiles provide insight into the mobility of P in these sediments and can be used to define zones of P enrichment, seasonal mobility and longer term mobility in the Wairewa sediments (Figure 3.32).

A long term flux occurs from deep anoxic, to shallow, less reducing sediments. Low redox potential causes P associated with reactive (BD-P), and more refractory (NaOH-rP), Fe (hydr)oxides and Fe-PO_4 phases, to be released. Higher pH in the deeper sediments may also result in P desorption from Fe and Al (hydr)oxides while burial and decomposition causes the progressive release of organic associated P. This P diffuses upward until it is adsorbed, predominantly to Fe (hydr)oxides under more oxidising conditions. Hence a long term upward flux involves P from the BD-P, NaOH-rP and Org-P fractions.

Seasonal changes in redox profile alter the depth at which upwardly diffusing P is immobilised on Fe (hydr)oxides. In early summer a more oxidising upper sediment profile results in an increased stability of Fe (hydr)oxides and hence an increased [BD-P] down to around 10 cm depth. Later in summer, during rapid increases in primary productivity, upward compression of sediment redox profiles reduces the stability of Fe

(hydr)oxides and releases P for further upward diffusion to the enrichment zone at the top of the sediment pile (Figure 3.32).

A further seasonal flux involves interaction between the enrichment zone and the water column where P release (discussed in Chapter 4) primarily from the BD-P in the surface sediments is taken up by primary producers. This P is then returned to the sediment as Org-P by sedimentation, where decomposition and/or burial result in P mineralisation.

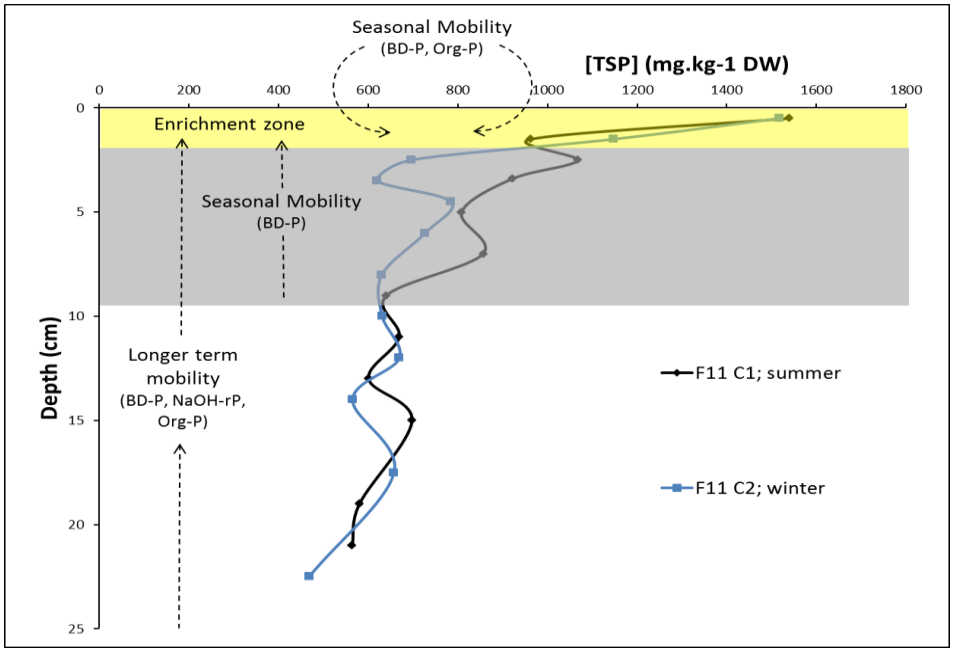

Figure 3.32 Zones of P enrichment, seasonal mobility and longer term mobility in the Wairewa sediments, evident in winter and summer cores. These zones are not physical boundaries, but rather are indicative of where movements of redox thresholds drive seasonal changes.

3.5 Conclusions

The binding of P in the Wairewa sediments is complex and dynamic. Figure 3.33 illustrates the key P binding mechanisms identified. The biological uptake of P and subsequent sedimentation of organic matter to the sediment surface, results in a large pool of organic P in the surface sediment especially during autumn and winter. Subsequent decomposition affects redox conditions, and results in the mineralisation of P to various inorganic P fractions. Additional P accumulates to these fractions by the sedimentation of inorganic P from the water column. Several of these fractions are mobile, in particular the P associated with Fe (hydr)oxides. In contrast the P retained in the more refractory organic fraction and that which is associated with detrital apatite are relatively immobile within the sediment profile.

Burial of the mobile P fractions, continued decomposition of organic material and the effect of the more reducing conditions occurring below the surface sediments, results in the release of bound P. This creates an upward flux of PO_4^{-3}, which is again immobilised in the shallower, more oxic sediments where PO_4^{-3} adsorbs to phases such as Fe (hydr)oxides.

In the surface sediments this cycle is affected by the rapid precipitation and dissolution dynamics of an amorphous Fe(III) (hydr)oxide such as ferrihydrite, and at depth by FeS_2 regulation of Fe availability. Secondary mineral phases such as $MnHPO_4$, strengite and vivianite may also exert some control over P binding in the sediments.

Significant seasonal changes occur in redox conditions, with more reduced sediments at the surface during winter, and a more oxidised upper sediment profile during the early summer growing season (prior to algal bloom formation). This leads to an increased pool of redox sensitive bound P in the upper sediments, which is available for release when redox profiles are compressed upward during periods of algal bloom formation.

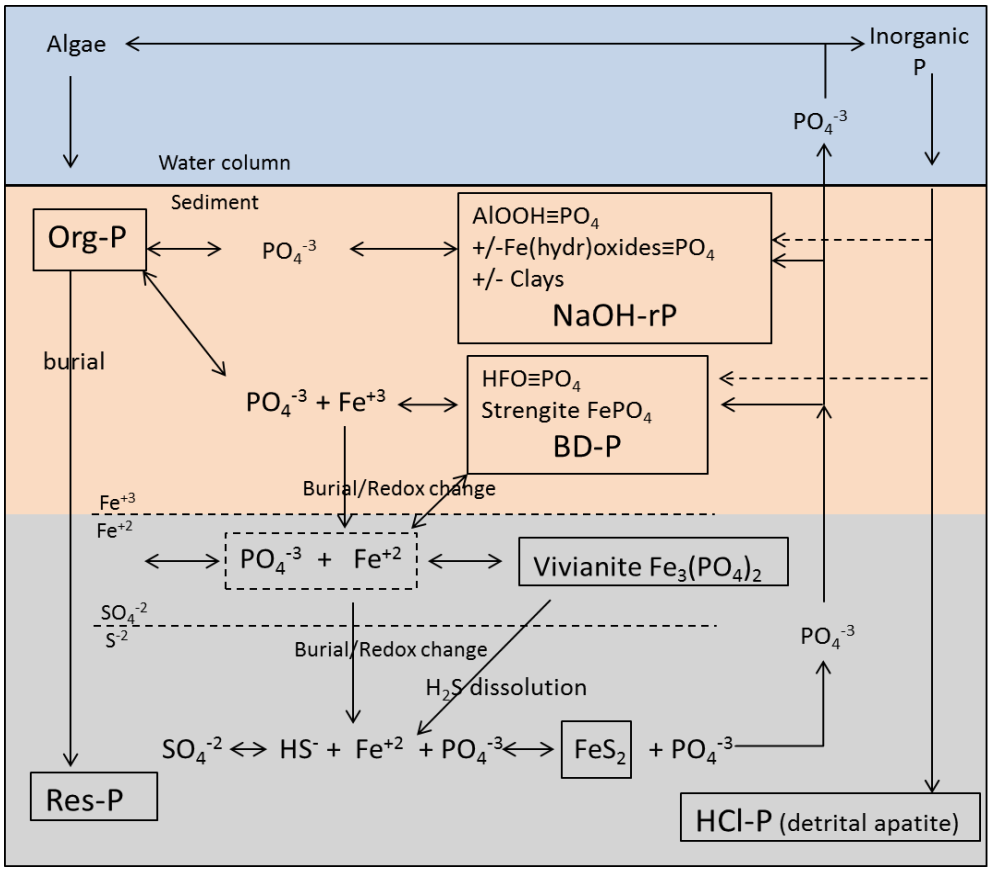

Figure 3.33 Schematic diagram of the key processes, mineral phases and P fractions involved in P binding in the Wairewa sediments. HFO = amorphous Fe (hydr)oxides. ≡ denotes adsorption.

3.6 Key Research Findings

- P enrichment was evident in the surface sediments of all cores, resulting in total sedimentary P concentrations of 1500 $mg.kg^{-1}$. This enrichment is due to long term, as well as seasonal fluxes of P from the deeper sediments.
- P mobility in the upper, more oxic sediments is largely controlled by reactive Fe (hydr)oxides.
- Redox conditions undergo seasonal changes and control Fe and S redox reactions which are key to P retention in the Wairewa sediments.
- Seasonal cycling occurs between pools of organic and Fe bound P in the surface sediments.
- Fe binding by FeS_2 precipitation immobilises Fe in the deeper, more reduced sediments. This decreases the upward flux of Fe^{+2} and hence decreases the Fe available to form P binding Fe (hydr)oxide phases in the oxic upper sediments.

Chapter 4: Phosphorus Release Mechanisms

4.1 Introduction

Internal loading of P from the sediments to the water column is a key process in Wairewa, especially during the summer months (Section 2.3.4). The release of organic P, as well as inorganic P adsorbed onto Fe and Al (hydr)oxides, in the large sedimentary P reservoir, results in an upwards flux of P towards the sediment/water interface. However mobility is generally decreased in the Fe (hydr)oxide rich surface sediments, resulting in the P enriched layer discussed in Section 3.4.1. In order for P to become bioavailable in the water column it must either be released from this surface sediment, or the P flux from deeper sediments must be able to pass through the surface sediments to reach the OLW. Various mechanisms have the potential to facilitate this process.

The coupling of the Fe and P cycles in lake systems has supported the long held hypothesis (Einsele, 1938; Mortimer, 1942) that aerobic conditions at the sediment/water interface support P retention, and that anoxic conditions result in P release (Hupfer and Lewandowski, 2008). With the high Fe:P ratios observed in the Wairewa sediments and the importance of redox dynamics in the sediment pile, oxygen generation and consumption processes in the water column may be expected to be important. The flux of organic matter from the water column to the sediment surface and the subsequent organic breakdown, and/or the deoxygenation of the OLW, results in reductive dissolution of Fe (hydr)oxides (Smolders et al, 2006; Koretsky et al, 2006; Ekholm and Lehtoranta, 2012), with consequent release of adsorbed P. This paradigm has informed general limnology, lake modelling and lake restoration for decades (Hupfer & Lewandowski, 2008).

However various studies have begun to cast doubt on the simplicity of an oxygen controlled, Fe and P solubility model (Gachter and Muller, 2003; Katsev et al, 2006; Ekholm and Lehtoranta, 2012). Several studies have demonstrated low P release during periods of water column anoxia (Caraco et al, 1991; Prairie et al, 2001), while conversely, others have shown significant PO_4^{-3} release during periods when the water column has remained oxic (e.g. Gao et al, 2012). One mechanism suggested to explain these exceptions is the retention of P by redox insensitive Al phases. While Al (hydr)oxide adsorption of P is not affected by redox, it is affected by pH. Elevated pH promotes the

desorption of PO_4^{-3} by the substitution by hydroxyl ions on Al and Fe (hydr)oxide surfaces, as well as on clays and organic particulates (Jacoby et al, 1982). Another mechanism inferred to explain exceptions to the classic oxygen control paradigm, involves high concentrations of SO_4^{-2} and the reductive dissolution of Fe (hydr)oxides (and Fe-phosphate minerals) by reduced HS^-/H_2S. This decreases the P binding by Fe phases, and immobilises Fe by FeS_2 precipitation, thus allowing upwardly diffusing PO_4^{-3} to overwhelm the adsorption capacity of the oxic surface sediments, and be released to the water column under oxic conditions (Gachter and Muller, 2003; Katsev et al, 2006; Koretsky et al, 2006).

Resuspension of sediment into the water column is also prevalent in shallow lakes and can result in a significant increase in [TP] in the water column (Kristensen et al, 1992), but this may or may not result in an increase in bioavailable P (Sondergaard et al, 2003). The direct contact of water and suspended sediment may result in the exchange of PO_4^{-3}, subsequently increasing or decreasing bioavailable PO_4^{-3} in the water column (Mayer and Gloss, 1980; Froelich, 1988; Wildman and Hering, 2011; Cyr et al, 2009). The zero equilibrium P concentration (EPC_0) is the threshold water [PO_4^{-3}] below which sediments in suspension release PO_4^{-3} to the surrounding water column, and above which the suspended sediment adsorbs PO_4^{-3} from the water (Cyr et al, 2009). This equilibrium dynamic has the potential to release significant amounts of PO_4^{-3} where the Fe:P ratio of the suspended sediment is low, and the concentration of readily exchangeable NH_4Cl-P is high (Søndergaard et al 1992).

Additional mechanisms which may affect P release to shallow lake water columns include the direct release from decomposing of organic material (Hupfer and Lewandowski, 2008), bioturbation which may result in release or retention of P, and gas ebullition due to microbial decomposition of organic matter in deeper sediments (Søndergaard et al, 2003). The relative importance of specific binding and release mechanisms are likely to be lake specific (Søndergaard et al, 2003), and this chapter presents research into the effect of key release mechanisms operating in the Wairewa sediments and water column. Key questions are;

- Does P release from the Wairewa sediments occur when the lake water column is oxic, and circum-neutral?

- Do changes in redox and pH conditions result in significant P release from the Wairewa sediments?
- Does salinity affect P release from the Wairewa sediments?

4.2 Methods

4.2.1 Phosphate Release Experiments

Phosphate release experiments were conducted to assess the importance of various release mechanisms, using two approaches; (i) slurry release experiments consisting of small amounts of sediment suspended in solution and shaken for a defined period of time, and (ii) core-incubation release experiments using intact cores in contact with the OLW. More specific details for the individual experiments are detailed below.

Sediment sampling was conducted as detailed in Section 2.2.4 from sites presented in Figure 3.1. Analysis for DRP was also as detailed in Section 2.2.4 while analysis for trace elements was as detailed in Section 3.2.2. All pore water concentrations presented in this chapter refer to 'total dissolved' concentrations, as analysed by ICP-OES, except for DRP where specified. Dissolved oxygen (DO), pH, electrical conductivity (EC) were all measured on a HACH HQ40d meter with calibrated DO, pH, and EC probes respectively. Temperature was obtained from the HACH DO probe. Redox potential was also measured on the HACH HQ40d meter with a calibrated ORP (Ag/AgCl) probe and results corrected for the standard hydrogen electrode according to the HACH ORP/Redox electrode User Instructions (DOC272.53.80033). Conversions between E_h and pe were by the following equation, where E_h is measured in volts;

$$pe = 16.9E_h \qquad \text{(eq 4.1)}$$

4.2.1.1 Unadjusted core-incubation experiment

In order to assess the background P release rates into an aerobic, circum-neutral water column, a core-incubation experiment was conducted in which adjustment of the OLW chemistry was kept to a minimum. Five cores were taken from Site F12 (Figure 3.1) in May 2013. These were transported in an insulated box to the laboratory where they were allowed to settle for 8 hours. DO was maintained at > 9 $mg.L^{-1}$ above all cores by bubbling air through the OLW using an aquarium air pump. pH remained in the range 7.10 - 7.40 and no pH adjustment was conducted. Temperature was maintained at 15-20 ^{o}C. 15 ml samples from the OLW were taken at periodic intervals over 14 hours,

and were filtered immediately through 0.45µm MF-millipore filters. These were frozen until analysis for DRP.

4.2.1.2 Equilibrium P concentration (EPC) slurry experiments

Two EPC experiments were conducted to ascertain the PO_4^{-3} equilibrium dynamics between resuspended surface sediments and oxygenated lake water with circum-neutral pH. The first was conducted in November 2014 on surface sediment (top 5 mm) from site F12. The second was conducted in May 2015 on surface sediment from site F10 (Figure 3.1). The method followed that described by Olila and Reddy (1993). Lake water was filtered (0.45 µm MF Millipore) and the DRP concentration established. This water was then spiked to known PO_4^{-3} concentrations using standard 2.5 $mg.L^{-1}$ phosphate solutions made from anhydrous KH_2PO_4 dissolved in deionised water. An accurately weighed wet sediment sample equivalent to between 1.07 - 1.27 g (dry weight) was added to 40 ml of the spiked lake water solutions to give a solid:solution ratio of between 1:30 - 1:40 (by weight). The concentrations of these sediment slurries were calculated allowing for contribution of pore water [PO_4^{-3}] in the wet sediment sample.

These slurries were then put onto an end over end shaker for 24 hr at room temperature. Water was then filtered (0.45 µm) and analysed for DRP. The P lost from the solution was plotted against the initial concentration. The x axis (concentration of initial solution) intercept is considered the 'Zero Equilibrium P Concentration' (EPC_0) which represents the water [P] below which sediments in suspension will release P to the water and above which resuspended sediments will adsorb P from the water (Cyr et al, 2009). In the first EPC_0 experiment the filtered lake water had pH = 7.13, DO = 9.88 $mg.L^{-1}$, EC = 3.14 $mS.cm^{-1}$. In the second experiment, in order to test the effect of salinity, lake water was filtered from two sites with differing EC, one from site F12 (pH= 7.51, DO=11.22 $mg.L^{-1}$, EC = 3.13 $mS.cm^{-1}$), the second from site F10 (pH = 7.81, DO = 11.35 $mg.L^{-1}$, EC = 8.33 $mg.L^{-1}$). Duplicate samples were run for both experiments.

4.2.1.3 Redox- core-incubation experiments

A core-incubation experiment was conducted to evaluate the release of PO_4^{-3} from sediment exposed to lowered redox conditions. Five cores were taken from Site F12 (Figure 3.1) in October 2014. These were transported in an insulated box to the laboratory where they were allowed to settle for 1 hour. The OLW in each core tube was then

equilibrated with the OLW in the other core tubes, and with 25 L of lake water, for 16 hours, via a flow through system with a flow rate of 5 $L.h^{-1}$ (Figure 4.1). At the end of this equilibration period the cores were isolated from each other and the OLW volume in each core was standardised to 1.5 L. E_h was adjusted in the OLW of four cores by the addition of 0.68 M $Na_2S_2O_4$, to various values between +450 and -300 mV. These are considered to represent a full range of conditions observed in actual lake settings (e.g. Moore and Reddy, 1994; Gomez et al, 1999; Christophoridis and Fytianos, 2006). Redox conditions were maintained at desired levels in all cores by bubbling air through the OLW using an aquarium air pump, and/or by further addition of $Na_2S_2O_4$. pH was maintained at circum-neutral levels by addition of 5 M HCl or 2 M NaOH as required. Temperature was maintained at 20 ^oC (+/- 1.5 ^oC). The incubation was run for 44 hours. Key parameters for the cores are presented in Table 4.1. 15 ml samples were taken at periodic intervals and filtered immediately through 0.45 µm MF-millipore filters. These were frozen until analysis for DRP.

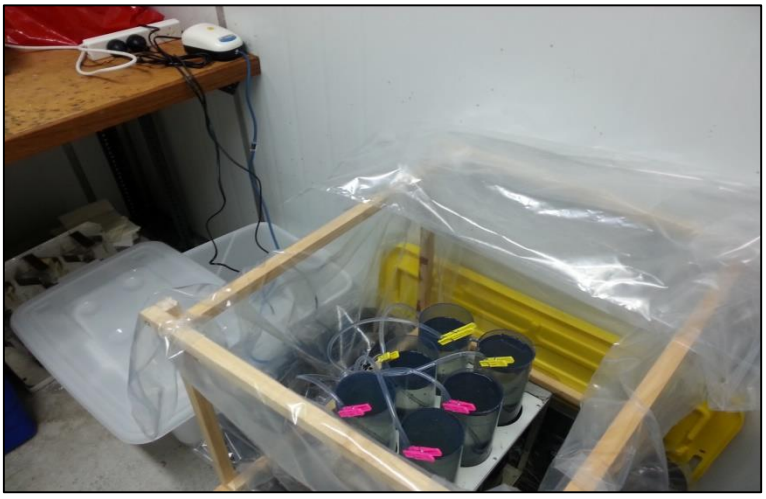

Figure 4.1 Core incubation experiment showing the flow through system used to equilibrate the OLW in the cores. The cores sit in a collection bin filled with lake water which is slowly pumped into all core tubes simultaneously. The OLW overflows the core tube and drains back into the collection bin.

A further redox core-incubation experiment was conducted in November 2014 to assess the effect of the redox at $E_h \approx 0$ and +100 mV. This used the same methodology as described above using three cores, one of which had a high [DO] maintained by air bubbling and two of which had reduced [DO], maintained as described above (Cores F and G, Table 4.1). DRP analysis was conducted on samples from Core F and G OLW.

After 48 hr the core with the oxic OLW and Core G were sectioned and pore water extracted under a N_2 atmosphere. The filtered (0.45 µm) pore water was then analysed for trace element chemistry.

Table 4.1 Key water chemistry parameters measured in the OLW of cores during 2 redox- core-incubation experiments. Experiments 1 and 2 were conducted in October and November 2014 respectively as described in Section 4.2.1. DO = $mg.L^{-1}$, E_h = mV, EC = ($mS.cm^{-1}$), Temperature= ^oC (+/- 1.5 ^oC)

	Experiment 1 Cores (Oct 14)					**Expt 2 Core (Nov 14)**		
	A	**B**	**C**	**D**	**E**	**Oxic**	**F**	**G**
DO	8.7	3.3	1.8	0	0	9.77	0	0
E_h (mean)	+450	+400	+370	-210	-300	+432	+110	0
E_h (range)	+455- +475	+354- +455	+330- +430	-110- -245	-276- -317	+376- +461	+60- +215	-50- +95
pH	7.05	6.94	6.93	6.89	6.83	7.33	7.08	7.03
EC	2.80	2.80	2.80	2.80	3.75	3.02	3.10	3.15
Temp	20	20	20	20	20	18.5	18.5	18.5

4.2.1.4 pH- slurry release experiment

A slurry release experiment was conducted in March 2013 to assess the effect of pH on phosphate release from surface sediments. The pH of twelve 220 ml samples of filtered (0.45 µm) lake water, was adjusted using 2.2 ml of NaOH solutions ranging from 0.001 to 0.05 M. These adjustments resulted in three samples for each of four pH groups, with the initial pH averaging 7.65, 8.82, 9.27 and 10.14 respectively. Oxic conditions were maintained and DO for the solutions ranged from 9.88 to 10.86 $mg.L^{-1}$.

Approximately 0.13 g of accurately weighed wet surface sediment (0.06 g DW), collected from site F12, was added to each sample and the slurries were then put on an end over end shaker for 24 hr. The final average pH of the four groups was 7.95, 8.37, 8.94 and 9.98. 15 ml samples were taken at periodic intervals and filtered immediately through 0.45 µm MF-millipore filters. These were frozen until analysis for DRP.

4.2.1.5 pH- core-incubation experiment

A core-incubation experiment was conducted in October 2013, to assess the effect of varying pH in the OLW, on PO_4^{-3} release from the sediments. Five cores were taken from Site F12 (Figure 3.1) in October 2014. These were transported in an insulated box to the laboratory where they were allowed to settle for 1 hour. The OLW in each core tube was then equilibrated with the OLW in the other core tubes and with an additional 25 L of lake water, for 19 hours via a flow through system with a flow rate of 2.6 $L.h^{-1}$. At the end of this equilibration period the cores were isolated from each other and the OLW volume in each core was standardised to 1.5 L. pH was adjusted and maintained in the OLW of the cores by addition of 2M NaOH or 5N HCl as required. pH was adjusted to an average of 5.99. 7.10, 7.93, 8.97 and 9.94, for the five cores respectively. DO was maintained at > 8 $mg.L^{-1}$ in all cores by bubbling air through the OLW using an aquarium air pump. Temperature was maintained at 20 ^oC (+/- 1.7 ^oC). 15 ml samples were taken at periodic intervals and filtered immediately through 0.45 µm MF-millipore filters. These were frozen until analysis for DRP.

After 48 hr, a short-lived resuspension event was simulated in the cores by using syringe driven OLW to stir up 2mm of the surface sediment. This was thoroughly mixed into the OLW. 15 ml samples were taken at 2, 15 and 30 min after the resuspension. These were filtered immediately as above and frozen prior to DRP analysis. The use of 2 mm of surface sediment was based on in-lake calculations of resuspended sediment during a wind event in July 2012 (see Section 5.2.7.1).

After completion of the incubation period, two cores (pH = 7.10 and 9.94) were sectioned and the pore water analysed for pH and DRP.

4.2.1.6 Salinity- core-incubation experiments

Two core-incubation experiments were conducted to evaluate the effect of varied salinity levels in the OLW, on the release of PO_4^{-3}. In the first experiment, six cores were taken from Site F12 (Figure 3.1) in February 2014. These were transported in an insulated box to the laboratory where they were allowed to settle for 1 hour. EC was used as a proxy for salinity, and the initial EC in the cores was 4.54 $mS.cm^{-1}$. EC in the lake had been around this level over the whole 2013-14 summer season. The OLW in each core tube was equilibrated with the OLW in the other core tubes and with an additional 60 L of low EC

water from the lake tributary, the Okuti River, for 139 hours The equilibration period was prolonged due to an undetected blockage in the flow through system. Equilibration occurred once this was addressed and a flow rate of 3.9 $L.h^{-1}$ was achieved. At the end of this equilibration period the cores were isolated from each other and the OLW volume in each core was standardised to 1.5 L. EC in the equilibrated OLW was 0.68 $mS.cm^{-1}$. This was left unadjusted in two cores while the other four cores were adjusted with filtered (0.45µm) sea water to EC of 2.09, 4.16, 6.22 and 8.25 $mS.cm^{-1}$ respectively. DO was maintained at > 8 $mg.L^{-1}$ in all cores by bubbling air through the OLW using an aquarium air pump. pH was maintained at circum-neutral levels by addition of 5N HCl or 2N NaOH as required. Temperature was maintained at 20 ^{o}C (+/- 1.7 ^{o}C). The core incubation experiment ran for 7 days. 15 ml samples were taken at periodic intervals and filtered immediately through 0.45µm MF-millipore filters. These were frozen until analysis for DRP.

The second core incubation experiment was started on 18 March 2014 after a natural 'fresh' event in the lake (a significant rain event on the 5 March 2014), resulted in a reduction of lake EC from the relatively consistent summer 2014 value of 4.5 $mS.cm^{-1}$ to 0.39 $mS.cm^{-1}$ (at Site F12). This experiment was conducted to evaluate the effect of this natural change in EC. Five cores were collected from site F12. One of these cores was sectioned and the pore water extracted as described in Section 2.2.4. Pore water was analysed for EC, pH, and DRP. Four cores were transported in an insulated box to the laboratory where the OLW volume in each core was standardised to 1 L. The cores were allowed to settle for 16 hr. EC had risen during the settling period and was left unadjusted in one core (EC=0.58 $mS.cm^{-1}$). Two cores were adjusted with filtered (0.45 µm) sea water to EC of 2.69 and 4.77 $mS.cm^{-1}$ respectively while the remaining core was adjusted to an EC of 0.328 $mS.cm^{-1}$ with filtered Okuti River water. DO was maintained at > 8 $mg.L^{-1}$ in all cores by bubbling air through the OLW using an aquarium air pump. pH was maintained at circum-neutral levels by addition of 5N HCl or 2N NaOH as required. Temperature was maintained at 18.5 ^{o}C (+/- 2.5 ^{o}C). The core incubation experiment was maintained for 5 days. 15 ml samples were taken at periodic intervals and filtered immediately through 0.45 µm MF-millipore filters. These were frozen until analysis for DRP.

Following the second salinity- core-incubation experiment, lake water was sampled for DRP and TP and analysed for EC along the length of the lake from north to south for reasons explained in Section 4.3.4.1.

4.2.1.7 Salinity- slurry release experiment (high pH)

Two slurry release experiments were conducted to assess the effect of increasing salinity on PO_4^{-3} binding/release in high pH water.

In the first of these filtered (0.45 µm) lake water was adjusted to approximately pH = 10 with 0.5M NaOH. EC was then adjusted in five separate 50 ml solutions to 1.09, 4.05, 5.97, 8.78 and 12.08 $mS.cm^{-1}$ respectively. An accurately weighed sample of approximately 0.11 g of wet surface sediment (from Site F12) was added to each solution and the samples placed on an end over end shaker for 24 hrs. Table 4.2 presents the key water chemistry parameters at the start and end of the experiment. 15 ml samples were taken at the start and end of the experiment. These were filtered immediately through 0.45 µm MF-millipore filters and were then frozen until analysis for DRP.

Table 4.2 Key parameters at the start and end of the first slurry release experiment assessing the effect of salinity on PO_4^{-3} release in high pH waters.

Solution	EC ($mS.cm^{-1}$)		pH		DO ($mg.L^{-1}$)
	Start	Finish	Start	Finish	Finish
1	1.09	1.10	10.00	8.95	7.55
2	4.05	4.09	10.03	9.53	7.63
3	5.97	6.02	10.03	9.61	7.60
4	8.78	8.89	10.02	9.52	7.75
5	12.08	12.18	10.02	9.52	7.64

The experiment was repeated using 12 samples, with steps of approximately 1 $mS.cm^{-1}$ between samples (1-12 $mS.cm^{-1}$). pH was checked and adjusted twice during the 24 hr on the end over shaker, using 0.5M NaOH.

4.2.2 Geochemical modelling

Geochemical modelling was undertaken to further investigate the effects of redox conditions, pH, temperature and salinity on the release of P from the Wairewa sediments.

The PHREEQC computer model was used as described in Section 3.2.5. Surface complexation modelling was undertaken using the generalised two-layer model of Dzombak and Morel (1990), to model the adsorption of P on a hydrous ferric oxide surface (HFO). Comprehensive thermodynamic data sets of complexation constants only exist for HFO and hence the modelling is conducted with respect to HFO surfaces only. Surface complexation with Al (hydr)oxides, clays and organic material etc, was not modelled in this process. Given the significance of Fe (hydr)oxides in the Wairewa sediments (Section 3.4) it is assumed that surface complexation modelling of HFO will give reasonable insight into the factors affecting P desorption from the surface sediments.

Solution chemistry for the modelling was taken as the surface sediment pore water (0-1 cm) from core F11 C4 (Table 3.4), which was sampled and processed under a N_2 atmosphere. The concentration of high- and low-affinity binding sites were calculated for the HFO surface using the site densities from Dzombek and Morel (1990) (0.005 and 0.2 mol.mol Fe^{-1}, respectively). An HFO surface area of 600 $m^2.g^{-1}$ was assumed (Dzombak and Morel, 1990). The mass of HFO in contact with the solution was entered as 5% of the [Fe] in the BD extract of core F11 C3, assuming an HFO stoichiometry of $Fe(OH)_3$. This proportion of the BD-Fe was based on adjustments of the [Fe] used in the 'pH effect' modelling as described below, to best fit data from the core-incubation experiments.

4.2.2.1 The effect of pH on surface complexation

The effect of pH on surface-complexation was modelled using a single step modelling process, assuming a constant mass of HFO surface. Complexation was modelled for that HFO surface at various pH values. A modelled desorption curve, as a function of pH, is presented in Figure 4.2. Modelling which assumed that 100% of the BD extract [Fe] (as HFO) was in contact with water, resulted in a curve that lay too far to the right i.e. desorption commenced at higher pH than was observed in the pH core incubation experiments (refer Section 4.3.3.2), indicating that too much Fe was assumed to be in contact with water. This high Fe surface area resulted in high adsorption of OH^- at the HFO surface which had a buffering effect on modelled pH. Table 4.3 compares the desorbed PO_4^{-3} for solutions of differing pH (as a percentage of the P desorption at pH= 10) observed in the pH-core-incubation release experiment, with that predicted by modelling of varying proportions of the [BD-Fe]. The root mean square error is used to assess which proportion of [BD-Fe] provided the best fit with the observed data. The

desorption curve which best fitted the observed PO_4^{-3} release at varying pH in the pH-core-incubation experiment was around 5 % of the [BD-Fe], present as HFO. This proportion of the BD-Fe was subsequently used in pH and redox modelling

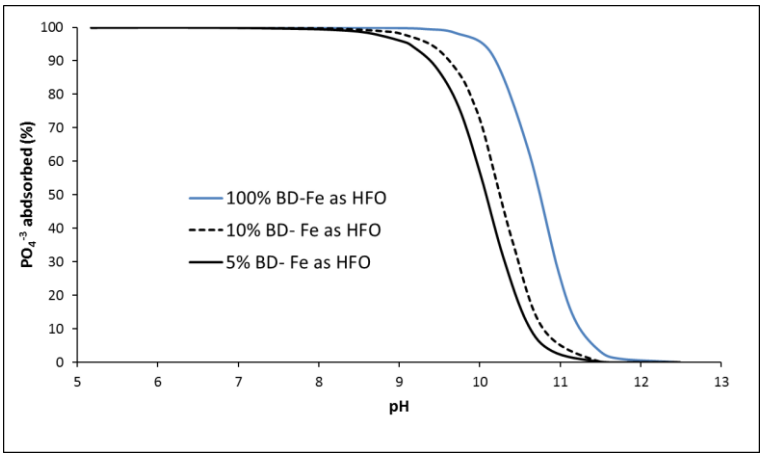

Figure 4.2 Modelled desorption curves which assume differing proportions of the BD-[Fe] is in contact with water. The 5 % [BD-Fe] curve provides the best fit for observed desorption in the core-incubation experiment.

Table 4.3 Comparison of observed (from the pH core incubation experiment) and modelled PO_4^{-3} release, for varying pH using PHREEQC and assuming HFO = varying proportions of [BD-Fe]. The values are as a % of the release in the pH= 10 solution (both observed and modelled). RMSE = root mean square error.

Solution pH	**Observed PO_4^{-3} release in core incubations (% of P release observed at pH=10)**	**Modelled PO_4^{-3} release (% of release in pH= 10)**		
		HFO=100% [BD-Fe]	**HFO=10% [BD-Fe]**	**HFO=5% [BD-Fe]**
10	100	100	100	100
9	7	2.93	6.73	7.20
8	3	0.4	0.79	1.59
7	0	0.1	0.29	0.42
RMSE (%)	0	2.79	1.29	0.85

The effect of varying temperatures and salinity on pH related desorption was also tested. Temperatures were selected to span the range seen in lake monitoring by Environment Canterbury (5 - 25 ^{o}C). Electrical conductivity was used as a proxy for salinity in the lake and also reflected a common EC range seen in lake monitoring data. For low EC conditions, the pore water chemistry of sample F11 S5 was used (Table 3.4), when lake

EC at the time of sampling was 0.736 mS.cm. For moderate EC conditions, F11 C4 pore water was used which reflects an OLW EC of 3.83 mS.cm. For high EC modelling F11 C4 0-1 cm pore water chemistry was used, but with Na, Cl, S, K, Ca and Mg all elevated to concentrations reflecting a water solution with EC = 12.6 $mS.cm^{-1}$. (These were estimated from the relationship between average sea water concentrations and conductivity). The [HCO_3] from F11 C4 was used. Assumed concentrations ($mg.L^{-1}$) for the high salinity solution are as follows; [Na] = 2949, [Cl] = 4660, [S] = 725, [K] = 804, [Ca] = 615, [Mg] = 1523.

4.2.2.2 Redox effect on surface-complexation

For modelling of redox related effects, the modelling was conducted in two steps. In the first step, the solution was equilibrated with the mass of HFO in order to determine the extent of precipitation or dissolution of the HFO surface under the varied environmental conditions (redox, salinity). The second step then modelled surface complexation between the equilibrated solution and HFO surface, to assess the extent of P release/uptake due to dissolution/precipitation of the equilibrated HFO surface, in response to the varied modelling conditions. The concentration of P in the solution was assumed to be 5% of the [P] in the BD extract for F11 C3, and the following data was used; particulate Fe mass of 0.0773 g (0.00138 mol), HFO mass of 0.148 g, mass of high and low affinity binding sites of 6.92 x 10^{-6} and 2.80 x 10^{-4} mol respectively, and a [TD-P] in solution of 4.82 $mg.L^{-1}$. The impacts of temperature and salinity on these redox related effects were then modelled as discussed above for the pH modelling.

4.3 Results

4.3.1 P release to an oxic, circum-neutral water column

The release of P into oxic, circum-neutral pH OLW was investigated by the use of both core incubation experiments and EPC slurry experiments. The “unadjusted” core-incubation experiment was conducted to provide a background P release rates, which could then be compared with P release from redox, pH and salinity adjusted core-incubation experiments. The EPC experiments were conducted to gain insight into the equilibrium dynamics between suspended sediment and the water column.

4.3.1.1 P release from undisturbed bed sediments

In the "unadjusted" core-incubation experiment (Figure 4.3 and Table 4.4), P was not released from the sediment cores, (1 core did produce an average release rate of 1 $mg.m^{-2}.day^{-1}$, which is considered to be within levels of experimental uncertainty). As these cores did not undergo a prior equilibration period, the P uptake (i.e. negative release rates in Table 4.4) observed in cores 2-5 may reflect re-equilibration following core disturbance during the core sampling and transport. The significantly elevated water column [P] in Core 1 and Core 5 supports this notion that disturbance during coring and transport resulted in elevated [P] in the water column.

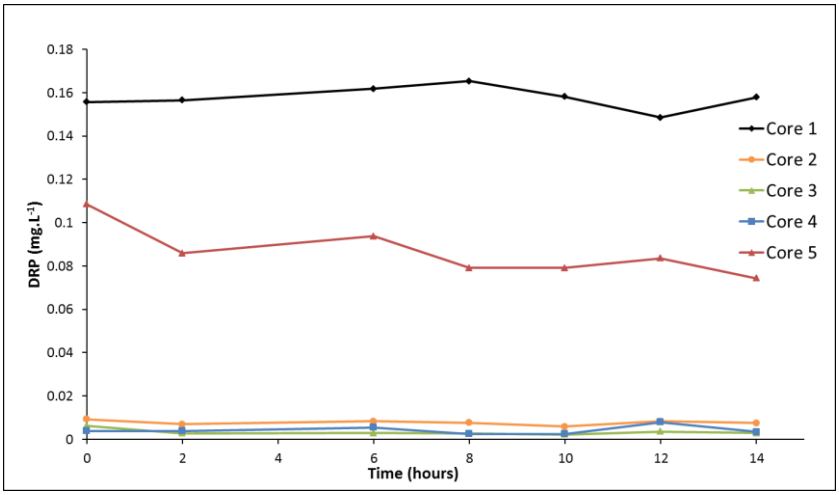

Figure 4.3 DRP concentration changes with time in the OLW during the unadjusted core-incubation experiment.

Table 4.4 Average (14 hour) release rates observed during the non-adjusted core-incubation experiment.

Core	Release Rate ($mg.m^{-2}.day^{-1}$)
1	1.01
2	-0.638
3	-1.01
4	-0.144
5	-12.1

4.3.1.2 P release from resuspended sediment

Graphs used to ascertain EPC_0 for the two EPC experiments are presented in Figures 4.4 and 4.5 respectively, while the resulting EPC_0 values are presented in Table 4.5. In the

first experiment, conducted in November 2014 on sediment from site F12, the duplicate samples provide good agreement with the EPC_0 value of 0.012 $mg.L^{-1}$. In the second experiment conducted in May 2014 using sediment from site F10 in two solutions of moderate EC (3.13 $mS.cm^{-1}$) and high EC (8.33 $mS.cm^{-1}$), the duplicate samples also provided good agreement. The F10 sediment EPC_0 values were an order of magnitude lower than those for the F12 sediment, indicating a lower P binding affinity in the F12 sediments. As the solutions had circum-neutral pH, were well oxygenated, and one of the F10 solutions had similar EC to F12, these differences must be due differences in the sediments rather than the solutions. However, as the sediments were sampled on different dates, whether these differences are spatial or temporal has not been determined. Surface sediments sampled from F10 and F12 on approximately the same dates (although on different dates to the sampling for the EPC experiments) indicated that the sites had similar concentrations of reactive Fe, but F10 had higher Org- and NaOH-P concentrations.

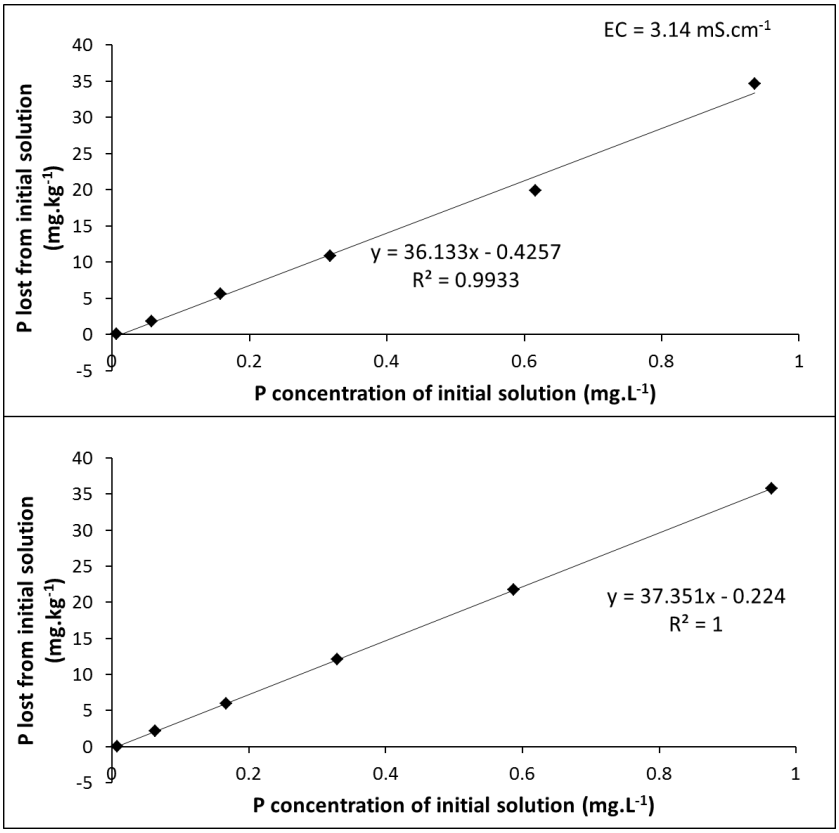

Figure 4.4 P lost from spiked lake water solutions (per kg of added sediment) vs initial solution P concentrations, for duplicate EPC experiments using sediment from site F12. Linear regression equations and regression coefficients are shown. The x axis intercept represents the EPC_0 presented in Table 4.5.

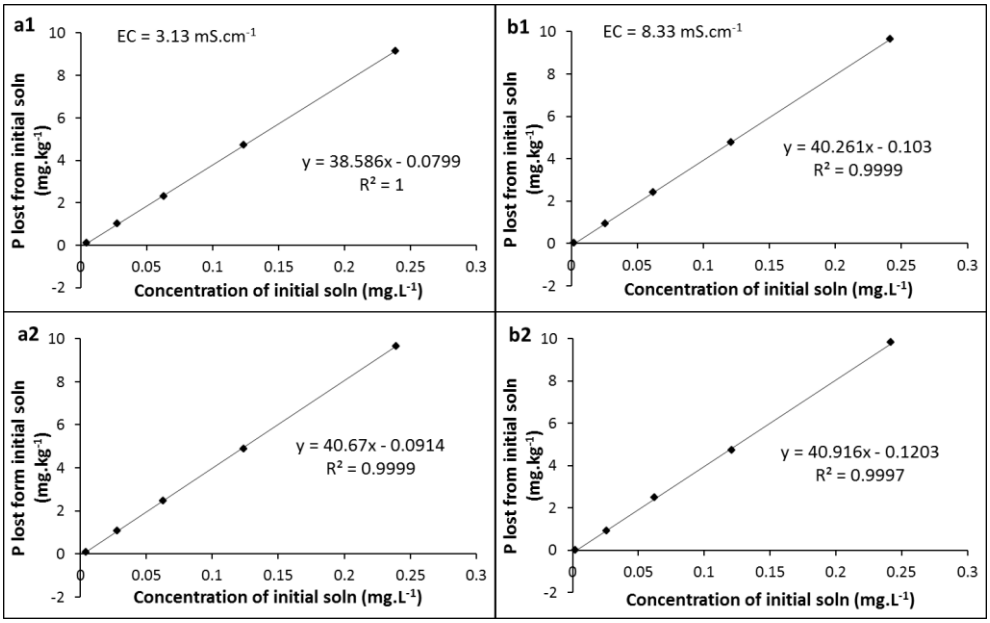

Figure 4.5 P lost from spiked lake water solutions (per kg of added sediment) vs initial solution P concentrations for duplicate EPC experiments using sediment from site F10. Linear regression equations and regression coefficients are presented. The x axis intercepts represent the EPC_0 concentrations in Table 4.5.

Table 4.5 EPC_0 concentrations for sediment from sites F12 and F10. For F10 sediments the experiment was repeated in moderate and high EC water. EC = $mS.cm^{-1}$

	EPC_0 ($mg.L^{-1}$)		
	F12	**F10**	
		EC = 3.13	**EC = 8.33**
	0.0115	0.0021	0.0026
	0.0121	0.0022	0.0029
Mean	0.0118	0.0022	0.0028
SD	0.0004	7.07×10^{-5}	0.0002

4.3.2 Redox-related P release

Redox related P release was investigated through the use of core-incubation experiments and geochemical modelling.

4.3.2.1 P release from bed sediments

Phosphorus release over time and calculated release rates from the redox- core-incubation experiments are presented in Figure 4.6 and Table 4.6 respectively. P release was negligible for all cores when [DO] > 0 $mg.L^{-1}$. As the OLW became increasingly reducing, P release increased, beginning at around E_h= 100 mV. Release rates increased rapidly under lower redox conditions, with average rates reaching 20-64 $mg.m^{-2}.day^{-1}$ at

E_h values of -210 and -300mV respectively. Maximum release rates of 385-865 $mg.m^{-2}.day^{-1}$, were recorded on the rising limb of the major peaks seen in Figure 4.6. The cause of these peaks is uncertain as EC, pH and E_h remained relatively constant but the synchronised peaks in the two cores suggests an analytical issue. P release in the low E_h cores showed no sign of diminishing in the 48 hours of the experiment. It is possible that an increase in [S] due to the addition of NaS_2O_4 (to decrease E_h), may have enhanced P release in the Eh = -210 and -300 mV cores, however research into the effects of increased salinity (Section 4.3.4) indicates that this effect is likely to be negligible at the circum-neutral pH, maintained during these redox- core-incubation experiments.

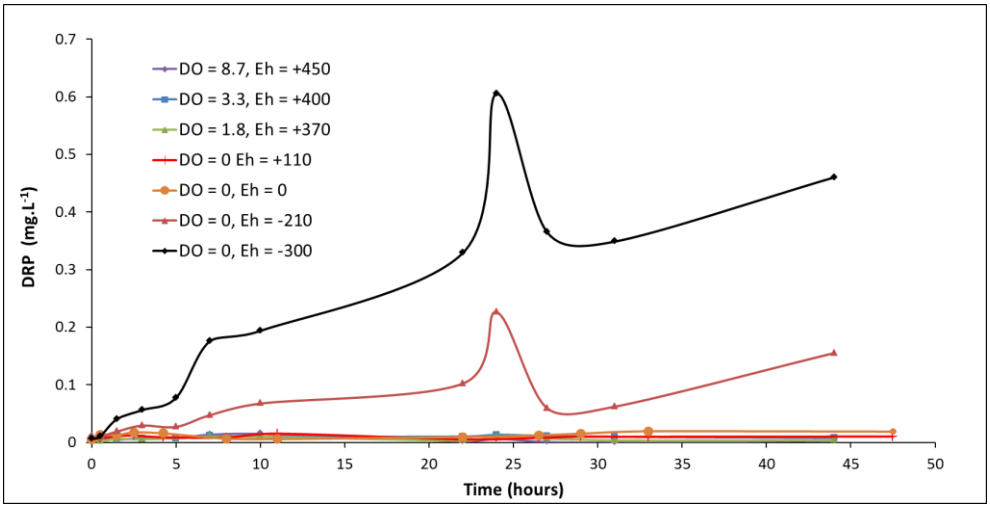

Figure 4.6 DRP concentration changes over time during the DO core-incubation experiment. DRP is as measured in the OLW. OLW DO concentrations are in $mg.L^{-1}$ and E_h is in mV. Results are from the October 2014 experiment except the results for E_h = 0 and +110 mV which are from the November 2014 experiment.

Table 4.6 Average and maximum release rates observed during the redox core-incubation experiment. E_h = oxidation-reduction potential.

Redox Condition		**Release Rate ($mg.m^{-2}.day^{-1}$)**		
DO ($mg.L^{-1}$)	**E_h (mV)**	**Average (first 3 hr)**	**Maximum 2 hour period**	**Average (44 hr)**
8.7	+450	-8.36	13.2	-0.900
3.3	+400	3.72	13.9	0.303
1.8	+370	-5.58	-0.449	-0.577
0	+110	15.2	14.0	0.754
0	0.00	32.2	29.6	2.79
0	-210	41.8	385	20.6
0	-300	110	865	64.0

The effect of a change in redox conditions in the OLW on sediment pore water can be seen in Figure 4.7. Increased pore water [TD-Fe] indicated that 48 hours of anoxic conditions in the OLW decreased pore water redox potential to a sediment depth of around 3 cm. The pore water redox potential was low enough to cause $Fe^{+3} \rightarrow Fe^{+2}$ reduction, with a coincident increase in pore water [TD-P]. Pore water [TD-Mn] was also significantly increased in the core with anoxic OLW, and was affected to a deeper sediment depth.

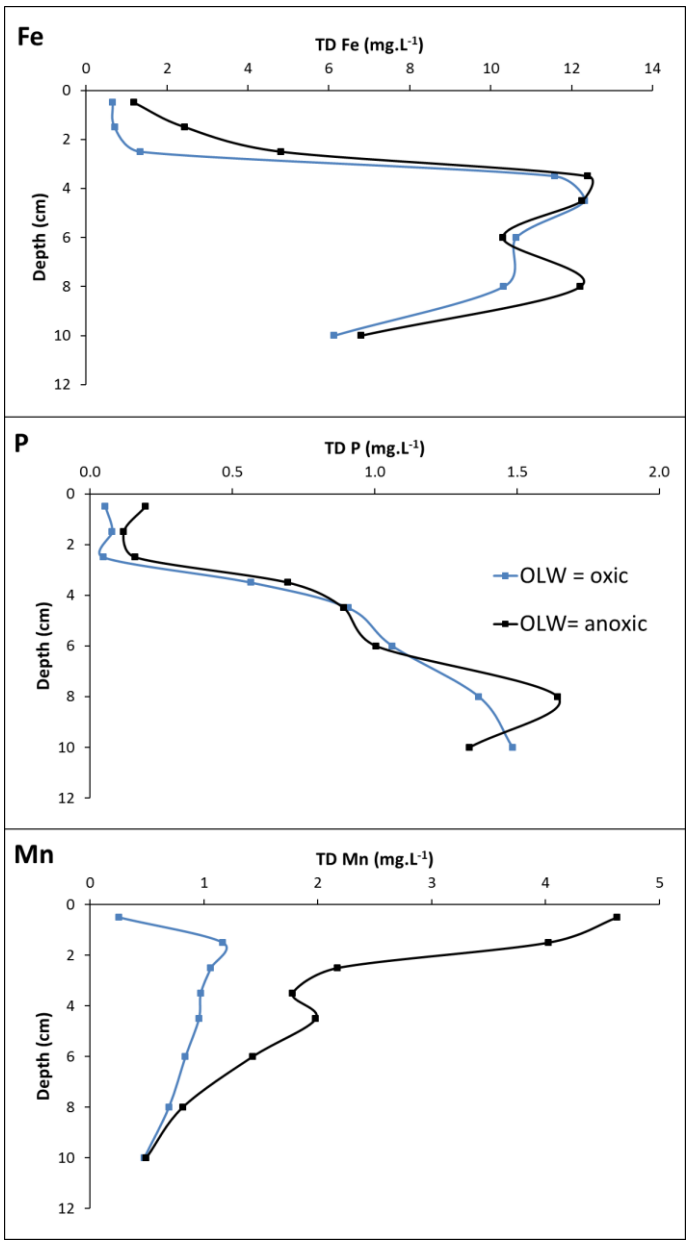

Figure 4.7 Total dissolved concentrations of Fe, P and Mn measured in the pore waters of two cores, after 48 hours of a core-incubation experiment in which the OLW of one core was maintained under oxic conditions and the other was deoxygenated to DO = 0 $mg.L^{-1}$, E_h = 0 mV. Depth is below sediment/water boundary.

4.3.2.2 Geochemical modelling of redox effects on P release

Figure 4.8 presents the results of surface complexation modelling under varying redox conditions. As the HFO surface begins to dissolve at around pe < 6 (E_h = 355 mV), the proportion of P adsorbed to the HFO surface begins to decrease, resulting in an increase in the proportion of [P] in solution. The dissolution is limited until pe < 2 (E_h = 120 mV), where dissolution increases significantly as redox conditions become progressively more reducing. The beginning of HFO dissolution at pe < 6 occurs as oxygen becomes unavailable as an electron acceptor (Table 3.5), and Fe reduction begins. The beginning of significant dissolution at E_h = 120 mV was consistent with the core incubation experiment where significant release began at around E_h = 110 mV.

The effect of low temperatures can also be seen in Figure 4.8. Reducing the temperature from 20^{o}C to 5^{o}C moves the dissolution curve slightly to the right. At 5^{o}C, rapid dissolution with decreasing redox conditions occurs at pe < 3 rather than at pe < 2 (at 20^{o}C). The reduction of an HFO surface and subsequent release of redox sensitive P is therefore thermodynamically favoured at lower temperatures, but only a minor difference is evident.

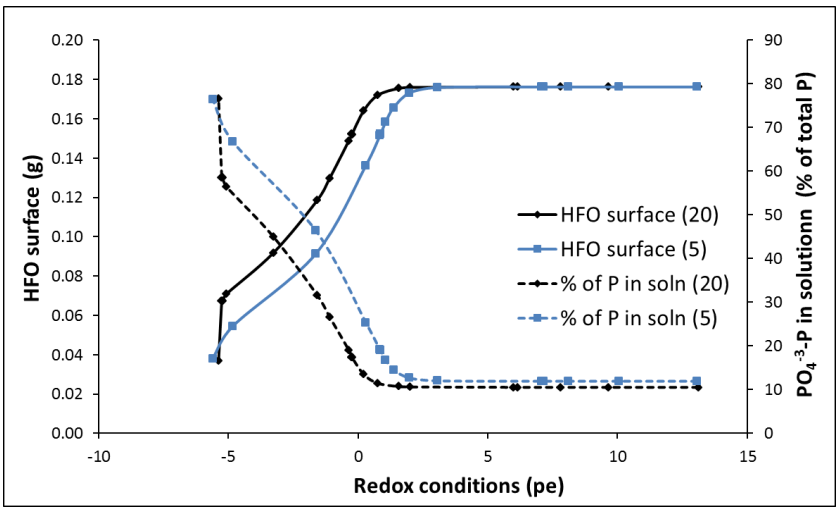

Figure 4.8 Modelled P desorption under various redox conditions at two solution temperatures (20^{o}C and 5^{o}C). The mass of HFO surface in contact with 1 kg of pore water is shown on the left-hand x axis, while the mass of PO_4^{-3} in solution (as a % of total P) is on the right x axis.

4.3.3 pH-related P release

4.3.3.1 P release from resuspended sediments

Figure 4.9 presents the results of the pH- slurry release experiment. P release was observed in the pH = 7.83 (average) solution, but reached an equilibrium with no further release or uptake within a few hours. At pH ≥ 8.6, however, P release was initially very rapid, especially within the first hour, and continued throughout the experiment albeit at a lower rate. At pH = 9.09 and pH = 9.98 similar initial release curves were observed, but higher release rates occurred after 4 hours.

The experiment allowed calculation of release rates per kg of sediment, which were converted to release rates per m^2 (Table 4.7), to allow comparison with release rates from the core-incubation experiments. This conversion assumed sediment densities of 2.81 $kg.m^{-2}$ as calculated for the surface sediment (0-1 cm) from core F11 C3 (Table 3.8), and 2 mm of surface sediment resuspended into the slurry. As sediment density was not calculated at a resolution finer than 0-1 cm, it has also been assumed that the density is consistent throughout the top 1 cm. Density may in fact decrease upwards in this surface sediment fraction, so these calculated areal release rates may be an over-estimation. Areal release rates were high for all solutions and increased with pH.

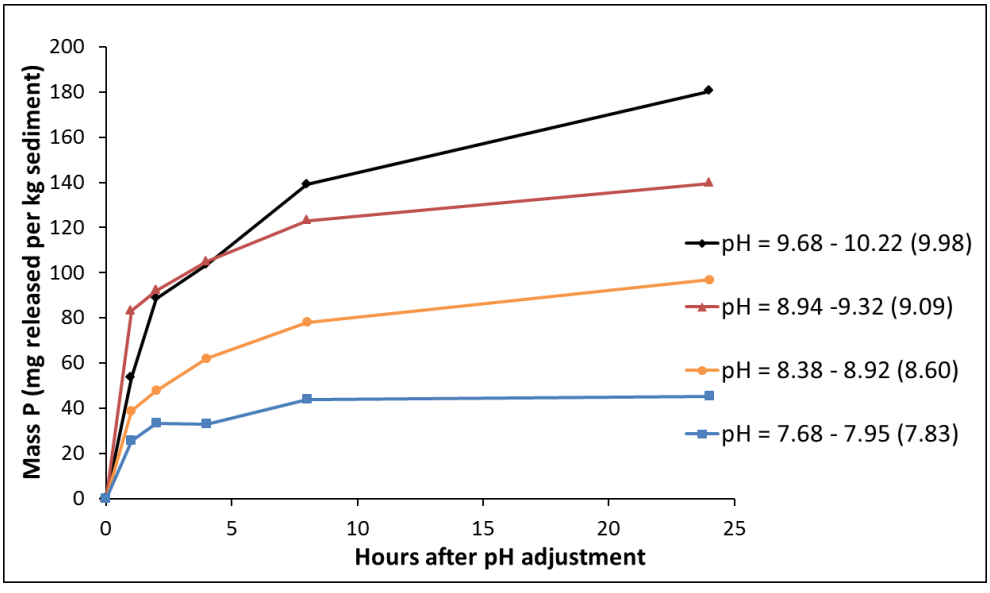

Figure 4.9 Mass of P released over time during the pH slurry release experiment. Sediment refers to dry weight. The plot legend shows the pH range observed during the experiment + (the average over 24 hours).

Table 4.7 Average and maximum release rates observed during the pH- slurry release experiment. Rates from the experiment were calculated per kg of sediment (dry weight), and then converted to areal release.

Average pH	Release Rate ($mg.kg^{-1}.day^{-1}$)		Release Rate ($mg.m^{-2}.day^{-1}$)	
	Average (24 hours)	Maximum	Average (24 hours)	Maximum
7.83	45.2	615	25.4	345
8.60	96.9	930	54.4	522
9.09	140	1200	78.4	1120
9.98	180	1290	101	722

4.3.3.2 P release from bed sediments

Phosphorus release over time, and calculated release rates from the pH- core incubation experiment, are presented in Figure 4.10 and Table 4.8 respectively. The release of P was negligible for an OLW of pH = 7.10, but was higher at pH close to 8, while the most significant P release was observed at pH > 9. As the experiment progressed a significant dip occurred in [DRP], in the pH = 9.94 core, at time = 20 hours. This resulted from a short-lived drop in the pH of the OLW to pH = 9.19, illustrating the pH sensitivity of the sediment P release/uptake processes.

The P release rates are modest compared to the rates seen in both the pH- slurry release and the redox- core-incubation experiments.

Table 4.8 Average and maximum release rates observed during the pH- core incubation experiment.

pH	Release Rate ($mg.m^{-2}.day^{-1}$)		
	Average (first 4 hr)	Maximum observed	Average (46 hr)
7.10	0.425	8.36	0.573
7.93	4.18	6.97	2.24
8.97	4.18	5.57	3.27
9.94	18.1	60.36	11.07

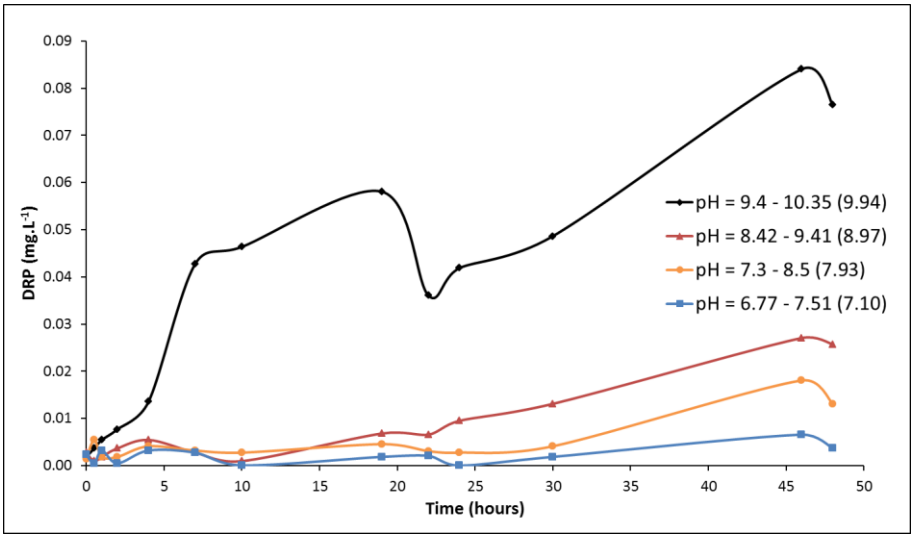

Figure 4.10 DRP concentration in OLW over time during the pH core-incubation experiment. The pH range observed during the experiment, and the average pH over 48 hours (in parentheses) are shown.

The effect of a pH change in the OLW, on sediment pore water, can be seen in Figure 4.11a. After 48 hours of pH = 9.40 - 10.35 in the OLW, pH had increased from 7.07 to 9.03 in the pore water in the top 1 cm of sediment. Pore water pH was elevated to a depth of around 6 cm, but the effect below 1 cm was less (pH = 7.55 at 1-2 cm depth) and these pH increases were insufficient to cause significant P release from the sediment. Pore water [DRP] had increased significantly (x 50) in the top 1 cm, but was unaffected at depths below 1cm (Figure 4.11b).

The effect of the simulated short-term resuspension of the top 2 mm of sediment in varying pH OLW can be seen in Figure 4.12. In the lower pH OLW, resuspension resulted in a short term decrease in [DRP], while in the higher pH OLW the [DRP] immediately increased. At pH = 7.93 and 8.97, this was followed by a subsequent decline in [DRP] back to pre-suspension levels, while at pH = 9.94, the initial release was sustained for 15 mins and then decreased.

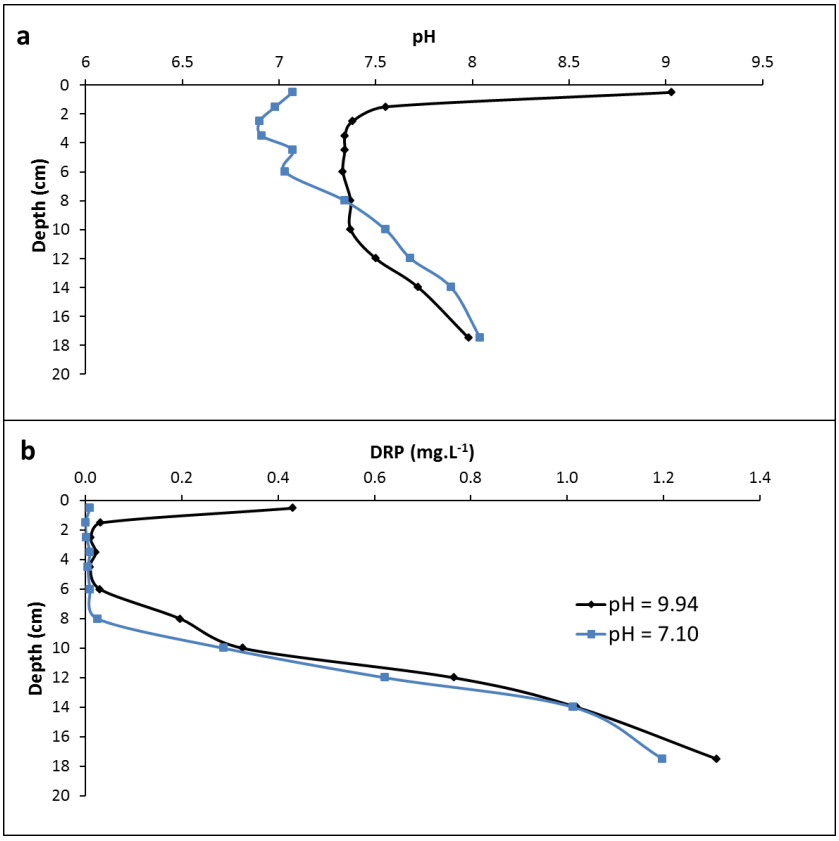

Figure 4.11 The effect of the pH of the over-lying water column (OLW) on (a) pore water pH, and (b) pore water DRP concentration, in the sediment cores, after a 48 hour core-incubation period. Depth is below sediment/water boundary. pH is the average measured in the OLW over the 48 hours of the experiment.

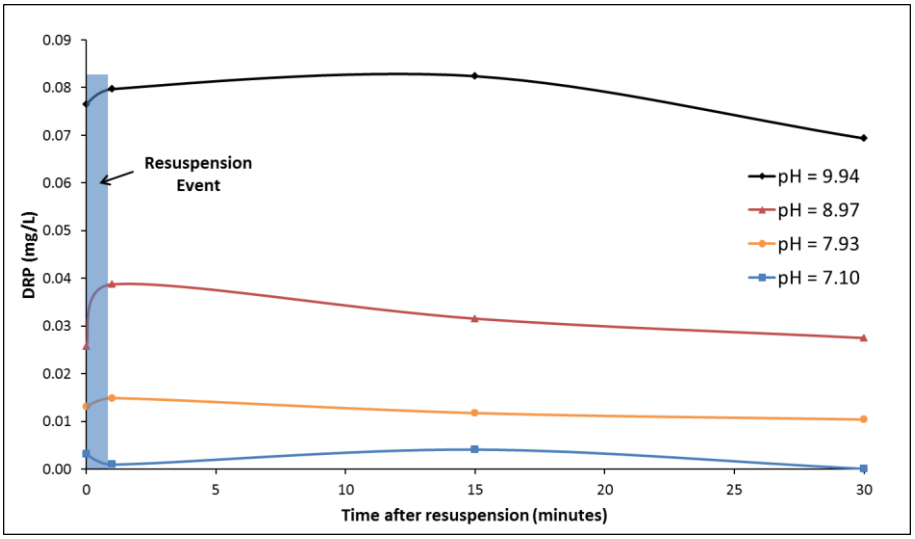

Figure 4.12 DRP concentration change over time in the OLW during following a simulated sediment resuspension event at the end of a pH core-incubation experiment. pH is the average measured in the OLW for each core, over the 48 hours of the experiment.

4.3.3.3 Geochemical modelling of pH related P release

Figure 4.13 presents the modelled adsorption curve for variable pH using core F11 C4 pore water at 20^{o}C, assuming an HFO surface of 5% of [BD-Fe]. With increasing pH, adsorption decreased at pH > 8.5, with complete desorption at pH ≈ 11.5. The steepest part of the curve lies between pH ≈ 9.5 and 10.7. This is consistent with the release rates observed in the pH- related slurry, and core incubation experiments. Changing the temperature of the modelling simulation to 5 and 25 ^{o}C had almost no effect on pH related desorption.

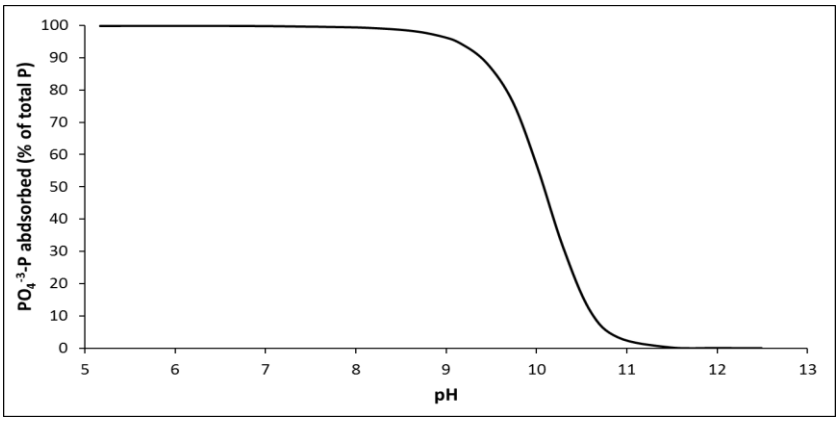

Figure 4.13 Modelled adsorption curves for F11 C4 pore water chemistry, HFO surface = 5% BD-Fe and temperature = 20 ^{o}C.

4.3.4 Salinity effects on P release

The effect of varied salinity in the OLW on P release was investigated through the use of slurry experiments, core-incubation experiments and geochemical modelling. The core-incubation experiments provided information on the effect of changing salinity in the lake OLW, during oxic and circum-neutral pH conditions. The slurry experiments and geochemical modelling investigated the effect of salinity on pH and redox-related P release.

4.3.4.1 P release from bed sediments

The results of the February 2014 salinity- core-incubation experiment are presented in Figure 4.14. The original EC of the OLW prior at the time of core collection, was 4.54 mS.cm^{-1}. After dilution and equilibration, the EC of 0.68 mS.cm^{-1} was adjusted to the EC's shown in Figure 4.14. There was then a period of around 24 hr with no release of P from the cores. After 24 hr however, P release began, with the greatest release

occurring in the cores with an OLW EC lower than the pre-equilibration EC (i.e. EC < 4.54 $mS.cm^{-1}$). This correlation is shown in Figure 4.15. Figure 4.14 also provides the change in EC over the duration of the experiment. For cores with EC < 4.54 $mS.cm^{-1}$ (pre-equilibration EC), EC increased over time. The core with OLW EC close to the pre-equilibration EC showed little change over the experiment, while the cores with EC > than pre-equilibration EC, showed a decrease in EC.

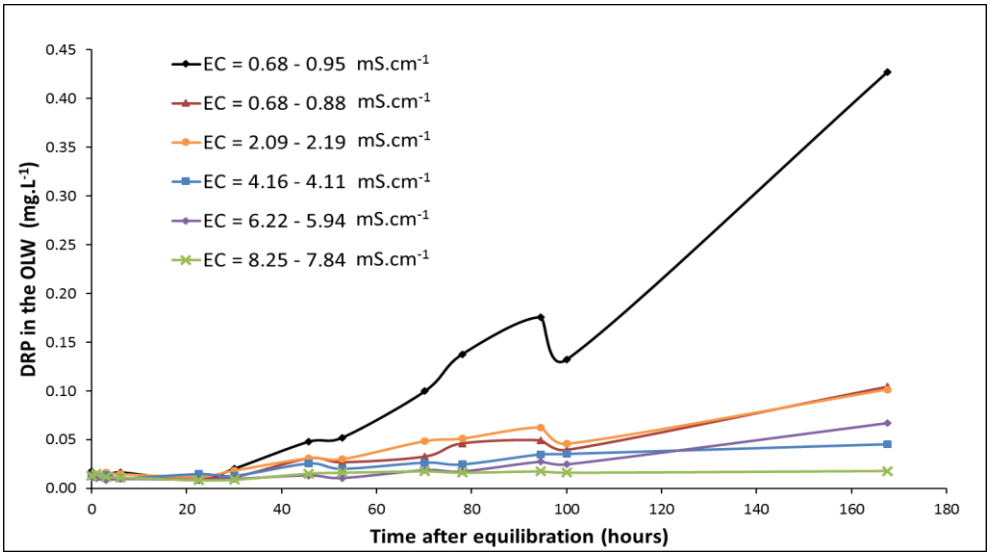

Figure 4.14 DRP concentration changes over time during the February 2014, salinity core-incubation experiment. EC denotes the change in EC in the OLW, from the start to end of the experiment.

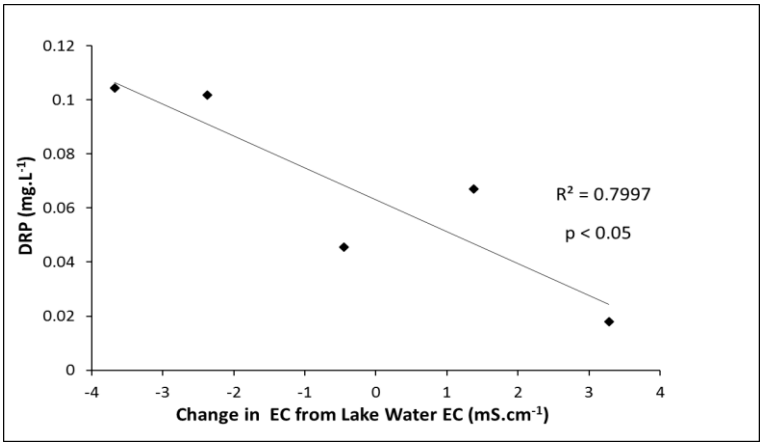

Figure 4.15 The final DRP concentration vs the change in EC from pre-equilibration EC to the EC at the end of the salinity- core-incubation experiment (February experiment),

The results of the second salinity- core-incubation experiment are shown in Figure 4.16 with the release rates presented in Table 4.9. This experiment was conducted 13 days after a significant rain event in the catchment resulted in a natural 'freshening' of the north end of the lake. This provided an opportunity to assess whether the results of the

first salinity- core-incubation experiment (Figure 4.14) would be seen for a naturally occurring dilution of lake EC.

The results of this second experiment were very similar to the first, with P release facilitated by dilution of the OLW EC. The core in which the EC was diluted to 0.34 $mS.cm^{-1}$ (less than the 'natural' freshening event), had the greatest P release, while the unadjusted core (EC = 0.58 $mS.cm^{-1}$) had the second highest P release. The cores in which EC was adjusted upward, toward the summer average lake EC of 4.54 $mS.cm^{-1}$, had significantly lower release rates. With time, the EC in the OLW tended towards a value somewhere between the usual summer EC (4.54 $mS.cm^{-1}$) and the 'new' freshened lake value (0.39 $mS.cm^{-1}$) as shown in Figure 4.17. Hence a freshening of the OLW after a period of stable, EC conditions in the lake, appears to promote P release from the sediments.

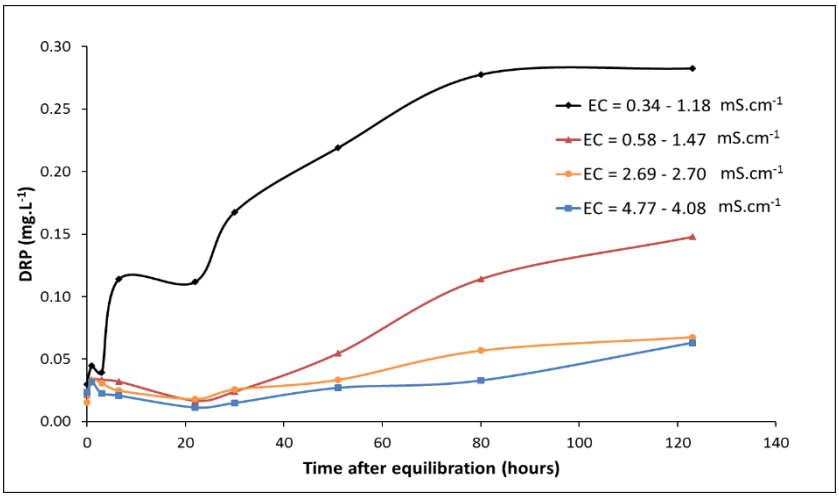

Figure 4.16 DRP concentration changes in the OLW over time, during the March 2014 salinity core-incubation experiment, conducted following an influx of fresh water into the lake. 'EC =' denotes the change in EC from the start to end of the experiment.

Table 4.9 Average and maximum release rates observed during the March 2014 salinity core-incubation experiment. The maximum release rates for all cores except EC = 0.34-1.18 $mS.cm^{-1}$, occurred during the first hour of the experiment.

EC	Release Rate ($mg.m^{-2}.day^{-1}$)		
$mS.cm^{-1}$	Average (first 5.5 hours)	Maximum	Average (123 hrs)
0.34-1.18	78.2	132	12.7
0.58-1.47	-1.52	72.5	6.35
2.69-2.70	-9.12	109	2.63
14.77-4.08	-12.2	50.2	1.99

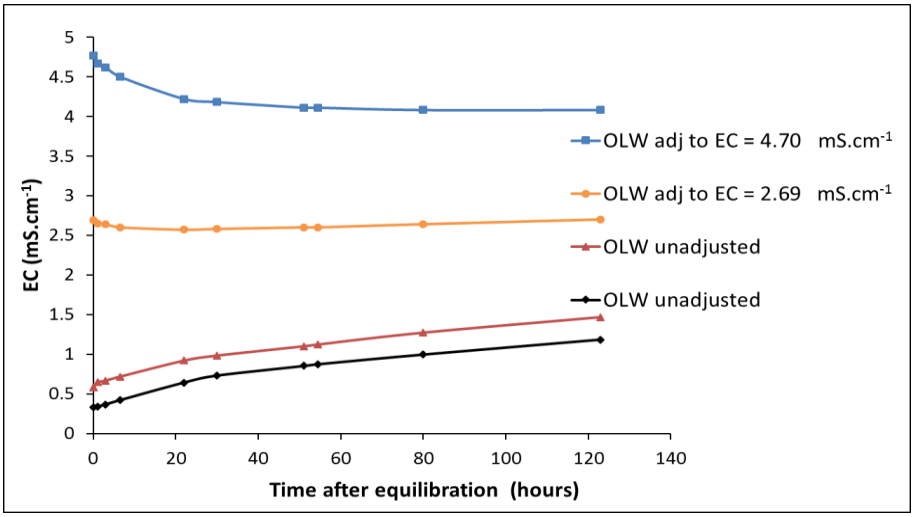

Figure 4.17 Changes in EC over time during the salinity- core-incubation experiment March 2014, when a natural rain event reduced EC in the lake 13 days prior to collection.

This equilibration of EC in the pore water and in the OLW, resulting from the freshening of the lake, can be seen in Figure 4.18a, for a core taken and sectioned at the lake on the 18 March 2014. At depth the pore water EC is still at pre-freshening level of around 4 $mS.cm^{-1}$, while in the OLW the EC is at the post-freshening level of 0.39 $mS.cm^{-1}$. In between there is a steep EC gradient.

In the core incubation experiment an unadjusted core (EC = 0.58 $mS.cm^{-1}$), sectioned at the end of the experiment (3 April 2014), also shows the equilibration of the OLW and pore water EC (Figure 4.18a). This is similar to another core sampled and sectioned at the lake on the 2 April 2014, which confirmed that the process apparent in the near-surface sediments of the experimental cores, was also occurring in the lake itself.

The effect of these changes in OLW EC, on pore water and OLW [DRP], is shown in Figure 4.18b. The low EC core from the salinity- core-incubation experiment (March 2014) shows an increase in [DRP] in both the OLW and pore water at the end of the experiment, relative to the in-situ core (18 March 2014). This is due to either a release of P from the adjacent sediment, or an increased flux of dissolved P from deeper sediments. Conversely, the higher EC adjusted core (in which the OLW EC was close to pre-freshening levels- Figure 4.17) had lower pore water [DRP] over the whole sediment profile. This may be due to a decreased flux of DRP from the deeper sediment.

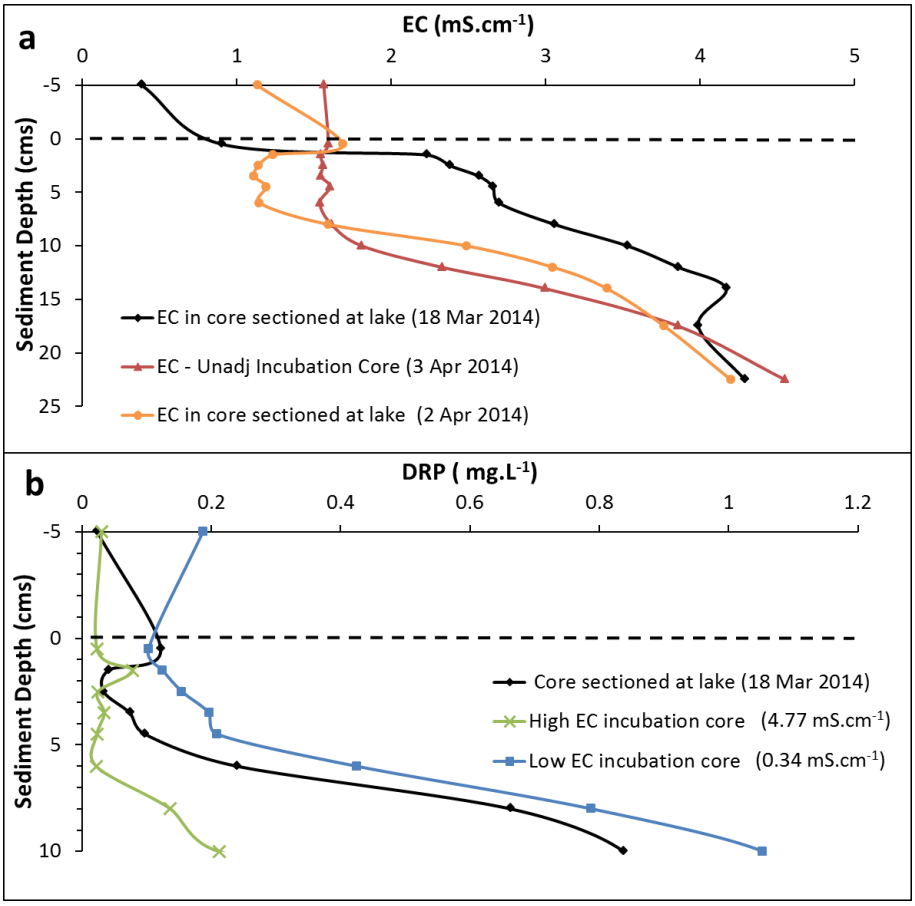

Figure 4.18 The effect of EC changes in the overlying water column (OLW) on sediment pore water (a) EC and (b) DRP. Sediment depths of < 0 indicate the OLW. EC incubation cores were sectioned in the laboratory after the March salinity- core incubation experiment.

Following the results of these salinity- core-incubation experiments, the lake surface water was sampled from north to south to see if any evidence could be found of a relationship between EC and [DRP] in the lake water. Figure 4.19a presents the EC gradient present in the lake on the 26 March 2014, 21 days after the 'freshening' rain event, with the north end of the lake significantly fresher than the south. Figure 4.19b-c presents the relationships between EC, and [DRP] and [TP], respectively. While the correlations were not particularly strong and are not statistically significant, the north (fresher) end of the lake had higher [DRP] than the south (higher EC) end, despite the opposite trend in [TP]. DO of the bottom OLW was > 8.9 $mg.L^{-1}$ at all sites except F10 (DO= 5.71 $mg.L^{-1}$) and pH was circum-neutral at all sites.

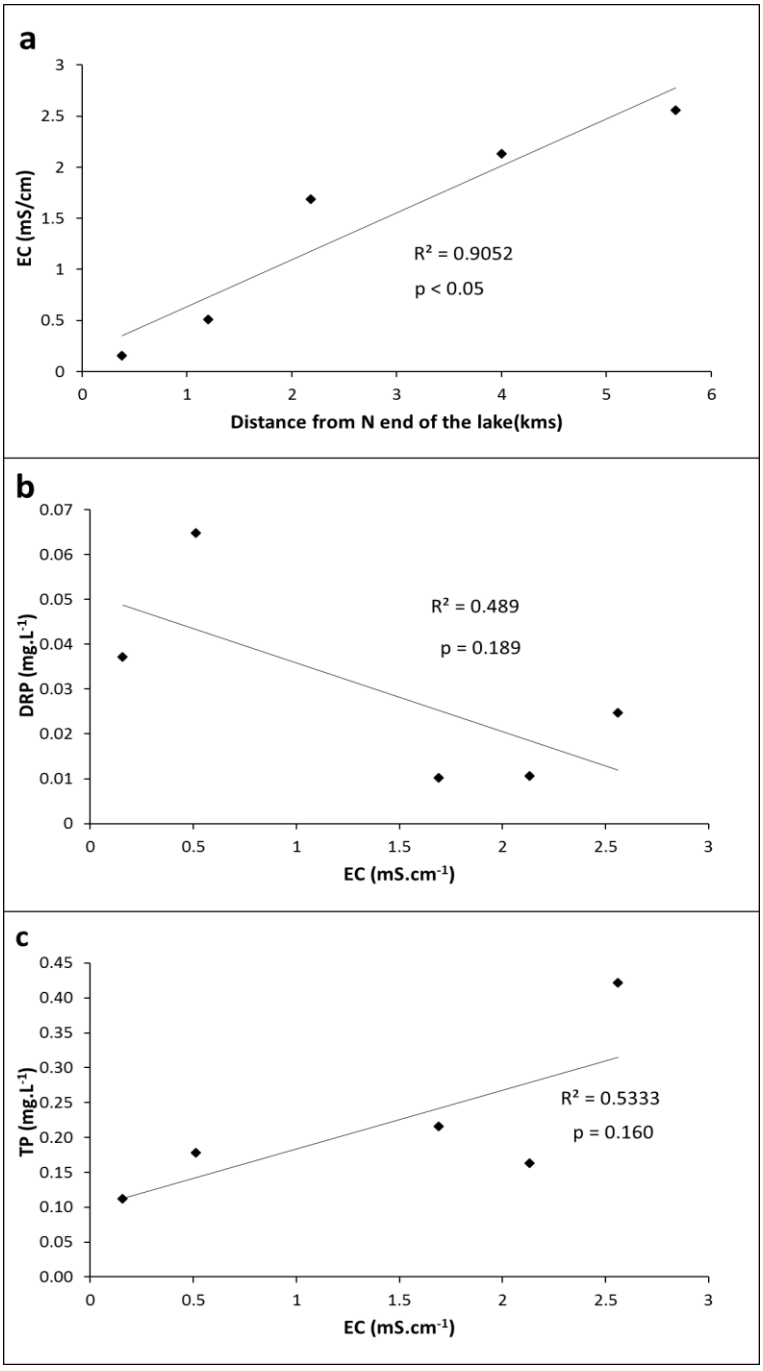

Figure 4.19 Lake gradients on 26 March 2014 showing; (a) EC along the lake following a significant influx of fresh water on 5 March 2014, and concentrations of (b) DRP vs EC and (c) TP vs EC, at five sites along the lake. The main source of freshwater is the lakes main tributary, the Takiritawai River which enters at the north end of the lake.

4.3.4.2 P release from resuspended sediment at high pH

Figure 4.20 presents the results of the two slurry release experiments conducted to assess the effect of salinity on P desorption from suspended sediments in high pH solutions. A

pH of 10 was used in the experiment as this falls in the steepest part of the pH desorption curve (Figure 4.13). A pH of 10 is also observed in the lake (refer Chapter 5).

The results of the first experiment (Figure 4.20a) show a weak correlation between desorption at pH ≈ 10 and increasing EC (R^2= 0.50). However the second experiment shows a weak negative correlation (Figure 4.20b). Neither correlation is statistically significant. Hence the effect of increased salinity on high pH-related desorption was inconclusive.

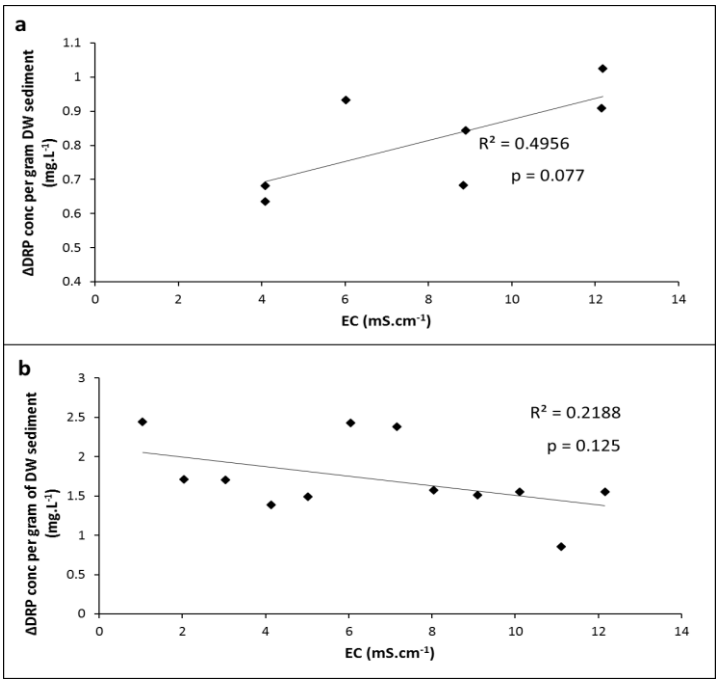

Figure 4.20 Results from two slurry release experiments testing the effect of different salinities on P adsorption, in high pH (pH=10) water. (a) The initial experiment in which pH was not adjusted during the experiment and the average pH = 9.54 at the end (pH= 10.02 at the start), and (b) the second experiment in which pH was adjusted and the average pH = 10.02 at the end (pH =10.08 at the start).

4.3.4.3 Geochemical modelling of salinity effects on P release

Effect on pH-related desorption

Geochemical modelling was undertaken to determine the effects of salinity on both pH- and redox related P release. The effect on pH related P release is presented in Figure 4.21. Increased salinity moved the modelled adsorption curve to the left. The pH_{50} (pH at which 50 % of PO_4^{-3}-P is adsorbed) moved from 10.25 for EC = 0.74 $mS.cm^{-1}$, to 9.65 for EC = 12.6 $mS.cm^{-1}$. At high EC, PO_4^{-3} adsorption decreased, while Mg adsorption increased (Table 4.10).

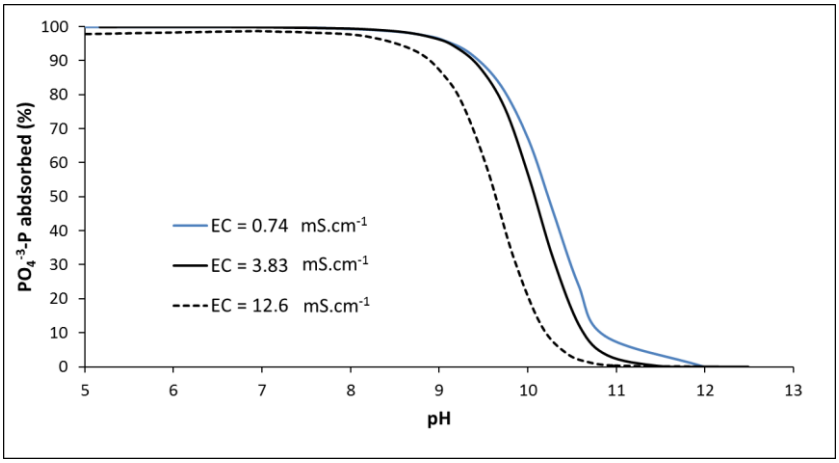

Figure 4.21 Modelled pH adsorption curves for varying levels of salinity in the lake.

Table 4.10 Changes of adsorbed species (% of total adsorption sites filled) in low EC (EC = 0.736 mS.cm^{-1}) and high EC (EC = 12.6 mS.cm^{-1}) lake water solutions modelled at pH = 10 and 5% [BD-Fe] as HFO. Mass of total adsorption sites is the same for both salinity scenarios.

Surface complex (total)	Adsorption sites filled (% of total sites)	
	Low EC	High EC
Tot ≡PO_4	2.0	1.0
≡OMg^+	49.0	66.2
≡O^-	44.8	31.5
≡OH	3.2	0.3
≡OCa^+	0.7	0.9
≡$OHCa^{+2}$	0.2	0.0
≡$OHSO_4^{-2}$	0.0	0.3
≡OZn^+	0.1	0.1

Effect on redox-related P release

The effects of variable salinity on P release under changing redox conditions are presented in Figure 4.22. Increased salinity moves the dissolution curve to the right resulting in the steeper part of the curve beginning at a higher pe. More rapid dissolution of the HFO surface with decreasing redox conditions begins at pe < 2 in the higher salinity as opposed to pe < 1 in the lower salinity. As a result there was a decrease in the total adsorption sites available at pe < 2 in the high salinity solution. The increased HFO dissolution resulted in the proportion of [P] in solution, increasing in the high salinity solution, for all pe values. This was a result of both the decrease in HFO surface at pe < 2 and subsequent decrease in number of adsorption sites, and competition for available adsorption sites from the higher ionic strength solution.

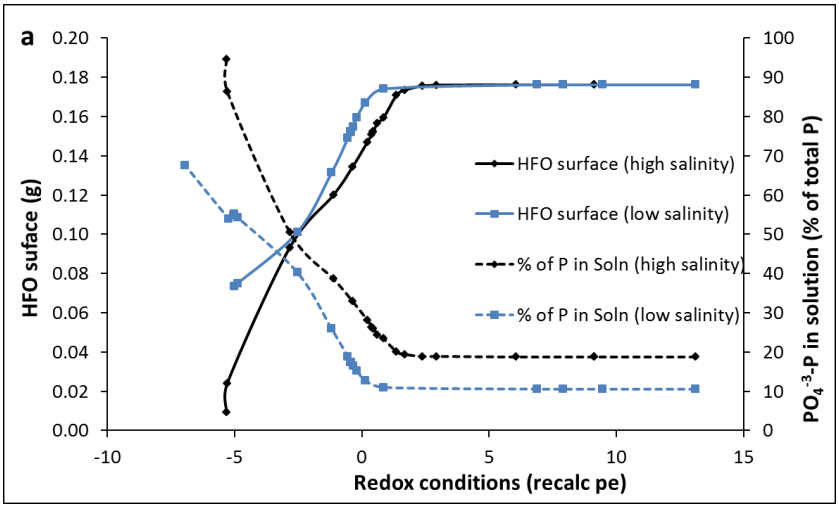

Figure 4.22 Modelled responses to varying redox conditions in high and low salinity solutions, showing the mass of HFO surface in contact with 1 kg of pore water, and PO_4^{-3}-P in solution as a % of total dissolved and adsorbed P.

4.4 Discussion

4.4.1 The release of P in an oxic, circum-neutral water column

The sediments of Wairewa provide a major sink for P sequestration in the lake but a significant proportion of this P reservoir occurs in mobile forms (Chapter 3), and periods of significant P release from the sediments has been shown to occur (Chapter 2). P release to oxic and circum-neutral pH water columns has been reported in various studies (Kim et al, 2003; Cyr et al, 2009), and Steinman et al (2009) reported P release rates under aerobic conditions of 0 - 1.54 $mg.m^{-2}.d^{-1}$ in a shallow lake in Michigan (USA). However P was not released from undisturbed Wairewa cores under oxic and circum-neutral pH conditions.

Phosphorus equilibrium concentrations refer to the water column [DRP] concentration below which P will be released from the sediment (Cyr et al, 2009). Such EPC_0 values of between 0.007 – 0.119 $mg.L^{-1}$ have been reported in shallow polymictic lakes (Cyr et al, 2009) and the EPC_0 values determined for Wairewa sediments are at the lower end of this spectrum and therefore have a high binding capacity. The Wairewa EPC_0 values were also highly variable and more work is required to determine whether this variability is spatial, temporal or both. However, given the negative release rates from the core incubations under oxic conditions, and the low EPC_0 for the sediment, equilibrium

concentrations are unlikely to be a significant driver of P release, even during sediment resuspension.

Søndergaard et al (1992) found significant release of P (60-70 $mg.m^{-2}.d^{-1}$) from resuspended sediments in the shallow Lake Arresø. These high rates were attributed to low Fe:P ratios (2.2) and high [NH_4Cl-P]. Jensen et al (1992) also found an inverse relationship between Fe:P ratios and aerobic P release in 15 Danish lake sediments. In the Wairewa sediments, the ratios of reactive Fe:P (Table 3.10), are significantly higher than those reported by Søndergaard et al (1992) and the proportion of NH_4Cl-P is much lower. The high Fe:P ratio, low [NH_4CL-P] and the ubiquity of wind-induced resuspension in Wairewa, compared with the variable timing of the algal bloom events, suggest that P release associated with sediments resuspended into an oxic, circum-neutral pH water column, are unlikely to result in P loading significant enough to sustain algal bloom formation (see also Chapter 5).

4.4.2 Redox-related P release

The binding mechanisms of P in the sediments of Wairewa (refer to Chapter 3) suggest that low redox conditions in the water column are likely to result in P release from the sediment. The redox sensitive BD-P fraction comprises 25% of the [TSP] and even though the comparison of geochemical modelling and core-incubation results indicated that a small proportion of the BD-extracted Fe and P is in contact with surrounding water, this still constitutes a large P reservoir available for such redox mediated release.

Core incubation experiments indicated that negligible P release occurs until complete deoxygenation of the water column has occurred (E_h < 100 mV). Significant P release began between E_h =100 and 0 mV (see Table 4.11). Geochemical modelling predicted significant HFO dissolution and resulting P release at E_h = 60 to 0 mV. The agreement between modelled HFO dissolution, and significant experimental P release under reducing conditions, supports the notion that HFO is a major P-binding phase in these sediments. Moore and Reddy (1994) found similar results with P release occurring at around Eh = 0 mV in muddy sediments from a shallow lake in Florida. Christophoridis and Fytianos (2006) also found P release from lake sediments began at around 100 mV, while Gomez et al (1999) found the reduction of goethite (Fe(OOH)) began between Eh =100 and -50 mV at pH = 7, in the sediments of a shallow coastal lagoon in France.

P release in the Wairewa sediments was greatly increased under even more reducing conditions (Eh < -210 mV). Increased pore water [Fe] and [P] down to 3 cm, and [Mn] down to 8 cm, showed the depth to which sediments were affected by only 48 hours of lowered redox conditions in the OLW.

The range of average redox-related P release rates seen in the Wairewa sediment core incubations (0.7 – 64 $mg.m^{-2}.d^{-1}$, Table 4.11) was at the high end of values reported elsewhere in the literature. Steinman et al (2009) reported release rates between 0.8 and 15.6 $mg.m^{-2}.d^{-1}$, while Kim et al (2003) also reported release rates of 15 $mg.m^{-2}.d^{-1}$, both from anaerobic sediments in shallow eutrophic lake systems. Burger et al (2007), recorded release rates of 2.2 to 85.6 $mg.m^{-2}.d^{-1}$ in Lake Rotorua. These were largely independent of [DO], but they were dependent on the rate of organic matter decomposition in the surface sediment, and hence are likely to still be redox-related as this decomposition utilises oxygen and nitrate in the sediment. The maximum rates of P release seen in the Wairewa sediments were very high in the highly reducing water columns (14- 865 $mg.m^{-2}.d^{-1}$), and exceeded the 100 - 200 $mg.m^{-2}.d^{-1}$ rates reported by Søndergaard et al (1990) from Lake Søbygard in Denmark, hwoever the highest rates in Wairewa may be due to an indeterminate analytical error (see Section 4.3.2.1). The latter was measured during a period of phytoplankton population collapse and hence a rapid supply of organic material to the sediment surface. Chen et al (2014) also found enhanced P release due to the addition of cyanobacterial biomass, which resulted in increased Fe and sulfate reduction. The Wairewa average, and maximum release rates, under reducing conditions, show the potential to significantly and rapidly increase the [P] in the lake water column (Table 4.11). For example, under redox conditions where Eh = -210 mV, a TP concentration increase such as that observed in the lake water column in March-April 2013 (0.077 $mg.L^{-1}$, refer Section 2.3.4), could be sourced from the sediment in 6 days, at the average flux rate, or just 8 hours, at the maximum flux rate. This assumes the entire lake bed is experiencing these redox conditions. The validity of this assumption is discussed in Chapter 5.

Geochemical modelling suggested that lower temperatures thermodynamically favour slight increases in reductive dissolution of reactive Fe (hydr)oxides. However this does not take temperature effects on biological activity into account, with higher temperatures in the lake likely increasing microbially-mediated mineralisation of organic material and hence dissimilatory Fe reduction (Søndergaard et al, 2003; Alghren et al, 2011). Various

studies have found increased rates of P release from sediments at higher temperatures. For example, Chen et al, (2014) reported increases in Fe and SO_4 reduction, as well as P release due to temperature increases from 15 to 25^oC, while Kim et al (2003) measured a five-fold increase in release rate between 2 and 25^oC. Jensen and Andersen (1992) reported that lakes with a high component of Fe-bound P, displayed the strongest temperature effect. They also noted a decrease in the depth of the oxidised surface sediment layer with increasing temperatures. Thus, although the effect of temperature was not investigated in the laboratory setting for Wairewa sediments, higher temperatures are considered likely to increase redox related P release in Wairewa.

Table 4.11 Potential increases (Inc) in OLW P concentration, calculated from experimentally-derived P release rates (RR), for the average lake area and volume over the P budget period (refer Chapter 2). EC is not presented for the 'Salinity Related Release' section, as the release rates are not a function of EC, but are rather a function of the difference between EC in the pore water and OLW (see Section 4.3.4).

Redox-Related Release

E_h (mV)	Average RR ($mg.m^{-2}.d^{-1}$)	Inc in OLW [P] ($mg.L^{-1}.d^{-1}$)	Max RR ($mg.m^{-2}.d^{-1}$)	Inc in OLW [P] ($mg.L^{-1}.d^{-1}$)
+110	0.754	0.0005	14.0	0.009
0	2.69	0.002	29.6	0.019
-210	20.6	0.013	385	0.243
-300	64.0	0.040	865	0.541

pH-Related Release

Slurry Experiment			Core incubation experiment		
pH	RR ($mg.m^{-2}.d^{-1}$)	Inc in OLW [P] ($mg.L^{-1}.d^{-1}$)	pH	RR ($mg.m^{-2}.d^{-1}$)	Inc in OLW [P] ($mg.L^{-1}.d^{-1}$)
7.83	25.4	0.010	7.10	0.573	0.0004
8.60	54.4	0.034	7.93	2.24	0.001
9.09	78.4	0.050	8.97	3.27	0.002
9.98	101	0.064	9.94	11.07	0.007

Salinity Related Release

Release Rate ($mg.m^{-2}.d^{-1}$)	Increase in OLW [P] ($mg.L^{-1}.d^{-1}$)
1.99	0.001
2.63	0.002
6.35	0.004
12.7	0.008

Sediment resuspension into a low redox water column was not investigated in this study, as low dissolved oxygen conditions in shallow lakes such as Wairewa, are likely to result from quiescent conditions due to a lack of wind or sheltered areas in the lake such as macrophyte beds. Resuspension is unlikely to occur in these conditions.

4.4.3 pH related P release

Elevated pH is expected to increase dissolved [P] in surrounding water, through desorption of P from sediment surfaces due to hydroxyl ion competition for adsorption sites (Jacoby et al, 1982; Søndergaard et al, 2003). High pH is likely to mobilise P associated with the NaOH-rP fraction (Chapter 3), that is P adsorbed to Fe, Al, and Mn (hydr)oxides as well as organic particulates and clays. Surface adsorbed P in the BD-P fraction is also likely to be affected by high pH, and in the Wairewa surface sediments during summer, approximately 30% of the [TSP] was found to be susceptible to P release under high pH conditions (refer to Chapter 3)

Core incubation and slurry experiments indicated that pH-related P release was significant at pH > 9. These observations were consistent with the geochemical modelling, which showed the adsorption edge at 9 > pH > 11.5. The modelling also suggested that temperature variation over the range 5 – 25 ^{o}C, was unlikely to have an effect on pH desorption. Other studies have also shown a pH ≈ 9 to be a critical P desorption threshold in sediments (e.g. Gao et al, 2012). Release rates were relatively modest for the core incubation experiments (11.07 $mg.m^{-2}.d^{-1}$ at pH ≈ 10), compared to the higher redox-related rates seen in reduced sediments (E_h < -200 mV). The pH-related release rate observed for Wairewa sediments, fell somewhere between the rate of 5.6 $mg.m^{-2}.d^{-1}$ (pH = 10) reported by Jacoby et al (1982), and the rate of 29 $mg.m^{-2}.d^{-1}$ (pH = 9.5) reported by Gao et al (2012).

The elevation of surface sediment (0-1 cm) pore water [DRP] observed in Figure 4.11, was a response to elevated pore water pH. 48 hours of exposure to OLW with elevated pH (pH ≈ 10) resulted in pore water pH increasing from pH ≈ 7 to pH ≈ 9. The increased pH in the pore water below this (5-7 cm), was insufficient to cause a pH-related increase in [DRP], but suggested that over time these deeper sediments would also undergo P desorption as the pore water pH increased. This was also observed in freshwater sediments of the Potomac River (USA) by Bailey et al (2006), who observed pH > 9 in

pore water at 4-8 cm depth, after a week-long incubation of a sediment core with pH ≈ 10 in the OLW. Søndergaard et al (1990) noted increased pH and [P] down to 8-10 cm in Lake Søbygaard sediment during summer, with 9 < pH < 10 down to 5cm. They ascribed this to photosynthetically elevated pH in the OLW. Such increases in pore water [DRP] are likely to result in increased flux rates to the OLW, as was observed by Gao et al (2012) in the sediments of a shallow fresh-water estuary system in Chesapeake Bay (USA). Hence it may be expected that prolonged periods of elevated pH in the OLW will result in an increased concentration of pore water DRP, which may in turn, sustain a prolonged flux of P from the sediment to the OLW.

Despite lower release rates than those associated with low redox conditions, high pH conditions might be expected to persist over longer periods of time and pH-related release in Wairewa has the potential to significantly increase the water column [P]. At pH ≈ 10, for example, a daily increase in the water column [P] of 0.007 $mg.L^{-1}.d^{-1}$ (Table 4.11) is possible, assuming the high pH occurs throughout the lake. This could account for the 0.077 $mg.L^{-1}$ increase in [TP] observed in March-April 2013 (Section 2.3.4) in just 11 days, and rates are easily high enough to explain the fastest rate of [TP] increase (Figure 2.11). The release rate at pH ≈ 9 could provide the same [TP] increase in 39 days, only three days longer than the period over which the actual increase was seen to occur. However the [TP] increase was not steady over this time (Figure 2.11) and the pH ≈ 9 release rate, was not enough to explain the more rapid periods of [TP] increase observed.

The release rates seen in the pH-slurry release experiment were significantly higher than the core incubation rates (Figure 4.23), even allowing for possible over-estimation of sediment density (Section 5.2.7.1). The water-sediment ratio therefore has an important effect on pH-related release rates. This was also evident in the geochemical modelling, where the amount of HFO surface in contact with the surrounding water made a significant difference to the position of the pH adsorption edge (Section 4.2.2.1). Resuspension of sediment into a high pH OLW is, therefore, likely to result in high P release rates, and the pH-slurry release experiment indicated continued P desorption for at least 8 hours during resuspension. The resuspension event simulated at the end of the pH core–incubation experiment (Figure 4.12) confirmed that resuspension of sediment into the high pH water results in an increase in the OLW [P]. The initial release rate seen in the pH ≈ 10 core was 580 $mg.m^{-2}.d^{-2}$, similar to the maximum rates measured in the slurry release experiment. However the decrease in [P] in the 25 minutes following this initial

increase, suggested that the increase in [P] was largely due to the mixing of pore water into the OLW, and the P was subsequently re-adsorbed onto the resuspended sediment. Such mixing of pore water into the OLW may also explain the initial increase in [DRP] observed in the low pH slurry release experiment.

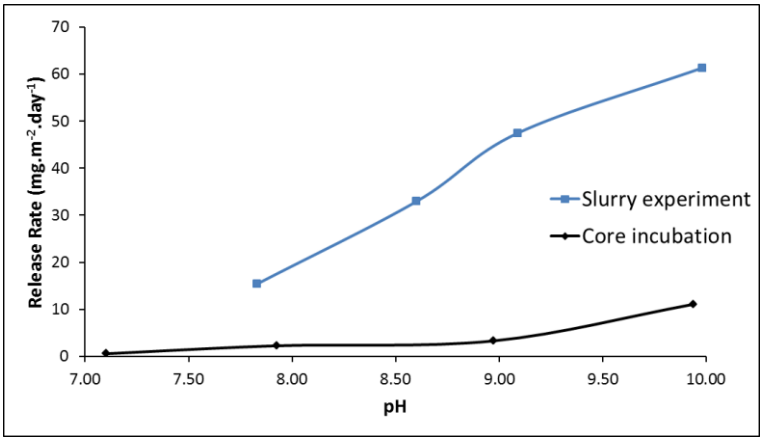

Figure 4.23 A comparison of pH-related P release rates in the core-incubation and slurry release experiments.

The effect of simultaneous high pH and low redox conditions was not investigated in this research. High concentrations of redox insensitive Al (hydr)oxides have the potential to decrease anoxia-related P release by adsorbing P released from Fe (hydr)oxides (Kopacek et al, 2005). If the adsorption capacity of the Al (hydr)oxides is reduced by elevated pH then it may be expected that anoxia-induced P release will be enhanced. However Gao et al (2012) reported that oxygen consumption in the sediment decreased as pH increased, which may promote less reducing conditions. Increased pH also lowers the redox threshold at which Fe (hydr)oxide reduction will occur. For example, Gomez et al (1999) reported reduction thresholds of +100 - -50 mV at pH = 7, -100 mV at pH = 8 and -150 mV at pH = 9. More work is needed to fully understand the combined effect of high pH and low redox conditions in the lake sediment.

4.4.4 Salinity-related P release

Significant effects on the biogeochemistry of water and sediments have been documented along estuarine salinity gradients, and as a result of sea water inundations of freshwater sediments (e.g. Weston et al, 2011; Wong et al, 2015). Various studies have reported increased nutrient release as a result of increased salinity in OLW (e.g. Fox et al, 1986; Gardolinski et al, 2004; Weston et al, 2006; Hartzell and Jordan, 2012). Mechanisms

cited to explain this include, ion exchange with adsorbed PO_4^{-3} (Gardolinski et al, 2004; Ahmed et al, 2008), the increased reductive dissolution of Fe (hydr)oxides and Fe-phosphate minerals due to increased, bacterially mediated, SO_4^{-2} reduction (Katsev et al, 2006), and the immobilisation of Fe as FeS and FeS_2 (Hupfer and Lewandowski, 2008).

The results of the salinity- core incubation experiments in this study, however, showed an opposite effect, with P release being greater in the lower salinity OLW (Figure 4.14, 4.16). Release rates at the lowest salinity were as significant as the rates observed in the pH- core-incubation experiment (Table 4.11). An examination of EC trends in the OLW during the experiment, as well as pore water EC and DRP concentrations following these experiments, indicated that the rate of [P] and EC increase in the OLW was influenced by the gradient between pore water and OLW salinity, which promoted solute movement from high to low concentrations. This trend was seen in both the cores where salinity was adjusted in the OLW, and where OLW underwent a natural 'freshening' by a freshwater influx to the lake. Reported chemical diffusion rates in sediments due to seawater inundation are variable. Weston et al (2011) reported increased pore water $[Cl^-]$ at depths >16 cm three months after inundation, while much more rapid diffusion rates were reported by Santos-Echeandia et al (2010), in intertidal fine sediments, with equilibration between sediment pore water (to 5 cm) and OLW, achieved within 50 mins. In this study, P release occurred in the salinity- core-incubation experiments after about 24 hours and pore water EC appeared to have equilibrated to a depth of 5-7 cm 28 days after the 'freshening' rain event (Figure 4.18a). This is an equilibration rate of 0.25 $cm^{-1}.d^{-1}$, somewhat quicker than the 0.18 $cm^{-1}.d^{-1}$ reported by Weston et al (2011).

It is uncertain whether the P release into the lower salinity OLW is due to the same diffusive mechanism driving EC equilibration, or to an advective transport mechanism. However the increased DRP down to around 4-5 cm in the pore water of the low EC core (Figure 4.18b), suggests either in-situ P release or diffusion of P from the deeper sediments. The experimentally observed release of DRP into the low salinity OLW, is consistent with the higher [DRP] seen in the lower salinity lake-water at the north end of Wairewa following the 'freshening' rain event on 5th March 2014 (Figure 4.19), and suggests that this mechanism of P release has the potential to be a significant source of P to the lake OLW. The frequency of such P release episodes and their potential effect on primary productivity is uncertain. However no reports of a similar mechanism of P

release have been found in the literature, and the mechanism is likely to be unique to systems such as ICOLLs, which may experience significant periods of stable salinity followed by a rapid freshening of the OLW. This is a fundamentally different system to estuarine or tidal settings where salinity fluctuations are frequent and episodic.

The longer term effects of higher salinity in the OLW, has not been observed experimentally in this study of Wairewa, but may be expected to follow more widely reported trends of higher salinity promoting P release. Geochemical modelling suggested that increased salinity would increase pH-related desorption of P from Fe (hydr)oxide surfaces, and a similar effect may be expected for Al (hydr)oxide and other adsorbing surfaces. The proportion of PO_4^{-3} adsorbed to the HFO surface at pH > 8.5 was significantly decreased in higher salinities due to the increased adsorption of competing ions. Hence while the experimental work (slurry-release experiment) was inconclusive with respect to the effect of salinity on P desorption in high pH water, the modelling tends to support the hypothesis that higher salinity will result in some P release due to competition for adsorption sites. This is consistent with other studies. Gardolinski et al (2004) reported rapid release of dissolved P from sediments in higher salinity solutions while Hawke et al (1989) found substantially greater PO_4^{-3} adsorption on goethite in a 10% seawater solution compared to a 100% seawater solution. Ahmed et al (2008) also found competition between SO_4^{-2} and PO_4^{-3} for adsorption sites, and that PO_4^{-3} release was enhanced by synergistic effects between Na and SO_4^{-2}. It seems likely then that a combination of high pH (pH > 8.5-9) and high salinity will enhance P release in Wairewa, especially where sediment is resuspended into the water column.

Geochemical modelling also indicated that increased salinity would enable the reductive dissolution of the HFO surface at higher E_h, thereby promoting P release. This is due to the increased abiotic reduction of HFO by H_2S formed by SO_4^{-2} reduction. In low SO_4^{-2} systems, reduction of Fe (hydr)oxides is predominantly by an enzymatic dissimilatory reaction mediated by Fe reducing bacteria. In higher SO_4^{-2} systems the dissimilatory, bacteria mediated reduction of SO_4^{-2} to H_2S allows the abiotic reduction of Fe (hydr)oxides to proceed by the equation (Lehtoranta et al, 2009);

$$2FeOOH + 3H_2S + 4H^+ \rightarrow 2FeS + S^0 + 4H_2O. \qquad \text{(eq 4.2)}$$

Spiteri et al (2008) noted similar results from modelling of PO_4^{-3} adsorption on a model Fe-oxide, where a decrease in adsorption site density due to reductive dissolution of Fe-oxide was caused by sulfate reduction resulting from increased salinity. This was also observed experimentally by Weston et al (2006), who noted an increase in Fe reduction and PO_4^{-3} release following salinity intrusion in flow through reactor experiments. Wong et al (2015) also noted increased concentrations of Fe^{+2} resulting from reductive dissolution of Fe oxyhydroxides following sea water inundation of coastal floodplain sediments. This relatively rapid mechanism of P release (days to weeks, Weston et al, 2006) is also linked to longer term release of P by the immobilisation of Fe as FeS_2, and the dissolution of Fe-phosphate minerals as discussed in Section 3.4.3.

4.5 Conclusion.

The surface sediments of Wairewa are enriched in mobile fractions of P and as such are susceptible to mechanisms which cause the release of this P into sediment pore water and the OLW. EPC experiments and the high reactive-Fe:P ratio indicate that the sediments have a high binding affinity, and that P release under oxic and circum-neutral pH conditions in the water column is likely to be limited, even during periods of sediment resuspension. In contrast, sedimentary P release associated with low redox conditions is potentially a major source of P to the OLW. Significant P release begins at $E_h < 100$ mV (pe < 2), when all DO in the water column has been exhausted. P release rates under highly reducing conditions ($E_h < -200$ mV) were at the high end of rates reported in the literature, and reflect the importance of P binding to Fe (hydr)oxide surfaces, in these sediments. The observed release rates have the potential to account for the rapid, algal bloom-associated, increases in [TP] observed in Wairewa.

pH-related P release increases significantly at pH > 9. High pH release rates are lower than those associated with low redox conditions, but still have the potential to account for algal bloom-associated increases observed in the OLW [TP], if high pH is maintained in the water column. Sediment resuspension into a high-pH water column can significantly enhance release of P to the water column.

High salinity in the OLW may increase pH-related P release by competitive desorption, a mechanism which will increase P release in the lake, especially during resuspension events. High salinity is also expected to increase the reductive dissolution of Fe

(hydr)oxides and Fe–phosphate minerals, resulting of P release from the sediments. Increased SO_4^{-2} reduction due to increased salinity, may also result in the long term immobilisation of Fe as FeS_2 in the deeper sediments, resulting in a decreased upward flux of Fe^{+2}, and hence a decrease in the Fe binding potential of the oxic surface sediment. If the upward flux of PO_4^{-3}saturates this binding potential, PO_4^{-3} release to the OLW may increase. Rain events in the catchment can create salinity gradients between high salinity pore water and low salinity OLW, which may enhance the release of P to the OLW. This mechanism is likely to be specific to ICOLL type settings where prolonged periods of higher salinity in the lake may be followed by a sudden 'freshening'.

4.6 Key Research Findings

- P release from sediments (including resuspension) into an oxic, circum-neutral pH OLW, is negligible due to the high ratio of reactive-Fe to P in the surface sediments.

- Significant redox-related P release begins once DO is completely depleted in the OLW, and Eh < 100 mV (pe < 2).

- Redox-related P release rates of 21 and 64 $mg.m^{-2}.d^{-1}$ were observed at Eh ≈ -200 and -300 mV, respectively

- pH-related P release increased significantly at pH > 9, and release rates of up to 100 $mg.m^{-2}.d^{-1}$ were observed (pH ≈ 10).

- Resuspension of sediment into high pH OLW will result in higher rates of P release, than from stable bed sediments.

- High salinity increases pH-related P release, reductive dissolution of Fe (hydr)oxides, and Fe immobilisation as FeS_2, and hence decreases sedimentary P binding capacity.

- Salinity gradients across the sediment/water interface, resulting from freshening events in the lake, may increase the release of P to the OLW.

Chapter 5: Environmental Conditions Affecting Phosphorus Binding and Release

5.1 Introduction

The P budget presented in Chapter 2 of this research indicates that the fluctuations in water column [TP] cannot be explained by external P loading. Internal loading of P to lake systems, primarily as release from sediments, is a widely reported phenomenon (eg: Burger et al, 2007; Søndergaard, 2007; Das et al, 2009;), and a flux of P from the sediments to the water column is the simplest explanation of the discrepancy seen in Wairewa. Given the correlation between TP and chl-*a* during times of high biomass, this internal load may be particularly important in satisfying primary productivity-related P demand, during bloom formation. The flux of P to the water column will be controlled by the environmental conditions which affect sedimentary P binding and release. The research in Chapters 3 and 4 of this study, indicated that dissolved oxygen (DO) concentration, pH and salinity in the lake are likely to be important factors in promoting release from bed sediments. Chapter 4 also indicated that desorption from resuspended sediment is dependent on high pH in the water column, and other studies have also noted the contribution of entrained pore water to internal P loading, during sediment resuspension (e.g. Das et al, 2009).

Stratification commonly controls [DO] in lake bottom waters, where it can promote development of an anoxic hypolimnion, within which high concentrations of soluble P can accumulate (Wetzel, 2001). However, Wairewa is a shallow, windswept lake which can be expected to generally have a well-mixed, oxygenated water column. The regime in Wairewa is more likely to involve diurnal stratification or short periods of more prolonged stratification, interrupted by wind-driven mixing (polymixis). Stratification in such systems may require an additional factor such as macrophyte beds, which may prevent water column mixing (Cooke et al, 2005), or changes in salinity, which may cause density stratification (e.g. McCorquodale and Georgiou, 2004).

Elevated primary productivity resulting from eutrophication processes, may also affect bottom water [DO] due to flux of organic material to the sediment surface and subsequent

decomposition (Chen et al, 2014). Such primary productivity is also likely to increase water column pH via photosynthesis by either macrophytes and/or phytoplankton.

This chapter presents research into the environmental conditions that exist in Wairewa and their effect on P binding and release mechanisms. Key questions are

- Do concentrations of DO in the lake decrease enough to promote P release, and if so, what factors drive such deoxygenation?
- Does pH become elevated enough to promote P release, and is so what factors drive this increase?
- What effect does salinity have on P dynamics in the lake,
- Does pore water contribute to P loading during sediment resuspension?

5.2 Methods

5.2.1 Study design

A number of investigations were undertaken to provide insight into the key questions presented in Section 5.1. Dissolved oxygen conditions were investigated by deployment of DO data loggers at five locations around the lake. In addition oxygen profiles across the sediment-water interface were obtained at different times of the year. pH conditions were determined by the deployment of a pH data logger near the north end of the lake, which could then be compared with time series pH data collected by ECan near the southern end of the lake.

The effect of macrophyte beds on oxygenation of the sediment-water interface was investigated by the positioning of DO data loggers, and the measurement of oxygen profiles across the sediment-water interface in sediment cores, inside and outside of the beds. In addition, thermistor strings inside and outside of beds, were used to record water column temperature profiles. The effect of macrophytes on water column pH could be determined from the comparison of data from the northern data logger (inside macophyte beds) and the ECan time series data (no macrophytes). The role of the macrophyte beds in P release was also investigated by spot sampling across a macrophyte bed margin, and by pore water and sediment sampling from inside and outside macrophyte beds.

The effect of salinity was investigated by the measurement of salinity gradients along the lake and the deployment of dissolved oxygen loggers at the southern end of the lake,

where salinity was higher. The long-term effect of salinity was investigated by sampling of sediment pore waters from each end of the lake.

Sediment resuspension was investigated by the analysis of suspended particulate material in the water column prior to and during wind events.

Details of the methodology of these investigations is provided below.

5.2.2 Dissolved oxygen conditions

Data loggers, positioned 5 cm above the lake sediment surface, were used to analyse and record dissolved oxygen (DO) concentrations and temperature at 15 min intervals at the sites detailed in Figure 5.1 and Table 5.1. Loggers were calibrated in the laboratory prior to deployment, and ongoing calibration was conducted by spot analysis using a HACH HQ40d meter with a laboratory calibrated DO probe. Two types of loggers were used; Onset HOBO DO Loggers (U26-001) were deployed in two locations (Table 5.1), data from which were downloaded using a HOBO waterproof shuttle (U-DTW-1), and processed using HOBOware Pro v3.3.2 software. Three D-Opto Loggers were also deployed, data from which was processed using D-Opto Logger V3 software.

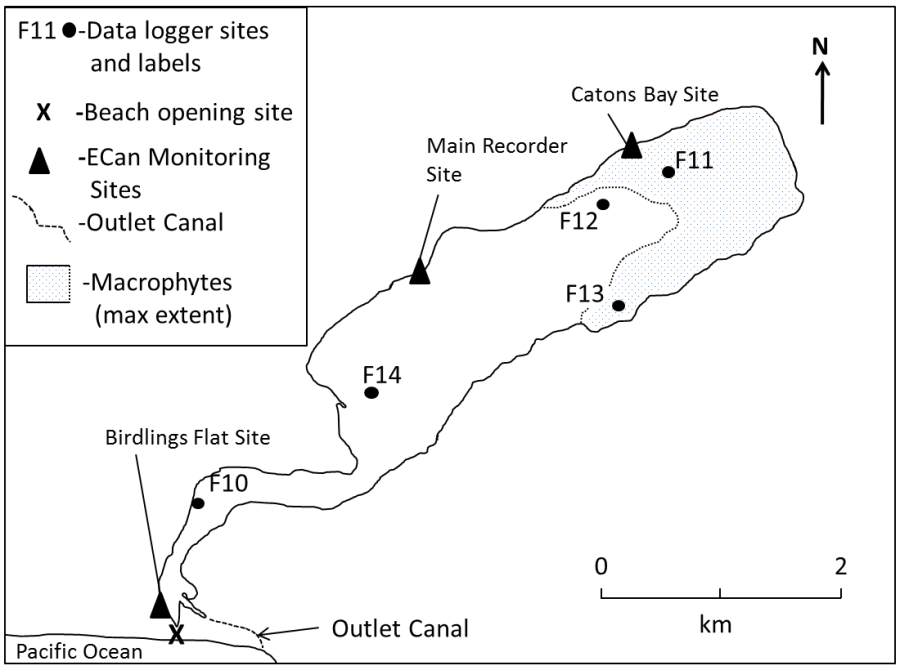

Figure 5.1 Map of Wairewa showing data logger sites as well as the sites used by ECan for routine lake monitoring. The maximum extent of tall growing, submerged macrophytes, observed during the research project, are indicated. Also indicated is the original beach site used for opening the lake to the sea pre 2010, and the outlet canal used to open the lake since 2010 (these sites are referred to in Chapter 6)

DO gradients across the sediment-water interface were analysed using a PreSens Microx TX-3 meter and a calibrated fibre-optic microsensor in a needle type housing. Data was processed using Microx TX3 software version TX3v520. The microsensor was attached to an aluminium rod and analysis increments were controlled by use of a micrometer. Gradients were analysed in cores collected as described in Section 2.2.4.

5.2.3 pH conditions

pH was recorded every 15 minutes, at site F11, for the period specified in Table 5.1, using an Omega OM-CP PH101 pH and temperature logger with a calibrated Omega PHE7352-15-PT100 pH probe. The probe was positioned 5 cm above the sediment/water interface. Data were processed using Omega OM-CP v 2.07.0 data logging software.

Table 5.1 Deployment details for data loggers used in time series data collection. DO and pH sensors were positioned 5 cm above the sediment surface, while temperature was recorded at depths of 0, 40, 80, 120 cm above the sediment surface.

Variable	Site	Logger Type	Dates deployed
DO	F10	D-Opto	17 May 13 - 11 Feb 14
	F11	D-Opto	20 Feb 13 - 13 Dec 13
	F12	D-Opto	1 Mar 13 – 11 Feb 14
	F13	HOBO	16 May 13 - 6 Jul 14
	F14	HOBO	16 May 13 - 6 Jul 14
pH	F11	Omega	22 Mar 13 – 12 Nov 13
Temperature	F11	Campbell Scientific	15 Jan 13 – 21 Jan 13 and 25 Mar 13 – 22 Jun 13
	F12	Campbell Scientific	2 Feb 13 – 25 Mar 13

5.2.4 General water and sediment analysis

Water, sediment and sediment pore water samples taken during the various investigations described below, were collected and analysed for phosphorus as detailed in Sections 2.2.4 and 3.2.1. Water chemistry parameters (DO, pH, EC, TP, DRP), and trace element chemistry in sediment pore water, were analysed as detailed in Section 3.2.2.1.

5.2.5 The effect of macrophyte beds on environmental conditions

5.2.5.1 Temperature stratification

Temperatures were measured at 15 min intervals by Campbell Scientific P/N 9661 temperature sensors, deployed as a thermistor chain. Sensors were deployed at 0, 40, 80 and 120 cm above the sediment surface. Data were logged on a Campbell Scientific CR10 data logger housed in a floating waterproof housing. Processing was conducted using Campbell PC208W 3.3 logger support software. Only one thermistor chain was available and it was deployed between sites F11 and F12 over the dates specified in Table 5.1

5.2.5.2 Sampling across a macrophyte bed margin

A particularly large, dense bed of surface-reaching *Myriophyllum triphyllum* formed near the north end of the lake in late November 2013 (Figure 5.2). The *Myriophyllum* bed persisted throughout December, with increasingly senescing margins. A thick algal bloom was observed within the bed throughout mid-December (Figure 5.3).

Figure 5.2 The dense bed of flowering *Myriophyllum* on 6 December 2013.

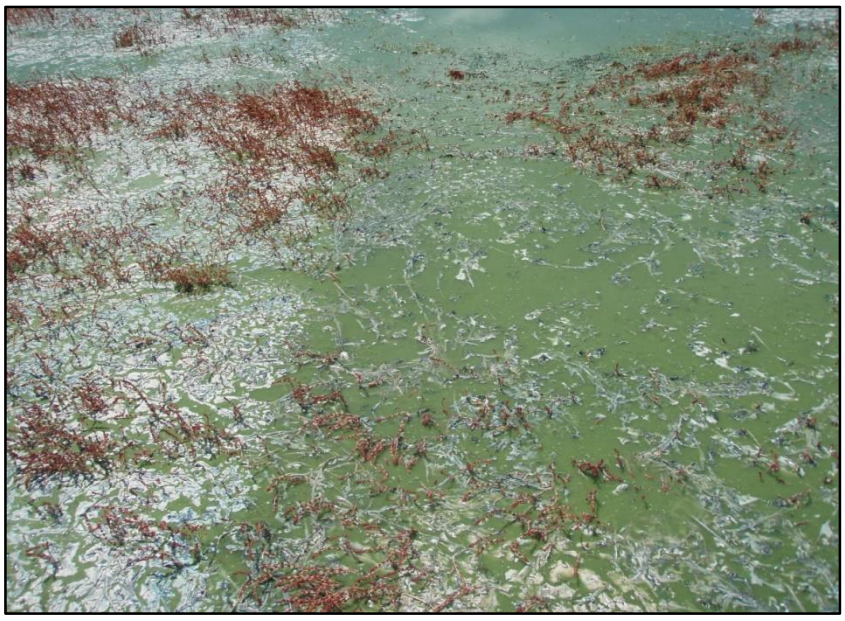

Figure 5.3 A thick bloom of cyanobacteria within the *Myriophyllum* bed.

Observations of water column pH, [DO], [TP] and [DRP], as well as [DRP] in the surface sediment pore waters (0-1 cm), were made on the 13 December 2013, during the decline of the macrophyte bed margins. The water column observations were made at 5 cm below the surface and 5 cm above the sediment. Three sites were sampled, one in the main lake water column (20 m outside the macrophyte bed), one within the senescing margin, which was characterised by scattered, ragged macrophyte plants, and one within the main body of the macrophyte bed.

5.2.5.3 Pore water chemistry

The conditions observed in the macrophyte beds, particularly with regards to DO, might be expected to produce geochemical differences within the sediments, relative to areas without macrophyte beds. To investigate this, pore water chemistry was analysed from two sediment cores (processed under a N atmosphere), both sampled on the 23 December 2013, one from the macrophyte dense area of site F11, and one from site F12 (no macrophytes).

5.2.5.4 Sedimentary P fractions

To investigate the effect of macrophyte beds on sedimentary P fractionation, surface sediments were sampled periodically throughout the summer season of 2012-13 from site F11 (macrophyte beds) and site F12 (no macrophytes). Sequential chemical extractions

(see Section 3.2.3.4) were undertaken on these samples, as well as an analysis of organic matter content (see Section 3.2.3.1).

5.2.6 The effect of salinity

5.2.6.1. Salinity gradient in the lake

EC was used as a proxy for salinity, and surface conductivity was measured along the lake on three separate occasions; 2 November 2011, 8 April 2013, and 26 March 2014.

5.2.6.2 Pore water chemistry

The effect of long-term differences in lake salinity on the pore water chemistry of the sediments, was investigated by sampling two cores on the same day (20 October 2014), one from site F10 at the southern end of the lake, and one from site F12 at the northern end.

5.2.7 Sediment resuspension

5.2.7.1 Depth of sediment disturbance

The mass of sediment resuspended into the lake water column, and the sediment depth from which resuspension occurs, were calculated by determining the total suspended solids (TSS) in the water column at the beginning and end of a discrete wind event on the lake. TSS was determined by filtering lake water through a pre-weighed 0.45 µm filter paper, which was then dried at 105^{o}C for 24 hours prior to re-weighing. This was conducted on 25 July 2012, then again on 27th and 30 July, during which time the wind rose from 0 to 21 km.hr^{-1} as measured using a hand-held Silva ADC anemometer. The change in mass of TSS in the lake could then be calculated using the lake level at the ECan Main Recorder site, and the lake level to volume relationship described in Section 2.2.3. At the same time the sediment load entering the lake from the Okana and Okuti Rivers was determined by spot gauging of flow rate (as described in Chapter 2) and TSS determination as described above. The sediment load in the water column resulting from resuspension was then calculated as the change in lake TSS minus the external load TSS.

The depth of sediment disturbed by resuspension was then calculated using the area of lake sediment, derived from the lake level to area relationship described in

Section 2.2.6.2, and the 0-1cm sediment density presented in Table 3.8. This method describes the depth of sediment disturbed by a discrete wind event and does not allow for repeated or continuous wind events. In addition the density used is an average for the surface sediment (0-1 cm), and if actual densities in the upper few mm of the sediment were lower, this would increase the depth of disturbace required to acccount for the observed increases in water column TSS.

A maximum possible depth of sediment disturbed by resuspension was then calculated using the difference between the minimum (1 $mg.L^{-1}$) and maximum (430 $mg.L^{-1}$) inorganic-SS (ISS) concentrations from the ECan monitoring data set. ISS was calculated by subtracting volatile-SS from TSS. The depth of sediment disturbance was then calculated as above (using the minimum and maximum ISS to represent the suspended sediment at the beginning and end of the resuspension event, respectively). This method did not allow for the resuspension of settled organic material, or the impact of external load on the SS, but should allow for the effect of prolonged and/or repeated wind events.

5.2.7.2 Changes in lake water [TP] due to pore water P release

The change in water column [TP] concentration that was due to the release of dissolved P in sediment pore water, was then calculated using the sediment disturbance depth calculated as above, the pore water mass/area presented in Table 3.8 (0-1 cm), the pore water concentration of TD-P presented in Table 3.4 (0-1 cm), and the average lake areas and volumes during the budget period presented in Chapter 2.

5.3 Results

5.3.1 Dissolved oxygen concentrations

The five DO loggers deployed in the lake provided data on spatial and temporal variability of dissolved oxygen concentrations in the lake. Figure 5.4 presents the DO data for the five sites. The lake water was generally well oxygenated with a common diurnal cycle of overnight decreases in concentration, and daytime recoveries. The winter period had higher concentrations than summer due to the higher oxygen saturation possible in cooler waters. Despite these general trends, the [DO] showed periods of high variability and significantly decreased concentration. These decreases were generally short-lived, although a more prolonged event occurred at site F11 in November 2013. DO concentrations of 0 $mg.L^{-1}$ were rare, but spot analyses in the lake indicated that complete

deoxygenation at the sediment surface could occur when the [DO] at 5 cm above the sediment (the position of the DO loggers) was as high as 2 $mg.L^{-1}$. This is consistent with Aigars (2001), who reported deoxygenation of sediment while the OLW [DO] was 3 $mg.L^{-1}$

Low oxygen events were usually not coincident across the lake, indicating that conditions leading to declining oxygen concentrations were often spatially discrete. For instance the period of low oxygen at site F11 in November 2013 was not evident elsewhere in the lake, even at the nearest site, F12. In particular, the sites at the southern end of the lake (F10, F14) demonstrated significantly different DO patterns than the sites at the northern end (F11, F12). This was observed especially during the period May-July 2013, when frequent low DO concentrations occurred at the southern end but not at the northern end of the lake. In general, during the period when data was collected from all sites (mid-May to mid-December 2013), the southern sites experienced more episodes of [DO] < 2 $mg.L^{-1}$ than the northern sites (i.e. 1 episode of [DO] < 2$mg.L^{-1}$ at site F11, 8 episodes at site F10). The major deoxygenation event in November 2013, at site F11, coincided with the beginning of an algal bloom event in the lake. This bloom continued through to late February 2014 and was a period of significant variability in [DO] across the lake.

Rates of net decline in bottom water [DO] were calculated from the time series data and varied from -0.44 to -1.17 $mg.L^{-1}.hr^{-1}$. These decline rates indicated that a decrease in [DO] from 10 to 0 $mg.L^{-1}$ could occur in 9 - 23 hours.

5.3.1.1 Sediment-water interface

Oxygen conditions across the sediment-water boundary at different times of the year, are presented in Figure 5.5. Despite the higher oxygen concentrations in the OLW during winter (discussed above), the winter profile had the lowest oxygen conditions in the water at the sediment surface (2.29 $mg.L^{-1}$), and the shallowest oxic sediment depth (1.5 mm). The summer profile with no algal bloom had 3.69 $mg.L^{-1}$ at the sediment surface and the sediment was oxic to approximately 2.25 mm depth. The presence of a bloom increased water column oxygen and oxygen at the sediment surface (5.52 $mg.L^{-1}$) during the day, although in the early morning, after night respiration, oxygen concentrations were lower throughout the profile than in late afternoon. The effect of bioturbation is suspected in the 'Summer, bloom, 1625' profile in Figure 5.5, with a sudden increase in oxygen levels at around 2 mm and oxic sediments to around 6 mm depth.

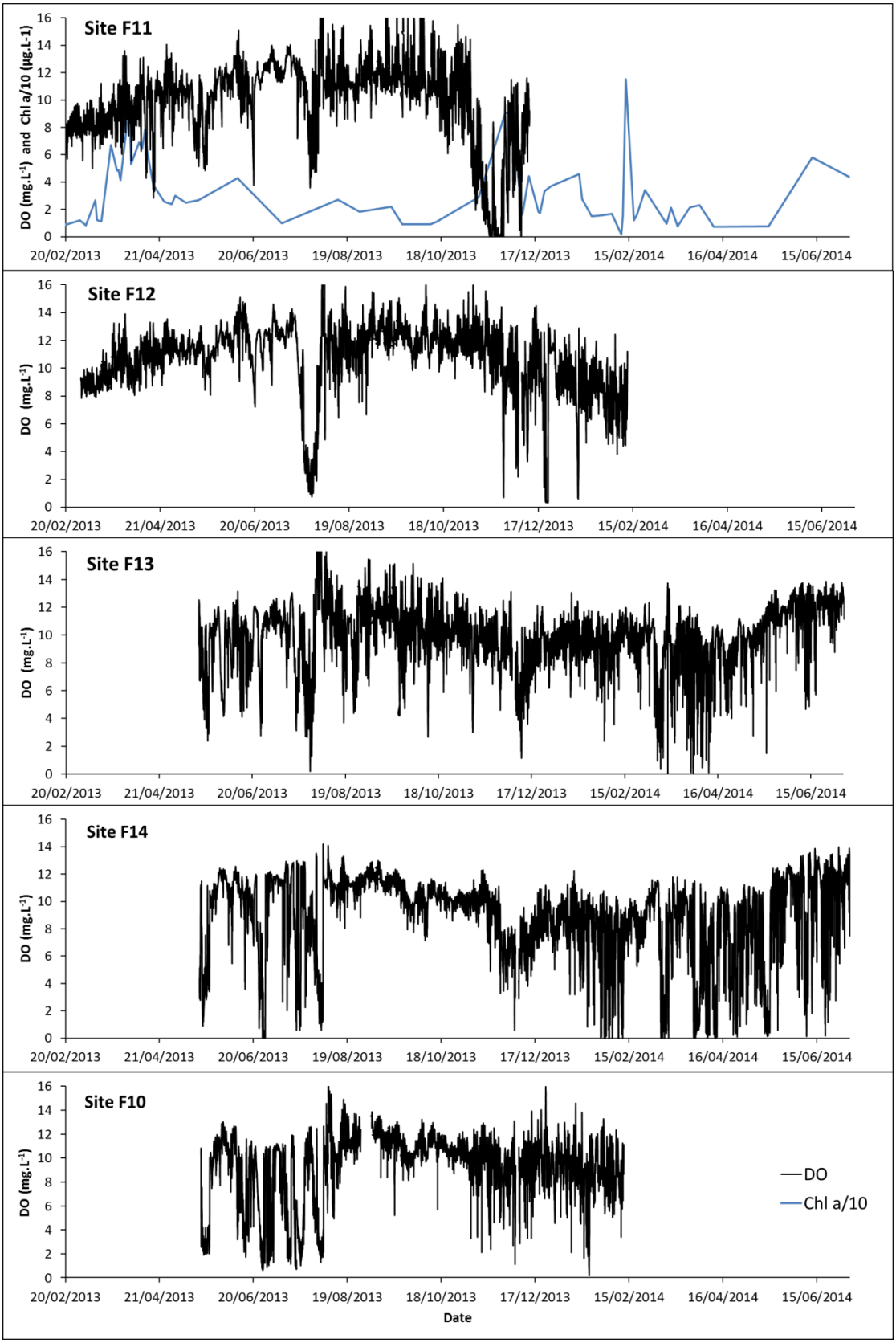

Figure 5.4 Dissolved oxygen data, analysed 5 cm above the sediment-water interface, every 15 minutes, at 5 locations. The lake [chl-*a*] for the same time period, from ECan data and analyses by the author, is also presented on the F11 plot.

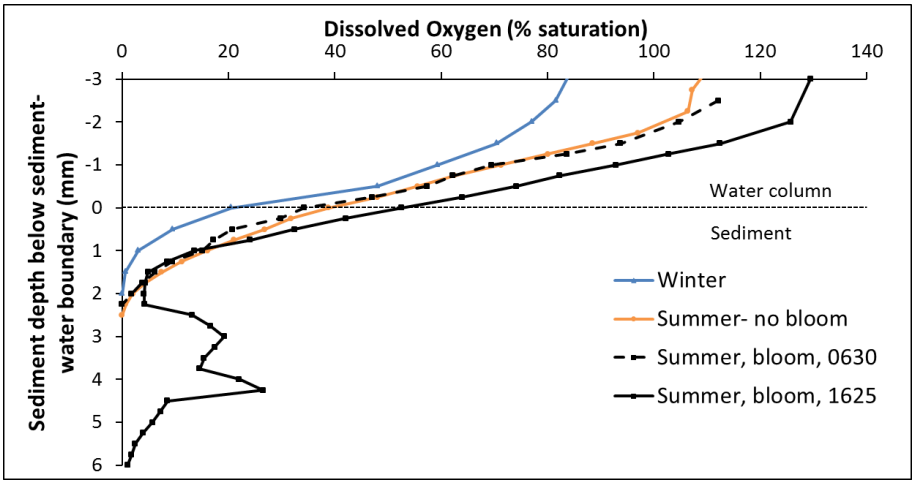

Figure 5.5 Oxygen profiles across the sediment/water boundary at site F12 at different times of the year. The summer bloom profiles were measured on the same day, and (b) sites F11 and F12. Analysis on each day was within 1 hour of each other.

5.3.2 pH

Continuous pH data for the period March – December 2013, for site F11, is presented in Figure 5.6. This site is positioned in semi-permanent, tall-growing, submerged macrophyte beds at the north end of the lake (Figure 5.1). Also presented is the continuous (15 min interval) pH data collected by ECan at the Main Recorder site. This logger is calibrated every 4-6 months and data processed to calibration points (A Ring, ECan, *pers comm)*

pH was generally slightly elevated above neutral, reflecting the high primary productivity in the lake. Summer pH was generally higher than winter but high variability was evident year-round. The ECan pH data was generally slightly lower than the F11 data, possibly due to differing calibrations, however for large parts of the period, the data from both sites showed similar trends. There were however, discrete time periods when the two data sets decoupled. This was seen between 25 July and 4 August and during October-November, 2013. At the end of September the pH increased markedly at site F11, probably reflecting the beginning of growth in the macrophytes around this site. At the recorder site, which has few macrophytes, pH showed little increase. In contrast, at the during November, pH at site F11 began to decrease, while at the recorder site pH increased. These opposing trends coincided with the development of the algal bloom in November 2013 (see Figure 5.4).

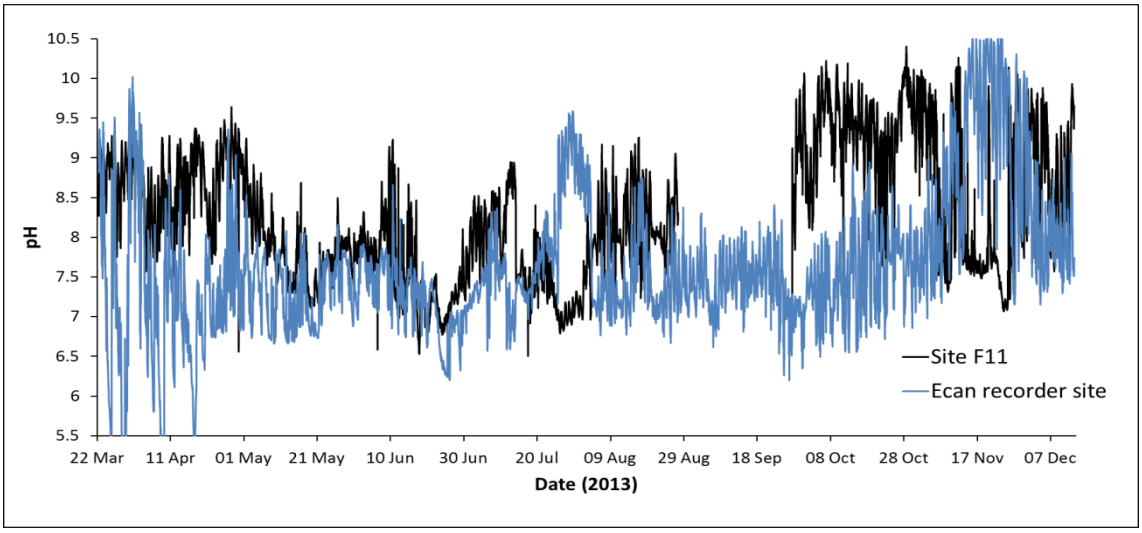

Figure 5.6 pH data recorded every 15 minutes at two sites. The F11 site data was recorded by the author while the ECan recorder site data was recorded by ECan.

5.3.3 The effects of macrophyte beds on environmental conditions

Tall growing, submerged macrophytes were unevenly distributed in the lake with abundant beds of *Myriophyllum sp.* developing at the north end of the lake (Figure 5.1) and few growing elsewhere. The area and density of the *Myriophyllum* beds were observed to go through several cycles of expansion and decline during the research period, typically expanding during early summer, clear water periods, and declining as concentrations of cyanobacteria increased. *Ruppia sp.* was observed periodically at the southern end of the lake. Area and densities of *Ruppia* growth were not accurately determined but appeared to be low and highly variable. In addition to the effects on pH discussed in Section 5.3.2, the macrophytes were observed to change various environmental parameters in the lake. These are discussed in the sections below.

5.3.3.1. Temperature stratification and dissolved oxygen

The difference that the presence of macrophyte beds makes on thermal stratification of the lake water column can be seen in Figure 5.7. A thermistor chain was deployed at sites F11 and F12 over different time periods and hence direct comparison of the two sites at the same time was not possible. Despite this limitation there was a clear difference in frequency of thermal stratification between the two sites. Site F11, which was in an area of abundant macrophyte beds (Figure 5.1) displayed regular diel stratification, with upper water column temperatures increasing relative to deeper waters during the late morning

and afternoon, and cooling again over night. Equilibration typically occurred in the early hours of the morning (after 12 to 20 hours duration). However, on several nights (e.g. 21-22 January, 11-12 April 2013), the water column did not re-equilibrate and thermal stratification persisted through the night and into the following day, (around 40 hours duration). In contrast at site F12, where few macrophytes existed, there was little evidence of temperature stratification and only two significant stratification events were observed (16 February and 20 March), neither of which lasted more than a single night (Figure 5.7). Suppression of wind-induced turbulence at the water surface in the macrophyte beds was observed frequently (e.g. Figure 5.8), which may be related to the higher frequency and longer duration of thermal stratification observed at the site with abundant, macrophytes.

Figure 5.9 plots the difference in temperature between the bottom water and water 120 cm above the bottom, as well as the DO concentrations at the respective sites. 10 hour moving averages, based on DO decline rates discussed in Section 5.3.1, were used to smooth the variability in temperatures. These plots confirm the greater strength and frequency of stratification at site F11, relative to site F12. DO concentrations decreased in response to the prolonged stratification events at site F11. No [DO] decreases were observed at F12. These trends were consistent with the observation that the longest period of deoxygenated bottom water observed from the DO data loggers, occurred in the macrophyte beds (Figure 5.4, site F11, November 2013).

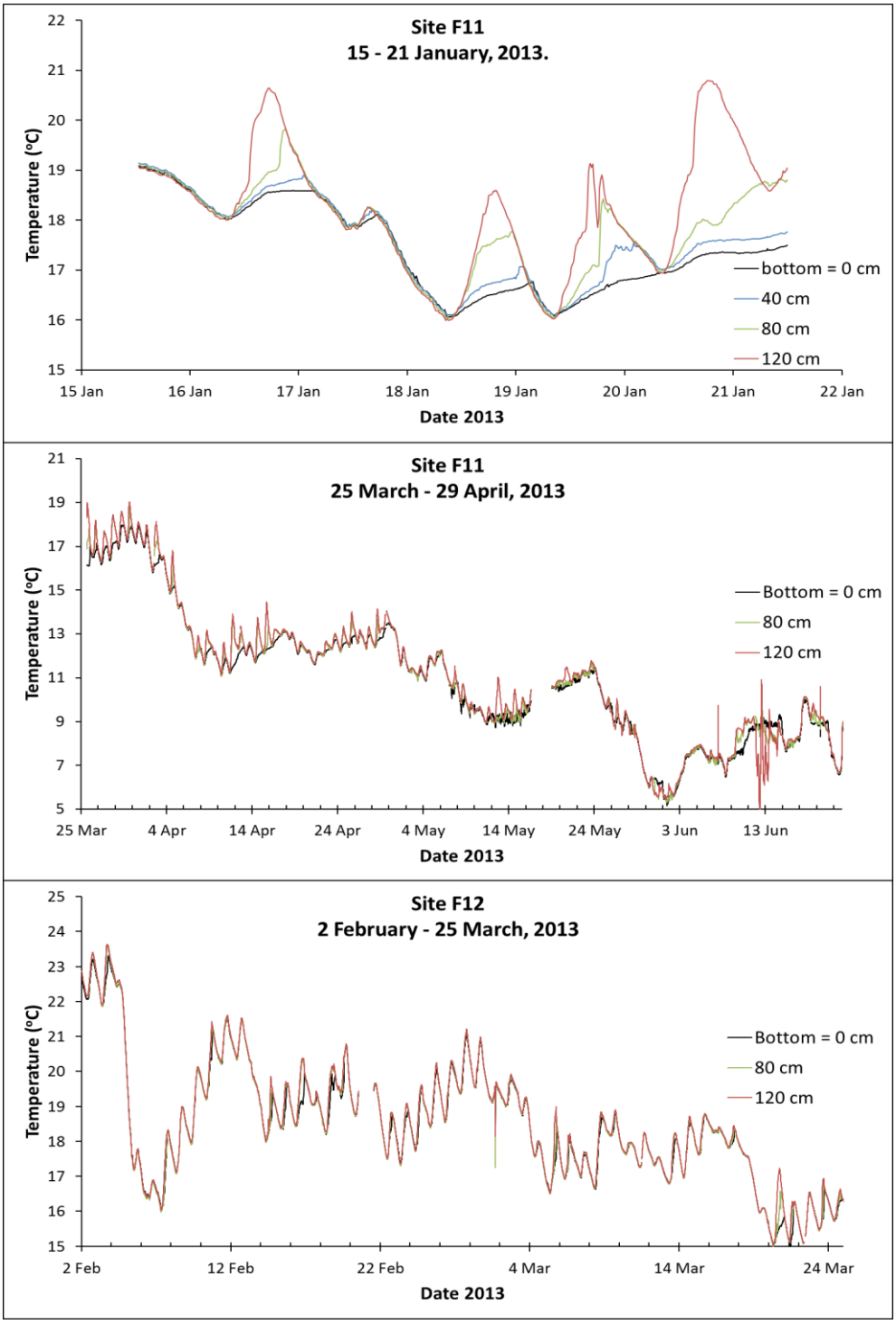

Figure 5.7 Water temperature with depth profiles at two sites, F11 and F12, which had dense macrophytes, and no macrophytes, respectively. Distances were as measured above the sediment surface. Note different date series and scale for each plot.

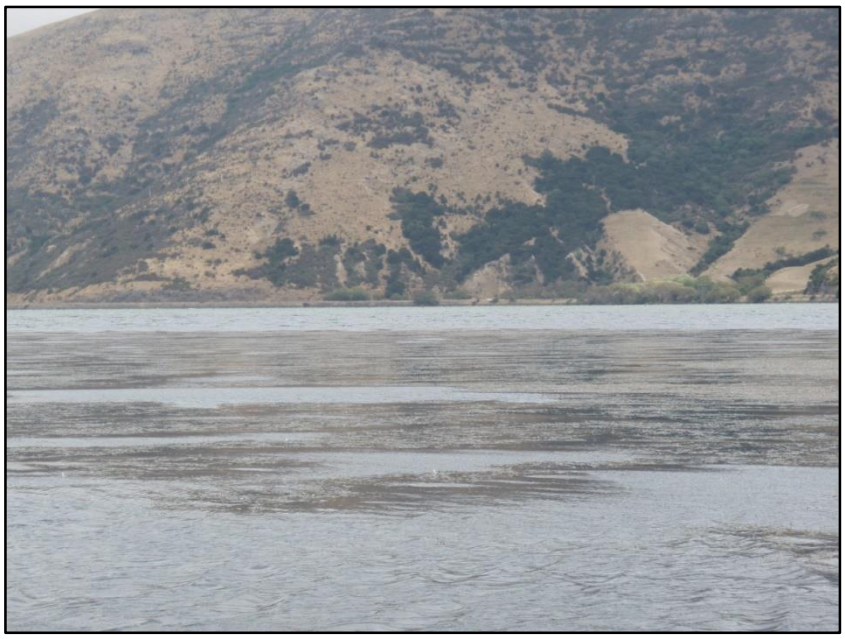

Figure 5.8 The reduction of wind-induced water turbulence, by tall-growing, submerged macrophyte beds in Wairewa.

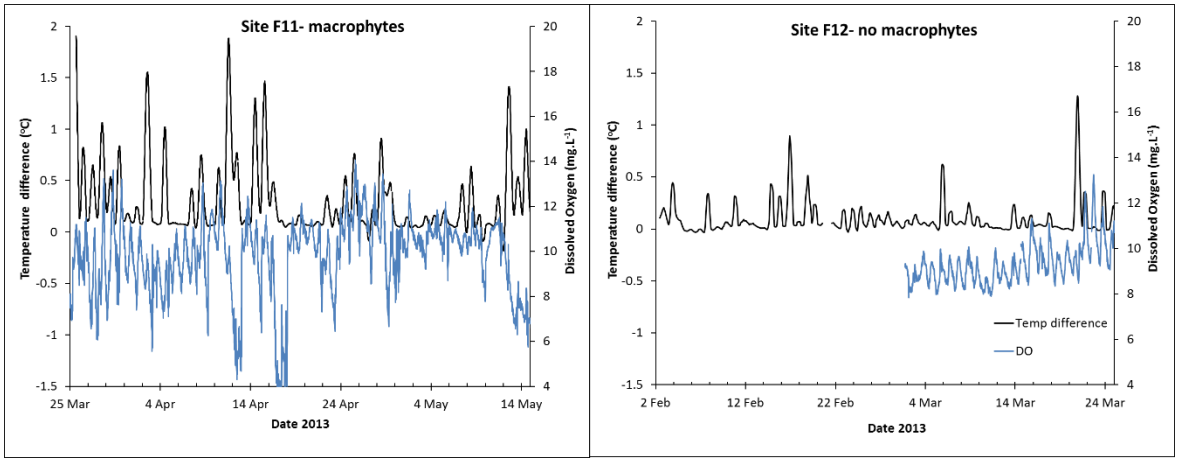

Figure 5.9 Differences in water temperatures between the lake bottom and 120 cm above lake bottom, at two sites, plotted as 10 hour moving averages, as well as bottom water DO at the two sites. The plot is for 51 days (different dates) at each site. DO data was not collected for the entire period at site F12.

5.3.3.2 Oxygen conditions across the sediment water interface

Figure 5.10 presents oxygen conditions across the sediment-water interface at two sites F11 (inside macrophyte beds), and F12 (no macrophyte) on days with different algal bloom conditions. Prior to the formation of the algal bloom (5 March) the two oxygen profiles were similar within the upper 0.75 mm of the sediment, despite a more oxygenated OLW at F11, however the oxic layer at F12 was thicker at 1.75 mm, as

opposed to 1.25 mm at F11. After the initiation of an algal bloom (which began between the 14th and 21st March), the water column and upper sediment were more oxygenated than on 5th March. Again the OLW at F11 was more oxygenated, however within the sediments the oxygen saturation at F11 was consistently lower than at F12 at similar sediment depths, and the oxic layer at F11 was thinner at 2 mm, than at F12 where the oxic layer was 3mm thick.

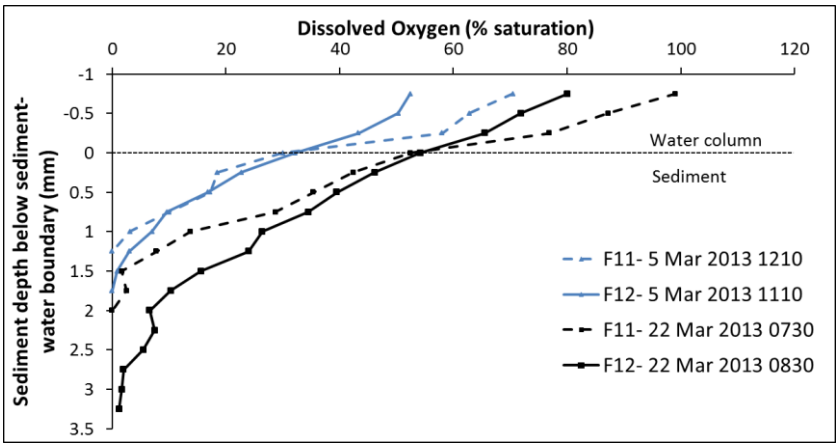

Figure 5.10 Oxygen profiles across the sediment/water boundary at sites F11 (in macrophyte beds), and F12 (no macrophytes) on two different days. On the 5th of March there was no algal bloom present, whereas on the 22 March an algal bloom had begun.

5.3.3.3 Sampling across a macrophyte bed margin

The results from spot sampling across a macrophyte bed margin are presented in Figure 5.11. The OLW, outside the macrophyte bed, was well oxygenated throughout the water column, with a slightly higher [DO] and pH at the surface, than at the bottom. [DRP] was low and consistent throughout the water column, while [TP] increased slightly with depth. The pore water [DRP] in the surface sediment (0-1 cm) was similar to that in the over-lying water column. In contrast, the water column inside the macrophyte bed and in the senescing margin had low DO concentrations in the bottom water, an elevated surface pH, and elevated [DRP] and [TP] in the bottom water. The odour of hydrogen sulphide was evident in the bottom water, both inside the macrophyte bed and in the senescing margin. DRP and TP concentrations were highest in the bottom waters of the senescing edge, where a visible accumulation of black particulate matter was present on the sediment surface which, under SEM-EDS analysis was shown to be organic matter (not

presented). The [DRP] in the surface sediment pore water (0-1 cm) of the senescing margin was further elevated.

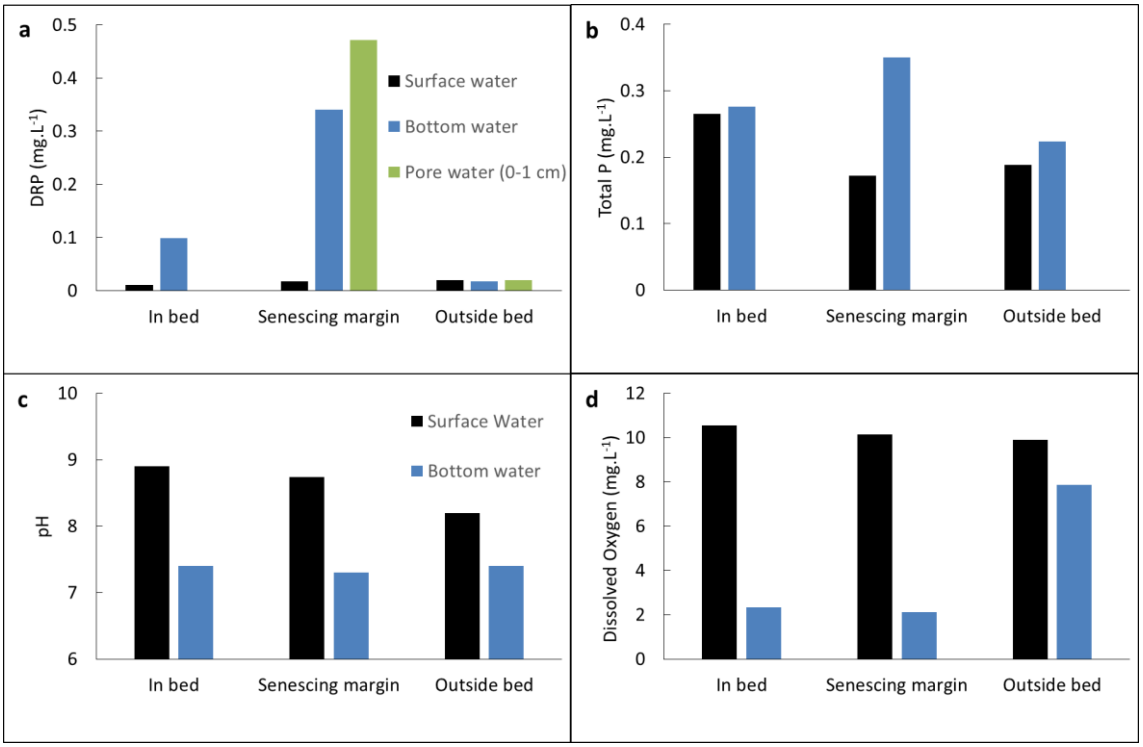

Figure 5.11 Water quality parameters analysed on 13 December 2013, at sites outside (main lake water column), inside, and on the senescing margin of the macrophyte bed depicted in Figure 5.13. The bottom water measurement was from 5 cm above the sediment and surface water 5 cm below the surface. Total depth was approximately 190cm. DRP was also analysed in the pore water of the surface sediment (0-1 cm)

5.3.3.4 Pore water chemistry

Pore water chemistry, sampled on the same day from the sites F11 (macrophyte beds) and F12 (no macrophytes) is presented in Figure 5.12. Raw data for the analysis of site F11 was presented in Table 3.4, and for site F12 is presented in Appendix 2.

Significant differences between the two sites were evident. Total dissolved Fe, P and Mn concentrations were much higher in the F11 pore water, relative to F12, and the [TD-Fe] peak was closer to the surface. The [TD S] was lower in the F11 pore water, and decreased rapidly immediately below the sediment surface. These trends were consistent with a more upwardly compressed redox profile and more reducing conditions at the sediment surface (See Chapter 3), at the macrophyte-dense site, relative to the site with no macrophytes.

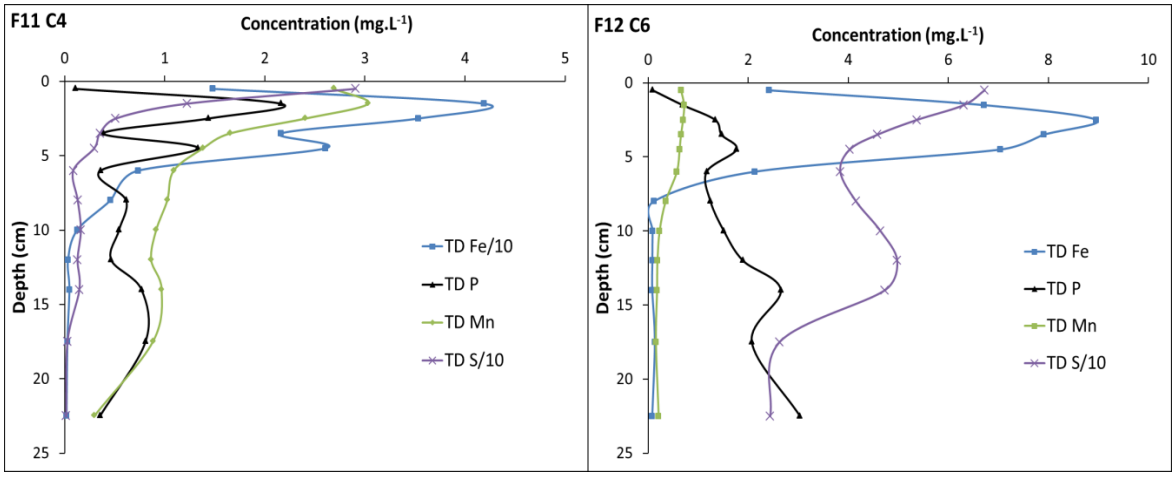

Figure 5.12 Pore water chemistry in two sediment cores sampled on the same day, one from site F11, an area with dense macrophyte beds, and one from site F12 with no macrophyte beds. Note the different units of Fe concentration used.

5.3.3.5 Sedimentary P fractions

The results of the sedimentary P fractions analysed over the summer of 2012-13 at sites F11 and F12 are presented in Figure 5.13. The data is also presented in Appendix 1.

At the macrophyte-dense site (F11), a progressive increase in TP through the summer season was evident, with accompanying increases in organic matter, BD-P, NaOH-rP Org-P, and Res-P. The increases in organic matter, TP, Org-P and Res-P are likely due to the senescence of macrophytes (see Chapter 3 for a discussion of these P fractions). The growth of algae on macrophytes (Figure 5.14) was observed during periods when the macrophyte beds were observed to decline in area and density, and in Figure 5.13 (a) the increases in the various P fractions are most pronounced after mid-March, when a cyanobacteria bloom began. The increase in BD-P and NaOH-rP is likely due to the decomposition of sedimented organic matter and the subsequent release of P for adsorption onto Fe and Al (hydr)oxides (see Chapter 3).

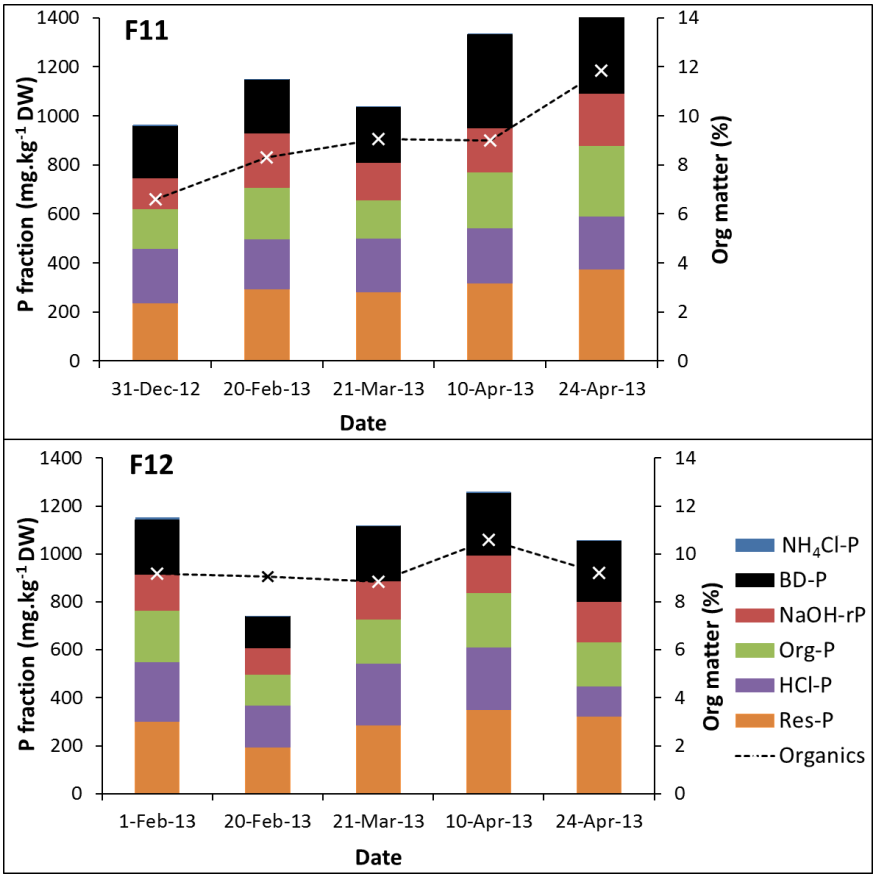

Figure 5.13 P fractionation in surface sediments (0-1 cm) at sites (a) F11, and (b) F12 sampled over the summer season of 2012-13.

Figure 5.14 Algal growth on macrophytes in samples recovered from senescing macrophyte beds in March 2013.

5.3.4 The effect of salinity

5.3.4.1 Salinity gradients along the lake

Figure 5.15 presents the results of surface water EC analysis at various sites along the lake on three different days. There was a consistent gradient along the lake on all 3 sampling dates, with higher EC at the southern end, closest to the sea.

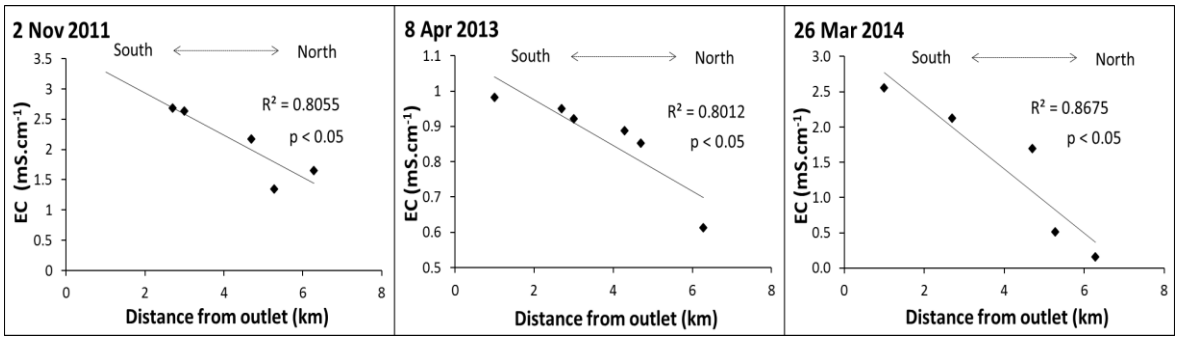

Figure 5.15 Electrical conductivity gradients along the lake on three separate sampling dates.

5.3.4.2 Pore water chemistry

Figure 5.16 presents the depth profiles for sediment pore water chemistry at the two sites F12 (north end) and F10 (south end) cores sampled on the 20th October 2014. The pore water trace element chemistry is also presented in Appendix 2. At the time of sampling there was only a small difference in water column salinity (F10 EC = 3.33 $mS.cm^{-1}$, F12 EC = 2.97 $mS.cm^{-1}$), however long-term salinity is higher at the southern end than further north (see Section 5.4.3.1), and pore water chemistry may be expected to reflect these prevailing conditions.

The EC in the surface sediment pore waters reflected that of the overlying water column, but was higher in the F10 core, and steeply increased with depth, reflecting the longer term trend of higher salinity at this site. pH was also higher at the F10 site, below the surface sediments, again reflecting the higher long term salinity. The salinity conditions were also reflected in the [TD-S] and [TD-Na] profiles. The two sites had similar concentrations in the surface sediment, but immediately below the surface, the pore water of F10 had higher concentrations of both Na and S, and both these increased with depth, reflecting the longer term trend of higher salinity at this site.

The [TD-Mn] and [TD-Fe] showed similar trends near the surface at both sites, but peak concentrations were much lower at F10 and the concentration began to decrease at a shallower depth. In contrast the [TD-P] was higher above 10 cm depth in the F10 core, and demonstrated a distinct peak, whereas in the F12 core the [P] was much lower and increased consistently with depth. The [TD-Al] showed similar trends between the two sites but was elevated at depths below 10 cm in the F12 core relative to F10.

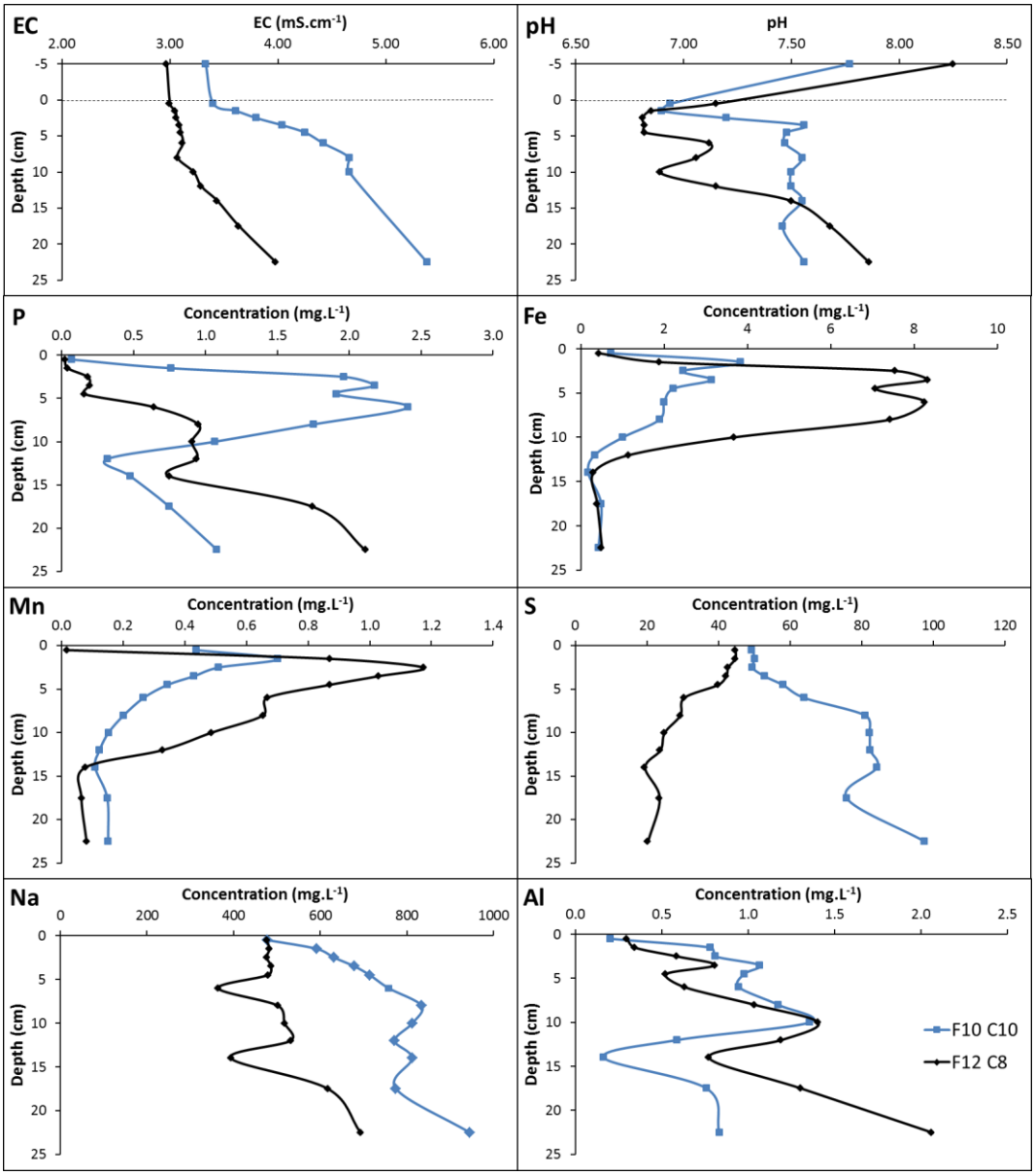

Figure 5.16 Pore water chemistry profiles with depth for sediment cores from two sites, F10 and F12, at the southern and northern end of the lake respectively. Concentrations are total dissolved. Sampling was conducted on the same day (20 Oct 2014).

5.3.5 Sediment resuspension

5.3.5.1 Depth of sediment disturbance

Sediment resuspension calculations conducted during a discrete, two day wind event, indicated that sediment to a depth of 0.72 mm, was resuspended into the water column. The maximum sediment disturbance depth was 2.4 mm.

5.3.5.2 Change in lake water [TP] due to pore water P release

Pore water release due to sediment disturbance to a depth of 0.72 mm across the whole lake, was calculated to increase the water column [P] by 0.0001 $mg.L^{-1}$, while disturbance to a depth of 2.4 mm would increase the water column [P] by 0.0004 $mg.L^{-1}$. By way of sensitivity analysis, disturbance to a depth of 10 mm (4 x greater than the maximum disturbance depth), would increase the water column [P] by 0.002 $mg.L^{-1}$

5.4 Discussion

5.4.1 General DO and pH conditions

The Wairewa water column is generally well mixed and oxygenated reflecting its shallow nature and windy catchment. This was consistent with the generally oxic layer found in the surface sediments, although the oxic layer only penetrated a few millimetres into the sediment. This thin oxic 'cap' is consistent with results from other studies in lake sediments (e.g. Ekholm & Lehtoranta, 2012). The differences in the thickness of the oxic sediments observed between summer and winter were also consistent with the more reduced winter sediment discussed in Chapter 3. However the bottom water [DO] patterns did display high variability, both spatially and temporally. This data highlighted a complex picture of spatially discreet deoxygenation events, occurring in the lake at various times. Vertical gradients of [DO] in lake water columns are well documented (e.g. Wetzel, 2001), however such spatially variable oxygen dynamics occurring across a relatively small and morphologically simple lake, appear to be less well documented.

The well mixed water columns common in shallow lakes (Søndergaard et al, 2003), and the windy nature of the Wairewa catchment meant that periods of low [DO] in the bottom waters, were of short duration. The longest event lasted approximately 13 days at site F11, with the next longest duration being 4 days at Site F14. Most other low [DO] events were of two days duration or less. Oxygen depletion rates in Wairewa indicated that

complete deoxygenation of the bottom water was possible in 9 - 24 hours. This is consistent with research in Lake Horowhenua where bottom water deoxygenation was calculated to occur in about a day (Gibbs, 2011). These rapid oxygen depletion rates indicated that relatively short periods of quiescence in the lake can result in low [DO] events, however the long periods without low [DO] events at, for example, site F12, indicated that additional environmental factors leading to water column stratification were required for bottom water deoxygenation to occur, as discussed in Sections 5.4.2.1, 5.4.3.1 and 5.4.5.

Elevated pH occurred throughout the year with pH > 8 commonly occurring during winter and pH reaching 10.5 during summer. Again spatial and temporal variability was observed in the time series data, where significant differences were observed between ECan's Main Recorder site and Site F11, and a range from 4.90 to 10.02 was recorded over a few days. pH > 9 was recorded over much of the summer period and pH > 10 occurred for significant periods of time.

The logger data for DO and pH collected for this research, in combination with time series data for EC, pH, lake level and wind, collected by ECan as part of lake monitoring, allowed various key drivers of conditions likely to affect P binding and release, to be identified.

5.4.2 The role of macrophyte beds

Macrophyte beds have significant effects on water quality parameters, particularly in shallow lake systems (Wetzl, 2001). The tall growing submerged macrophytes such as those in Wairewa may enhance water clarity by decreasing sediment resuspension, as well as decreasing algal growth through competition for nutrients, and providing habitat for phytoplankton grazing organisms (Takamura et al 2003). Such mechanisms underlie the theory of alternative stable states, whereby shallow lakes may exist in a clear-water state, dominated by macrophytes, or a turbid state, dominated by phytoplankton. Lakes may 'flip between these states and often show hysteresis when efforts such as nutrient load reduction, are made to shift a lake back to the clear water state (Scheffer and Nes, 2007).

The macrophyte beds in Wairewa are largely restricted to the northern end of the lake and cover approximately a third of the lake area at their maximum extent (Figure 5.1). However the area and density of the macrophyte beds was observed to vary significantly

during the research period and appeared to undergo a cycle of expansion and contraction at least partly related to algal biomass in the lake. Summer periods of low [chl-*a*], such as that during most of the summer of 2012-13, allowed extensive development of the macrophyte beds, which was followed by an algal bloom and associated macrophyte senescence. Hence Wairewa did not appear to demonstrate longer term hysteresis but rather the macrophyte biomass fluctuated over relatively short time periods (months). The macrophyte beds had significant impacts on P binding and release mechanisms, and periods of rapid growth produced self-limiting conditions, where macrophyte-associated P release, appeared to support the growth of phytoplankton. These are discussed below.

5.4.2.1 Stratification, organic flux and dissolved oxygen

The density of macrophytes is known to increase the vertical temperature gradient in shallow lakes (Herb and Stefan, 2004) and this was observed in Wairewa where thermal stratification was common in the macrophyte beds and uncommon outside of them. Generally, such stratification lasted only overnight but on occasion mixing did not occur and stratification lasted through the following day and night. Such stratification has the potential to decrease the [DO] of the bottom waters in the lake (Welsh and Eller, 1991) This was observed in Wairewa with the declines in bottom water [DO] resulting from the longer periods of thermal stratification within the macrophyte beds. In addition the longest period of low [DO] ([DO] < 2 $mg.L^{-1}$) observed during the period of time series data collection, occurred at site F11 in the macrophyte beds, in November, 2013. The spot analyses in the dense macrophyte bed which formed in late 2013 (Figure 5.11), also indicated a strong vertical gradient in [DO].

The oxygen demand at the sediment surface is likely to be higher in macrophyte beds than outside them, due to the increased supply of organic matter to the sediment surface (Herb and Stefan, 2004). In the Wairewa macrophytes, the flux of organic matter and the increased likelihood of thermal stratification resulted in a more reduced sediment profile, a thinner oxic surface layer and an upwardly compressed redox profile in the sediments underlying the macrophyte beds. These trends indicated that P release was more likely from sediments within the macrophyte beds relative to those elsewhere. Evidence of this was seen in the spot analyses in the dense macrophyte bed, where a nine fold increase in bottom water [DRP] was observed relative to outside the bed. The key role of the organic matter flux was evident from the further three-fold increase in [DRP] observed in the bottom water of the senescing margin of the bed. The prolonged low [DO] event in

November 2013 at site F11, coincided with the beginning of macrophyte senescence and provided further evidence of the critical role of the flux of organic matter resulting from the decomposition of the macrophyte beds. In a global sensitivity analysis, Katsev et al (2006) reported that the flux of organic matter to the sediment surface is the most important factor in determining the magnitude of P release in lake systems. In addition to the increased oxygen demand, decomposing organic matter may release P directly to the water column (Barko and Smart, 1980; Wetzl, 2001).

The prolonged low [DO] event at site F11 observed in November 2013 (13 days), also coincided with a substantial increase in planktonic [chl-*a*]. This suggested that periods of low [DO] in the macrophyte beds have the potential to release enough P from the sediments to trigger and sustain an algal bloom event. If the P release rates calculated for low [DO] in Chapter 4 are applied to the maximum area of macrophyte beds for this time period, increases in lake water [P] of 0.05 - 0.14 $mg.L^{-1}$ are possible (release rates for Eh=-210 and -300 mV respectively). The increase in [TP] during the November 2013 bloom event was not measured, however, during the algal bloom event in March – April 2013, discussed in Section 2.3.4 (which had a higher [Chl-a], 141 $\mu g.L^{-1}$ as opposed to 90 $\mu g.L^{-1}$ for the November 2013 event), the [TP] increased by 0.077 $mg.L^{-1}$. Hence the possible release of P from the sediments underlying the macrophyte beds over the November 2013 low [DO] event, was more than enough to trigger and sustain the growth of an algal bloom.

5.4.2.2 pH

Macrophyte beds are known to strongly influence water column pH, and rapid changes may occur during periods of intense photosynthesis or respiration (Serafy and Harrell, 1993; Cooke et al, 2005). The research discussed in Chapters 3 and 4 of this research, indicated that pH has a significant effect on P binding and release in the Wairewa sediments. This is consistent with Barko and James, (1998) who reported that P release from oxic sediments was doubled by an increase in pH from 8 to 9.

The effect of macrophyte growth was evident in the time series pH data collected at site F11. pH at this site rapidly increased in the spring of 2013 and was consistently > 9, regularly > 9.5 and not infrequently > 10. During November the pH in the macrophytes at site F11 decreased markedly. This was possibly due to a decrease in growth and photosynthesis due to senescence in response to algal growth, or simply a response to the

decreased light penetration resulting from macrophyte or phytoplankton density. In contrast the pH at the Main Recorder site (no macrophytes) increased substantially over the same period, reflecting the increasing phytoplankton biomass and probably, therefore, the rate of photosynthesis in the lake. This trend appeared to be reversed in late November 2013 when chl-*a* concentrations decreased from their peaks and substantial macrophyte growth occurred at the north end of the lake.

From September to November 2013 the macrophyte area experienced pH > 9 for approximately 40 days. At the bed sediment release rates calculated in Chapter 4 (pH > 9, release rate = 3.27 $mg.m^2.d^{-1}$) this has the potential to raise the whole lake [TP] by 0.023 $mg.L^{-1}$. Resuspension into high pH water column may raise [P] by more than this (see Section 5.4.4.2)

5.4.3 The role of salinity

5.4.3.1 The effect on sedimentary P-binding potential

The variability in salinity observed in Wairewa is due to a balance between freshwater influx at the northern end of the lake and sporadic sea water influx at the southern end of the lake. This dynamic produces a consistent salinity gradient along the lake, which has resulted in the significant differences observed in sediment chemistry between the northern and southern end of the lake. The trends observed in pore waters, with decreased [TD-Fe] and increased [TD-P] in the near surface sediments, at the higher salinity site (F10), were consistent with the mechanisms likely to result from increased [SO_4], which were discussed in Chapter 3. In sediments with low redox potential, increased [SO_4], which is reduced to [HS^-], increases the immobilisation of Fe as FeS_2. The resulting decrease in the upward flux of Fe^{+2}, decreases the P binding potential of the surface sediments. This mechanism has been noted in reviews of eutrophication processes as a key component in the long-term P-binding potential of sediments (e.g. Smolders et al, 2006; Katesev et al, 2006). In addition increased concentrations of reduced S increase the reductive dissolution of Fe (hydr)oxides (Katsev et al 2005; Weston et al, 2006: Lehtoranta et al, 2009) and reduce the stability of Fe-PO_4 mineral phases (Gachter and Muller, 2003), while SO_4 may compete with PO_4^{-3} for adsorption sites (Gardolinski et al, 2004; Spiteri et al, 2008). These processes all decrease P retention in the sediments.

This control of P availability by the SO_4^{-2} mediated solubility of Fe (hydr)oxides has been observed along estuarine salinity gradients in various studies. Hartzell & Jordan (2012)

found that decreases in pore water [Fe^{+2}] coincided with SO_4^{-2} reduction and increases in pore water [PO_4^{-3}] at similar salinities in four estuaries of Chesapeake Bay. Jordan et al, (2008) found similar trends, along with a coincident decrease in sequential extraction derived sediment [Fe-P]. Caraco et al (1990) studied 48 different aquatic systems and found that P derived from organic decomposition was immobilised in freshwater systems by P mineral formation or sorption, while less immobilisation occurred in marine and brackish sediments.

The effect of [SO_4] on sedimentary P-binding, means that long-term increases in salinity are likely to decrease the P-binding potential in in Wairewa sediments. This hypothesis was examined using long-term monitoring data from ECan for the period 1995- 2014. Non-parametric Spearman-rank order correlations were calculated for EC, Chl-a and lake level which could not be transformed to normal distribution (analysis conducted in Sigmaplot 13 statistical software, www.sigmaplot.com). Chlorophyll-*a* has been used here as a proxy for biologically available P which has been released from the lake sediments and taken up by algae. While this is not perfect, it is considered an improvement on using the analysed DRP concentrations due to the poor temporal resolution of DRP sampling, coupled with the reactivity of DRP in the water column. Changes in [TP] are also unlikely to represent a good indicator of bio-available P release, due to the extent of sediment resuspension in the lake. The chl-*a* data was dominated by periodic, very high concentrations, which were related to blooms of cyanobacteria. This is seen in the Figure 1.6 (a) where the mean chl-*a* concentrations are near or above the 75th percentile, and maximum values are an order of magnitude above the mean. These peaks were likely to skew any background correlation and for this reason peaks > 50 $\mu g.L^{-1}$ were removed. As the effects of salinity and lake level were likely to play out over medium to long time frames, 4 month moving averages were used in an attempt to ascertain changes resulting from longer term geochemical processes (as opposed to shorter term processes such as density stratification) and to smooth short term variability in the correlations.

Over the period 1995-2014, around 60% of the variability in [chl-*a*], could be explained by changes in salinity concentrations, with higher [chl-*a*] at times of high EC. This correlation supports the pore water evidence as well as the modelling evidence from Chapter 3, that salinity has a significant effect on long term P binding in Wairewa. The

lake level explains around half the variation in [chl-*a*] relative to salinity and some of this may be explained by the correlation between EC and lake level.

Table 5.2 Spearman's rank-order correlations for chl-*a* , lake level and EC data, from long term monitoring data collected by ECan. r_s is the Spearman's rank-order coefficient. Lake level (LL) and EC data were transformed to 4 month moving averages, while chl-*a* was transformed to 4 month moving averages from data with peaks >50 $\mu g.L^{-1}$ removed.

	March 1995 – October 2014		
	EC vs chl-*a*	**LL vs chl-*a***	**LL vs EC**
r_s	0.57	-0.313	-0.362
p	<0.001	<0.001	<0.001

The observations discussed above indicate that elevated salinity in the lake produces sediments with lowered P binding potential, and may predispose the lake to higher levels of P supported phytoplankton productivity. This is consistent with the pattern observed during this research period (November 2011 – December 2014) in which higher salinity during winter and spring produced earlier algal bloom events during the spring-summer (Figure 5.17)

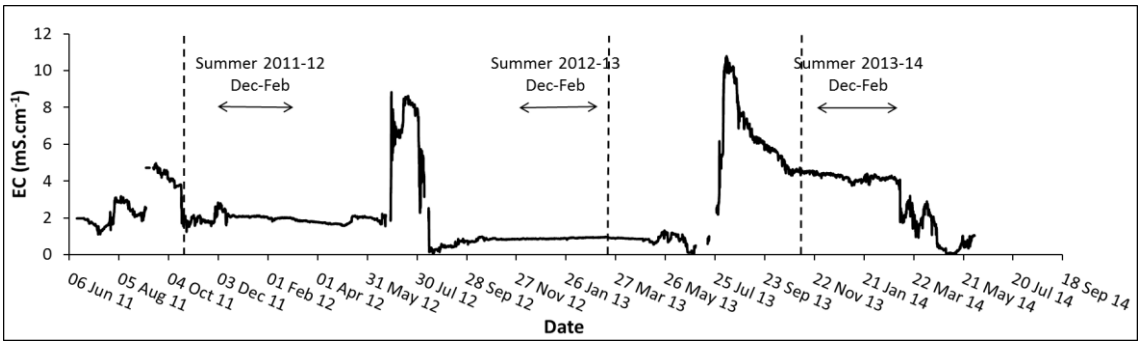

Figure 5.17 EC in Wairewa over the research period with the beginning of algal bloom events (dotted lines) indicated. The summer months of December-February are indicated for reference. Higher EC during winter and spring was associated with earlier onset of algal blooms relative to the summer months (December-February). EC data is from ECan lake monitoring.

5.4.3.2 Salinity induced stratification and dissolved oxygen

When the time series of DO data from this research was compared against EC and lake level data, it was apparent that during periods of rapid changes in lake level and/or EC, DO demonstrated high variability and episodes of low concentration. This pattern was mainly apparent at the southern end of the lake where EC was generally higher. Figure 5.18 (a) presents DO data for site F14, for the period June 2013- July 2014, and compares it to lake level and EC data from ECan lake monitoring.

Rapid increases in lake level were associated with large flood events in the catchment, and rapid falls with the subsequent artificial lake openings used to control flooding (see Chapter 2). It is evident in Figure 5.18 that these events were associated with rapid changes in salinity, as represented by EC. For example the time periods prior to early August 2013, and between early March and June 2014, were characterised by large changes in level and EC. During these periods, site F14 experienced very high variability in [DO], with multiple low [DO] events. This relationship was especially evident during the 21-22 June and 30-31 July 2013 as well as 1 April, 7 March and 18 April, 2014 flood/opening events and associated changes in EC. The large increase in EC in late July/early August 2013, also coincided with a low [DO] event. Similar patterns were observed in the data from site F10 (Figure 5.18 b), but much less DO variability was observed at sites nearer the north end of the lake (see Figure 5.4) over the same period. An explanation for this pattern is that intrusions of saline water, were causing density stratification and allowing bottom water deoxygenation at sites F10 and F14 over this period. An alternative explanation is that low [DO] events over these periods are associated with an increased organic flux due to the load of external flood-associated organic matter, and the collapse of phytoplankton populations due to turbidity, though this is not consistent with the absence of DO depletion at the north end of the lake during the same period.

Towards the end of the June–July 2013 period of variable bottom water [DO], a synchronous low [DO] event occurred at all data logger sites (26 July-2 August). This occurred immediately after the very rapid and substantial increase in EC at the Main Recorder site (≈ 30 July, 2013, Figure 5.18). This increase was likely due to an influx of sea water at some stage after the June/July 2013 lake opening. The northward spread of this seawater and consequent water column stratification, may explain the rare, lake-wide, low DO event. A lag between a sea water influx at the south end of the lake and a salinity related low [DO] event further north, is consistent with lag periods of up to forty days between EC increases at Birdlings Flat (see Figure 5.1) and Catons Bay, evident in the ECan monitoring data, as well as the persistent EC gradient observed along the lake.

Figure 5.18 (b) presents the DO data from site F10 along with 10 hour wind run data for a NE wind direction (from ECan lake monitoring) for the period 1 June- 23 August 2013. The 10 hour interval for the wind run was used to smooth the highly variable wind data and was based on DO decline rates discussed in Section 5.3.1, where 10 hours of

quiescence appeared to be the minimum required for potential deoxygenation of bottom waters to occur. The wind run for NE wind was used as this direction was likely to produce the greatest turbulent mixing at the southern end of the lake. Peaks in the wind run coincided with high [DO] concentration, with generally low [DO] in between, indicating that over this period the bottom waters at the southern end of the lake, deoxygenated rapidly in the absence of significant wind. This seems to support the notion of density driven stratification causing the observed deoxygenation. The end of this period of [DO] variability occurred on 4 August 2013 (see dotted orange lines on Figure 5.18 a, b), immediately after the rapid rise in EC and lake-wide low [DO] event discussed above. A strong wind event on 4 August appeared to mix the lake sufficiently to prevent ongoing stratification, and ushered in a period of much lower [DO] variability, during which bottom waters were less likely to deoxygenate during low-wind periods (see post-4 August 2013, Figure 5.18 (b)).

Hence the relationships between lake level, EC, wind and low DO concentrations appear to indicate that salinity induced stratification may be a key factor in bottom-water deoxygenation during periods of fresh- and sea-water influxes in Wairewa. Such trends have been previously documented in the Wilson Inlet ICOLL, in Western Australia where prolonged vertical salinity gradients were observed in response to fresh- and sea-water inflows. These resulted in low bottom-water DO concentrations, and significant P release (Twomey and Thompson, 2001). McCorquodale and Georgiou (2004) have also reported salinity stratification and resulting deoxygenation in bottom waters in a shallow, generally well mixed lake in Louisiana, USA.

The release of bioavailable P during the low [DO] events described above, may explain winter peaks in Chl-a that occurred during the periods of salinity-induced DO variability, in June-July 2013 (13 June 2013, Chl-a = 28.6 $\mu g.L^{-1}$; 19 July 2013, Chl-a = 44 $\mu g.L^{-1}$) and again in June 2014 (12 June 2014, Chl-a = 58 $\mu g.L^{-1}$). Winter blooms of cyanobacteria have been relatively common in Wairewa since at least 1996, and appear to be associated with the large changes in EC accompanying winter flood/lake opening events. Figure 5.19 illustrates this association over the period 2006-2010. The summer bloom that began in October 2011 (Figure 5.17), also coincided with a major change in lake EC and may be related to a stratification and deoxygenation event. The mechanism discussed in Section 4.4.4 whereby 'freshening' events in the lake may result in significant P release, may also have played a role in the October 2011 bloom event.

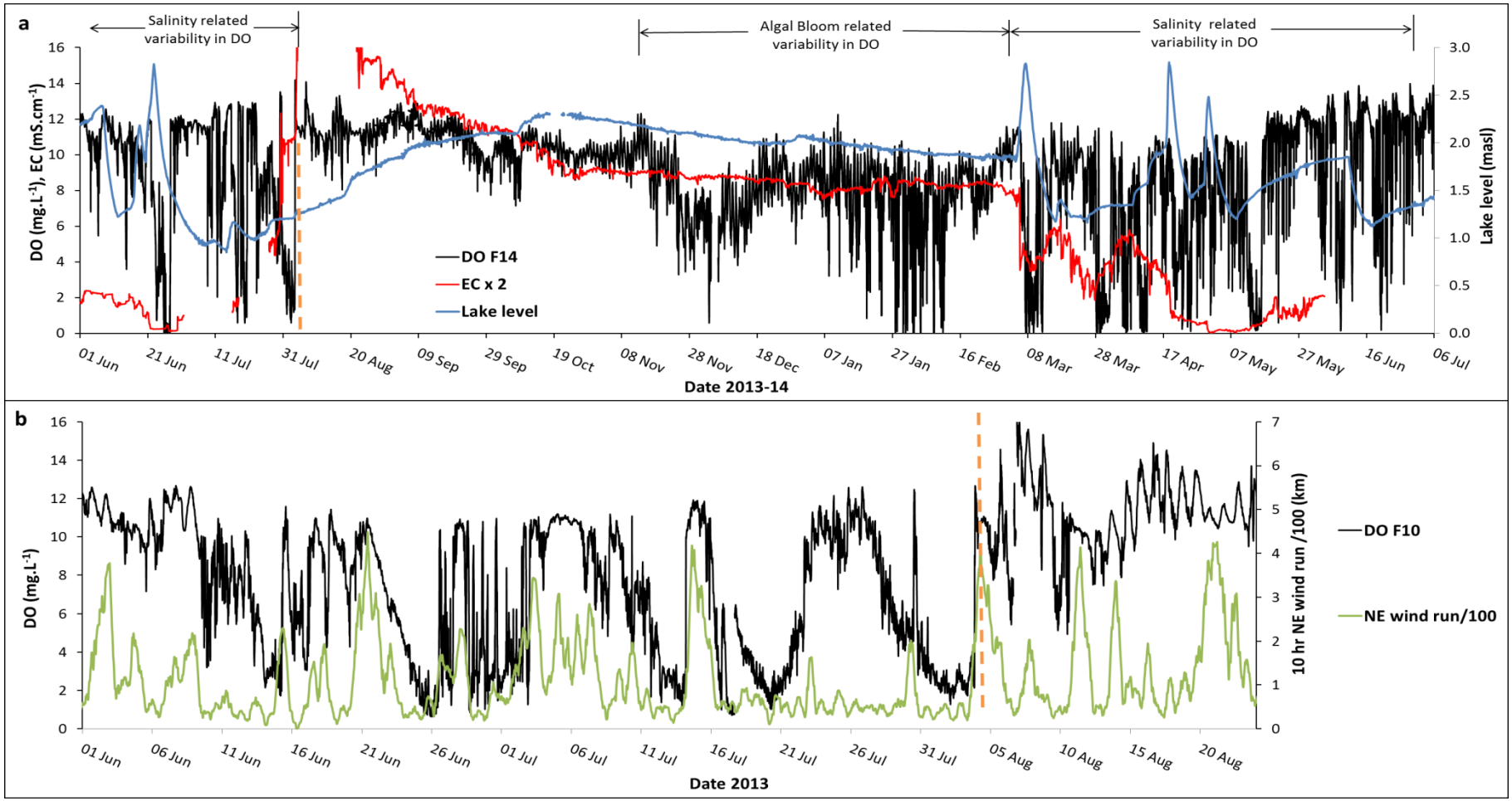

Figure 5.18 Selected water column parameters for sites at the southern end of the lake. (a) Site F14 [DO] plotted with EC and lake level, and, (b) site F10 [DO] plotted with EC, lake level and 10 wind-run for north-easterly winds. The orange dotted line in plot (a) and (b) indicates the wind-induced mixing event of 4 August 2013. The key factors driving periods of variability in [DO] are indicated on plot (a). Note the different time scales. EC, lake level and wind data are all from ECan lake monitoring data.

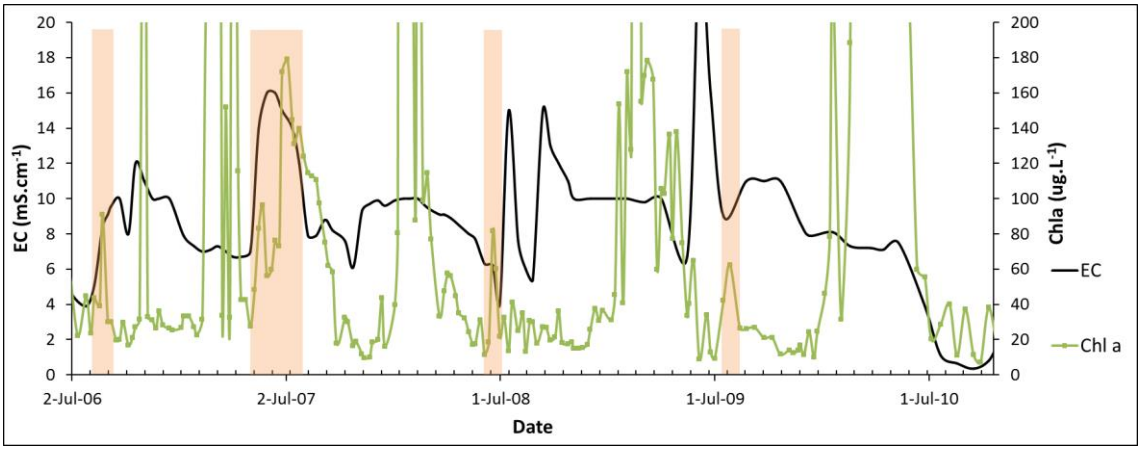

Figure 5.19 Electrical conductivity and chl-*a* concentrations in Wairewa over the period of winter 2006- winter 2010. Winter algal bloom events associated with significant changes in EC are indicated by the coloured bars. Data is from ECan lake monitoring.

5.4.4 The role of wind

5.4.4.1 Stratification and lake mixing

The windy nature of the Wairewa catchment ensures that the water column in Wairewa is generally well mixed. The mean wind velocity during this research period (from ECan lake monitoring data) was 4.2 $m.s^{-1}$ and Kleeburg and Dudel (1997) demonstrated that wind velocities of > 4 $m.s^{-1}$ are capable of completely mixing a water column down the 6 m depth, although this is likely to depend on factors such as the strength of stratification. Strong winds then, may mitigate the stratifying effects of macrophytes and salinity discussed above, and Figure 5.18 b showed the effect of partial wind mixing during periods of salinity stratification. As discussed in Section 5.4.3.2, a wind event also appeared to completely mix the lake after a period in which the DO dynamics of the north and south end of the lake were decoupled. Hence it was observed that wind had a critical role in the mixing and oxygenation, both vertically and horizontally, of the lake water column.

5.4.4.2 Sediment resuspension.

Sediment resuspension has been noted as an important factor in the cycling of nutrients between sediments and the water column in lake systems (e.g. Schallenberg and Burns, 2004), however in the case of P, this cycling is often in particulate form (measured as TP) which may not increase bioavailable P (e.g. Kristensen et al, 1992, Søndergaard, 2007). As discussed in Section 4.4.1 it appears unlikely that the resuspension of Wairewa

sediment into an oxic, circum-neutral water column, will result in the release of significant amounts of DRP by desorption from the particulate material. The effect on [TP] in the water column from the release of pore water during resuspension, has been noted in several studies (e.g. Das et al 2009), however it is apparent for the calculations in this research that pore water, mixed into the water column of Wairewa during resuspension, is unlikely to be a significant source of bioavailable P under oxic, circum-neutral conditions.

In contrast the resuspension of sediment in a high pH water column has the potential to release significant amounts of P. In field experiments in a shallow lake in Finland, Niemisto et al (2011) found resuspension during low pH periods increased water column [TP] but not [DRP], however during periods of high pH (pH > 9) significant increases in [DRP] were observed. Using release rates calculated in Chapter 4 for sediment shaken in water at pH > 9, disturbance of the sediment to a depth of 0.72 mm could increase the whole lake water column by 0.018 $mg.L^{-1}.d^{-1}$. Disturbance to a depth of 2.4 mm could increase the whole lake water column by 0.060 $mg.L^{-1}.d^{-1}$. Hence this may be a significant source of P to the water column during summer when macrophyte and cyanobacteria mediated pH is high. However despite the fact that sediment resuspension in Wairewa is very common, including during high pH periods in early summer, algal blooms do not develop as a matter of course. The relationship between resuspension, pH and bloom development may be self-limiting, as sediment resuspension will increase turbidity, decreasing light penetration and photosynthesis, and hence pH (Teng et al, 2007).

5.4.5 The effect of cyanobacteria blooms

Algal blooms are common events in the lake and their effects on oxygen and pH have a significant effect on the environmental conditions which affect P binding and release. The presence of such blooms in Wairewa led to elevated pH in the lake with pH > 10 at times. As discussed above and in Chapters 3 and 4, this may lead to significant P release from the sediment. Xie et al (2003) noted such P release during microcosm experiments in the hypereutrophic Lake Donghu in China, with major increases in both TP and DRP resulting from high pH during *Microcystis* blooms. In Wairewa, a bloom affecting the whole lake for a period of 30 days, could increase lake water column [TP] by 0.06 $mg.L^{-1}$ (based on lake area, volume, and the release rates for pH > 9, Table 4.11).

Periods of algal bloom in Wairewa, are also associated with periods of variability in [DO] in the lake bottom waters (Figure 5.18). Early November – late February 2014, was one such period which was characterised by high chl-*a*, and significant episodes of low bottom water [DO]. The oxygen profiles across the sediment-water interface indicated an increase in sediment oxygenation during algal blooms, however the profile during a bloom was analysed very early in the bloom cycle and deoxygenation of the lake bottom water may occur due to a flux of biomass to the sediment surface as algal populations fluctuate. The organic flux is likely to be increased by elevated macrophyte senescence in Wairewa during algal blooms. This was apparent from the the visual observations of declining macrophyte area and density during algal growth, the observations made across the senescing margin of a macrophyte bed, and the increase in sedimentary P fractions in the macrophyte beds after the beginning of an algal bloom. The decomposition of this biomass increases the oxygen demand and deoxygenates the bottom waters, leading to the release of Fe-bound P to the water column. Such processes were evident in the sulphide odour and high [DRP] observed in the bottom water of the dense macrophyte bed investigated in November 2013, and in the compressed redox profiles observed in the pore waters of the PBI sediment cores discussed in Chapter 3. Chen et al (2014) investigated the effect of adding cyanobacterial biomass to the sediments of the eutrophic Lake Taihu in China. Addition of such biomass resulted in sedimentary Fe reduction as well as SO_4 reduction and the formation of FeS/FeS_2. Significant P release accompanied these processes. Søndergaard et al (1990) also noted very high P release rates of 100-200 $mg.P.m^2.d^{-1}$ during collapses of phytoplankton populations in the shallow Danish lake, Lake Søbygard. Hence algal blooms may produce self-sustaining cycles of sedimentary P release.

5.5 Conclusions

Water quality conditions in Wairewa are poor with high and highly variable concentrations of P and common algal blooms. Internal loading of P from the sediments to the water column is key to initiating and sustaining these bloom events. Figure 5.20 presents the key biogeochemical processes, and 'drivers' of those processes, which have been identified in Wairewa as leading to sedimentary P release.

Episodes of low [DO] in the bottom-water of the lake were common, although generally short-lived and not consistent across the lake. The longest such episode observed in the

lake, was linked to thermal stratification in the macrophyte beds at the northern end of the lake, and appeared to trigger the algal bloom which began in late November 2013. Low [DO] in the bottom-waters and prolonged periods of DO variability also appeared to result from density stratification due to changing lake salinity. These changes occurred as a result of flood events in the catchment and subsequent lake openings. Such salinity induced stratification and deoxygenation, may have had a role in triggering the algal bloom in October 2011. Wind was key to mitigating both thermal and density driven stratification, as well as to mixing the variable salinity and DO conditions which arose at opposite ends of the lake during flood/lake opening events. Also producing periods characterised by wide fluctuations in [DO] and deoxygenation of lake bottom-waters, were the algal blooms themselves. This resulted from the flux of organic material to the sediment surface and subsequent high oxygen demand due to mineralisation of the organics. The effect of such organic fluxes was also evident in the macrophyte beds, particularly when increases in algal growth resulted in macrophyte senescence.

The release of P from the sediments due to high pH is also a key process in the lake. High pH was produced in the macrophyte beds and during algal blooms with prolonged periods of pH > 9. The release of P from bed sediments during these long periods of high pH, has the potential to significantly increase water column [TP].

Salinity plays a key role in P release beyond its role in density stratification, by decreasing the P binding capacity of the sediments. Elevated SO_4 concentrations result in increased sulphides in the reduced sediments. These increase the reductive dissolution of P binding Fe (hydr)oxides, dissolve Fe-PO_4 phases and immobilise Fe as FeS_2.

The resuspension of sediment in the lake is thought to play a limited role in the release of bioavailable P, except during periods of high pH. At such time significant rates of P release from resuspended sediment are possible, but resuspension related turbidity may have a negative impact on photosynthetically increased pH.

During the growing season the lake went through periods of time when macrophytes increased in area and density, followed by periods dominated by algal growth. The growth of macrophytes appears to be self-limiting via the agenct of macrophyte induced P release (pH or DO mediated). Such P release promotes and/or sustains algal growth which, along with direct algal growth on the macrophytes induces macrophyte

senescence, resulting in further P release and bloom development. P release is increased during periods of high and/or rapidly changing salinity.

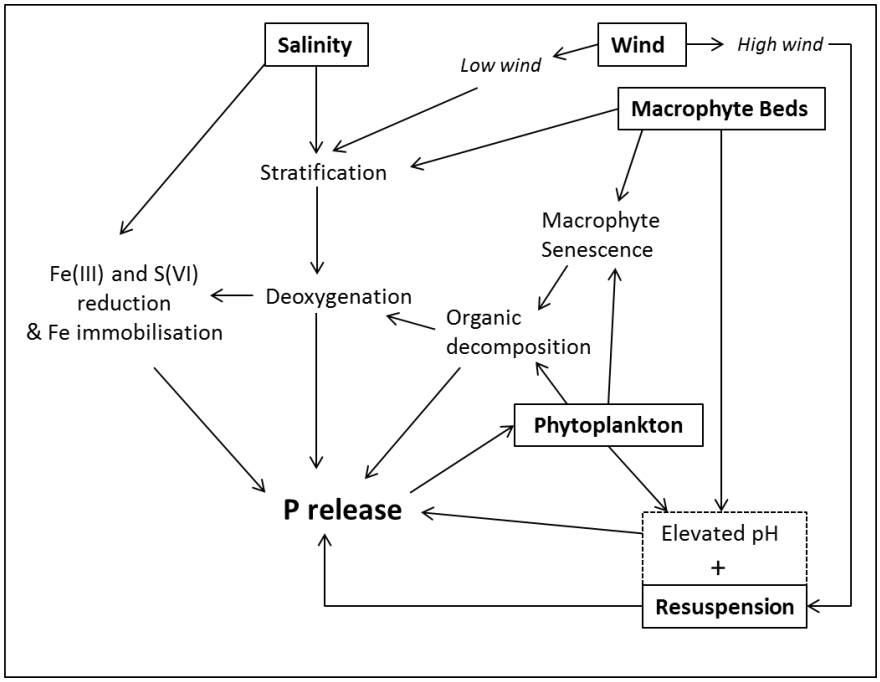

Figure 5.20 Biogeochemical processes leading to internal P loading in Wairewa. Key physical 'drivers' are in boxes. The dotted box around 'elevated pH' indicates that the elevated pH is key to the role of resuspension in P release.

5.6 Key research findings

- Bottom water anoxia occurs in Wairewa as 'patchy', spatially discrete, short lived (days, occasionally weeks) events.
- Bottom water anoxia results from thermal stratification in macrophyte beds, fluxes of organic material to the sediment from macrophytes and cyanobacteria, and probable density stratification due to rapid changes in salinity.
- Estimated P release from observed anoxic events is enough to explain observed increases in water column [TP] associated with algal blooms.
- Macrophytes and algal blooms produce pH conditions compatible with significant sedimentary P release.
- P released from pore water during sediment resuspension is unlikely to be a significant source of internal P loading.

Chapter 6: Synthesis and Lake Management

6.1 Introduction

Water quality parameters in Wairewa reflect a hypertrophic lake system which has experienced algal blooms since at least 1907 (Main et al, 2003). This state is due largely to the major increases in P rich sediment eroding to the lake, as a result of catchment deforestation following European settlement (Lynn, 2005; Woodward and Schulmeister, 2005). Chapters 2-5 of this research have quantified the flux of P from the catchment to the lake, and illuminated the key processes and mechanisms by which P is bound in the sediments, and released to the lake water column.

This chapter brings together the research presented in those chapters by way of a hypothetical year-long time line in which P dynamics in the catchment are described as they may occur during a given year. The timing, interaction between, and relative importance of, the various processes discussed, may vary from year to year, and several of the processes are likely to occur year round. However the seasonal framework provides a useful structure with which to summarise the key processes involved in P cycling in Wairewa. Such an annual cycle in P dynamics is presented in Figure 6.1. These P dynamics are then used to inform a brief discussion on management options for the lake. No research was conducted on the efficacy of various management options but an extensive literature exists on the subject, which has allowed an informed appraisal of the Wairewa situation.

6.2 Synthesis; A hypothetical year in the life of Wairewa.

Winter

The flux of P from the catchment is the ultimate source of P in the lake system. More than 7000 kg $P.yr^{-1}$ is delivered to the lake, predominantly in particulate form associated with major flood events. These flood events commonly occur during the winter months and lead to major fluctuations in the lake level which, in turn, lead to artificial lake openings in order to alleviate local flooding. Such openings are the major factor in the loss of around 30% of the total P inflows, to the sea. Retention of P in the lake system is high, at around 70 % of the P influx.

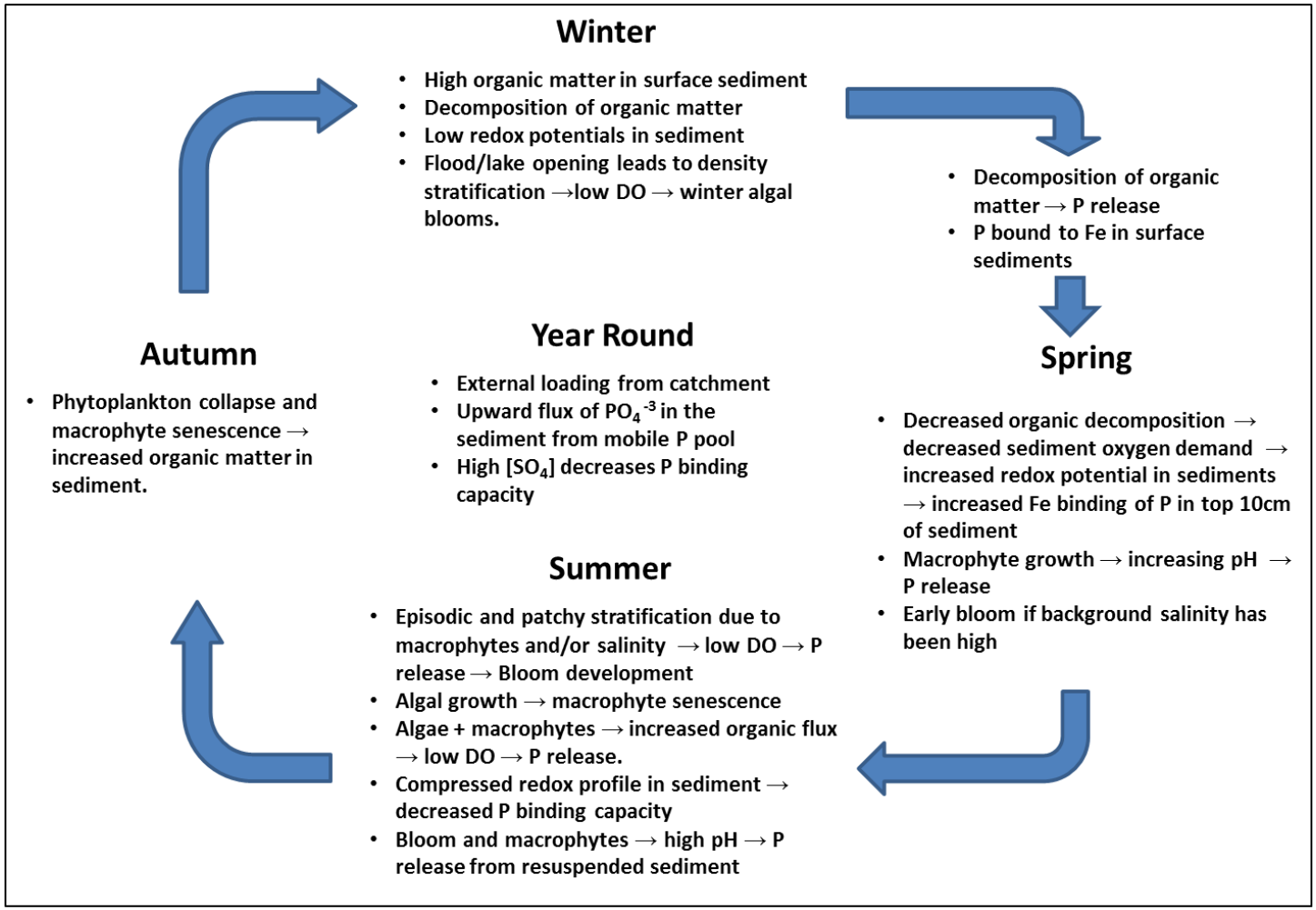

Figure 6.1 An annual cycle of P dynamics in Wairewa.

Such high retention and sedimentation of particulate material, at a rate of 2.4 mm.yr-1, leads to the vast majority of P in the lake system being sequestered in the lake sediments where it provides a source for the internal P loading required to explain many of the significant variations in [TP] associated with algal bloom events.

The slow burial of this P over time leads to changes in form, and fluxes of P from deeper to shallower sediments. With burial, PO_4^{-3} is progressively released due to decomposition of organic material, reductive dissolution of P binding Fe phases and desorption from Al phases. This PO_4^{-3} then undergoes an upward flux, while P associated with apatite and refractory organics is progressively and permanently buried. An upward flux of soluble Fe^{+2} also occurs, which is immobilised at the sediment depth at which redox conditions allow precipitation of Fe(III) phases. These redox sensitive ferric Fe phases, predominantly Fe (hydr)oxides such as ferrihydrite and goethite, are the key P binding phases in the upper sediment, along with pH sensitive, Al (hydr)oxides.

The flood events and artificial lake openings, often lead to significant changes in lake salinity. High SO_4 concentrations accompanying increased salinity, lead to higher sulphide concentrations in the reduced sediments. This in turn leads to reductive dissolution of Fe (hydr)oxides and Fe(II)-PO_4 minerals, as well as the immobilisation of Fe in the reduced sediments as FeS/FeS_2. Hence, prolonged higher salinities in the lake, often occurring over the winter months, decrease the binding potential of the sediment and lead to increased P release and higher background levels of phytoplankton in the water column. The flood/lake opening events also lead to salinity driven, density stratification of the lake water column. When this is not re-mixed by wind events it leads to bottom water deoxygenation, reduction of Fe (hydr)oxide minerals in the surface sediments, and subsequent release of P, leading to winter algal blooms.

In addition, during autumn/winter, mineralisation of the elevated organic matter which results predominantly from the sedimentation of summer algal populations, produces lowered redox potentials at the sediment surface. This results in a thinner 'cap' of oxic sediment at the surface and a decreased proportion of P bound to Fe (hydr)oxides.

Spring

As the spring/early summer season begins and decomposition exhausts the remaining labile organic matter in the surface sediments, oxygen demand at the sediment surface is

decreased and redox potentials in the upper sediment increase. This results in the ongoing upward flux of ferrous Fe being immobilised at deeper levels in the sediment, and a subsequent increase in sediment binding potential, which was observed as an increase in Fe-bound P in the upper 10 cm of the pre-bloom sediment cores.

Macrophyte growth increases the area and density of macrophyte beds at the northern end of the lake. The resulting increased photosynthetic activity, increases pH resulting in the desorption of P from Al and Fe (hydr)oxides.

Summer

The combination of high pH and/or prolonged high [SO_4] increases the flux of P from the sediment to the water column, and hence the background cyanobacteria populations in the lake. The resulting increase in organic flux as well as increasing nocturnal respiration, increases the oxygen demand at the sediment surface and hence the oxygen decline rate during periods of stratification. Such stratification occurs in the macrophyte beds, and/or due to summer-flood related salinity stratification as discussed above, and can result in periods of deoxygenation of the bottom waters, releasing significant amount of P, which drive and sustain algal bloom formation. P release rates due to a deoxygenation event in the macrophyte beds could increase the whole-lake water column [P] by 0.004 - 0.011 $mg.L^{-1}.d^{-1}$. A bloom, which appeared to be related to salinity driven stratification occurred in early October 2011, while macrophyte driven stratification resulted in bloom development in November 2013. Such blooms decrease light penetration in the lake and, along with algal growth directly on the macrophytes, begin a cycle of macrophyte senescence, thus further increasing the organic flux to the sediment. This flux during bloom events results in periods of significant variability in bottom water [DO]. These processes decrease redox potentials in the sediment, resulting in the upwardly compressed redox profiles seen in the PBI cores, and the release of P from the redox sensitive Fe (hydr)oxides in the upper 10 cm of the sediment.

The bloom events also sustain high pH in the lake and at pH > 9, P will be released from resuspended sediment. Resuspension in the lake is ubiquitous, with disturbance of the sediments during discrete wind events to a depth of 0.7 mm, and to maximum depths of 2.4 mm. Such sediment disturbance results in minimal release of pore water P, but P release, due to desorption from resuspended Al and Fe hydroxide particulates, may

increase lake water P concentrations by 0.018 $mg.L^{-1}.d^{-1}$. However, resuspension during non-bloom periods of high pH is common, and bloom development often does not occur, hence some additional factor such as light availability, may be limiting biological uptake, or repeated resuspension may reduce the likely P release rates.

Autumn

The cause of collapses in lake cyanobacteria populations is uncertain, but may be due to nutrient or light limitation, or trophic interactions (Jeppesen et al, 1990). Such collapses, when they occurred during the summer growing season, were observed to result in an increase in macrophyte growth, resulting in another cycle of macrophyte growth followed by cyanobacteria growth. Regardless of whether or not such a cycle occurs, or the bloom dominates throughout summer, the end of the summer growing season will see an increase in organic matter and organic-P in the surface sediment as primary productivity decreases. This flux of such organic matter from cyanobacteria and macrophytes, as well as the continued flux of P from the lake catchment, increases the organic content and the Org-P fraction in the surface sediment. Mineralisation of the organic material then re-establishes the reduced redox profile of the winter sediment pile.

6.3 Management Implications

The management of lake nutrient loads has the potential to significantly reduce eutrophication and cyanobacteria blooms (Heisler et al, 2008), however attempts to restore water quality in lakes already suffering from eutrophication, have had mixed results (Reitzel et al, 2005; Gibson et al, 2001). In particular, many shallow lakes, with large sedimentary P reservoirs, have resisted restoration efforts in the form of reduction in external loads, due to internal P loading (Søndergaard et al, 1990; Cooke et al, 2005; Schindler, 2012), Such internal loading typically lasts 10-15 years after reductions in external loads (Jeppesen et al, 2005) and may last more than twenty years (Kangur et al, 2013). Results of long-term, whole ecosystem studies indicate that the control of P is the key to controlling eutrophication and remediating lake systems (Schindler et al, 2008; Schindler, 2012), and the identification of lake-specific sources and processes which result in P loading, is likely to improve restoration results by providing direction for more targeted and cost effective interventions. The results of the mass-balance P budget established in Chapter 2 provides clear guidance for catchment managers.

Management of the Wairewa lake environment will need to respond to the following two phosphorus loading issues.

- The transport of P to the lake during high intensity, low frequency flood events, especially from the Okana sub-catchment.
- The release of P to the lake water column, from the large reservoir of P-bearing sediments.

6.3.1 Management of External P loading

While changes in water column TP concentrations, which support changes in primary productivity, were driven largely by internal loading processes, these are a legacy of decades of high external loading to the lake and a high phosphorus retention coefficient. Such legacy issues are common (Jarvie et al, 2013) and have been linked to poor responses to implemented P management interventions (McDowell et al, 2004). As such, management of the external P load is critical to long term rehabilitation. The work presented in Chapter 2 of this research formed the basis of a report to ECan (Waters. S. 2014. Phosphorus Loading to Lake Forsyth/Te Roto o Wairewa. Preliminary Results for a Lake Phosphorus Budget. *WCFM Report 2014-006*) which has helped inform the draft Wairewa/Lake Forsyth variation to the Land and Water Regional Plan.

The identification of CSA has the potential to significantly improve the cost effectiveness of management interventions (Doody et al, 2012). The Wairewa P budget, clearly indicates that targeted measures to control P transport should be aimed at the Okana sub-catchment and should aim to reduce flood-associated transport of particulate material. The naturally P-rich soils of the catchment suggest that these measures should aim to reduce erosion through riparian zone development and hill-slope erosion control measures, such as changes in soil, crop and stock management (Ekholm & Lehtoranta, 2012; Schoumanns et al, 2014). A more detailed understanding of land use practises in the Okana CSA would inform the efficacy of targeting these transport processes. If practises such as fertiliser applications are resulting in excess P loading to catchment soils, over and above crop requirements, then simply addressing transport mechanisms may result in a shift in the P legacy from the lake to the catchment soil. This is unlikely to create a long term solution to the water quality issues in the lake (Jarvie et al, 2013). More detailed work on the Okana CSA may identify smaller source areas and more

specific transport mechanisms and land use issues, which would allow even better targeting of management interventions.

The P budget can also inform specific management projects. The quantification of the flood associated P load to Lake Forsyth is important in assessing the suggested options for the control of sediment and nutrient load to Lake Forsyth. These include a constructed wetland for nutrient stripping and a sedimentation basin (Painter, 2014). However the capacity of such structures means that the highest flood flows are usually diverted directly to the lake. For example, analysis for the lake budget indicated that 50% of the total annual external P load was transported during 7 days of peak Okana River flows (June, 2013). The major effect that single flood events have on annual TP loads means that, in particular, those years which experience larger flood events, will deliver very significant P loads to the lake despite costly infrastructure approaches. Analyses of the efficacy of such management interventions need to account for the large amounts of P transport during uncaptured peak flood flows. At the very least, such infrastructure approaches will need to be part of a wider program including catchment and riparian, erosion control.

The budget suggests that an attractive option is to attempt to reduce the hydraulic retention time for the lake and hence increase flushing rates and reduce P retention. However the construction of a permanent opening to achieve such outcomes would have to overcome the problems associated with a very high energy coastline and the rapid transport of gravel northward along the coast. As such it is likely to be a very costly exercise and may well be short lived.

6.3.2 Management of Internal Loading

The P budget for Wairewa presented in Chapter 2, indicated that internal P loading from the sediment reservoir, especially during low flow summer months, was a key factor in the significant changes in lake P concentration associated with algal blooms. The appropriateness of any management intervention designed to address this internal P load, is likely to reflect the lake-specific dynamics that drive P release from the sediments. Hence the research in Chapters 3-5 detailing P binding and release mechanisms in the lake, provided valuable insight into the likely responses to the various management approaches.

A range of management options have been attempted around the world, for the control of internal P loading to lakes. Physical methods include sediment dredging and engineering solutions such as enhancing outlet flows. Chemical methods range from the artificial oxygenation of bottom water to sediment capping with various P inactivation agents. Biological controls may include harvestable floating wetlands, the permanent establishment of macrophyte beds or increasing the populations of algae-grazing zooplankton.

6.3.2.1 Physical methods

A change in opening regime

A physical management intervention has already been implemented at Wairewa and changes in water quality are examined here to provide an insight into the efficacy of the intervention. A change to the lake opening regime was instigated in late 2009. Rather than openings being conducted via a bulldozed trench directly through the beach barrier, the new regime involves the lake being opened via an outlet canal (see Figure 5.1), which has allowed better control over opening durations and lake levels. The change has had significant effects on water quality parameters in the lake. Table 6.1 presents key statistics for selected parameters, from the time periods pre- and post-change in opening regime. A third period of time is also presented (Oct- 2010-Oct 2014, Table 6.1 (c)), which was assessed in order to ascertain whether a period of post-change equilibration in the lake, made any further difference to water quality.

TP and chl-*a* concentrations were lower in the post-change period. DO concentrations were largely unchanged, but pH was lower in the post-change period, likely resulting from the decrease in chl-*a* concentrations. Average lake levels and water temperatures both increased in the post-change period, while EC was significantly lower after the regime change. Turbidity decreased slightly from 29.36 in the pre-change period, to 24.09 NTU in the post-change period. These trends all continued into the post-equilibration time period (Oct 2010-Oct 2014) and it is apparent that the change in opening regime significantly improved lake water quality, and further improvement occurred after an equilibration period of approximately one year.

While a range of interconnected factors may account for the observed improvement in lake water quality, the primary, underlying physical changes resulting from the change in

opening regime, will be in lake depth and salinity. Better control over opening durations has resulted over better control over lake levels, and over the amount of sea water entering the lake during openings. This was observed in the increase in lake level, and the decrease in EC, discussed above.

Table 6.1 Key statistics for selected water quality parameters in Wairewa from long-term lake monitoring data collected by ECan, over varying time periods associated with the changed lake opening regime. (a) Pre-regime change, (b) Post-regime change, and (c) the period of time from approx. 1 year after the regime change to Oct 2014.

(a) Mar 1995 - Dec 2009

	TP	chl-*a*	Level	Cond	Temp	DO	pH
	$mg.L^{-1}$	$\mu g.L^{-1}$	masl	$mS.cm^{-1}$	^0C	$mg.L^{-1}$	
mean	0.25	97.5	1.59	9.91	13.25	10.26	8.24
SD	0.30	351	0.36	4.94	5.07	1.69	0.54
Median	0.15	34.8	1.63	8.40	13.05	10.30	8.10
Range	0.004-2.80	0.1-6790	0.37-2.98	0.62-36.0	2.40-25.10	4.30-15.60	6.50-9.90
n	489	702	5261	570	682	217	566

(b) Jan 2010 - Oct 2014

	TP	chl-*a*	Level	Cond	Temp	DO	pH
	$mg.L^{-1}$	$\mu g.L^{-1}$	masl	$mS.cm^{-1}$	^0C	$mg.L^{-1}$	
mean	0.17	92.75	1.77	2.73	14.38	10.35	7.97
SD	0.19	340	0.30	2.38	4.84	1.77	0.49
Median	0.11	26.50	1.79	2.00	15.25	10.30	7.90
Range	0.03-1.10	1.40-3265	0.89-2.98	0.29-10.41	4.50-22.2	6.98-16.6	7.00-9.40
n	58	98	1753	59	106	101	58

(c) Oct 2010 - Oct 2014

	TP	chl-*a*	Level	Cond	Temp	DO	pH
	$mg.L^{-1}$	$\mu g.L^{-1}$	masl	$mS.cm^{-1}$	^0C	$mg.L^{-1}$	
mean	0.12	36.03	1.79	2.39	14.66	10.11	7.88
SD	0.10	55.85	3.03	2.01	4.79	1.67	0.36
Median	0.09	20.50	1.82	1.80	15.50	10.00	7.90
Range	0.03-0.60	1.40-360	0.89-2.78	0.29-10.4	4.50-22.2	6.98-16.10	7.00-9.00
n	48	76	1453	49	84	79	51

In order to understand the relative contributions of lake level and EC to the sedimentary release of bio-available P, the correlation between these factors and chl-*a* was

investigated. Data for lake levels, EC and chl-*a*, was not normally distributed and could not be transformed. Hence a non-parametric test of correlation, the Spearman's Rank-Order correlation was used, and the results of these analyses are presented in Table 6.2. The approach to this statistical analysis is the same as that discussed in Section 5.4.3.1.

Table 6.2 The effect of the change in lake opening regime on Spearman's rank-order correlations for chl-*a*, lake level and EC data, from long term monitoring data collected by ECan. r_s is the Spearman's rank-order coefficient. Lake level (LL) and EC data were transformed to 4 month moving averages, while chl-*a* was transformed to 4 month moving averages from data with peaks >50 $\mu g.L^{-1}$ removed.

	Pre-change			**Post-change**			**Entire period**		
	Mar 1995- Dec 2009			**Jan 2010- Oct 2014**			**Mar 1995 – Oct 2014**		
	EC vs chl-*a*	**LL vs chl-*a***	**LL vs EC**	**EC vs chl-*a***	**LL vs chl-*a***	**LL vs EC**	**EC vs chl-*a***	**LL vs chl-*a***	**LL vs EC**
r_s	0.50	-0.28	-0.31	0.41	-0.28	-0.17	0.57	-0.313	-0.362
p	<0.001	<0.001	<0.001	<0.01	0.133	0.28	<0.001	<0.001	<0.001

Over the entire period of long term data collection (1995- 2014), EC had a significant, strongly positive correlation to chl-*a* concentrations in the lake, and explained nearly twice as much variability as lake level, which had a significant, negative correlation with chl-*a*. EC and lake level also displayed a significant negative correlation. These various correlations are similar for the time period prior to the change in opening regime and remained significant. After the change in opening regime the correlation between lake level and chl-*a*, and between level and EC are no longer statistically significant. EC continues to display a significant, but lower, positive correlation with chl-*a*.

The improvements in water quality in Wairewa, following the change in opening regime in late 2009, provide an example of an already successful intervention which may have the potential to provide further improvements. The evidence indicated that the documented improvements were likely due to the reduction of background salinity in the lake. Observations outlined in Chapter 5 also indicated that reducing the frequency of major changes in salinity may also prove beneficial. A weir has been suggested across the northern end of the southern 'neck' of the lake. Such a weir may allow a more consistent lake level and allow more control over the sea water incursions associated with lake openings and beach overtopping events. Such control over salinity should decrease SO_4 related P release, increase the P binding potential of the sediments and reduce density

related stratification. If the lake was kept consistently higher, this may also have the effect of decreasing resuspension into high pH waters.

Other physical methods

Another physical method used in the control of P control in lake systems is sediment removal. Successful lake remediation using such techniques has been reported. Lake Trummen in Sweden experienced a 90% reduction in water column TP concentrations, and a dramatic decrease in blue-green algae biomass after the removal of lake sediments to the depth of 1 m. Improvements have been long-term and benthic communities recovered rapidly (Cooke et al, 2005). In a comparative study, the dredging of the Danish Lake Brabrand appeared to speed up the recovery of the lake following a reduction of external P loading, relative to Lake Søbygard which was not dredged (Søndergaard, 2007). However significant issues arise with dredging including cost, in-lake effects on biological communities and disposal of sediment (Cooke et al, 2005). In Wairewa the dredging of sediment to 5 cm depth would require removal and disposal of 365 000 tonnes of sediment (wet weight) and would remove around 106 tonnes of P, 20% of the TP pool in the top 25 cm. More importantly around 52 tonnes of this would be P from the 'mobile P' pool (NH_4Cl-P + BD-P + NaOH-rP + Org-P). This would remove 30 % of the mobile P from the top 25cm. Dredging to 10 cm depth would remove 750 000 tonnes of sediment and 91 tonnes of 'mobile P', 50% of the mobile-P pool in the top 25 cm. However the continuing upward flux of P is, over time, likely to reestablish the P enriched, surface layer in the lake sediments.

6.3.2.2 Chemical treatments

Various methods exist which aim to immobilise P within the sediment. The oxygenation of bottom waters has been used in a number of lakes around the world, however results are mixed. While oxygen levels are generally increased, the effect on P release is more variable (Cooke et al, 2005), and Gachter and Muller (2003) reported that 15 years of hypolimnetic oxygenation had not decreased P release from the sediments of Lake Sempach in Switzerland. Certainly in the case of Wairewa, the size of the lake as well as the spatial and temporal variability in anoxic conditions, is likely to render mechanical oxygenation of the lake bottom water impractical.

A number of chemical addition methods have been utilised, which aim to increase the binding potential in lake sediments. $Ca(NO_3)_2$ has been added to lake sediments in combination with $FeCl_3$ and $CaCO_3$, to increase P binding via decreased Fe reduction, and increase the decomposition rate of organic material via denitrification. The $FeCl_3$ increases Fe binding of P, while the $Ca(NO_3)$ increases redox potential, and the $CaCO_3$ buffers pH. This treatment may also increase the Fe binding potential of the sediment by decreasing the production of sulphides (due to decreased SO_4 reduction), and hence decreasing the immobilisation of Fe at depth. This method is not in widespread use but has been proposed for use in Lake Onondaga in New York (Effler and Matthews, 2008), and has been trialled successfully in Lake Lyng in Denmark where significant decreases in hypolimnetic P concentrations were recorded during years of nitrate addition (Søndergaard, 2007).

Other methods include the addition of P inactivation agents which aim to 'cap' the sediment and block the release of P during anoxic events in the lake bottom water. Such methods may be passive, which physically block diffusion of PO_4^{-3} from the underlying sediments, or active, which aim to increase P binding (Hickey and Gibbs, 2009). Passive methods are likely to be impractical in a lake as large and windy as Wairewa. Amongst active methods, alum ($Al_2(SO_4)_3$), is possibly the most commonly used P inactivation agent. At $6 < pH < 8$, alum produces a precipitate of $Al(OH)_3$ which has high P sorption characteristics and is stable in anoxic conditions, thus decreasing P release from the sediments during periods of low bottom water oxygen concentrations (Cooke et al, 2005). This has been used successfully in various lake systems. A trial in Lake Sonderby in Denmark, saw the lake-wide addition of alum in 2001. Average summer TP concentrations declined from 1.28 and 1.3 $mg.L^{-1}$ to 0.09 and 0.13 $mg.L^{-1}$, in the two pre- and post-treatment years respectively (Reitzel et al, 2005). However, significant issues may arise from such additions, including Al^{+3} toxicity at $pH < 5.5$ (Reitzel et al, 2003). The addition of the acidic sulphate salt may result in a pH low enough for this toxicity to be problematic, and hence the pH buffering capacity of the lake system is important. Wairewa has a low alkalinity ($Ca < 6$ $mg.L^{-1}$) and any high addition of alum would require simultaneous addition of a buffering agent. Adding SO_4 to the lake system may also increase long term immobilisation of Fe in the sediment. In addition continual sediment resuspension may cause disruption and redistribution of the $Al(OH)_3$ floc, and the use of such redox insensitive binding agents does not solve P release associated with

high pH. Other inactivation agents such as modified zeolites or Phoslock™, a La modified bentonite clay, may address some of these issues but cultural sensitivities to the addition of chemical agents to Wairewa may also be significant.

6.3.2.3 Biological methods

The macrophytes in Wairewa produce low-oxygen, stratified conditions, increase pH, and provide a significant source of organic material to the sediment. Hence control of the macrophyte beds may seem to provide an obvious mechanism by which to control internal P release in Wairewa. Such control of macrophyte beds was suggested by James et al (2002) for a eutrophic lake in Wisconsin as a way of removing P in macrophyte biomass and reducing pH. Macrophyte control is also used where species reach nuisance levels. However macrophytes also have many beneficial attributes in lake systems and are seen as key to the maintenance of a clear water state (Sondergaard, 2007), providing biological structure and habitat, and reducing sediment resuspension (Cooke et al, 2005). In the absence of a significant legacy pool of sedimentary P, macrophytes would be beneficial, however in Wairewa they create self-limiting conditions by facilitating significant P release. Hence control of macrophytes in Wairewa may have some benefits, however a much broader understanding of their role in the lake, other than just the biogeochemical impact on P release, would be required.

Biological control of trophic webs has also been used to control eutrophication in lake systems. Such methods include manipulation of fish species to remove zooplanktivorous species and thus increase zooplankton grazing of phytoplankton (Søndergaard, 2007). Such control mechanisms are beyond the scope of this biogeochemical focussed research.

6.3.3 Conclusions

Any attempt to improve water quality in Wairewa must begin with the control of external P loading. The export of P from the catchment, predominantly in particulate associated form during flood events in the Okana sub-catchment is the ultimate source of P in the lake system. Attempts to control internal loading without controlling the flux of P from the catchment are doomed to failure. However if the external P load is significantly reduced, the legacy of decades of high P loading is likely to result in a delayed water quality response due to internal loading from the sedimentary P reservoir. This is likely to be particularly pronounced in an ICOLL such as Wairewa due to the high P retention

resulting from limited lake openings. Hence, a long time frame (decades) for recovery should be accepted and/or the control of internal loading must be attempted.

A range of interventions aimed at the control of internal P loading, have been suggested and trialled in lake systems around the world. Each method has potential benefits and shortcomings which are often lake specific. Hence a program of assessing Wairewa's suitability for the various methods is required. Hickey and Gibbs (2009) provide a useful decision framework for some of these methods and the research presented in this study provides an understanding of the mechanisms of P binding and release on which to base such decision making. This research indicates that control of salinity in the lake shows particular promise and is likely to have already had significant positive effects on P release in the lake. Methods used in the control of salinity would have the likely added benefit of the maintenance of deeper lake levels, which may decrease resuspension. Sediment removal has the potential to significantly reduce the sedimentary P reservoir and thus speed up the lake response to reductions in external loading. The deepening of the lake will also decrease resuspension, but such dredging is likely to be expensive and presents issues with the disposal of large amounts of sediment. Sediment capping with P inactivation agents may be effective but would require extensive trials to assess their efficacy, longevity and ecological impact in the Wairewa environment.

Chapter 7: Conclusions

7.1 P dynamics in Lake Wairewa

The understanding of P loading dynamics is of critical importance in the management of of shallow, coastal lake systems which often have poor water quality. ICOLL's in particular are likely to have low flushing rates and hence retention of the external P load is typically high. This provides a legacy reservoir of P in the lake sediments, which is then available for internal loading processes that may trigger and sustain high rates of phytoplankton productivity. This research has quantified the external P flux to eutrophic Te Roto o Wairewa/Lake Forsyth, and identified the key P binding and release mechanisms occurring in the lake sediments, as well as the environmental conditions controlling these mechanisms. The research provides critical insights for the management of water quality issues in Wairewa, and has important implications for understanding P dynamics and eutrophication management in other ICOLL systems. A summary model of the P dynamics in Wairewa is presented in Figure 7.1.

7.1.1 The mass-balance P budget

A mass-balance P budget was established for the lake, allowing the P flux from the catchment to the lake to be calculated, as well as quantification of areal loading rates and a P retention coefficient for the lake. The external load of P to the lake was mainly associated with flood-borne particulate material, and low frequency, large flood events carried the vast majority of P to the lake. Significant differences in calculated catchment P export rates in the various sub-catchments enabled the identification of critical source areas.

The high P retention (R_P = 0.7) in the lake has resulted in a very large legacy reservoir of P in the sediments. The high rates of sediment resuspension, as well the temporal and spatial variability of environmental conditions leading to P release, make quantification of the annual internal P load problematic. However mass balance calculations indicated that the flux of P from the sediments is substantial and exceeded the external P load during low flow summer months. Increases in [TP] observed during algal bloom events could only be explained by the flux of PO_4^{-3} from the sediment to the lake water column.

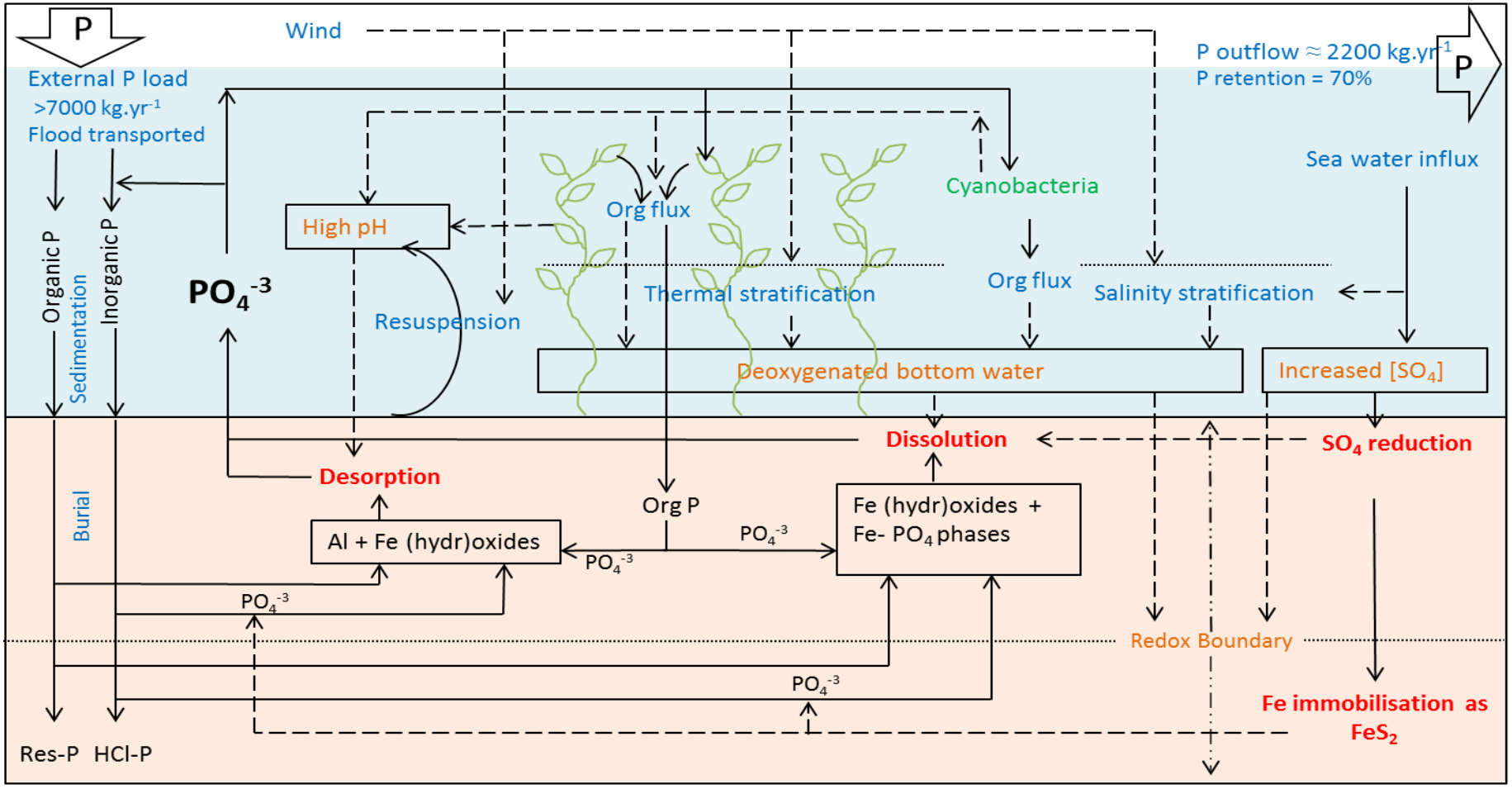

Figure 7.1 Key mechanisms and processes affecting P dynamics in Wairewa. Text colours indicate the following; Black = P chemical species or an important mineral phase, Blue = physical process, Red = geochemical process, Orange = geochemical condition, Green = biological P sink/source. Line types indicate; Solid line = transfer/transport, Dashed line = an effect, Dotted line = Boundary or condition threshold, Dash-dot line = mobility of redox boundary. Macrophyte beds are indicated by the green plant symbols.

7.1.2 Factors controlling P binding in the sediment

Factors controlling P fractionation, binding and mobility in the sediment reservoir were, identified, based on chemical sequential extractions, pore water chemistry and geochemical modelling. The binding of P in the Wairewa sediments is complex and dynamic. The flux of organic matter to the sediment, creates a large pool of organic P in the surface sediment, especially during autumn and winter. Subsequent decomposition results in the mineralisation of P to various inorganic P fractions which also accumulate due to the sedimentation of inorganic P from the water column. Some of these fractions are mobile, (loosely bound-P, P associated with Fe and Al (hydr)oxides, and the labile organic P fraction), and comprise a significant portion (up to 60 %) of the sedimentary P pool. In contrast the P retained in the more refractory organic fraction and that which is associated with detrital apatite are relatively immobile within the sediment profile and are progressively buried. Burial of the mobile P fractions, continued decomposition of organic material and the effect of the more reducing conditions occurring below the surface sediments, results in the release of bound P and an upward flux of PO_4^{-3}. This is then immobilised in the more oxic sediments near the sediment surface, where PO_4^{-3} adsorbs to phases such as Fe and Al (hydr)oxides.

Significant seasonal migration of the redox boundary in the sediment pile was observed, with more reduced sediments at the sediment surface during winter, and a more oxidised upper sediment profile during the early summer growing season (prior to algal bloom formation). This leads to an increased pool of redox sensitive sediment-bound P in the upper sediments, which is available for release when the redox boundary migrates upward during periods of increased organic decomposition.

7.1.3 Factors promoting P release to the water column

The high reactive Fe:P ratio in the surface sediments means that P release is unlikely under oxic, circum-neutral conditions in the water column, even during sediment resuspension. A possible exception to this is during periods when the salinity in the OLW is significantly lower than that in the sediment pore water, following a ‘freshening’ event in the lake. Salinity may be a significant driver of P dynamics in the lake with elevated salinity expected to enhance P release through competitive adsorption, increased reductive dissolution of Fe (hydr)oxides, and increased Fe immobilisation by FeS_2

precipitation in the reduced sediments. Prolonged high salinity levels in the lake were associated with elevated primary productivity and, reduced salinity explained much of the improvement in water quality parameters observed in ECan monitoring data, following the change in the lake opening regime

Redox- and pH-related release rates were sufficient to explain observed increases in [TP] associated with algal bloom events.

Redox-related P release occurred when DO is completely consumed and E_h < 100mV. Under even more reducing conditions, release rates were significantly increased. Periods of low [DO] in the lake bottom waters were generally short-lived and spatially discrete. They were associated with low wind periods leading to thermal stratification in macrophyte beds, and with density stratification driven by salinity changes associated with flood/lake opening events. Some such events coincided with algal bloom development. Low [DO] also occurred during periods of high flux of organic material to the lake sediments, from algal biomass and/or senescing macrophytes.

Periods of macrophyte and/or algal growth resulted in pH > 9 in the lake water column, for prolonged periods of time, and pH > 10 periodically. Experimentally determined pH-related P release rates were significant at pH > 9, and appeared to be key in producing the north-south gradients in [TSP] observed during summer months. P release rates were greatly increased during sediment resuspension into a high pH water-column, but increased primary productivity may be mitigated by decreased light penetration through the water column.

7.2 Implications for lake management

The management of P loading in Wairewa must begin with the reduction of the external P load, as this is the ultimate source of P in the lake system. A > 50% reduction in external P load is required to meet areal loading guidelines, which have been suggested for New Zealand ICOLL systems (e.g. Wriggle, 2012). To achieve this, management interventions will need to target the P associated with particulate material transported during large flood events, particularly from the Okana sub-catchment.

Lake responses to a reduction in external P load are likely to be very slow due to the large legacy reservoir of P in the lake sediments. The flux of P from this reservoir to the lake water column is likely to support primary productivity in the lake for many years. The

change in lake opening regime since late 2009, has resulted in water quality improvements which may be due to the control of salinity fluctuations, the overall lower salinity in the lake, and the decreasing sediment resuspension into a high pH water column resulting from higher lake levels. Further control of salinity and lake level may offer additional water quality improvements. Sediment dredging, the addition of P inactivation agents to the lake sediment, and biological control methods are all possible management interventions, but would all require further work to determine their potential consequences, as well as their efficacy.

7.3 Recommendations for future research

The P budget provided insight into which sub-catchments experienced the highest P export rates, however the source of this P was not investigated. Further research into this could refine the critical source areas and provide better guidance for targeted catchment management interventions. The flow of groundwater in the catchment is poorly resolved. Direct measurement of ground water movements and P concentrations, particularly across the gravel beach barrier would help refine the lake P budget as would research into the effect of bird movements, excretion and feeding habits.

This work did not specifically investigate the relative roles of nutrients and light in the limitation of primary productivity. Work aimed at understanding such limitation and probable temporal changes in limitation would be valuable.

The EPC_0 experiments indicated significant differences in the P binding capacity of various lake sediments, however it was uncertain if these were due to spatial or temporal variation in sediment sampling. Experiments conducted on sediments collected at the same time and from more sites around the lake, may provide clarification. More detailed work on the geochemical effects of salinity change, may also shed more light on how salinity affects P binding capacity.

Various mechanisms of P release that were not investigated in this research, but have been reported in the literature as having an effect on sediment-bound P, could be examined. Andersen (1982), amongst others (e.g. Xie et al 2003), reported that elevated levels of NO_3-N supress P release from lake sediments by buffering the redox potential in the surface sediments. The direct release of P from organic decomposition has been identified as significant by a number of authors (e.g. Hupfer and Lewandowski, 2008;

Ahlgren et al, 2011), while bioturbation and gas ebulition resulting from organic decomposition in the sediments, have both been implicated in sedimentary P release (Søndergaard, 2007). The potential effect of bioturbation was evident in the number of chironomids and oligcheates observed in the Wairewa sediments, as well as in the oxidation 'halos' around burrows in the sediment.

P release rates determined in this research were all derived experimentally in the laboratory. The applicability of these to the wider lake setting is unproven. Better resolution of the release of bioavailable P, particularly during sediment resuspension into high-pH OLW, would be invaluable for the quantification of an annual internal P load in this lake. This would require understanding the interactions between PO_4^{-3} release, phytoplankton productivity and light.

During the course of this research it was noted the [TSP] decreased at the northern end of the lake during summer producing a consistent north-south gradient that equilibrated during autumn and winter. These trends occurred over two summers, but the causes were not sufficiently resolved to present in the main work of this thesis. It appeared that the northern TSP decrease occurred predominantly in the NaOH-rP fraction, and may have been due to pH-related P release in the macrophytes at the north end of the lake. An increase in organic matter and the external load of P from the main lake tributary, may then 'top up' the TSP over winter. Redox changes in the macrophytes, salinity gradients, and the concentration of algal populations due to the prevailing NE wind, may also have an influence. Further work is required to determine the mechanisms behind this phenomenon.

The role of the macrophyte beds was highlighted in this research. Further insight could be gained from a more detailed survey of plant species distribution, areal extent and ecosystem impacts of the macrophytes in Wairewa. This, coupled with the resuspension and pH research, may also provide further understanding of the summer north-south gradients in [TSP] discussed above.

A lower salinity tolerance of 2 PSU has been suggested for *Nodularia spumigens* (Rakko and Seppala, 2014), however blooms of this species have occurred in Wairewa at salinities of around 0.5 ppt (≈ 0.5 PSU). In addition blooms of *Anabaena* (supposedly less tolerant of salinity) have occurred at higher salinities than those at which *Nodularia*

blooms have been observed. Work on understanding the population dynamics and environmental tolerances of these species in Wairewa would be useful.

Finally, ecological modelling of the lake system would provide valuable insight into the interplay of the various mechanisms affecting P dynamics, as well as allowing modelling of the effects of management interventions. Such modelling may shed further light on the hydrodynamics of salinity stratification and lake mixing processes, and would benefit from more detailed time series information on sea water inflow and density stratification.

References

Abell, J.M., Ozkundakci, D., Hamilton, D.P., Miller, S.D. 2011. Relationships Between Land Use and Nitrogen and Phosphorous in New Zealand Lakes. *Marine And Freshwater Research, 62, 162–175*

Abell, J.M., Ozkundakci, D., Hamilton, D.P. 2010. Nitrogen and Phosphorus Limitation of Phytoplankton Growth in New Zealand Lakes: Implications for Eutrophication Control. *Ecosystems 13(7). 966-977.*

Ahlgren, J., Reitzel, K., De Brabandere, H., Gogoll, A., Rydin, E. 2011. Release of Organic P Forms from Lake Sediments. *Water Research 45. 565-572.*

Ahmad, Z., Faridulah, El-Sharkawi, H., Irshad, M., Honna, T., Yamamoto, S., Al-Busaidi, A.S. 2008. Changes in Water-Extractability of Soil Inorganic Phosphate Induced by Chloride and Sulfate Salts. *Environmental Science and Pollution Research 15(1). 23-26.*

Aigars, J. 2001. Seasonal Variations in Phosphorus Species in the Surface Sediments of the Gulf of Riga, Baltic Sea. *Chemosphere 45. 827-834.*

Andersen, J.M. 1982. Effect of Nitrate Concentration in Lake Water on Phosphate Release from the Sediment. *Water Research 16. 1119-1126.*

Andersen, D.T., Sumner, D.Y., Hawes, I., Webster-Brown, J., McKay, C.P. 2011. Discovery of Large Conical Stromatolites in Lake Untersee, Antarctica. *Geobiology 9. 280-293.*

Anderson, G. 1976. An Ignition Method for Determination of Total Phosphorus in Lake Sediments. *Water Research 10. 329-331.*

Apello, C.A.J., Postma, D. 1999. A Consistent Model for Surface Complexation on Birnessite (-MnO2) and its Application to a Column Experiment. *Geochimica et Cosmochimica Acta 63(19/20) 3039-3048.*

APHA 4500-P. In Standard Methods for the Examination of Water and Wastewater. 21st Ed. 2005. Eaton, A.D.C., Rice, E.W., Greenberg, A.E. *American Public Health Association; American Water Works Association; Water Environment Federation: Washington DC, USA.*

ARS, 2012. Agricultural Research Service (downloaded from http://www.ars.usda.gov /Research/docs.htm?docid=10621, May 2014).

Asselman, N.E.M., 2000. Fitting and Interpretation of Sediment Rating Curves. *Journal of Hydrology 234. 228-248.*

Bailey, E., Owens, M., Boynton, W., Cornwall, J. 2006. Sediment Phosphorus Flux: pH Interaction in the Tidal Freshwater Potomac River Estuary. Interstate Commission on the Potomac River Basin. *UMCES report TS-505-08-CBL, 1-91.*

Barber, T.M. 2002. Phosphate Adsorption by Mixed and Reduced Iron Phases in Static and Dynamic Systems. *Unpublished MSc Thesis, Stanford University, U.S.A.*

Barko, J.W., James, W.F. 1998. Effects of Submerged Aquatic Macrophytes on Nutrient Dynamics, Sedimentation and Resuspension. *In;* The Structuring Role of Submerged Macrophytes in Lakes. Ed's; Jeppesen, E., Søndergaard, M., Søndergaard, M., Christoffersen, K. *Springer, Tokyo.*

Barko, J.W., Smart, R.M. 1980. Mobilization of Sediment Phosphorus by Submersed Freshwater Macrophytes. *Freshwater Biology 10. 229-238.*

Bengtsson, A., Sjoberg, S. 2009. Surface Complexation and Proton-promoted Dissolution in Aqueous Apatite Systems. *Pure and Applied Chemistry 81(9) 1569-1584.*

Berg, U., Neumann, T., Donnert, D., Nuesch, R., Stuben, D. 2004. Sediment Capping in Eutrophic Lakes- Efficiency of Undisturbed Barriers to Immobilise Phosphorus. *Applied Geochemistry 19 (11). 1759-1771.*

Bostrom, B., Persson, G., Broberg, B. 1988. Bioavailability of Different Phosphorus Forms in Freshwater Systems. *Hydrobiologia 170. 133-155*

Burger, D.F. 2006. Dynamics of Internal Nutrient Loading in a Eutrophic, Polymictic Lake (Lake Rotorua, New Zealand) *Unpublished Doctorate Thesis, University of Waikato, New Zealand.*

Burger, D.F., Hamilton, D.P., Hall, J.A., Ryan, E.F. 2007. Phytonplankton Nutrient Limitation in a Polymictic Eutrophic Lake: Community Versus Species-Specific Responses. *Fundamental and Applied Limnology Archiv fur Hydrobiologie 169(1). 57-68.*

Burger, D.F., Hamilton, D.P., Pilditch, C.A. Gibbs, M.M. 2007. Benthic Nutrient Fluxes in a Eutrophic, Polymictic Lake. *Hydrobiologia 584. 13-25.*

Burns, N., Bryers, G., Bowman, E. 2000. Protocol for Monitoring Trophic Levels in New Zealand Lakes and Reservoirs. *Ministry for the Environment. Wellington, New Zealand. Available from; http://www.mfe.govt.nz/publications/fresh-water-environmental-reporting/protocol-monitoring-trophic-levels-new-zealand.*

Caraco, N.F., Cole, J.J., Likens, G.E. 1990. A Comparison of Phosphorus Immobilization in Sediments of Freshwater and Coastal Marine Sediments. *Biogeochemistry 9. 277-290.*

Caraco, N.F., Cole, J.J., Likens, G.E. 1991. Phosphorus Release from Anoxic Sediments: Lakes that Break the Rules. *Verhandlungen des Internationalen Verein Limnologie 24. 2985-2988.*

Carpenter, S.R., Caraco, N.F., Correll, D.L., Howarth, R.W., Sharpley, A.N., Smith, V.H. 1998. Nonpoint Pollution of Surface Waters with Phosphorous and Nitrogen Reviewed work. *Ecological Applications 8 (3) 559-568*

Cassidy, R., Jordan, P. 2011. Limitations of Instantaneous Water Quality Sampling in Surface-Water Catchments: Comparison with Near-Continuous Phosphorus Time Series Data. *Journal of Hydrology, 405. 182-193.*

Chang, H., Matijevic, E. 1983. Interactions of Metal Hydrous Oxides with Chelating Agents: III. Adsorption on Spherical Colloidal Hematite Particles. *Journal of Colloid and Interface Science 92(2). 479-488.*

Charlton, S.R., Macklin, C.L., Parkhurst, D.L. 1997. PHREEQCI- A Graphical User Interface for the Geochemical Computer Model PHREEQC. *United States Geological Survey, Water Resources Investigations Report 97-4222. Lakewood Colorado.*

Chen, M., Ma, L.Q. 1998. Comparison of Four USEPA Digestion Methods for Trace Metal Analysis Using Certified and Florida Soils. *Journal of Environmental Quality. 27(6). 1294-1300.*

Chen, M., Ye, T., Krumholz, L.R., Jiang, H. 2014. Temperature and Cyanobacterial Bloom Biomass Influence Phosphorus Cycling in Eutrophic Lake Sediments. *PLoS ONE 9(3). 1-10.*

Christophoridis, C., Fytianos, K. 2006. Conditions Affecting the Release of Phosphorus from Surface Lake Sediments. *Journal of Environmental Quality. 35. 1181-1192.*

Cooke,G.D., Welch, E.B., Peterson, S.A., Nichols, S.A. 2005. Restoration and Management of Lakes and Reservoirs. 3rd Ed. *Taylor and Francis Group, Boca Raton, Florida.*

Condron, L.M., Newman, S. 2011. Revisiting the Fundamentals of Phosphorus Fractionation of Sediments and Soils. *Journal of Soils and Sediment 11.830-840.*

Crowe, S.A., Roberts, J.A., Weisner, C.G., Fowle, D.A. 2006. Alteration of Iron-Rich Lacustrine Sediments by Dissimilatory Iron-Reducing Bacteria. *Geobiology 5(1). 63-75*

Cyr, H., McCabe, S.K., Nurnberg, G.K. 2009. Phosphorus Sorption Experiments and the Potential for Internal Phosphorus Loading in Littoral Areas of a Stratified Lake. *Water Research 43. 1654-1666*

Daniel, T.C., Sharpley, A.N., Lemunyon, J.L. 1998. Agricultural Phosphorus and Eutrophication: A Symposium Overview. *Journal of Environmental Quality. 27(2). 251-257*

Danz, M.E., Corsi, S.R., Graczyk, D.J., Bannerman, R.t. 2010. Characterisation of Suspended Solids and Total Phosphorus Loadings from Small Watersheds in Wisconsin. *USGS Scientific Investigations Report 2010-5039.*

Das, B.K. 2008. Lakes: Water and Sediment Geochemistry. *Satish Serial Publishing House. Delhi, India.*

Das, S.K., Routh, J., Roychoudhury, A.N., Klump, J.V., Ranjan, R.K. 2009. Phosphorus Dynamics in Shallow Eutrophic Lakes: An Example from Zeekoevlei, South Africa. *Hydrobiologia 619(1). 55-66.*

Degens, B.P., Donohue, R.D., 2002. Sampling Mass Loads in Rivers- A Review of Approaches for Identifying, Evaluating and Minimising Estimation Errors. *Water and Rivers Commission, Water Resources Technical Report WRT 25. Government of Western Australia.*

Dehvari, A. 2014. Estimation of Surface Runoff and Sediment Yield using WEPP Model in Southern Ontarion, Canada. *International Journal of Agricultural and Crop Sciences. 7 (11) 876-889.*

De Vicente, I., Huang, P., Andersen, F.O., Jensen, H.S. 2008. Phosphate Adsorption by Fresh and Aged Aluminium Hydroxide. Consequences for Lake Restoration. *Environmental Science and Technology 42. 6650-6655.*

Diffuse Sources/NIWA. 2012. Waituna Catchment Loads. *Unpublished report prepared for Environment Southland, New Zealand.*

Dillon, P.J. 1975. The Phosphorus Budget of Cameron Lake, Ontario: The Importance of Flushing Rate to the Degree of Eutrophy of Lakes. *Limnology and Oceanography, 20(1). 28-39.*

Dodds, W.K., Bouska, W.W., Eitzmann, J.L., Pilger, T.J., Pitts, K.L., Riley, A.J., Schlosser,J.T., Thornbrugh, D.J. 2009. Eutrophication of US Freshwaters: Analysis of Potential Economic Damages. *Environmental Science and Technology 43(1). 12-19.*

Doody, D.G., Archbold, M., Foy, R.H., Flynn, R. 2012. Approaches to the Implementation of the Water Framework Directive: Targeting Mitigation Measures at Critical Source Areas of Diffuse Phosphorus in Irish Catchments. *Journal of Environmental Management 93. 225-234.*

Downs, T.M., Schallenberg, M., Burns, C.W. 2008. Responses of Lake Phytoplankton to Micronutrient Enrichment: A Study in Two New Zealand Lakes and an Analysis of Published Data. *Aquatic Science70. 347-360.*

Drake, D.C., Kelly, D., Schallenberg, M., Ponder-Sutton, A., Enright, M. 2009. Shallow Coastal Lakes in New Zealand: Assessing Indicators Of Ecological Integrity and their Relationships to Broad-Scale Human Pressures. NIWAClient Report CHC2009-004, Christchurch: 1–79

Drake, D.C., Kelly, D., Schallenberg, M. 2011. Shallow Coastal Lakes in New Zealand: Current Conditions, Catchment Scale Human Disturbance, and Determination of Ecological Integrity. *Hydrobiologia 658. 87-101.*

Duzgoran-Aydin, N.S., Avula, B., Willett, K.L., Khna, I.A. 2011. Determination of total and partially extractable solid-bound element concentration using collision/reaction cell inductively coupled plasma-mass spectrometry and their significance in environmental studies. *Environmental Monitoring and Assessment. 172(1) 51-66.*

Dzombak, D.A., Morel, F.M.M. 1990. Surface Complexation Modelling: Hydrous Ferric Oxide. *John Wiley & Sons Inc. U.S.A.*

EBOP, 2007. Proposed Lakes Rotorua and Rotoiti Action Plan. *Environment Bay of Plenty. Environmental Publication. 2007/11.*

EC, 2000. Directive Establishing a Framework for Community Action in the Field of Water Policy. *Water Framework Directive 2000/60/EC, European Commission.*

ECan. 2013. Resource Consent Application. Artificial Opening of Wairewa/Lake Forsyth. *downloaded from; http://ecan.govt.nz/publications/Consent%20Notifications/wairewa-opening-application.pdf, on 1 February 2014.*

Effler, S.W., Matthews, D.A. 2008. Implications of Redox Processes for the Rehabilitation of an Urban Lake, Onondaga Lake, New York. *Lake and Reservoir Management. 24(2). 122-138.*

Einsele, W. 1938. Uber Chemische und Kolloidchemische Vorgange in Eisen-Phosphat-Systemen unter Limnischen and Limnogeologischen Gesichtpunkten. Archiv fur Hydrobiologie 33. 361-387

Ekholm, P., Lehtoranta, J. 2012. Does Control of Soil Erosion Inhibit Aquatic Eutrophication. *Journal of Environmental Management 93. 140-146.*

Enyard.A. 1994. Relationship of Well- and Poorly Crystallized Iron Oxides with Phosphate and Water Retention by Soils, A Review. *Mineralogy and Petrology Acta 36. 343-350*

Fagel, N., Alleman, L.Y., Granina, L., Hatert, F., Thamo-Bozso, E., Cloots, R., Andre, L. 2005. Vivianite Formation and Distribution in Lake Baikal Sediments. *Global and Planetary Change 46(1-4) 315-336.*

Fangueiro, D., Bermond, A., Santos, E., Carapuca, H., Duarte, A. 2002. Heavy Metal Mobility Assessment in Sediments Based on a Kinetic Approach to EDTA Extraction: Search for Optimal Experimental Conditions. *Analytica Chimica Acta 459(2). 245-256.*

Fox, L.E., Sager, S.L., Wofsy, S.C. 1986. The Chemical Control of Soluble Phosphorus in the Amazon Estuary. *Geochimica et Cosmochimica Acta 50(5) 783-794.*

Fischer, H.B., List, E.J., Koh, R.C.Y., Imberger, J., Brook, N.A., 1979. Mixing in Inland and Coastal Lakes. *Academic Press Inc, New York. 483pp.*

Friedl, G., Wehrli, B., Manceau, A. 1997. Solid Phases in the Cycling of Manganese in Eutrophic Lakes: New Insights from EXAFS Spectroscopy. *Geochimica et Cosmochimica Acta 61(2). 275-290.*

Froelich, P.N. 1988. Kinetic Control of Dissolved Phosphate in Natural Rivers and Estuaries: A Primer on the Phosphate Buffer Mechanism. *Limnology and Oceanography 33(4-2)649-668*

Gachter, R., Muller, B. 2003. Why the Phosphorus Retention of Lakes Does Not Necessarily Depend on Oxygen Supply to Their Sediment Surface. *Limnology and Oceanography 48(2)929-933.*

Gao, L., Zhou, J.M., Yang, H., Chen, J. 2005. Phosphorus Fractions in Sediment Profiles and Their Potential Contributions to Eutrophication in Dianchi Lake. *Environmental Geology 48. 835-844.*

Gao, Y., Cornwell, J.C., Stoecker, D.K. Owens, M.S. 2012. Effects of Cyanobacterial-Driven pH Increases on Sediment Nutrient Fluxes and Coupled Nitrification-Denitrification in a Shallow Water Estuary. *Biogeosciences 9. 2679-2710*

Gardolinski, P.C.F.C., Worsfold, P.J., McKelvie, I.D. 2004. Seawater Induced Release and Transformation of Organic and Inorganic Phosphorus from River Sediments. *Water Research 38. 688-692.*

Gburek, W.J., Sharpley, A.N., Heathwaite, L., Folmar, G.J. 2000. Phosphorus Management at a Watershed Scale: A Modification of the Phosphorus Index. *Journal of Environmental Quality. 29.*

Gerard, F. 2015. Clay Minerals. Iron/Aluminium Oxides and their Contribution to Phosphate Sorption in Soils- A Myth Revisited. *Geoderma 262. 213-226.*

Geurts, J.J.M., Smolders, A.J.P., Banach, A.M., van de Graaf, J.P.M., Roelofs, J.G.M., Lamers, L.P.M. 2010. The Interaction Between Decomposition, Net N and P Mineralization and their Mobilization to the Surface Water in Fens. *Water Research.44. 3487-3495.*

Gibbs, M. 2011. Lake Horowhenua Review: Assessment of Opportunities to Address Water Quality Issues in Lake Horowhenua. *National Institute of Water and Atmospheric Research Client Report No HAM2011-046. Hamilton New Zealand*

Gibson, C.E., Wang, G., Foy, R.H., Lennox, S.D. 2001. The Importance of Catchment and Lake Processes in the Phosphorus Budget of a Large Lake. *Chemosphere, 42. 215-220.*

Golterman, H.L. 1988. The Calcium-and Iron Bound Phosphate Phase Diagram. *Hydrobiologia 159. 149-151.*

Gomez, E., Durillon, C., Rofes, G., Picot, B. 1999. Phosphate Adsorption and Release from Sediments of Brackish Lagoons: pH, O_2 and Loading Influence. *Water Research 33(10). 2437-2447.*

Gunnars, A., Blomqvist, S., Johansson, P., Andersson, C. 2002. Formation of Fe(III) Oxyhydroxide Colloids in Freshwater and Brackish Seawater, with Incorporation of Phosphate and Calcium. *Geochimica et Cosmichimica Acta 66. 745-758.*

Hamilton, D.P., Mitchell, S.F. 1997. Wave-induced shear stresses, plant nutrients and chlorophyll in seven shallow lakes. *Freshwater Biology 38(1). 159-168.*

Hammender, K. 2013. Sediment Discharge Estimation for Steep Terrain Catchments with Loess Soil in New Zealand. *Unpublished thesis, University of Natural Resources and Life Science, Vienna, Austria.*

Hawes, I., Safi, K., Webster-Brown, J., Sorrell, B. and Arscott, D. 2011. Summer-winter transitions in Antarctic ponds: II. Biological responses. *Antarctic Science.*23: 243-254.

Hawke, D., Carpenter, P.D., Hunter, K.A. 1989. Competitive Adsorption of Phosphate on Geothite in Marine Electrolytes. *Environmental Science and Technology 23. 187-191.*

Hartzell, J.L., Jordan, T.E. 2012. Shifts in the Relative Availability of Phosphorus and Nitrogen Along Estuarine Salinity Gradients. *Biogeochemistry 107(1). 489-500.*

Heisler, J., Glibert, P.M., Burkholder, J.M., Anderson, D.M., Cochlan, W., Dennison, W.C., Dortch, Q., Gobler, C.J., Heil, C.A., Humphries, E., Lewitus, A., Magnien, R., Marshall, H.G., Sellner, K., Stockwell, D.A., Stoecker, D.K., Suddleson, M. 2008. Eutrophication and Harmful Algal Blooms: A Scientific Consensus. *Harmful Algae 8. 3-13.*

Herb, W.R., Stefan, H.G. 2004. Temperature Stratification and Mixing Dynamics in a Shallow Lake with Submersed Macrophytes. *Lake and Reservior Management 20(4). 296-308.*

Heiri, O., Lotter, A.F., Lemcke, G. 2001. Loss on Ignition as a Method For Estimating Organic and Carbonate Content in Sediments: Reproducibility and Comparability of Results. *Journal of Paleolimnology. 25. 101-110.*

Hickey, C.W., Gibbs, M.M. 2009. Lake Sediment Phosphorus Release-Decision Support and Risk Assessment Framework. *New Zealand Journal of Marine and Freshwater Research.*

Ho, H.H., Swennen, R., Cappuyns, V., Vassilieva, E., Gerven, T.V., Tran, T.V. 2013. Speciation and Mobility of Selected Trace Metals (As, Cu, Mn, Pb and Zn) in Sediment with Depth in Cam River-Mouth, Haiphong, Vietnam. *Aquatic Geochemistry 19. 57-75.*

Horowitz, A.J., Elrick, K.A. 1987. The Relation of Stream Sediment Surface Area, Grain Size and Composition to Trace Element Chemistry. *Applied Geochemistry 2. 437-451.*

Horrell, G. 1992. Lake Ellesmere Water Balance Model: Variable Analysis and Evaluation. *Unpublished Masters Thesis, University of New South Wales.*

Hupfer, M., Lewandowski, J. 2008. Oxygen Controls the Phosphorus Release from Lake Sediments- a Long Lasting Paradigm in Limnology. *Internationals Reviews in Hydrobiology 93(4-5). 415-432.*

Jacoby, J.M., Lynch, D.D., Welch, E.B., Perkins, M.A. 1982. Internal Phosphorus Loading in a Shallow Eutrophic Lake. *Water Research 16. 911-919*

Jalali, M., Moharami, S. 2013. Kinetics of Iron and Manganese Release from Contaminated Calcareous Soils. *Communications in Soil Science and Plant Analysis 44(22) 33650-3380*

James, W.F., Barko, J.W., Eakin, H.L., Sorge, P.W. 2002. Phosphorus Budget and Management Strategies for an Urban Wisconsin Lake. *Lake and Reservoir Management 18(2). 149-163.*

Jarvie, H.P., Sharpley, A.N., Spears, B., Buda, A.R., May, L., Kleinman, P.J.A. 2013. Water Quality Remediation Faces Unprecedented Challenges from "Legacy Phosphorus". *Environmental Science and Technology, 47. 8997-8998.*

Jellyman, D., Cranwell, I. 2007. The Status of Eel Stocks in Wairewa (Lake Forsyth). Ministry of Fisheries. *New Zealand Fisheries Assessment Report 2007/11.*

Jensen, H.S., Andersen, F.O. 1992. Importance of Temperature, Nitrate, and pH for Phosphate Release fromAerobic Sediments of Four Shallow, Eutrophic Lakes. *Limnology and Oceanography 37. 577-589.*

Jensen, H.S., Kristensen, P., Jeppesen, E., Skytthe, A. 1992. Iron:Phosphorus Ration in Surface Sediment as an Indicator of Phosphate Release From Aerobic Sediments in Shallow Lakes. *Hydrobiologia 235/236. 731-743.*

Jeppesen, E., Søndergaard, M., Sortkjaer, O., Mortensen, E., Kristensen, P. 1990. Interactions between phytoplankton, zooplankton and fish in a shallow, hypertrophic lake: a study of phytoplankton collapses in Lake Søbygard, Denmark. *Hydrobiologia, 191. 149-164.*

Jeppesen, E., Søndergaard, M, Jensen, J.P., Havens, K., Anneville, O., Carvalho, L., Coveney, M.F., Deneke, R., Dokulil, M., Foy, B., Gerdeaux, D., Hampton, S.E., Kangur, K., Kohler, J., Korner, S., Lammens, E., Lauridsen, T.L., Manca, M., Miracle, R., Moss, B., Noges, P., Persson, G., Phillips, G., Portielje, R., Romo, S., Schelske, C.L., Straile, D., Tatrai, I., Willen, E., Winder, M. 2005. Lake Responses to Reduced Nutrient Loading- an Analysis of Contemporary Long-Term Data from 35 Case Studies. *Freshwater Biology 50. 1747-1771.*

Johnes, P.J. 2007. Uncertainties in Annual Riverine Phosphorus Load Estimation: Impact of Load Estimation Methodology, Sampling Frequency, Baseflow Index and Catchment Population Density. *Journal of Hydrology 332. 241-258.*

Jones, C., Crowe, S.A., Sturm, A., Leslie, K.L., MacLean, L.C.W., Katsev, S., Henny, C., Fowle, D.A., Canfield, D.E., 2011. Biogeochemistry of Manganese in Ferruginous Lake Matano, Indonesia. *Biogesciences. 9. 2977-2991*

Jordan, T.E., Cornwall, J.C., Boyton, W.R., Anderson, J.T. 2008. Changes in Phosphorus Biogeochemistry Along an Estuarine Salinity Gradient: The Iron Conveyor Belt. *Limnology and Oceanography 53(1). 172-184*

Kangur, M., Puusepp, L., Buhvestova, O., Haldna, M., Kangur, K. 2013. Spatio-Temporal Variability of Surface Sediment Phosphorus Fractions and Water Phosphorus Concentration in Lake Peipsi (Estonia/Russia). *Estonian Journal of Earth Sciences 62(3). 171-180.*

Katsev, S., Tsandev, I., Heureux, I.L., Rancourt, D.G. 2006. Factors Controlling Long-Term Phosphorus Efflux from Lake Sediments: Exploratory Reactive Transport Modelling. *Chemical Geology 234. 127-147.*

Kawashima, M., Tainaka, Y., Hori, T., Koyama, M., Takamatsu, T. 1986. Phosphate Adsorption onto Hydrous Manganese(IV) Oxide in the Presence of Divalent Cations. *Water Research 20(4) 471-475.*

Kelly, D., Shearer, K., Schallenberg, M. 2013. Nutrient Loading to Shallow Coastal Lakes in Southland for Sustaining Ecological Integrity Values. *Cawthron Report No 2375, Prepared for Environment Southland.. http://www.cawthron.org.nz/publication/science-reports/nutrient-loading-shallow-coastal-lakes-southland-sustaining-ecological-integrity-values/*

Kim, L., Choi, E., Stenstrom, M.K. 2003. Sediment Characteristics, Phosphorus Types and Phosphorus Release Rates Between River and Lake Sediments. *Chemosphere 50. 53-61.*

Kinsand, A., Noges, P. 2003. Sediment Phosphorus Release in Phytoplankton dominated versus Macrophyte Dominated Shallow Lakes: Importance of Oxygen Conditions. *Hydrobiologia 506-509. 129-133.*

Kiov, T., Noges, T., Laas, A. 2011. Phosphorus Retention as a Function of External Loading, Hydraulic Turnover Time, Area and Relative Depth in 54 Lakes and Reservoirs. *Hydrobiologia, 660. 105-115.*

Kleeberg, A., Dudal, G.E. 1997. Changes in Extent of Phosphorus Release in a Shallow Lake (Lake Grober Muggelsee, Germany, Berlin) due to Climatic Factors and Load. *Marine Geology 139. 61-75.*

Kopacek, J., Borovec, J., Hejzlar, J., Ulrich, K., Norton, S.A., Amirbahman, A. 2005. Aluminium Controls of Phosphorus Sorption by Lake Sediments. *Environmental Science and Technology 39. 8784-8789.*

Koretsky, C.M., Haas, J., Miller,D., Ndenga, N.T. 2006. Seasonal Variations in Pore Water and Sediment Geochemistry of Littoral Lake Sediments (Asylum Lake, MI, USA). *Geochemical Transactions 7(11)*

Kristensen, P., Sondergaard, M., Jeppesen, E. 1992. Resuspension in a Shallow Eutrophic Lake. *Hydrobiologia 228. 101-109.*

Kumar Das, S., Routh, J., Roychoudhury, A.N., Klump, J.V., Ranjan, R.K. 2009. Phosphorous Dynamics in Shallow Eutrophioc Lakes; An Example from Zeekoevlei, South Africa. *Hydrobiologia 619. 55-66.*

Laflan, J.M., Flanagan, D.C., Engel, B.A. (2004). Soil Erosion and Sediment Yield Prediction Accuracy using WEPP. *Journal of the American Water Resources Association. 40.289-297.*

Larned, J.M. Schallenberg, M, 2006. Constraints on Phytoplankton Production in Lake Ellesmere. *National Institute of Water and Atmospheric Research, Client Report CHC2006-101.*

Le, C., Zha, Y., Li, Y., Sun, D., Lu, H. Yin, B. 2010. Eutrophication of Lake Waters in China: Cost, Causes and Control. *Environmental Management. 45. 662-668.*

Lehtoranta, J., Ekholm, P., Pitkanen, H. 2009. Coastal Eutrophic Thresholds: A Matter of Sediment Microbial Processes. *Ambio 38(6) 303-308.*

Letcher, R.A., Jakeman, A.J., Merritt, W.S., McKee, L.J., Eyre, B.D., Baginska, B., 1999. Review of Techniques to Estimate Catchment Exports. *Environmental Protection Authority, Water Sciences Section, New South Wales.*

Li, W., Pierre-Louis, A., Kwon, K.D., Kubicki, J.D., Strongin,D.R., Phillips, B.L. 2013. Molecular Level Investigations of Phosphate Sorption on Corundum (α-Al_2O_3) by ^{31}P Solid State NMR, ATR-FTIR and Quantum Chemical Calculation. *Geochimica et Cosmochimica Acta 107. 252-266.*

Lijklema, L., Hieltjes, H.M. 1982. A Dynamic Phosphate Budget Model for a Eutrophic Lake. *Hydrobiologia 91. 227-233.*

Lukkari, K., Hartikainen, H., Leivuori, M. 2007. Fractionation of Sediment Phosphorus Revisited. 1: Fractionation Steps and Their Biogeochemical Basis. *Limnology and Oceanography: Methods 5. 433-444.*

Lynn, I. 2005. Lake Wairewa/Lake Forsyth: Potential Sources of Phosphorous to the Lake. *Wairewa Programme Report Series 2005/01.*

Mayer, L.M., Gloss, S.P. 1980. Buffering of Silica and Phosphate in a Turbid River. *Limnology and Oceanography 25(1). 12-22*

Main, M.R., Lavender, R.M., Hayward, S. 2003. The Okana River: Assessment of Water Quality and Ecosystem Monitoring, July 1992 to May 2002 and Water Quality Implications for Lake Forsyth/Wairewa. *Environment Canterbury Technical Report U03/20.*

McCorquodale, J.A., Georgiou, I. 2004. Modelling Freshwater Inflows in a Shallow Lake. *Archives of Hydro-Engineering and Environmental Mechanics 51. 3-12.*

McDowell, R.W., Biggs, B.J.F., Sharpley, A.N., Nguyen, L. 2004. Connecting Phosphorus Loss from Agricultural Landscapes to Surface Water Quality. *Chemistry and Ecology, 20(1).*

Meals, D.W., Cassell, E.A., Hughell, D., Wood, L., Jokela, W.E., Parsons, R. 2008. Dynamic Spatially Explicit Mass Balance Modelling for Targeted Watershed Phosphorus Management. 1. Model Development. *Agriculture, Ecosystems and Environment, 127. 189-200.*

Miller, J. 2013. Investigating Sources of Sediment Input to Lake Forsyth/ Wairewa. *Waterways Center for Freshwater Management Report 2013-003, University of Canterbury, New Zealand.*

Moore, P.A., Reddy, K.R. 1994. Role of Eh and pH on Phosphorus Geochemistry in Sediments of Lake Okeechobee, Florida. *Journal of Environmental Quality 23(5). 955-964*

Morris, K., Bailey, P.C., Boon, P.I., Hughes, L. 2003. Alternative Stable States in the Aquatic Vegetation of Shallow Urban Lakes. II. Catastrophic Loss of Aquatic Plants Consequent to Nutrient Enrichment. *Marine and Freshwater Research 5. 201-215.*

Mortimer, C.H. 1942. The Exchange of Dissolved Substances Between Mud and Water in Lakes. *Journal of Ecology 30. 147-201.*

Moss, B., Jeppesen, E., Sondergaard, M., Lauridsen, T,L., Liu, Zhengwen, L. 2013. Nitrogen, macrophytes, shallow lakes and nutrient limitation: resolution of a current controversy? *Hydrobiologia 710. 3-21.*

Nash, J.E., Sutcliffe, J.V. 1970. River Flow Forecasting through Conceptual Methods. Part 1- A Discussion of Principles. *Journal of Hydrology, 10. 282-290.*

Ngwick, B., Sigg, L. 1997. Dissolution of Fe(III) (hydr)oxides by Metal EDTA Complexes. *Geochimica et Cosmochimica Acta 61(5). 951-963*

Niemisto, J., Holmroos, H., Horppila, J. 2011. Water pH and Sediment Resuspension Regulating Internal Phosphorus Loading in a Shallow Lake- Field Experiment on Diurnal Variation. *Journal of Limnology 70(1). 3-10.*

Nyenje, P.M., Meijer, L.M.G., Foppen, J.W., Kulabako, R., Uhlenbrook, S. 2014. Phosphorus Transport and Retention in a Channel Draining an Urban, Tropical Catchment with Informal Settlements. *Hydrology and Earth Systems 18. 1009-1025.*

Oelbner, W., Guth, U. 2003. Determination of Carbon Dioxide Dynamics in Lakes. *Proceedings of ICGG7 50-52. Retrieved from copernicus.org/ICGG7/extended abstracts/icgg00010.pdf*

Olila, O.G., Reddy, K.R. 1993. Phosphorus Sorption Characteristics of Sediments in Shallow Eutrophic Lakes of Florida. *Archi fur Hydrobiologie 129(1). 45-65.*

Oxmann, J.F., Schwendenmann, L. 2015. Authigenic Apatite and Octacalcium Phosphate Formation Due to Adsorption-Precipitation Switching Across Estuarine Salinity Gradients. *Biogeosciences 12. 723-738.*

Ozkundakci, D., Hamilton, D.P., Gibbs, M.M. 2011. Hypolimnetis Phosphorus and Nitrogen Dynamics in a Small, Eutrophic Lake with a Seasonally Anoxic Hypolimnion. *Hydrobiologia 661. 5-20.*

Pacini, N., Gachter, R. 1999. Speciation of Riverine Particulate Phosphorus During Rain Events. *Biogeochemistry 47. 87-109.*

Painter, D. 2014. Reducing Sediment Input to Te Roto o Wairewa/Lake Forsyth. *Unpublished Environment Canterbury, Technical Report.R14/32. http://ecan.govt.nz/publications/ Reports/reducing-sediment-input-wairewa-forsyth.pdf*

Parkhurst, D.L., Appelo, D.L. 1999. Users Guide to PHREEQC (Version 2)- A Computer Program for Speciation, Batch Reaction, One Dimensional Transport and Inverse Geochemical Calculations. *Waters Resources Investigations Report 99-4259. United States Geological Survey, Denver, Colorado. Available from* http://wwwbrr.cr.usgs.gov/projects/ GWC_coupled/phreeqc/

PCE (Parlimentary Commissioner for the Environment). 2013. Water Quality in New Zealand: Land Use and Nutrient Pollution. *http://www.pce.parliament.nz.*

Perkins, R.G., Underwood, G.J.C. 2001. The Potential for Phosphorus Release Across the Sediment-Water Interface in an Eutrophic Reservoir Dosed with Ferric Sulphate. *Water Research 35(6). 1399-1406.*

Pettersen, K., Bostrom, B., Jacobsen, O. 1988. Phosphorus in Sediments- Speciation and Analysis. *Hydrobiologia 170. 91-101*

Pieri,L., Bitelli, M., Wu, J.Q., Dun, S., Flanagan,D.C., Pisa, P.R., Ventura, F., Salvatorelli, F. (2007). Using the Water Erosion Prediction Project (WEPP) Model to Simulate Field-Observed Runoff and Erosion in the Appenine Mountain Range, Italy. *Journal of Hydrology. 336. 84-97.*

Pionke, H.B., Gburak, W.J., Sharpley, N., Schnabel, R.R. 1996. Flow and Nutrient Export Patterns for an Agricultural Hill-Land Watershed. *Water Resources Research. 32(6) 1795-1804.*

Post, J.E. 1999. Manganese Oxide Minerals: Crystal Structures and Economic and Environmental Significance. *Proceedings of the National Academy of Sciences of the USA. 96(7) 3447-3454.*

Postma, D., Larsen, F., Hue, N.T.M., Duc, M.T., Viet, P.H., Nhan, P.Q., Jessen, S. 2007. Arsenic in Groundwater of the Red River Floodplain, Vietnam: Controlling Geochemical Processes and Reactive Transport Modelling. *Geochimica et Cosmochimica Acta 71(21). 5054-5071.*

Prairie, Y.T., De Montigny, C., Del Giorgio, P.A. 2001. Anaerobic Phosphorus Release from Sediments; A Paradigm Revised. *Verhandlungen des Internationalen Verein Limnologie 27. 4013-4020.*

Psenner, R., Bostrom, B., Dinka, M., Pettersen,K. 1988. Fractionation of Phosphorus in Suspended Matter and Sediments. *Arch. Hydrobiol. Beih. Ergebn. Limnol. 30. 98-109*

Quilbe, R., Rousseau, A.N., Duchemin, M., Poulin, A., Gangbazo, G., Villeneuve, J-P. 2006. Selecting a Calculation Method to Estimate Sediment and Nutrient Loads in Streams: Application to the Beaurivage River (Quebec, Canada). *Journal of Hydrology 326. 295-310.*

Quinn, J.M., Stroud, M.J., 2002. Water Quality and Sediment and Nutrient Export from New Zealand Hill Catchments of Contrasting Land Use. *New Zealand Journal of Marine and Freshwater Research, 36. 409-429.*

Rakko, A., Seppala, J. 2014. Effect of Salinity on the Growth Rate and Nutrient Stoichiometry Of Two Baltic Sea Filamentous Cyanobacterial Species. *Estonian Journal of Ecology 63(2). 55-70.*

Reid, M., Wybrow, R., Woodward, C. 2004. Managing Te Roto o Wairewa: Lessons from the Past. *Water and Atmosphere 12(4)*

Reitzel, K., Hansen, J., Jensen, H.S., Andersen, F.O, Hansen K.S. 2003. Testing Aluminium Addition as a Tool for Lake Restoration in Shallow, Eutrophic Lake Sønderby, Denmark. *Hydrobiologia, 506-509. 781-787.*

Reitzel, K., Hansen, J., Andersen, F.O., Hansen, K.S., Jensen, H.S., 2005. Lake Restoration by Dosing with Aluminium Relative to Mobile Phosphorus in the Sediment. *Environmental Science and Technology 39(11). 4134-4140.*

Reitzel, K., Ahlgren, H., DeBrabandere, H., Waldebak, M., Gogoll, A., Tranvik, L. 2007. Degradation Rates of Organic Phosphorus in Lake Sediments. *Biogeochemistry 82. 15-28.*

Reynolds, C.S., Davies, P.S. 2001. Sources and Bioavailability of Phosphorus Fractions: A British Perspective. *Biological Review 76. 27-64.*

Robertson, P. 2011. Diurnal Variation in Wairewa Water Quality. *Waterways Center for Freshwater Management Report 2011-003. University of Canterbury, New Zealand.*

Rosewell, C.J. 2001. Evaluation of WEPP for Runoff and Soil Loss Prediction in Gunnedah, NSW, Australia. *Australian Journal of Soil Research. 9. 230-243.*

Roy, P.S., Williams, R.J., Jones, A.R., Yassini, I., Gibbs, P.J., Coastes, B., West, R.J., Scanes, P.R., Hudson, J.P., Nicol, S. 2001. Structure and Function of South-East Australian Estuaries. *Estuarine, Coastal and Shelf Science 53. 351-384.*

Ruban, V., Lopez-Sanchez, J.F., Pardo, P., Rauret, G., Muntau, H., Quevauller, Ph. 1999. Selection and Evaluation of Sequential Extraction Procedures for the Determination of Phosphorus Forms in Lake Sediment. *Journal of Environmental Monitoring 1. 51-56.*

Rydin, E. 2000. Potentially Mobile Phosphorus in Lake Erken Sediment. *Water Research 34 (7) 2037-2042.*

Santos-Echeandia, J., Vale, C., Caetano, M., Pereira, P., Prego, R. 2010. Effect of Tidal Flooding on Metal Distribution in Pore Waters of Marsh Sediments and its Transport to the Water Column (Tagus Estuary, Portugal). *Marine Environmental Research 70. 358-367.*

Scanes, P. 2012. Nutrient Loads to Protect Environmental Values in Waituna Lagoon, Southland NZ. *Report prepared for Environment Southland. 10p. Available from http://www.es.govt.nz.*

Schaefli, B., Gupta, H.V. 2007. Do Nash Values have Value? *Hydrological Processes 21. 2075-2080.*

Scheffer, M., van Nes, E.H. 2007. Shallow Lake Theory Revisited: Various Alternative Regimes Driven by Climate. Nutrients, Depth, and Lake Size. *Hydrobiologia 584. 455-466.*

Schindler, D.W. 1977. The evolution of phosphorus limitation in lakes. *Science 195. 260-262.*

Schindler, D.W., 2006. Recent Advances in the Understanding and Management of Eutrophication. *Limnology and Oceanography 51(1 part2). 356-363.*

Schindler, D.W., 2012. The Dilemma of Controlling Cultural Eutrophication of Lakes. *Proceedings of the Royal Society B 279. 4322-4333.*

Schindler, D.W., Hecky, R.E., Findlay, D.L., Stainton, M.P., Parker, B.R., Paterson, M.J., Beaty, K.G., Lyng, M., Kasian, S.E.M. 2008. Eutrophication of Lakes Cannot be Controlled by

Reducing Nitrogen Input: Results of a 37-year Whole-Ecosystem Experiment. *Proceedings of the National Academy of Sciences of the United States of America, 105 (32)*

Schallenberg, M., Burns, C. 2004. Effects of Sediment Resuspension on Phytoplankton: Teasing Apart the Influences of Light, Nutrients and Algal Entrainment. *Freshwater Biology 49. 143-159.*

Schallenberg, M., Sorrell, B. 2009. Regime Shifts Between Clear and Turbid Water in New Zealand Lakes; Environmental Correlates and Implications for Management and Restoration. *New Zealand Journal of Marine and Freshwater Research 43. 701-712.*

Schallenberg, M., Larned, S.T., Hayward, S., Arbuckle, C. 2010. Contrasting Effects of Managed Opening Regimes on Water Quality in Two Intermittently Closed and Open Coastal Lakes. *Estauraine, Coastal and Shelf Science 86. 587-597.*

Schallenberg, M., Kelly,D. 2012. Ecological Condition of Six Shallow Southland Lakes. *MSI Envirolink Report prepared for Environment Southland. Cawthron Report No 2198 43p. Available from www.envirolink.govt.nz*

Schoumans, O.F., Chardon, W.J., Bechmann, M.E., Gascuel-Odoux, C., Hofman, G., Kronvag, B., Rubak, G.H., Ulen, B., Dorioz, J.M. 2014. Mitigation Options to Reduce Phosphorus Losses from the Agricultural Sector and Improve Surface Water Quality: A Review. *Science of the Total Environment 468-469. 1255-1266.*

Schwertmann, U., Carlson, L., Murad, E. 1987. Properties of Iron Oxides in Two Finnish Lakes in Relation to the Environment of Their Formation. *Clays and Clay Minerals. 35(4). 297-304.*

Serafy, J.E., Harrell, R.M. 1993. Behavioural Responses of Fishes to Increasing pH and Dissolved Oxygen: Field and Laboratory Observations. *Freshwater Biology 30. 53-61.*

Smolders, A.J.P., Lamers, L.P.M., Lucassen, E.C.H.E.T., Van der Velde, G., Roelofs, J.G.M. 2006. Internal Eutrophication: How it Works and What to Do About It- A Review. *Chemistry and Ecology 22(2). 93-111*

Spiteri, C., Van Capallen, P., Regnier, P. 2008. Surface Complexation Effects on Phosphate Adsorption to Ferric Iron Oxyhydroxides Along pH and Salinity Gradients in Estuaries and Coastal Aquifers. *Geochimica et Cosmochimica Acta 72. 3431-3445.*

Søndergaard, M., Jeppesen, E., Kristensen, P., Sortkjaer, O., 1990. Interactions Between Sediment and Water in a Shallow and Hypertrophic Lake: A Study on Phytoplankton Collapses in Lake Sobygard, Denmark. *Hydrobiologia 191. 139-148.*

Søndergaard, M., Kristensen, P, Jeppesen, E. 1992, Phosphorus Release from Resuspended Sedimetn in the Shallow and Wind Exposed Lake Arreso, Denmark. *Hydrobiologia 228. 91-99*

Søndergaard, M., Jensen, J.P., Jeppesen, E. 1999. Internal Phosphorous Loading in Shallow Danish Lakes. Hydrobiologia 408-409. 145-152.

Søndergaard, M., Jensen, J.P., Jeppesen, E. 2003. Role of Sediment and Internal Loading of Phosphorous in Shallow Lakes. *Hydrobiologia 506-509. 135-145.*

Søndergaard, M. 2007. Nutrient Dynamics in Lakes- with Emphasis on Phosphorus, Sediment and Lake Restoration. *Unpublished D. Phil. Thesis, National Environmental Research Institute, University of Aarhus, Denmark.*

Soons, J.M., 1998. Recent Coastal Changes in Canterbury- the Case of Lake Forsyth/Wairewa. *New Zealand Geographer 54(1).*

Stamm, C., Jarvie, H.P., Scott, T. 2014. What's More Important for Managing Phosphorus: Loads, Concentration or Both? *Environmental Science and Technology 48. 23-24.*

Stone, M., English, M.C. 1993. Geochemical Composition, Phosphorus Speciation and Mass Transport of Fine Grained Sediment in Two Lake Erie Tributaries. *Hydrobiologia 253. 17-29.*

Steinman, A., Chu, X., Ogdahl, M. 2009. Spatial and Temporal Variability of Internal and External Phosphorus Loads in Mona Lake, Michigan. *Aquatic Ecology 43. 1-18.*

Strauss, R., Bruemmer, G.W., Barrow, N.J. 1997. Effects of Crystallinity of Goethite II: Rates of Sorption and Desorption of Phosphate. *European Journal of Soil Science. 48. 101-114.*

Takamura, N., Kadono, Y., Fukushima, M., Nakagawa, M., Kim, B,O. 2003. Effects of Aquatic Macrophytes on Water Quality and Phytoplankton Communities in Shallow Lakes. *Ecological Research 18. 381-395.*

Teng, W., Guoxiang, W., Qiang, L. 2007. Effects of Water Turbidity on the Photosynthetic Characteristics of *Myriophyllum spicatum L. Asian Journal of Plant Sciences 6. 773-780.*

Tessier, A., Campbell, P.G.C., Bisson, M. 1979. Sequential Extraction Procedure for the Speciation of Particulate Trace Metals. *Analytical Chemistry 51(7). 844-851.*

Tiruta-Barna, L. 2008. Using PHREEQC for Modelling and Simulation of Dynamic Leaching Tests and Scenarios. *Journal of Hazardous Materials 157(2-3). 525-533.*

Trfunovic, S.R., Matovic, Z.D., Milovanovic, V. 2000. Maganese (II) Complexes with EDTA-type Ligands. The Molecular Structure of Aquo-dihydrogen(1,2-propanediamine-*N,N,N,N*_tetraacetate)manganese(ii) Trihydrate, [Mn($H_2$1,2-pdta)*H_2O)].3H_2O. *Transition Metal Chemistry 25. 680-685.*

Turner, B.L., Frossard, E., Baldwin, D.S. (Eds) 2005. Organic Phosphorus in the Environment. *CABI Publishing, Oxfordshire, United Kingdom.*

Turnipseed, D.P., Sauer, V.B. 2010. Discharge Measurements at Gauging Stations: U.S. Geological Survey Techniques and Methods book 3, Chapter A8. *United States Geological Survey http://pubs.usgs.gov/tm/tm3-a8/.*

Twomey, L., Thompson, P. 2001. Nutrient Limitation of Phytoplankton in a Seasonally Open Bar-Built Estuary: Wilson Inlet, Western Australia. *Journal of Phycology 37. 16-29.*

U.S. EPA (Environmental Protection Agency). 1994. Method 3051. Microwave assisted acid digestion of sediments, sludges, soils and oils. *US EPA, Office of Water, U.S. Government Printing Office. Washington D.C.*

U.S. EPA (Environmental Protection Agency). 1996. Environmental Indicators of Water Quality in the United States. *EPA 841-R-96-002. US EPA, Office of Water, U.S. Government Printing Office.*

Verma, A.K., Jha, M.K., Mahana, R.K. 2010. Evaluation of HEC-HMS and WEPP for Simulating Watershed Runoff Using Remote Sensing and Geographical Information System. *Paddy Water Environment 8. 131-144*

Verburg, P., Hamill. K., Unwin. M., Abell.J. 2010. Lake Water Quality in New Zealand 2010: Status and Trends. *NIWA Client Report HAM2010-107. Prepared for the Ministry for the Environment.*

Waters, A.S., Webster-Brown. J.G. 2013. Assessing Aluminium Toxicity in Streams Affected by Acid Mine Drainage. *Water Science and Technology 67(8). 1764-1772.*

Wang, X., Liu, F., Tan. W., Li, W., Feng. X., Sparks, D.L. 2013. Characteristics of Phosphate Adsorption-Desorption onto Ferrihydrite: Comparison with Well Crystalline Fe (Hydr)Oxides. *Soil Science 178(1) 1-11*

Weston, N.B., Dixon, R.E., Joye, S.B. 2006. Ramifications of Increased Salinity in Tidal Freshwater Sediments: Geochemistry and Microbial Pathways of Organic Matter Mineralization. *Journal of Geophysical Research. 111.*

Weston, N.B., Vile, M.A., Neubauer, S.C., Velinsky, D.J. 2011. Accelerated Microbial Organic Matter Mineralization Following Salt-Water Intrusion into Tidal Freshwater Marsh Soils. *Biogeochemistry 102. 135-151.*

Wentworth, C.K. 1929. Method of Computing Mechanical Composition in Sediments. *Geological Society of America Bulletin 40. 771-790.*

Weiner, E.R. 2008. Applications of Environmental Aquatic Chemistry: A Practical Guide 2nd Ed. *Taylor and Francis Group, Florida. U.S.A.*

Welsh, B.L., Eller, F.C. 1991. Mechanisms Controlling Summertime Oxygen Depletion in Western Long Island Sound. *Estuaries 14(3). 265-278.*

Wetzel, R.G. 2001. Limnology; Lake and River Ecosystems. *Academic Press, Elsevier. U.S.A.*

White, E. Payne, G., Pickmere, S., Woods, P. 1986. Nutrient demand and availability related to growth among natural assemblages of phytoplankton. *New Zealand Journal of Marine and Freshwater Research 20(2)199-208.*

Wildman, R.A., Hering, J.G. 2011. Potential of Release of Sediment Phosphorus to Lake Powell (Utah and Arizona) due to Sediment Resuspension During Low Water Level. *Lake and Reservoir Management 27(4). 365-375*

Wissmeier, L., Barry, D.A. 2010. Implementation of Variably Saturated Flow into PHREEQC for the Simulation of Biogeochemical Reactions in the Vadose Zone. *Environmental Modelling and Software 25(4) 526-538.*

Wong, V.N.L., Johnston, S.G., Burton, E.D., Hirst, P., Sullivan, L.A., Bush, R.T., Blackford, M. 2015. Seawater Inundation of Coastal Floodplain Sediments: Short-term Changes in Surface Water and Sediment Geochemistry. *Chemical Geology 398. 32-35.*

Woodward, C.A., Shulmeister, J. 2005. A Holocene Record of Human Induced and Natural Environmental Change from Lake Forsyth (Te Wairewa), New Zealand. *Journal of Paleolimnology 34. 481-501.*

Wriggle Coastal Management, 2012. Nutrient Load Criteria to Limit Eutrophication in Three Typical New Zealand Estuary Types - ICOLL's, Tidal Lagoon, and Tidal River Estuaries. *Report prepared for Environment Southland. Available from http://www.es.govt.nz.*

Xie, L.Q., Xie, P., Tang, H.J. 2003. Enhancement of Dissolved Phosphorus Release from Sediment to Lake Water by *Microcystis* Blooms- an Enclosure Experiment in a Hyper-eutrophic, Subtropical Chinese Lake. *Environmental Pollution 122. 391-399.*

Young, W.J., Marston, F.M., Davis, R.J. 1996. Nutrient Exports and Land Use in Australian Catchments. *Journal of Environmental Management 47(2): 165-183*

Appendix 1

Sediment; Sequential Chemical Extractions

1.1 Cores

Core F11 C1	Sample date = Dec 2011		Atmosphere = oxygen				Core type = PBI		
Depth cm	**NH4Cl -P**	**BD-P**	**NaOH-rP**	**Org-P**	**HCl-P**	**Res-P**	**TSP**	**NaOH only[1]**	**Org[2]**	**Carb[3]**
	mg.kg^{-1} DW								%	
0-1	8.96	332	283	255	236	424	1539		11.1	2.34
1-2	1.97	204	186	156	190	225	963		6.5	1.88
2-3	1.36	259	173	124	224	286	1068		6.5	
3-4	1.50	218	152	121	204	225	922		6.6	1.62
4-6	1.07	129	124	106	219	231	809		6.2	1.56
6-8	1.36	126	129	101	251	248	857		6.4	
8-10	3.04	66.9	85.4	61.3	231	194	641		5.8	1.76
10-12	1.07	59.2	97.8	67.5	235	209	669		5.5	1.76
12-14	1.09	45.1	80.4	47.4	239	189	601		5.0	1.74
14-16	2.77	55.4	93.3	64.1	243	240	698		5.4	
18-20	3.37	35.9	75.1	47.9	238	181	581		5.0	2.01
20-22	4.43	29.5	67.9	45.1	238	180	565		4.5	1.79
Core F11 C2	Sample date 17-Aug-12			Atmosphere oxygen			Core type = winter			
0-1	0.452	200	324	367	255	370	1517		15.6	1.61
1-2	0.000	153	173	199	288	334	1147		12.5	1.71
2-3	0.000	66.9	80.7	74.7	269	205	696		7.90	1.52
3-4	0.000	42.4	79.7	57.1	249	193	621		8.79	1.43
4-5	0.000	57.3	111	103	244	269	785		9.64	1.63
5-7	0.000	56.6	104	106	216	245	728		7.95	1.47
7-9	0.323	45.7	85.3	70.3	232	197	631		6.94	1.38
9-11	0.656	47.3	83.9	71.7	218	210	632		7.12	1.38
11-13	0.478	21.2	79.3	76.3	220	272	670		5.94	1.56
13-15	0.495	33.9	70.1	53.9	211	196	565			
15-20	2.00	46.6	96.1	71.3	240	202	658		5.50	1.66
20-25	3.76	21.9	50.0	39.9	190	163	469		4.75	1.36
Core F12 C7	Sample date 7-Oct-14			Atmosphere oxygen			Core type = PBI			
0-0.5	0.41	273	181	213	223	305	1196	317	9.26	2.37
0-1	0.90	474	248	168	345	314	1549	374	9.71	1.94
1-2	0.10	219	120	150	216	252	957	244	9.68	2.18
2-3	0.13	225	144	165	222	261	1016	287	10.4	2.15
3-4	0.05	171	124	141	226	251	913	165	9.46	2.16
4-5	0.02	155	131	148	231	268	933	234	10.6	2.47
5-7	0.00	80.0	97.0	103	237	218	736	130	8.90	2.31
7-9	0.86	35.6	70.2	81.2	227	194	609	102	7.37	2.29
9-11	0.23	39.5	74.2	75.1	221	206	616	84.8	6.71	2.00
11-13	0.40	13.4	38.9	49.1	206	150	458	48.8	5.66	1.80
13-15	0.38	21.2	38.8	54.8	199	143	458	43.2	5.30	0.95
15-20	0.530	16.9	44.3	62.9	210	174	508	48.7	5.57	1.80

Core F10 C9	Sample date = 10-Oct-14			Atmosphere = oxygen			Core type = PBI		
Depth	**NH4Cl-P**	**BD-P**	**NaOH-rP**	**Org-P**	**HCl-P**	**Res-P**	**TSP**	**NaOH only[1]**	**Org[2]**	**Carb[3]**
cm	mg.kg DW								%	
0-1	0.397	496	340	247	275	358	1716	610	14.5	3.15
1-2	0.171	482	328	176	284	331	1601	612	16.8	3.71
2-3	0.128	314	282	130	296	279	1302	445	17.7	3.94
3-4	0.141	392	278	129	311	285	1394	480	18.6	3.63
4-5	0.000	276	228	137	291	305	1237	360	16.7	3.92
5-7	0.224		154	96	258	253		247	14.4	3.66
7-9	0.211	99.4	115	91.0	274	256	835	144	11.2	2.51
9-11	0.268	79.8	99.8	94.7	277	271	823	120	9.77	2.68
11-13	0.167	71.6	91.5	95.5	289	272	820	111	11.0	2.63
13-15	0.009	61.3	86.5	89.8	288	259	784	108	10.8	2.61
15-20	0.318	49.9	84.4	75.3	314	238	762	102	9.92	2.59
20-25	0.280	58.8	88.5	153	333	247	880	112	10.5	2.79
Core F10 C9	Sample date = 10-Oct-14			Atmosphere = nitrogen			Core type = PBI			
0-1	1.61	404	340	184	292	345	1566			
1-2	0.335	384	352	136	311	354	1537			
2-3	0.000	304	284	93	278	339	1299			
3-4	0.000	276	272	87	316	299	1250			
4-5	0.000	232	233	117	264	322	1167			
5-7	0.000	185	177	99	292	293	1045			
7-9	0.097	90.5	126	43.5	284	266	809			
9-11	0.000	67.3	102	15.0	291	302	777			
11-13	0.000	57.9	99.3	62.9	291	278	789			
13-15	0.418	52.7	103.6	55.5	290	254	756			
15-20	1.78	40.6	97.6	48.4	301	237	727			
20-25	4.54	55.3	99.0	59.1	314	258	790			

1 = NaOH only = Extraction procedure used without BD step, i.e. NaOH step directly after the NH_4Cl step.
2 = Org = Organic matter determined by LOI
3 = Carb = Carbonate content determined by LOI

1.2 Surface sediments (0-1 cm)

Site	Date	NH_4Cl-P	BD-P	NaOH-rP	Org-P	HCl-P	Res-P	TSP	Org [1]	Carb[2]
		mg.kg^{-1} DW							%	
F1	2-Nov-11	0.518	303	172	96.9	230	266	1068	7.07	0.777
F2	2-Nov-11	0.177	335	239	168	270	374	1386	11.0	1.81
F3	2-Nov-11	0.549	198	197	152	238	250	1034	6.99	1.10
F4	2-Nov-11	2.03	248			146	314	1080	10.4	0.000
F5	2-Nov-11	0.000	119	147	108	255	274	903	7.98	1.50
F8	2-Nov-11	0.000	244	147	169	246	283	1090	7.91	1.46
F10	2-Nov-11	0.254	237	220	98.4	343	322	1221	9.84	2.14
F1	17-Aug-12	1.96	333	397	349	189	554	1824	9.27	2.52
F2	17-Aug-12	0.732	254	379	265	238	487	1624	11.6	2.92
F3	17-Aug-12	0.090	208	367	236	181	443	1435	8.88	2.30
F4	17-Aug-12	1.03	299	318	222	240	450	1530	11.1	2.36
F5	17-Aug-12	0.000	245	357	298	213	460	1572	15.7	3.14
F8	17-Aug-12	0.000	259	260	167	237	347	1270	9.70	1.73
F10	17-Aug-12	0.633	374	161	374	153	464	1527	12.1	2.94
F11	17-Aug-12	0.453	200	324	367	253	370	1515	15.6	1.20
F1	8-Apr-13	0.385	245	192	203	212	315	1168		
F2	8-Apr-13	4.93	399	265	287	276	459	1690		
F4	8-Apr-13	2.88	257	202	233	269	389	1353		
F7	8-Apr-13	5.60	262	140	180	173	218	979		
F8	8-Apr-13	4.11	364	189	253	220	252	1282		
F10	8-Apr-13	2.42	361	227	269	345	448	1653		
F11 S5	31-Dec-12	5.93	213	125	163	220	238	965	6.59	
F11 S9	20-Feb-13	0.290	218	222	210	204	294	1148	8.31	
F11 S11	21-Mar-13	0.445	226	154	154	220	281	1036	9.05	
F11 S14	10-Apr-13	5.65	380	182	227	227	317	1338	8.99	
F11 S16	24-Apr-13	4.28	321	213	288	216	374	1416	11.9	
F12 S1	1-Feb-13	8.83	229	150	213	248	303	1152	9.17	
F12 S2	20-Feb-13	2.37	132	111	127	175	194	742	9.06	
F12 S5	21-Mar-13	1.33	228	162	182	259	286	1118	8.85	
F12 S9	10-Apr-13	4.24	259	158	225	262	350	1259	10.6	
F12 S11	24-Apr-13	1.58	255	167	183	127	322	1057	9.23	

1= Org = organic material analysed as LOI
2=Carb= Carbonate content analysed as LOI

Appendix 2

Sediment; Pore-water chemistry- Trace element (ICP-OES)

Core F11 C1	Sample date = Dec 11			Atmosphere = oxygen			Core type = PBI			
Depth	**P**	**Al**	**Ca**	**Fe**	**K**	**Mg**	**Mn**	**Na**	**S**	**Zn**
cm					$mg.L^{-1}$					
0-1	0.858	0.017	10.3	0.049	19.5	25.0	0.081	173	15.0	0.001
1-2	1.32	0.020	12.4	0.523	22.8	27.0	0.434	179	9.16	0.003
2-3	2.51	0.019	13.9	2.63	25.8	28.5	0.765	219	4.93	0.002
3-4	2.69	0.027	17.2	2.23	31.1	37.3	0.640	269	7.89	0.003
4-6	3.01	0.026	19.4	4.32	25.9	46.5	0.528	310	2.02	0.009
6-8	2.97	0.036	23.2	3.75	33.3	55.7	0.448	385	2.25	0.003
8-10	2.00	0.041	26.7	2.15	38.6	63.6	0.445	447	2.67	0.001
10-12	1.37	0.036	30.7	1.49	40.6	75.2	0.533	521	1.63	0.002
12-14	1.26	0.040	37.7	0.793	53.4	92.6	0.477	655	2.02	0.002
14-16	1.12	0.039	39.0	0.591	57.4	97.2	0.511	694	1.51	0.001
18-20	0.999	0.060	42.7	0.250	68.7	106	0.476	795	1.55	0.002
20-22	0.795	0.054	39.6	0.120	70.3	95.7	0.295	768	3.80	0.002
Core F11 C2	Sample date = 17 Aug 2012				Atmosphere = oxygen			Core type = winter		
0-1	0.047	0.029	15.4	0.053	10.4	18.6	0.336	138	11.4	0.003
1-2	0.057	0.022	12.7	0.051	15.6	25.6	0.339	213	15.5	
2-3	0.169	0.027	14.4	0.061	29.7	36.7	0.267	408	27.2	
3-4	0.145	0.037	14.9	0.060	22.2	32.9	0.365	341	20.9	0.005
4-5	0.144	0.031	27.0	0.054	38.7	61.0	0.665	561	29.2	0.004
5-7	0.111	0.025	35.6	0.054	47.2	90.6	0.730	696	23.4	
7-9	0.139	0.019	32.2	0.046	43.8	88.0	0.631	619	5.91	
9-11	0.140	0.022	39.1	0.043	44.2	105	0.823	683	1.38	0.001
11-13	0.274	0.023	35.0	0.038	49.5	113	0.304	717	0.880	0.002
13-15	0.343	0.020	32.9	0.040	53.2	110	0.414	743	1.09	
15-20	0.497	0.019	25.5	0.049	47.9	89.3	0.223	659	1.15	
20-25	0.228	0.014	9.73	0.020	19.1	29.7	0.048	262	0.596	
Core F11 C3	Sample date = 5 Mar 2013				Atmosphere = oxygen			Core type = pre-bloom		
0-1	0.040	0.006	10.8	0.001	13.6	23.0	0.340	159	18.4	
1-2	0.038	0.005	10.5	0.002	13.3	22.3	0.343	157	18.9	
2-3	0.040	0.005	9.58	0.002	12.5	20.1	0.325	142	16.8	
3-4	0.106	0.019	10.3	0.011	13.7	21.9	0.179	155	17.7	
4-5	0.079	0.026	5.91	0.013	7.3	12.4	0.088	82	10.4	
5-7	0.235	0.050	8.47	0.024	12.4	18.6	0.063	134	14.0	
7-9	0.240	0.040	9.76	0.016	15.9	21.3	0.051	162	11.1	
9-11	0.615	0.083	10.2	0.039	19.8	23.4	0.076	191	2.75	
11-13	0.960	0.058	11.2	0.028	26.9	27.5	0.079	249	1.25	
13-15	1.33	0.025	13.1	0.020	34.8	34.2	0.131	329	0.779	
15-20	1.58	0.023	17.0	0.020	45.5	46.9	0.189	459	1.62	
20-25	1.71	0.011	25.1	0.002	70.8	72.1	0.096	703	4.05	

F12 C5	Sample date = 5 Mar 2013			Atmosphere = oxygen			Core type = pre-bloom			
Depth	**P**	**Al**	**Ca**	**Fe**	**K**	**Mg**	**Mn**	**Na**	**S**	**Zn**
cm					$mg.L^{-1}$					
0-1	0.038	0.010	10.4	0.003	12.7	22.1	0.131	156	20.9	
1-2	0.035	0.007	10.0	0.002	12.1	21.2	0.195	150	19.8	
2-3	0.034	0.007	9.76	0.003	11.6	21.3	0.194	150	19.7	
3-4	0.046	0.010	9.75	0.003	11.7	20.8	0.128	149	19.8	
4-5	0.049	0.016	9.12	0.008	12.2	20.7	0.074	151	20.3	
5-7										
7-9	0.122	0.114	8.28	0.035	12.8	18.0	0.032	153	19.4	
9-11	0.391	0.121	7.80	0.039	15.8	18.3	0.037	172	19.0	
11-13	1.04	0.206	7.02	0.065	19.9	19.5	0.011	217	14.2	
13-15										
15-20	2.97	0.068	10.9	0.020	38.7	33.5	0.013	468	9.07	
20-25	3.42	0.054	17.2	0.011	48.1	48.0	0.044	590	8.53	
F12 C6	Sample date = 23 Dec 2013			Atmosphere = nitrogen			Core type = PBI			
0-1	0.093	0.054	37.8	2.42	56.6	90.2	0.660	736	67.3	0.003
1-2	0.691	0.186	38.6	6.71	59.1	92.7	0.720	751	63.1	0.039
2-3	1.34	0.253	38.1	8.96	59.7	92.0	0.699	761	53.7	0.001
3-4	1.47	0.158	36.9	7.91	61.4	90.4	0.658	767	45.9	
4-5	1.77	0.260	37.3	7.04	66.2	91.4	0.630	795	40.3	0.003
5-7	1.17	0.282	38.0	2.13	71.9	96.6	0.576	848	38.4	0.007
7-9	1.25	0.268	39.5	0.115	78.6	103	0.351	904	41.6	0.007
9-11	1.51	0.139	41.6	0.091	83.2	109	0.231	947	46.5	
11-13	1.90	0.070	43.6	0.086	89.9	119	0.188	996	49.8	0.006
13-15	2.65	0.097	44.7	0.084	92.1	125	0.180	1014	47.3	0.088
15-20	2.07	0.099	37.5	0.134	75.2	106	0.158	799	26.3	0.054
20-25	3.04	0.054	45.1	0.083	103	133	0.212	1063	24.4	0.002
Core F10 C9	Sampling date = 10 Oct 2014			Atmosphere = oxygen			Core Type = PBI			
0-1	0.046	34.3	0.484	80.4	84.9	1.02	625	0.031	54.3	0.009
1-2	0.047	34.0	0.352	95.8	90.9	1.0	686	1.01	57.1	0.005
2-3	0.058	34.3	0.566	106	94.4	0.788	744	2.26	61.7	0.005
3-4	0.046	35.6	0.433	115	98.7	0.672	813	2.51	67.7	0.004
4-5	0.050	36.5	0.717	122	103	0.589	869	3.10	73.9	0.005
5-7	0.072	37.9	0.649	133	107	0.501	941	3.85	83.3	0.027
7-9	0.114	39.9	1.67	139	113	0.407	1053	2.68	103	0.007
9-11	0.076	41.1	1.00	137	114	0.330	1061	1.71	109	0.004
11-13	0.107	42.9	0.520	141	119	0.289	1099	1.68	111	0.003
13-15	0.153	43.0	0.191	139	118	0.194	1072	1.33	107	0.006
15-20	0.111	43.6	0.187	136	120	0.180	1052	1.16	101	0.007
20-25	0.145	46.5	0.127	137	123	0.200	1049	1.00	95.4	0.005

Core F10 C9	Sampling date = 10 Oct 2014			Atmosphere = nitrogen			Core Type = PBI		
Depth	**Al**	**Ca**	**Fe**	**K**	**Mg**	**Mn**	**Na**	**P**	**S**	**Zn**
cm	mg.L-1									
0-1	0.060	34.2	1.69	80.1	85.1	0.996	621	0.132	55.3	0.020
1-2	0.118	35.0	8.44	104	94.3	0.894	725	5.04	62.3	0.025
2-3	0.075	35.0	4.99	96.1	92.3	1.06	689	2.48	58.7	0.014
3-4	0.134	36.6	8.96	114	98.9	0.770	804	5.52	68.4	0.013
4-5	0.230	37.5	8.82	121	102	0.668	853	5.99	73.9	0.014
5-7	0.182	38.0	7.08	125	104	0.541	903	4.88	81.1	0.024
7-9	0.154	39.4	4.79	135	112	0.417	1022	3.64	101	0.009
9-11	0.076	41.1	1.84	138	115	0.335	1060	1.94	110	0.006
11-13	0.110	42.8	0.967	141	119	0.289	1095	1.80	112	0.006
13-15	0.140	42.9	0.347	138	118	0.193	1066	1.36	107	0.006
15-20	0.132	43.3	2.33	136	119	0.204	1043	1.11	98.2	0.017
20-25	0.143	47.6	0.217	140	125	0.200	1081	0.983	95.7	0.006
Core F12 C8	Sampling date = 20 Oct 2014			Atmosphere = oxygen			Core Type = PBI		
0-1	0.297	27.7	0.438	54.0	72.3	0.016	476	0.023	44.7	0.001
1-2	0.344	27.8	1.89	55.5	70.8	0.869	483	0.043	44.7	0.003
2-3	0.586	28.1	7.56	56.0	68.9	1.17	476	0.182	42.7	0.004
3-4	0.808	28.8	8.33	57.8	69.9	1.03	487	0.195	42.1	0.006
4-5	0.525	28.2	7.08	59.4	66.8	0.869	480	0.159	39.9	0.004
5-7	0.632	23.6	8.27	46.4	54.2	0.667	364	0.643	30.4	0.003
7-9	1.04	28.5	7.43	63.8	68.3	0.654	502	1.0	29.3	0.004
9-11	1.40	27.4	3.69	67.4	70.1	0.486	517	0.907	24.9	0.003
11-13	1.19	26.1	1.16	71.6	72.1	0.328	532	0.939	23.8	0.003
13-15	0.772	20.4	0.30	60.4	55.5	0.076	394	0.750	19.4	0.002
15-20	1.30	23.0	0.40	97.2	73.8	0.064	617	1.74	23.5	0.002
20-25	2.06	23.1	0.51	104	78.6	0.081	693	2.11	20.3	0.002
Core F10 C10	Sampling date = 20 Oct 2014			Atmosphere = oxygen			Core Type = PBI		
0-1	0.203	25.6	0.729	57.2	67.6	0.438	478	0.071	49.3	0.002
1-2	0.781	28.3	3.84	81.4	76.8	0.703	592	0.760	50.1	0.006
2-3	0.808	26.8	2.45	89.2	78.2	0.510	632	1.962	49.4	0.003
3-4	1.065	25.9	3.14	93.7	75.7	0.430	679	2.18	52.8	0.004
4-5	0.975	26.0	2.22	106	79.0	0.344	714	1.91	57.9	0.002
5-7	0.945	25.6	2.00	112	79.6	0.266	758	2.41	63.9	0.002
7-9	1.17	26.7	1.89	119	81.8	0.202	834	1.75	80.9	0.003
9-11	1.35	25.2	1.01	114	80.7	0.152	813	1.07	82.2	0.002
11-13	0.589	26.8	0.335	116	81.9	0.123	772	0.319	82.4	0.002
13-15	0.164	26.9	0.181	116	82.7	0.109	812	0.480	84.2	0.002
15-20	0.758	28.7	0.488	107	85.3	0.148	775	0.749	75.7	0.003
20-25	0.832	36.4	0.428	125	104	0.151	945	1.08	97.5	0.003